Modelling the Glucose-Insulin Regulatory System for Glycaemic Control in Neonatal Intensive Care

Aaron Le Compte

A thesis presented for the degree of
Doctor of Philosophy
in
Mechanical Engineering
at the
University of Canterbury,
Christchurch, New Zealand.

6 July 2009

Acknowledgements

I would like to thank a number of people who have made my time working on this research for the past few years a rewarding experience.

To my supervisors Prof. Geoff Chase and Dr. Geoff Shaw for their enthusiasm, optimism, inspiration and passion for this project.

To Dr. Adrienne Lynn, Dr. Glynn Russell and the staff of the Neonatal Department at Christchurch Women's Hospital who were a pleasure to work with during the clinical trials.

To my glycaemic control colleagues: Jason, Jess, Thomas, Chris, Paul, Jackie, Normy, Klaus and Amy, many of whom provided a solid foundation of research upon which this project was based, and to the other members of the Centre for BioEngineering for making our work environment enjoyable and productive. Special thanks to those who assisted with the clinical work and allowing the trials to run smoothly into the small hours of the night. Thanks also to Dr. Chris Hann and Dr. Dominic Lee for providing mathematical and statistical tools and support.

Finally, I would like to thank my parents and family for all of their support and encouragement during these years of research, and for their dedication in providing the best possible future for their children.

Contents

List of Figures

List of Tables

Nomenclature

Acronyms and abbreviations

ACF	Auto-correlation function
AR	Auto-regressive
BG	Blood glucose
CDF	Cumulative distribution function
CLD	Chronic lung disease
DFT	Discrete fourier transform
EBM	Expressed breast milk
ECF	Extra-cellular fluid
EGA	Error Grid Analysis
EGP	Endogenous glucose production
ELBW	Extremely low birth weight
HGI	Hyperglycemic Index
GLUT	Glucose transporter
IDDM	Insulin-dependent diabetes mellitus
ICU	Intensive care unit
IQR	Inter-quartile range
MPC	Model predictive control
NEC	Necrotising enterocolitis
NICU	Neonatal intensive care unit
NIRTURE	Neonatal insulin replacement therapy in Europe
NRLS	Non-linear recursive least square
NZ	New Zealand
PACF	Partial auto-correlation function
PET	Positron emission tomography
PID	proportional-integral-derivative
SD	standard deviation
SEM	Standard error for mean
SPRINT	Specialized Relative Insulin and Nutrition Tables
VBLW	Very low birth weight

Mathematical variables

α_G	Michaelis-Menten constant for insulin-stimulated glucose removal saturation [L/mU]
α_I	Michaelis-Menten constant for plasma insulin disappearance saturation [L/mU]
c	Variance estimator modification constant
CNS	Central nervous system glucose uptake [mmol/min]
EGP_{max}	Endogenous glucose production at zero insulin [mmol/min]
G	Blood glucose concentration [mmol/L]
I	Blood plasma insulin concentration [mU/L]
I_B	Endogenous insulin production [mU/L/min]
k	Rate of insulin transport and utilisation in the interstitium [1/min]
k_{pr}	Rise rate of exogenous plasma glucose appearance [1/min]
k_{pd}	Decay rate of exogenous plasma glucose appearance [1/min]
m_{body}	Body mass [kg]
n	Plasma insulin decay rate [1/min]
P_{TPN}	External nutrition infusion rate via parenteral route [mmol/min]
P_{EN}	External nutrition infusion rate via enteral route [mmol/min]
$\phi(x; x_i, sigma^2_{x_i})$	Normal probability distribution
p_G	Rate of endogenous glucose removal [1/min]
$p(x, y)$	Joint probability density function
$p(x\|y)$	Conditional probability density function
Q	Interstitium insulin concentration
S_I	Insulin sensitivity index
u_{ex}	exogenous insulin input
u_{ex}	Exogenous insulin infusion [mU/min]
$V_{G,frac}$	Glucose distribution volume as a fraction of body weight [L/kg]
$V_{I,frac}$	Insulin distribution volume as a fraction of body weight [L/kg]

Abstract

Hyperglycaemia is a common condition in the very low birth weight infant and is linked to mortality and increased risks of morbidities such as sepsis and retinopathy of prematurity. The preterm neonate is in a state of transition from complete dependence on the mother to physiological independence. Many metabolic regulation systems are under-developed, attenuating the natural metabolic hormonal control response. Tight regulation of glucose levels can significantly reduce the negative outcomes associated with hyperglycaemia, but achieving it remains clinically elusive for the neonate.

Glucose control in adult critical care is a highly researched topic, and several studies have demonstrated significantly improved outcomes with protocols that modulate the insulin and/or nutrition inputs into the patient. Despite the potential, no standard protocol exists for neonates. Glucose restriction is often used as a treatment for neonatal hyperglycaemia, however this deprives the infant of much needed energy for growth. Limited trials of insulin infusions have been reported, based on fixed protocols or ad-hoc clinical decisions that do not objectively account for an individual patient's metabolic state.

Model-based methods can deliver control that is patient-specific and adaptive to handle highly dynamic patients. A physiological model of the glucose-insulin regulatory system is presented in this thesis, adapted from adult critical care. This model has three compartments for glucose utilisation, effective interstitial insulin and its transport, and insulin kinetics in blood plasma, with emphasis on clinical applicability. The predictive control for the model is driven by the patient-specific and time-varying insulin sensitivity parameter. A novel integral-based parameter identification enables fast and accurate real-time model adaptation to individual patients and patient condition.

Validation on retrospective clinical data demonstrated the model's ability to capture the major dynamics of the glucose-insulin system in the critically ill neonate. Model fit and prediction performance analysis resulted in a similar level of performance as adult intensive care models and thus suitable for model-based targeted control. Comparison of insulin sensitivity profiles with adult critical care patients highlighted the glycaemic control problem as one of managing inter- and intra-patient variability.

Stochastic models and time-series methods for forecasting future insulin sensitivity are presented in this thesis. These methods can deliver probability intervals to support clinical control interventions. The risk of adverse glycaemic outcomes given observed variability from cohort-specific and patient-specific forecasting methods can be quantified to inform clinical staff. Hypoglycaemia can thus be further avoided with the probability interval guided intervention assessments.

Simulation studies of clinical control trials on 'virtual patients' derived from retrospective clinical data provided a framework to optimise control protocol design *in-silico*. Comparisons with retrospective control showed substantial improvements in glycaemia within the target 4 - 7 mmol/L range by optimising the infusions of insulin. The simulation environment allowed experimentation with controller parameters to arrive at a protocol that operates within the constraints imposed by the clinically fragile state of the preterm infant.

The resulting control system was piloted in seven 12-24 hour clinical trials at the Christchurch Women's Neonatal Department. Glucose levels were tightly controlled in all cases over a trial cohort that represented a wide range of patient conditions and severity of illness. Model predictive performance agreed with simulation results and the stochastic model forecast bounds maintained patient safety.

Overall, the research presented takes model-based neonatal glycaemic control from concept to proof-of-concept clinical pilot trials. The thesis develops the full range of models, tools and methods to optimise the protocol design and problem solution. This research thus provides a template for model-based glycaemic control development in general that could be extended to other glycaemic control and similar problems.

Chapter 1

Introduction

The survival of infants born before the full course of natural gestation is one of *the* primary concerns of the neonatal intensive care unit (NICU). Preterm infants represent a large, and growing, proportion of the neonatal critical care population. Hyperglycaemia, an excess of glucose in the bloodstream, is a common complication of prematurity, and may be caused by a number of factors related to immaturity of the glucose regulatory system and stress of critical care.

The etiology of hyperglycaemia shares some commonality with the well-researched adult critical care case. However, preterm neonates present a unique state of human development and exhibit significant differing physiologies. Thus, there is no simple translation of many treatments from the adult to the neonatal case, even if the therapeutics, insulin and all forms of nutrition, are similar.

Insulin is a potent metabolic hormone that regulates many aspects of endogenous glucose production and disposal. Tight blood glucose control methods employing infusions of insulin are gaining popularity amongst neonatal clinicians. However, great inter-patient heterogeneity is the hallmark of neonatal metabolism, making designing insulin protocols difficult. Model-based methods can capture the metabolic state of the infant in real-time and adapt control for optimal insulin dosing. These methods have the potential to make tight blood glucose control a clinical reality for improved outcomes amongst preterm infants in critical care.

This chapter will introduce the problem of blood glucose control in the context of neonatal intensive care. The control of hyperglycaemia is a well-researched area of adult critical care, where tight control has resulted in improved outcomes.

A growing body of evidence suggests control of blood glucose may improve neonatal outcomes as a parallel to the adult case. Adaptive, model-based control is introduced as a solution to account for the differing physiologies of the neonate versus the adult. Therefore, the primary goal of this research is to introduce model-based control methods to neonatal intensive care to elicit the improved outcomes that might be obtained by the provision of patient-specific tight control of blood glucose levels.

1.1 Preterm neonates

Preterm neonates are commonly classified by two criteria: gestational age at birth, and birth weight. Some correlation exists between the categories of birth weight and gestational age. Typical categories for birth weight are:

- Low birth weight (LBW): $<$ 2,500 g
- Very low birth weight (VLBW): $<$ 1,500 g
- Extremely low birth weight (ELBW): $<$ 1,000 g

Typical definitions of prematurity at birth are:

- Preterm: $<$ 36 completed weeks gestation
- Very preterm: $<$ 31 completed weeks gestation
- Extremely preterm: $<$ 27 completed weeks gestation

Due to increasing survival and prolonged hospital stay, extremely low birth weight (ELBW) infants now represent most of the patient days in the neonatal intensive care nursery [Farrag and Cowett, 2000].

Over the past 20-30 years the incidence of preterm birth in most developed countries has been about 5-10% of live births [Tucker and McGuire, 2004; Lumley, 2003]. The incidence in the United States is higher, at about 12% [Tucker and

McGuire, 2004]. Some evidence shows that this incidence has increased slightly in the past few years, but the rate of birth before 32 weeks' gestation is almost unchanged, at 1-2% [Tucker and McGuire, 2004; Darlow et al., 2003; Graafmans et al., 2001].

Most preterm births follow spontaneous, unexplained preterm labour, or spontaneous preterm pre-labour rupture of the amniotic membranes. The most important predictors of spontaneous preterm delivery are a history of preterm birth and poor socioeconomic background of the mother [Lumley, 2003; Tucker and McGuire, 2004]. About one quarter of preterm births occur in multiple pregnancies. Half of all twins and most triplets are born preterm [Tucker and McGuire, 2004; Kiely, 1998]. The incidence of multiple pregnancies in developed countries has increased over the past 20-30 years [Tucker and McGuire, 2004]. This rise is mainly because of the increased use of assisted reproduction techniques, such as drugs that induce ovulation and in vitro fertilisation [Lumley, 2003].

The rate of preterm birth varies between ethnic groups. In the United Kingdom, and even more markedly in the United States, the incidence of preterm birth in women of African descent is higher than that in Caucasian women of similar age [Demissie et al., 2001; Kiely, 1998]. The reason for this variation is unclear because differences remain after taking into account socioeconomic risk factors [Tucker and McGuire, 2004]. In New Zealand, Maori are over-represented in preterm births compared to NZ Europeans [Mantell et al., 2004].

Broadly, outcomes improve with increasing gestational age, although for any given length of gestation survival varies with birth weight. The outcomes for preterm infants born at or after 32 weeks of gestation are similar to those for term infants. Additionally, advancements in the care of very-low-birth-weight ($<$ 1,500g) infants have resulted in increased survival [Richardson et al., 1998; Darlow et al., 2003]. However, mortality rates are as high as 20% in those born less than 1kg [Beardsall et al., 2007b]. Most serious problems associated with preterm birth occur in the 1% to 2% of infants who are born before 32 completed weeks gestation, and particularly the 0.4% of infants born before 28 weeks gestation [Tucker and McGuire, 2004].

1.2 Significance of hyperglycaemia in preterm neonates

Clinically, in adults, hyperglycaemia can be a marker of severity of illness and is directly associated with mortality. In addition, it is also associated with increases in other negative clinical outcomes, including severe infection [Bistrian, 2001], sepsis and septic shock [Das, 2003; Branco et al., 2005; Oddo et al., 2004; Marik and Raghavan, 2004], myocardial infarction [Capes et al., 2000], and polyneuropathy and multiple-organ failure [Van den Berghe et al., 2001; Langouche et al., 2005]. In each of these cases or patient subgroups, lower blood glucose levels were associated with reduced mortality and/or complications. Similar studies have associated early hyperglycaemia (in a patient stay) with mortality in trauma patients [Laird et al., 2004; Jeremitsky et al., 2005; Holm et al., 2004]. Finally, there is also evidence of significant reductions in the need for dialysis, bacteremia testing and the number of blood transfusions with aggressive blood glucose control using intensive insulin therapy [Van den Berghe et al., 2001, 2003; Krinsley, 2003b]. All of these results point towards the conclusion that the control of blood glucose levels in adult critical care has a significant clinical impact.

Currently, the exact reasons for the reductions in mortality and other clinical outcomes in these adult cases are not fully known, but have been extensively analysed in these original and other works [Bellomo and Egi, 2005; Diringer, 2005; Finney et al., 2003; Krinsley, 2003a; Langouche et al., 2005; Mesotten et al., 2004; Van den Berghe, 2004b,a; Van den Berghe et al., 2005]. However, recent studies by Weekers et al. [2003] on a rabbit model do indicate some major causes. Specifically, tight glycaemic control reduces glucotoxicity due to high blood glucose, which in turn:

1. Reduces oxidative stress and superoxides.
2. Reduces stress hormone responses.
3. Reduces damage to the endothelium and vascular walls [Langouche et al., 2005].
4. Increases immune response and bacteriocidal activity.

These results have been supported by a variety of recent, closely related studies [Soop et al., 2002; Hansen et al., 2003; Jeschke et al., 2004; Butler et al., 2005;

Table 1.1: Associations between hyperglycaemia and worsened outcomes in neonates.

Investigators	Outcomes
[Heimann et al., 2007]	Mortality increased in subjects with median BG $\geq$ 8.3 mmol/L and gestational age $<$ 27 weeks.
[Alaedeen et al., 2006]	Hyperglycaemia correlated with prolonged ventilator dependence and increased hospital stay in preterm septic infants. Average maximum serum glucose level significantly higher in non-surviving infants (13.4 mmol/L vs 7.8 mmol/L). Increased odds of death and sepsis in infants with early severe (OR: 5.07, 95% CI: 1.06 - 24.3) and persistent severe hyperglycaemia (OR: 6.26, 95% CI: 0.73 - 54.0) over 201 patients.
[Hall et al., 2004]	Higher mortality for infants with maximum BG $>$ 11.9 mmol/L compared with maximum BG $<$ 11.9 mmol/L, and late mortality ($>$ 10 days from admission) significantly higher (29% vs 2%) Maximum BG significantly related to length of stay.
[Hays et al., 2006]	BG significantly associated with early death and severe intra-ventricular haemorrhage. Longer periods of hyperglycaemia during first week of life associated with longer hospital stay.
[Ertl et al., 2006]	Hyperglycaemia was an independent risk factor in development of retinopathy of prematurity.
[Garg et al., 2003]	Increased risk of retinopathy of prematurity for each 0.56 mmol/L increase in mean glucose level (OR: 2.7, 95% CI: 1.003-7.27)

Dandona et al., 2006; Gubern et al., 2006]. All of these studies examine aspects of systemic inflammation that is common in critical illness, immune response, and the resulting impact or damage at a cellular level.

An increasing body of recent literature links hyperglycaemia in preterm neonates to worsened outcomes, including an increased risk of further complications, such as sepsis, increased ventilator dependence, retinopathy of prematurity, hospital length of stay and mortality [Ertl et al., 2006; Garg et al., 2003; Hays et al.,

2006; Kao et al., 2006; Hall et al., 2004; Alaedeen et al., 2006; Heimann et al., 2007]. Hyperglycaemia may also cause an osmotic diuresis and intra-ventricular hemorrhaging [Hemachandra and Cowett, 1999; Ditzenberger et al., 1999]. High rates of proteolysis are also common in low birth weight infants, reducing muscle mass and inhibiting growth [Agus et al., 2006, 2004]. Specific studies are summarised in Table 1.1.

The incidence of hyperglycaemia is 45% to 80% in infants $< 1{,}500$ grams, with increased incidence associated with lower birth weight [Dweck and Cassady, 1974; Heimann et al., 2007]. Persistent hyperglycaemia has been observed in 20% to 50% of extremely low birth weight infants, even in patients with no family history of diabetes [Hays et al., 2006]. Hyperglycaemia commonly occurs in infants if the glucose load exceeds 12 grams/kg/day [Pildes and Pyati, 1986].

Despite the stature of hyperglycaemia as a widely recognised perturbation of metabolic homeostasis, a universally accepted operational definition of hyperglycaemia in very preterm infants is lacking [Hey, 2005]. Glucose control targets exhibit significant variation between clinics, as shown in Figure 1.1 [Alsweiler et al., 2007], and between reports of glucose control, which hampers comparisons between studies. A blood glucose concentration < 2.6 mmol/L can increase the risk of long term neurological deficiencies [Lucas et al., 1988], and is often cited as a limit for hypoglycaemia [Cornblath et al., 2000]. However, the precise upper limit for clinically desirable blood glucose concentration is still under debate [Cowett and Farrag, 2004; Alsweiler et al., 2007]. For this study the range of 4 - 7 mmol/L, as used in several adult studies, was considered the target range for normal glucose levels.

Thus, hyperglycaemia is a common problem in both adult and neonatal intensive care. The control of blood glucose has resulted in improved outcomes for adult patients. Neonatal hyperglycaemia is prevalent amongst the youngest patients and has been linked to deleterious effects in a similar pattern to adults, indicating tight blood glucose control may be beneficial for this vulnerable cohort.

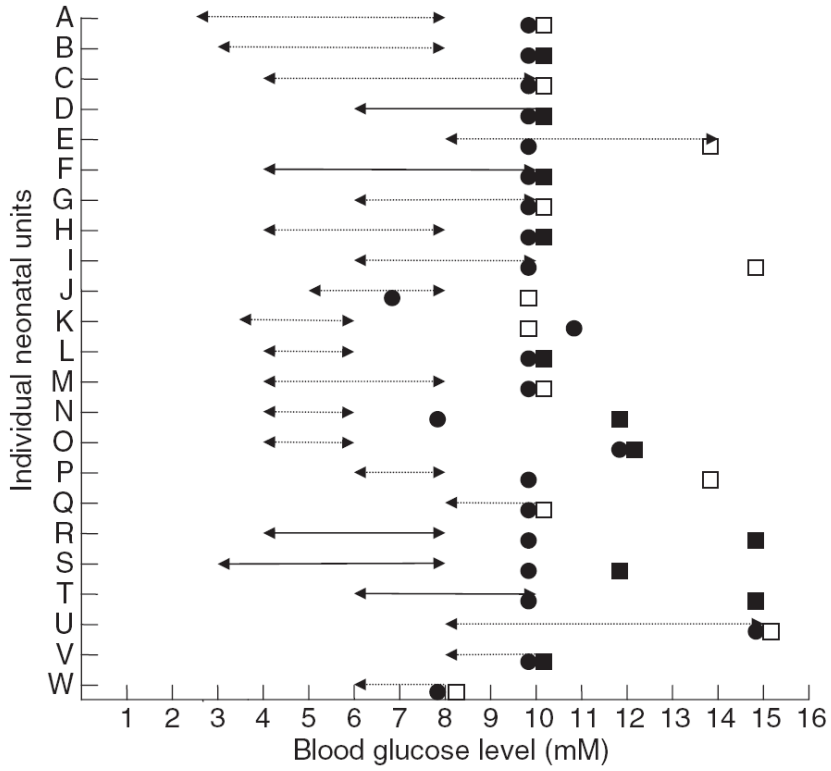

Figure 1.1: Definition of hyperglycaemia, criteria for starting insulin and blood glucose level target range for neonatal units in Australasia. Circles indicate definition of hyperglycaemia. Squares indicate threshold for commencing insulin infusions (filled squares include glycosuria in the criteria for starting insulin). Arrows represent target BG range. Blood glucose level expressed in mmol/L. Adapted from [Alsweiler et al., 2007].

1.3 Pathogenesis of hyperglycaemia

Hyperglycaemia in very sick patients is most likely an effect of stress and thus increased levels of catecholamines, which are known to stimulate glucose metabolism [Guyton and Hall, 2000; Vander et al., 2001]. In this regard, very premature infants are not different from older, critically ill patients. However, the glucose intolerance observed in otherwise healthy, premature infants receiving glucose infusions at rates exceeding their normal glucose turnover rate is specifically related to their immaturity. Conditions associated with hyperglycaemia in the neonate are summarised in Table 1.2.

Table 1.2: Conditions associated with hyperglycaemia in the neonate. Adapted from [Farrag and Cowett, 2000].

Origin	Condition or disease
Immature hepatic and pancreatic response to change in glucose concentrations	Very low birth weight and extreme prematurity
Elevated circulating levels of cortisol, glucagon and catecholamines	Stress, surgery, severe systemic illness (eg: respiratory distress, cardiac failure, sepsis, necrotising enterocolitis)
Drug related	Dexamethasone, methylxanthines (eg: theophylline), dopamine and administration of glucose at excessive rates
Reduction of glucose use	Administration of intravenous fat emulsion with/without amino acids

In the preterm infant, continuous glucose infusion is always required to maintain homeostasis and prevent hypoglycaemia. The conundrum is that many neonates develop hyperglycaemia during glucose infusion [Dweck and Cassady, 1974; Pildes and Pyati, 1986]. Hyperglycaemia is associated with many treatments that are presently considered standard care for the so-called micropremie, including administration of total parenteral nutrition and the use of dexamethasone for the treatment of bronchopulmonary dysplasia. Nutritional support regimes with high carbohydrate content are also provided to increase neonate weight, but often compound the counter-regulatory response [Alaedeen et al., 2006]. Additionally, lipids and lipid components in nutritional inputs, particularly free fatty acids, can also promote hyperglycaemia [Hemachandra and Cowett, 1999].

It has been shown that preterm infants can mount a hormonal response to stress similar to older critically ill patients [Barker and Rutter, 1996]. Sources of stress for these infants include respiratory distress, surgery and recurrent invasive procedures. Increased secretion of counter-regulatory hormones leads to a prominent rise in endogenously produced glucose and the rate of hepatic gluconeogenesis, as well as a reduction in insulin sensitivity [McCowen et al., 2001]. Inhibiting the physiological response to increased glycaemic levels are factors such as increased insulin resistance, absolute or relative insulin deficiency, and

drug therapy [Thabet et al., 2003; Hemachandra and Cowett, 1999; Goldman and Hirata, 1980; Farrag and Cowett, 2000].

The pathogenesis of stress-induced hyperglycaemia between critically ill adults and VLBW infants may differ. In particular, the development of hyperglycaemia in the neonate is unique in that several pathophysiologies are directly related to the immaturity of the glucose regulatory system:

Hepatic unresponsiveness to glucose infusions: The hepatic glucose production response to parenteral glucose infusion or increased glucose concentration is attenuated [Cowett et al., 1983].

Insulin resistance: Preterm infants require higher insulin levels than term infants to maintain euglycaemia [Mitanchez-Mokhtari et al., 2004], and peripheral glucose uptake is only increased with the exogenous delivery of insulin to 6-10x basal concentrations [Farrag and Cowett, 2000].

Impaired pancreatic β-cell secretion: The β-cells of hyperglycaemic preterm infants secrete increased amounts of pro-insulin, which is up to 10 - 16 times less active than regular insulin [Mitanchez-Mokhtari et al., 2004].

Immaturity of glucose transport system: The expression of glucose transporters (GLUT), which facilitate the movement of glucose across membranes of specific tissues, is dependent on maturation. The limited expression of GLUT-2 in the hepatocyte may explain the inability of the preterm neonate to suppress hepatic glucose production, and may explain the decreased sensitivity of the preterm pancreas to increased glucose concentrations [Raney et al., 2008]. The expression of insulin-sensitive GLUT-4 is limited in fetal tissues, increasing after birth to reach adult levels later on in life [Farrag and Cowett, 2000].

Limited number of insulin-dependent tissues: Very low birth weights infants have little skeletal muscle and adipose tissue and therefore have decreased peripheral glucose uptake [Raney et al., 2008].

Thus, hyperglycaemia as a response to the stress of critical illness is an origin of altered metabolic state common to both adults and neonates. Glucose intolerance in the neonate may also be due, at least in part, to immaturity, which adds a new dimension to this control problem.

Table 1.3: Principal actions of insulin [Ditzenberger et al., 1999].

Time category	Actions
Immediate: seconds	Increased transport of glucose, amino acids and potassium into insulin sensitive cells
Intermediate: minutes	Stimulates protein synthesis, inhibits protein degradation and activates enzymes necessary for glucose synthesis
Delayed: hours	Increases mRNA for lipogenic activities

1.3.1 The glucose-insulin regulatory system

After food is consumed, the body reduces the complex carbohydrate and sugar molecules to the simple six-carbon sugar known as glucose. Glucose is the body's fuel, and upon the reduction by the body, it is either utilised or stored. Sensing glucose in the bloodstream leads the β-cells in the pancreas to produce insulin. The concentration of insulin acts as the body's signal as to how to manage its storage and transportation needs, and thus determines the utilisation rate of the glucose.

Insulin is a small protein, which consists of 51 amino acids in two closely connected chains. Insulin molecules and their connecting fragments are then packed together in small granules in the β-cells, which are secreted through the islets of Langerhans in the pancreas. Along with β-cells, the 1 to 2 million islets of Langerhans contain α and δ cells which secrete glucagons and somatostatin respectively, which act as additional blood glucose regulatory hormones. The α, β and δ cells are approximately 25%, 60% and 10% of the total islets and are all very closely related [Guyton and Hall, 2000; Joslin, 1985].

The level of insulin in the bloodstream is the signal that facilitates the metabolic response to produce the desired effects, which are summarised in Table 1.3. A high insulin level promotes storage of glucose, and a low insulin level signals the need for the release of glucose fuels, currently in storage, back into the blood stream. A meal results in an increase of insulin concentration in the blood, due to the increased secretion of insulin by the β-cells, and signals the liver and muscles to consume the extra fuel (glucose) available. The liver stores glucose

as glycogen or fat, and the muscles utilise glucose primarily to repair damaged muscle cells, for energy storage as glycogen and lastly storage in the fat cells.

Counter regulatory hormones, such as glucagon and adrenaline, signal the liver to release glucose. Too much glucose removal from the blood-stream can result in dangerously low blood glucose levels. When the glucose available is not sufficient to supply the brain's requirements, hypoglycaemic symptoms include hunger, anxiousness, restlessness, agitation, perspiration, tachycardia (racing pulse) and palpitation (irregular and/or forced heart-beats). These symptoms are partly a result of the release of adrenaline by the body as a counter regulatory measure to restore normal blood glucose levels, as shown by Figure 1.2. When there is a deficit in the amount of insulin released, the signal is not available to the body to indicate it should remove glucose from the blood stream. The blood glucose level therefore rises and remains higher than the body's natural basal glucose level for an extended period, resulting in hyperglycaemia.

In the body's fasting state the organs must be supplied fuel (glucose) from the reserves in storage in the liver to retain function. The need for glucose reserves is indicated by a low insulin concentration in the blood. The brain is the body's priority for supply and continuously requires glucose. If the glucose is not available to supply all major organs, the energy requirement of the brain is still met by the liver's stored glycogen reserves. Neonates typically possess limited endogenous glycogen reserves, and it has been demonstrated that ketones provide a substantial proportion of the brain's energy requirements [Avery et al., 1994]. These dynamics are shown in Figure 1.3.

Insulin is an anabolic hormone and promotes growth, while lowering glucose levels [Vander et al., 2001]. However, endogenous deficiency or lack of effect due to high insulin resistance will have a negative impact on glycaemic levels [Thabet et al., 2003]. Additionally, studies have shown reduced proteolysis, and thus preservation of muscle mass associated with insulin therapy in neonates [Agus et al., 2006, 2004], independent of glucose infusion [Hertz et al., 1993]. Insulin also increases the activity of other enzymes, primarily those involved in glycogen, lipid and protein synthesis, and inhibits the activity of those that catalyse glucose degradation.

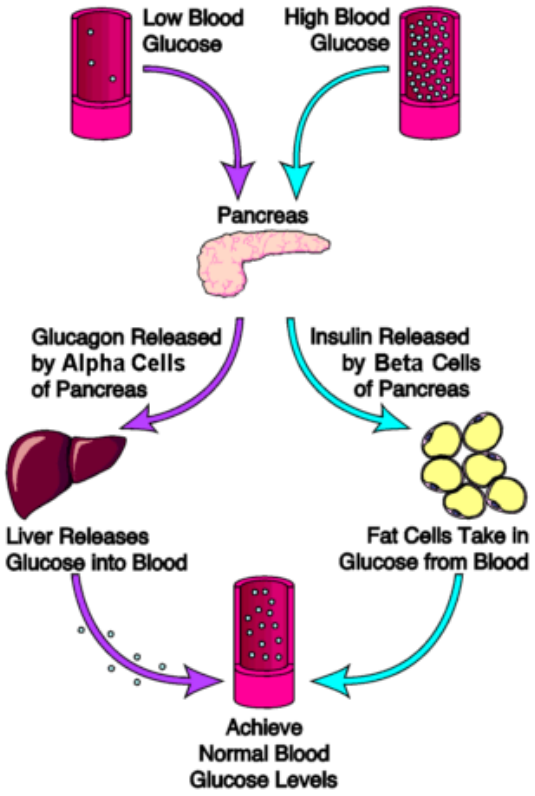

Figure 1.2: Effect of high and low blood glucose levels on the body. Adapted from endocrineweb.com.

1.4 Glucose control

Clinical interventions to control blood glucose levels typically focus on modulating two common exogenous inputs into this metabolic system: glucose and insulin. Hardware for implementing glucose control via modulating insulin and nutrition inputs is well developed and part of standard critical care equipment. Blood glucose sensors are widely available in a range of configurations from discrete and continuous point-of-care devices to laboratory-grade measurement systems [Chase et al., 2006a]. Thus, the success of a glucose control system depends upon disseminating the available clinical information into effective recommendations to direct glucose and insulin infusions.

Two landmark studies controlling blood glucose by modulating only the insulin input have shown the impact of tight control on mortality and other clinical outcomes in adults. First, van den Berghe and colleagues [2001; 2003] showed that tight blood glucose control to less than 6.1 mmol/L reduced cardiac surgical ICU patient mortality by up to 45% in a randomised controlled trial. Krins-

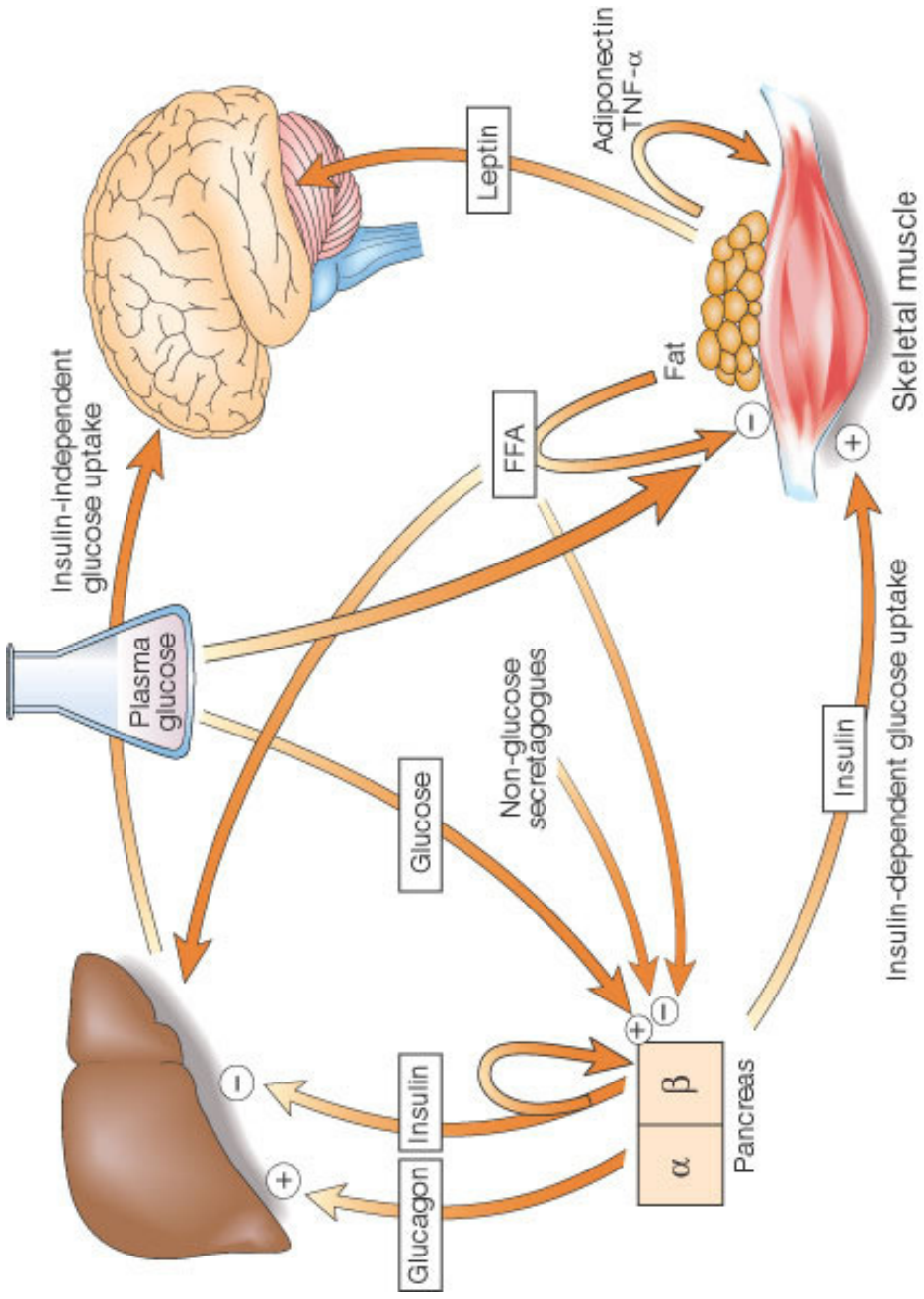

Figure 1.3: Major organs in the insulin-glucose dynamics system. Adapted from [Saltiel and Kahn, 2001].

ley and colleagues [2003b; 2004] reported a 17-29% total reduction in mortality over a wider, more critically ill, ICU population with a higher glucose limit of 7.75 mmol/L. However, this study was a comparison to a matched cohort of retrospective data with enough patients to show statistical significance for the intervention.

The SPRINT protocol [Chase et al., 2008b; Lonergan et al., 2006b,a] modulated both the insulin and nutrition inputs using a paper protocol that emulated model-based control. A 26%-35% reduction in hospital mortality for adult ICU patients compared to matched retrospective data was observed following the introduction of the protocol as a clinical practice change. Insulin effect saturation in adults often limits the gains that can be achieved through insulin-only protocols. Hence, the addition of nutrition modulation provides a non-saturable pathway to gain and maintain tight glucose control.

There is currently no best-practice method available for neonates. Hyperglycaemic infants are often treated by glucose restriction [Hemachandra and Cowett, 1999; Thabet et al., 2003; Farrag and Cowett, 2000]. However, prolonged severe glucose restriction may adversely affect the infant's nutritional status and may also be a reason for poor growth observed in these infants [Thabet et al., 2003]. The rate of fetal growth varies throughout gestation, increasing from 5 grams/day at the end of the first trimester to 30-35 grams/day at 32-34 weeks gestation [Zylberberg and Pepper, 2001].

Limited trials of glucose control using only insulin to control glucose in neonates have been reported [Meetze et al., 1998; Collins et al., 1991; Binder et al., 1989; Ostertag et al., 1986; Vaucher et al., 1982; Beardsall et al., 2007a, 2008; Vlasselaers et al., 2009; Kanarek et al., 1991; Thabet et al., 2003; Ng et al., 2005]. Positive outcomes of improved glycaemic control, glucose tolerance and growth have been reported [Binder et al., 1989; Collins et al., 1991; Kanarek et al., 1991; Thabet et al., 2003; Ostertag et al., 1986; Meetze et al., 1998; Vaucher et al., 1982]. Reduced proteolysis in response to insulin infusions has also been demonstrated in neonates [Poindexter et al., 1998; Agus et al., 2006, 2004]. However, most studies are limited by small study cohorts.

In particular, [Vlasselaers et al., 2009] used a relatively low target band of 2.6 - 4.4 mmol/L for preterm infants in their study that included older children,

and reported overall positive outcomes. However, these low glucose target levels were subject to debate [Fendler and Mlynarski, 2009; Van den Berghe et al., 2009]. The NIRTURE study [Beardsall et al., 2008] was a large, multi-centre randomised controlled trial that recruited 389 patients from 8 neonatal units. The goal of the study was to provide insulin replacement therapy to prevent catabolism, as opposed to directly combat hyperglycaemia. Thus, insulin, together with supplementary glucose, was infused into patients with and without hyperglycaemia, using a fixed weight-based protocol [Beardsall et al., 2007b]. The study was discontinued early due to concerns over excessive hypoglycaemia, which overshadowed the improved glucose tolerance and weight profile results. This latter result for the NIRTURE trial also highlights the requirement for glucose control protocols to account for the significant variations in patient condition, drug therapies and tolerance to glucose and insulin.

Fixed protocols do not account for inter-patient variation, and ad-hoc protocols that rely on clinician judgement increase clinician workload and the potential for variation due to subjective reasoning [Chase et al., 2006a, 2008a]. Model based methods allow information about the metabolic state of the patient, and infant in this case, to be inferred from serial blood glucose measurements and records of nutrition and insulin administration [Chase et al., 2007, 2006a; Hann et al., 2005]. Therefore, a model capturing the fundamental dynamics of the neonatal glucose regulatory system could be used to develop methods to better control blood glucose levels in this cohort, while also enhancing nutritional support and improving outcomes.

Thus, the current state of glucose control therapies in current clinical practice is that tight blood glucose control has been employed in adult intensive care via insulin and/or nutrition modulation with positive outcomes. Glucose restriction is a common treatment for hyperglycaemia in the neonate, but can result in negative growth outcomes [Mena et al., 2001]. All reported insulin infusion trials in neonates have used either fixed protocols or clinician judgment to determine insulin infusion rates. Hence, there is currently no standard protocol that accounts for specific patient sensitivity to glucose and insulin, and thus no protocol that is adaptive to patient-specific variability.

1.5 Model-based glycaemic control

Currently, most typical practice in intensive care glycaemic management using insulin for both adults and neonates is comprised of ad-hoc protocols based primarily on experience, where intravenous insulin is titrated against glucose measurements variably taken every 1–4 hours. When combined with the unpredictable and sudden metabolic changes that characterise this aspect of critical illness and/or clinical changes in nutritional support, this approach results in highly variable blood glucose levels. The overall result is sustained periods of hyper- or hypo- glycaemia, characterised by oscillations between these states. The situation is exacerbated by exogenous nutritional support regimes with high dextrose content. Hence, there is an emerging, strong need for the more rigorous analysis and methods that model-based control methods bring to this type of problem.

A physiological model that captures the glucose-insulin system dynamics is thus the basis for more optimally addressing the glycaemic control problem. Metabolic modelling of the glucose-insulin system has a very deep history in the published literature. The vast majority of these models have their roots in basic compartment modelling with differential equations [Carson and Cobelli, 2001]. To date, the primary use of metabolic models has been the development of model-based measures to assess metabolic parameters, with a particular focus on measuring insulin sensitivity [e.g. Bergman et al., 1979, 1981, 1985; Pacini and Bergman, 1986; Yang et al., 1987; Mari, 1998; Mari et al., 2001, 2003; Lotz et al., 2006, 2008; Toffolo et al., 1999, 2006].

However, a model for glycaemic control in intensive care needs to be applicable for real-time clinical control, addressing the needs and limitations typical of most ICUs. Metabolic models that are complex in physiological details, although accurate given rigorous laboratory data, are not often practical for real-time glycaemic control utilising less frequent and noisier blood glucose measurements. These issues will be explored with examples in Chapter 2. Therefore, a model suitable for glycaemic control in any type of intensive care setting needs to satisfy the following basic criteria:

- Accurately capture insulin and glucose pharmacokinetics and pharmacodynamics typical of critically ill patients.

- Feature a simple structure preferably requiring only blood glucose levels as physiological feedback.
- Address inter- and intra-patient variability over time.
- Have rapidly identifiable patient specific model parameters.

Given an accurate model satisfying these criteria, model-based glycaemic control can offer individualised control adaptable to the critically ill patient's highly dynamic physiological condition. Furthermore, such a physiological model may also be used as a patient simulator for protocol development given realistic patient specific parameters [Hann et al., 2005; Wong et al., 2006a; Lonergan et al., 2006b,a; Chase et al., 2007]. Additional knowledge of the critically ill population's variable dynamics can further enhance model-based control with more accurate predictive performance.

1.6 Control performance measures

Understanding the difficulties and defining desired controller performance is the first step to controller design. A variety of performance metrics have been used in different critical care glycaemic studies, with their differences often confounding direct comparisons between studies. These metrics can be summarised as four basic goals:

Mean blood glucose level: calculated over all measurements [Krinsley, 2004] or over limited measurements, such as first morning measurement [Van den Berghe et al., 2001, 2003]. The average is the simplest performance measure and the one used in both landmark clinical studies. However, it provides no further information on glucose excursions or tightness of control. An important consideration is the use of a trapezoidal mean to obtain the proper mean value if the sampling period is particularly irregular [Doran, 2004; Shaw et al., 2005]. In addition, an average value should utilise all blood glucose measurements and not just a morning average, as in Van den Berghe et al. [2001, 2006], which can hide variability and poor control.

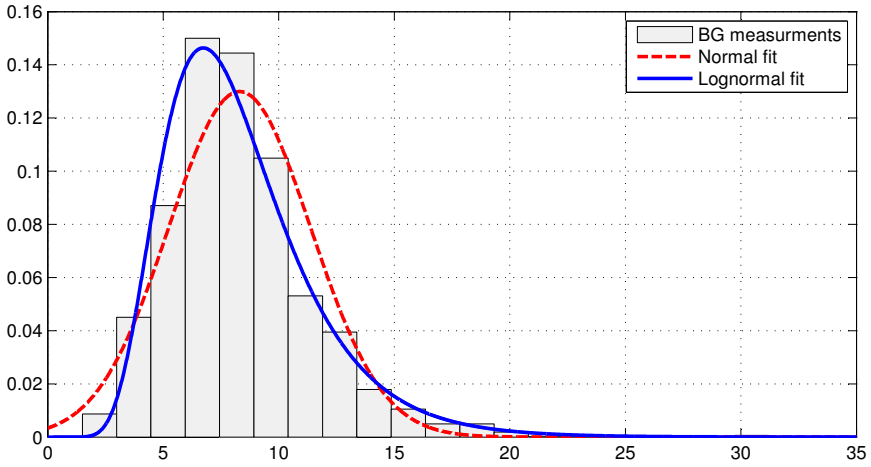

Figure 1.4: Comparison of normal and lognormal distributions fitted to a sample of 1,091 BG measurements from neonatal intensive care. The fitted lognormal distribution more accurately represents the underlying BG measurement distribution, compared to the symmetrical normal distribution.

Distribution of blood glucose level: Most studies report an average glycaemic level and standard deviation, assuming blood glucose measurements are normally distributed. As a negative blood glucose concentration is physically impossible, a log-normal distribution provides a more accurate representation of the underlying spread of measurements. Figure 1.4 provides an example of a typical distribution of BG measurements, and a comparison of fitted normal and lognormal probability density functions. Finally, empirical cumulative distribution functions provide a framework to display all measurements and allow interpretation of results for any desired glycaemic band.

Time in a glycaemic band: calculated as the time or percentage of measurements in a specific band, such as 4–6.1 mmol/L [Lonergan et al., 2006b; Wong et al., 2006a,b] or 4.5–6.1 mmol/L [Plank et al., 2006]. Maximising this metric is essentially equivalent to minimising the Hyperglycaemic Index (HGI) or area under the blood glucose level curve [Van den Berghe, 2004b; Vogelzang et al., 2004]. This metric provides a surrogate measure of the average value, as well as an indication of the tightness of the glycaemic control result. Using multiple overlapping or contiguous bands provides a good definition of the total glucose distribution under control.

Glucose variability: measured as the standard deviation or 90% interval over

the data. This metric has only been employed recently [Chase et al., 2005a; McDonnell et al., 2005] and measures the tightness of blood glucose control around the average or target value. It is also increasingly important in managing Type 1 diabetes [Kovatchev et al., 2004, 2005; Hirsch and Brownlee, 2005]. However, it provides no indication of the absolute glycaemic levels obtained and some methods assume normal or other statistical distributions that may not match the data. Hence, confidence intervals determined from the data may prove more useful. Note that recent studies indicate the variability in control may be a critical determinant of outcome [Chase et al., 2006b].

Hypoglycaemic episodes: measured as the number or percentage of measurements that are below a defined hypoglycaemic threshold. The typical definition is 2.2 mmol/L, although some studies use higher thresholds [Lonergan et al., 2006b; Plank et al., 2006]. Variability also captures some of this information when associated with the average or median glucose values. More importantly, this measure is a critical indicator of the safety of the control methods used.

Finally, clinical end-points such as mortality are a patient-specific outcome and tied to the control of glucose on a per-patient basis. Whole cohort results allow analysis of the full glycaemic control data set to assess outcomes such as hypoglycaemia, which has a typically low incidence rate but great clinical implications. Thus, each categorisation method provides a different insight into the data, and both are required to clearly describe the performance of a particular protocol [Goldberg et al., 2006].

1.7 Specific considerations for neonatal control

Blood glucose control for the neonate poses several challenges that differ from the adult critical care case. Absolute blood volumes in preterm infants are relatively small [Cassady, 1966; Leipala et al., 2003; Avery et al., 1994]. Thus, the number of blood glucose measurement must be optimised to a minimum useful number to conserve volume.

Endogenous energy supply stores are limited in preterm infants at birth as fat accretion does not occur until the 3rd trimester [Hume et al., 2005; Avery et al., 1994; Mena et al., 2001]. Thus, preterm infants must be constantly fed to provide enough energy for basal requirements in addition to growth [Hay et al., 1999]. In contrast, the adult can tolerate periods of reduced caloric intake. Tight glucose control may allow clinicians to more actively manage nutrition. The primary goal of premature infant nutrition is to achieve weight gain comparable to fetal growth without additional stress to immature metabolic and excretory functions [Ditzenberger et al., 1999]. Thus, it is desirable to administer adequate calories to facilitate growth, whilst maintaining glucose homeostasis. Overfeeding can lead to excessive oxidation demands for respiration, taxing the premature lung [Poindexter et al., 1998], and over-aggressive nutrition regimes may lead to obesity and insulin resistance in later life [Hay, 2006].

Many pharmacokinetic studies routinely performed in adults are technically and ethically difficult in the preterm neonate [Farrag and Cowett, 2000]. Thus, adapting known physiology from the adult case with available data for the neonate is important to develop a clinically sound model of the glucose-insulin regulatory system for the preterm neonate.

1.8 Preface

Preterm infants represent a significant proportion of the neonatal population. Hyperglycaemia is an altered state of metabolic homeostasis that commonly afflicts the youngest and sickest infants. A growing body of evidence links the degree of hyperglycaemia to increased morbidity and mortality, and reflects similar findings in the adult critical care case. Tight glucose regulation through insulin and/or nutrition modulation has shown positive outcomes in adults. However, such a level of tight control has not yet been achieved for the preterm neonate.

The pathophysiology of hyperglycaemia exhibits some marked differences in the neonate compared to the adult case, and the goals for tight control in neonates emphasise nutrition and growth outcomes in addition to the protective effects of insulin and normoglycaemia. Significant physiological differences means there is no simple translation of adult therapies to the unique neonatal case.

Model-based methods can identify patient-specific parameters in real-time and adapt control, and provide a pathway for clinically realistic glycaemic control systems that handle the great heterogeneity that is the hallmark of neonatal glucose metabolism. This thesis presents the adaptation of a validated glucose-insulin regulatory system model to the unique case of the neonate. Stochastic modelling of the insulin sensitivity parameter is used to forecast likely changes in condition to enhance safety against hypoglycaemia and manage intra-patient variability. Simulations performed on virtual patients are used to optimise protocol performance *in-silico*, and the system is piloted in a series of 24-hour clinical trials.

Chapter 2 reviews models of glucose and insulin pharmacokinetics that have been applied to control of glycaemia in critical care. A model that accounts for the unique physiology of the neonate is developed.

Chapter 3 presents the integral-based parameter identification method, and adapts model parameters based on available neonatal data.

Chapter 4 presents the validation of the neonatal glucose-insulin model on retrospective data, including assessments of model fit and prediction performance, and suitability for use in real-time clinical control.

Chapter 5 develops methods for insulin sensitivity variation forecasting. Stochastic and time-series analysis techniques are used to generate likelihood bands for future blood glucose concentration to improve control performance and add safety.

Chapter 6 presents simulated control trials on 'virtual patients' as a tool to optimise controller robustness and performance prior to any clinical implementation.

Chapter 7 presents the pilot trials of the model-based glucose control system in the Christchurch Women's Hospital Neonatal Department.

Chapters 8 and 9 summarise the key aspects of the thesis and present possible future improvements and applications for this research.

Chapter 2

Model development

2.1 Introduction

The dynamics of the human glucose-insulin system have been extensively studied. A number of researchers have created models with different levels of detail and complexity to suit different clinical or research applications. In particular, many models have been designed to provide model-based measures to assess metabolic parameters, with a particular focus on measuring insulin sensitivity [e.g. Bergman et al., 1979, 1981, 1985; Pacini and Bergman, 1986; Yang et al., 1987; Toffolo et al., 1999, 2006; Mari, 1998; Mari et al., 2001, 2003]. Several researchers have constructed control system models to dose insulin infusions for the control of blood sugar levels [Chase et al., 2006a; Deutsch et al., 2004]. Biomedical control system models can capture, as well as predict, patient behaviour. Such a model offers a safe and fast means for protocol development without the limitation of clinical data scarcity [Chase et al., 2007]. However, control system models must often work with clinically available data in real-time, which limits feasible model complexity and detail compared to models designed to illuminate human physiology in research settings [Chase et al., 2006a].

To date, no model has specifically accounted for the glucose-insulin dynamics of the preterm neonate. Whilst it has been shown that major metabolic markers and control systems are present from a very early age, significant physiological and hormonal differences imply existing control system models will require adaptation to provide a clinically acceptable level of performance. The clinically fragile nature of preterm neonates means that pharmacokinetic data from invasive tests is limited due to technical, clinical and ethical constraints. Thus, knowledge

gained from control system modelling in adults can guide model development in neonates.

This chapter examines several forms of existing metabolic control-relevant models that have been used in adult intensive care. A neonatal control system model is developed from this foundation that utilises available physiological data. To make this transition, several model parameters are adapted from the adult to the neonatal case based on clinical data.

2.2 Models in critical care

Intensive care represents a highly controlled environment where most glucose-insulin system inputs and outputs can be accounted for and thus modelled. However, the stress of critical illness can significantly disturb the glucose-insulin regulatory system from a healthy baseline [McCowen et al., 2001; Capes et al., 2000; Van den Berghe et al., 2001; Mizock, 2001; Thorell et al., 2004; Bloomgarden, 2003; Christensen, 2001; Coursin and Murray, 2003; Esposito et al., 2003; Finney et al., 2003; Umpierrez et al., 2002]. This situation is exacerbated by the myriad of medications administered to the critically ill, many of which exhibit highly patient-specific effects on glucose metabolism. Such detailed pharmacodynamic information may not be measurable in a typical clinical setting. Thus, any control system model must make a compromise between physiological validity, clinical applicability and mathematical identifiability, as shown schematically in Figure 2.1.

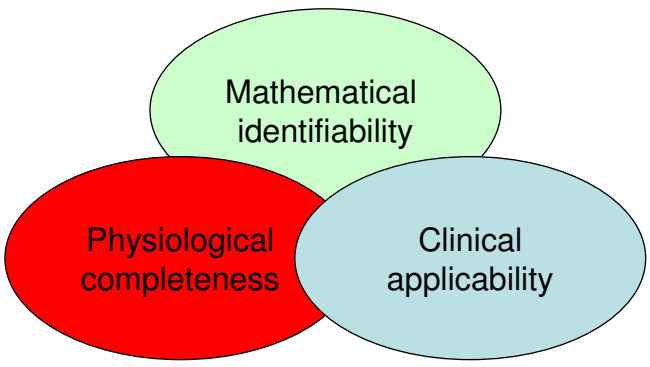

Figure 2.1: Competing requirements of modelling in a critical care environment

There have been several metabolic models used in clinical examination of critical care patients and glycaemic control [Wong et al., 2006a,b; Hovorka et al., 2004; Chee et al., 2003a,b; Plank et al., 2006], as reviewed in [Chase et al., 2006a]. Each model is substantially different, based in part on the modelling direction taken or clinical focus. A common theme, and benefit, is the ability to tailor insulin dosage to the current, inferred, patient condition. The first model is that of Chee and colleagues [2003a; 2003b] who used an optimised PID form of control.

$$\text{Insulin increment} = \begin{cases} 4\,\text{U/hr, if}\,\|\overline{W}_{zone}\| > 4.5 \\ 2\,\text{U/hr, if}\,3.6 \leq \|\overline{W}_{zone}\| \leq 4.5 \\ 1\,\text{U/hr, if}\,2.7 \leq \|\overline{W}_{zone}\| \leq 3.6 \\ 0\,\text{U/hr, if}\,\|\overline{W}_{zone}\| < 2.7 \end{cases} \tag{2.1}$$

where:

$$\left\|\overline{W}_{zone}\right\| = \frac{1}{\sum_{i=1}^{24} i}\left(\sum_{n=1}^{24} n.W_{zone}[n]\right) \tag{2.2}$$

$$\text{Bolus} = \begin{cases} 6\,\text{U/hr, if}\,\Delta y_{proj} \geq 2\,\text{mmol/L} \\ 4\,\text{U/hr, if}\,1 \leq \Delta y_{proj} < 2\,\text{mmol/L} \\ 0\,\text{U/hr, if}\,\Delta y_{proj} < 1\,\text{mmol/L} \end{cases} \tag{2.3}$$

$$\Delta y_{proj} = \left(\frac{\sum_{i=1}^{6} X_i Y_i}{\sum_{i=1}^{6} X_i^2}\right).\Delta x \tag{2.4}$$

$$X_i = x_i - \tilde{x} \text{ and } Y_i = y_i - \tilde{y} \tag{2.5}$$

$$\tilde{x} = \frac{x_{max} + x_{min}}{2} \text{ and } \tilde{y} = \frac{y_{max} + y_{min}}{2} \tag{2.6}$$

where:

Table 2.1: Sliding table with BG zone assignment. Adapted from [Chee et al., 2003b].

BG range (mmol/L)	Insulin dose (U/hr)	Assigned zone
> 20.0	4	6
15.1 - 20.0	3	5
12.1 - 15.0	2	4
10.1 - 12.0	2	3
8.1 - 10.0	1	2
6.1 - 8.0	1	1
0.0 - 6.0	0	0

x_{max} = maximum time value in the 30-min window
x_{min} = minimum time value in the 30-min window
y_{max} = maximum BG value in the 30-min window
y_{min} = minimum BG value in the 30-min window

The integral control (Equation 2.1) is implemented when sliding tables do not provide adequate glycaemic reduction and the amount of additional insulin is calculated using Equation 2.2, a normalized weighted average of the BG zones shown in Table 2.1 using a 2-hour triangular window. Derivative control is implemented using Equations 2.3-2.6. Expert control is implemented by keeping an active sliding table and 'offsetting' the recommended sliding table input according to several conditions, based on Equations 2.3-2.6, in order to determine the control input.

The ideal weighting values used in this form of control may be difficult to ascertain from physiological data, and thus would require re-tuning for each unique clinical population or individual patient. In particular, given the significant metabolic differences in the neonate compared to the adult critical care patient, any tuning would be based on current clinical judgement and/or require extensive testing. Additionally, as this model is designed from a control viewpoint, with little specific physiological dynamics, inferences of patient condition are not easily linked to known physiology in the same way a physiologically-based control model can.

The second model is that of Hovorka et al, which has been used in clinical practice to provide blood glucose control for patients with Type 1 diabetes [Hovorka et al., 2004] and, in similar form, for 48 hour trials on cardiac surgery

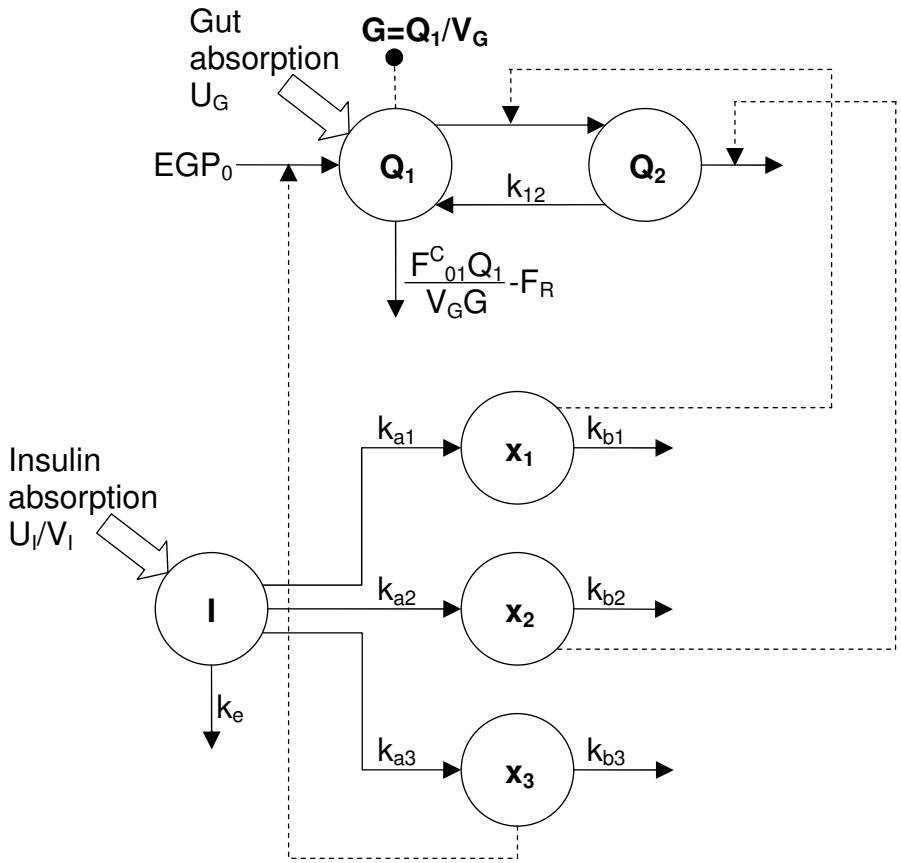

Figure 2.2: Compartmental model of glucose-insulin system (Adapted from [Hovorka et al., 2004])

patients with stress-induced hyperglycaemia [Hovorka et al., 2007; Plank et al., 2006]. The overall structure of the model is shown in Figure 2.2.

$$\begin{aligned}\dot{Q}_1(t) = &-\left[\frac{F^c_{01}}{V_G G(t)} + x_1(t)\right] Q_1(t) + k_{12} Q_2(t) \\ &-F_R + U_G(t) + EGP_0[1 - x_3(t)]\end{aligned} \tag{2.7}$$

$$\dot{Q}_2(t) = x_1(t) Q_1(t) - [k_{12} + x_2(t)] Q_2(t) \tag{2.8}$$

$$y(t) = G(t) = Q_1(t)/V_G \tag{2.9}$$

$$F_{01}^{c} = \begin{cases} F_{01} & \text{if } G \geq 4.5 \text{ mmol/L} \\ F_{01}G/4.5 & \text{otherwise} \end{cases} \tag{2.10}$$

$$F_R = \begin{cases} 0.003(G-9)V_G & \text{if } G \geq 9 \text{ mmol/L} \\ 0 & \text{otherwise} \end{cases} \tag{2.11}$$

$$U_G(t) = \frac{D_G A_G t \exp\left(-t/t_{max,G}\right)}{t_{max,G}^2} \tag{2.12}$$

$$\dot{S}_1(t) = u(t) - \frac{S_1(t)}{t_{max,I}} \tag{2.13}$$

$$\dot{S}_2(t) = \frac{S_1(t)}{t_{max,I}} + \frac{S_2(t)}{t_{max,I}} \tag{2.14}$$

$$\dot{I}(t) = \frac{U_I(t)}{V_I} - k_e I(t) \tag{2.15}$$

where:

$$U_I(t) = S_2(t)/t_{max,I} \tag{2.16}$$

$$\dot{x}_1(t) = -k_{a1}x_1(t) + k_{b1}I(t) \tag{2.17}$$

$$\dot{x}_2(t) = -k_{a2}x_2(t) + k_{b2}I(t) \tag{2.18}$$

$$\dot{x}_3(t) = -k_{a3}x_3(t) + k_{b3}I(t) \tag{2.19}$$

where Q_1 and Q_2 represent masses of glucose in the accessible and inaccessible compartments, k_{12} the transfer rate between the inaccessible and accessible compartments, V_G the distribution volume of the accessible compartment, y and G the measurable glucose concentration, and EGP_0 the endogenous glucose production extrapolated to zero insulin concentration. F_{01}^{c} is the total non-insulin-dependent glucose flux corrected for the ambient glucose concentration and F_R is the renal glucose clearance above the glucose threshold of 9 mmol/L. $U_G(t)$ is the

gut absorption rate, dependent upon the carbohydrates digested, D_G, carbohydrate bio-availability, A_G, and the time-of-maximum appearance rate of glucose in the accessible compartment, $t_{max,G}$. The insulin subsystem is described by Equations 2.13-2.15. S_1 and S_2 are a two-compartment chain for absorption of subcutaneously administered rapid-acting insulin, $u(t)$ the insulin input (bolus/infusion), and $t_{max,I}$ the time-to-maximum insulin absorption. $I(t)$ is the plasma insulin concentration, k_e is the fractional elimination rate and V_I the distribution volume. The insulin action subsystem consists of three components, endogenous glucose production, transport/distribution and disposal (x_1, x_2 and x_3). Finally, k_{ai} and k_{bi} $(i = 1, \ldots, 3)$ represent the activation and deactivation rate constants of insulin action respectively.

Overall, the model uses 9 population values or generic constants, and requires a further 6 patient specific parameters to be identified. Nonlinearity comes from insulin action on parameters of glucose production, glucose distribution/transport and glucose disposal, and difference in the activation/deactivation profile of the three insulin actions. As a result it requires a significant number of measurements to be identifiable for controlling a specific patient.

This model represents an approach aimed for the physiologically descriptive sector of the modelling space described in Figure 2.1. In particular, this model defines insulin sensitivity as a ratio of 'activation' and 'deactivation' rates for insulin in a remote, unmeasurable compartment: k_{bi} and k_{ai} $(i = 1, \ldots, 3)$ respectively. This relatively detailed physiological modelling allows the separation of insulin action into specific effects on disposal, transportation and suppression of endogenous glucose production. The separation of these effects allows measurement of their temporal variation to a challenge in insulin and/or glucose through double-labelled tracer studies, showing its original focus and use for physiological research [Hovorka et al., 2002].

The compartmental form of Equations 2.17-2.19 can capture 'delay' and 'memory' effects of insulin action on the relevant glucose uptake and metabolism pathways. The double-labelled tracer study is a relatively intensive study in terms of blood requirements. Thus, gathering such dense data may be technically difficult in the preterm neonate, which is the focus of this thesis.

Reported data has been collected from healthy, adult patients, and showed

substantial inter-subject variation [Hovorka et al., 2002]. It is expected in critical care that the relationship of insulin effects on metabolism may be different. In particular, varying levels of circulating counter-regulatory hormones typical of stress-induced hyperglycaemia may change rapidly with patient condition and enhance such inter-patient and intra-patient variability.

Finally, Chase and colleagues used a model loosely based on Bergman's minimal model [Bergman et al., 1987] with additional non-linear terms and a grouped term for insulin sensitivity [Chase et al., 2007; Wong et al., 2006b,a]. This model has been employed in several critical care glycaemic control trials using different control approaches, as well as in retrospective analyses [Lonergan et al., 2006b; Chase et al., 2007, 2008c, 2005c,b; Wong et al., 2005, 2006b,a].

$$\dot{G} = -p_G G - S_I(G + G_E)\frac{Q}{1 + \alpha_G Q} + P(t) \tag{2.20}$$

$$\dot{Q} = -kQ + kI \tag{2.21}$$

$$\dot{I} = -\frac{nI}{1 + \alpha_I I} + \frac{u_{ex}(t)}{V} \tag{2.22}$$

$$P(t_i < t < t_{i+1}) = \bar{P}_{i+1} + (P(t_i) - \bar{P}_{i+1})e^{-k_{pd}(t-t_i)} \text{where } \bar{P}_{i+1} < P(t_i) \tag{2.23}$$

$$P(t_i < t < t_{i+1}) = \bar{P}_{i+1} + (P(t_i) - \bar{P}_{i+1})e^{-k_{pr}(t-t_i)} \text{where } \bar{P}_{i+1} > P(t_i) \tag{2.24}$$

where $G(t)$ is the plasma glucose above an equilibrium level, G_E, and $I(t)$ is the plasma insulin resulting from exogenous insulin input, $u_{ex}(t)$. The effect of previously infused insulin being utilised over time is represented by $Q(t)$, with k accounting for the effective life of insulin in the system. Patient endogenous glucose clearance and insulin sensitivity are p_G and S_I, respectively. V is the insulin distribution volume and n is the constant first order decay rate for insulin from plasma. Total plasma glucose input is denoted $P(t)$. Michaelis-Menten functions are used to model saturation, with α_I used for the saturation of plasma insulin disappearance, and α_G for the saturation of insulin-dependent glucose

clearance [Hann et al., 2005; Chase et al., 2005c]. The parameters k_{pr} and k_{pd} relate to the effective half lives of glucose transport from gut to plasma for both increasing (k_{pr}) and decreasing (k_{pd}) feed rates respectively, and $\bar{P}_{i+1}$ are the steps in enteral glucose feed rates.

The final two equations account for glucose appearance from enteral nutrition via feeding tube as the glycaemic control studies using this model [Chase et al., 2005a; Wong et al., 2006a] modulate both insulin and nutrition inputs to reduce plasma glucose levels. This approach thus looks at both sides of the glucose balance, exogenous insulin removal of glucose and glucose appearance from exogenous nutrition, to reduce glycaemic levels in the face of insulin resistance and insulin saturation.

Modulating nutritional dextrose inputs also provides a physiologically non-saturable path to reduce plasma glucose, at least to the point of eliminating nutritional input entirely. It is important to note that this approach is focused on controlling the dextrose carbohydrate content exacerbating hyperglycaemia, rather than the overall nutritional profile. This last issue could be practically addressed, for example, by separating the dextrose and protein-fat nutritional inputs infused.

The model of Equations 2.20 - 2.24 has been extensively validated in long-term data fitting [Hann et al., 2005]. As noted, its clinical validity is well established in glycaemic control in ICU. In all these cases, the insulin sensitivity term S_I was found to be the dominant term driving control system dynamics, and thus has been used as the major parameter that is time-varying, patient-specific and fitted to measured data as required. The physiological and clinical relevance of this S_I value has also been seen in the very high correlations to the euglycaemic clamp [Lotz et al., 2006, 2008].

2.3 Neonatal BG system model

The model of Chase et al shown in Equations 2.20 - 2.24 is used as a starting point from which a neonatal glucose-insulin system control model will be developed, based on success in real-time glycaemic control, long-term patient parameter identification, and virtual-patient simulation for *in-silico* protocol development

[Chase et al., 2007; Lonergan et al., 2006b].

The model will be adapted with reference to specific relevant elements of neonatal physiology that are particularly different to adults, and to account for relevant neonatal physiological data present in literature. Population parameter values used in the model will thus be derived from available literature sources. The final model is presented in summary form in Section 2.4, but Figure 2.3 presents an overall schematic of the model structure.

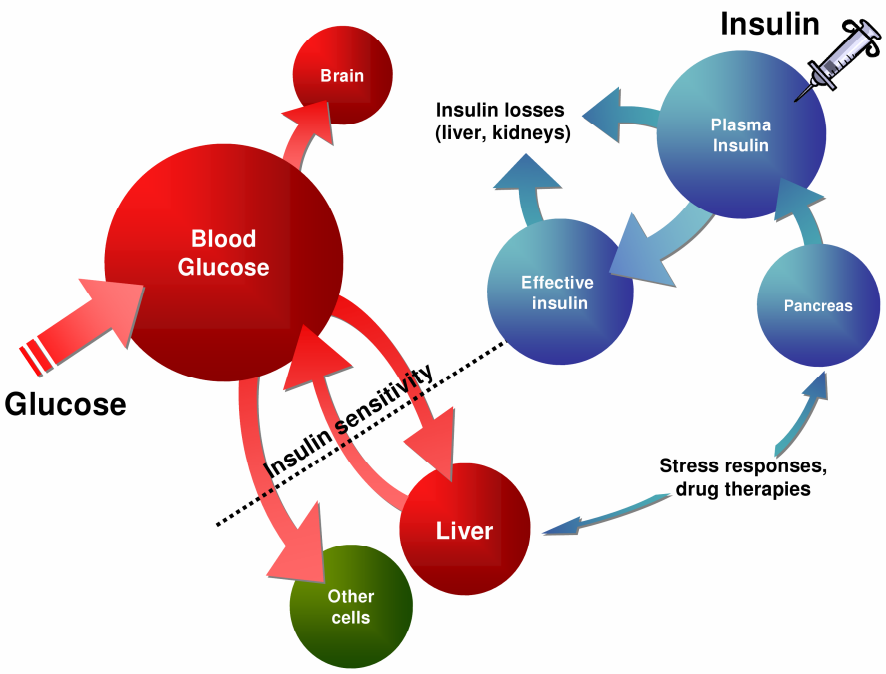

Figure 2.3: Basic outline of the fundamental physiology of glucose sources, insulin sources and their utilisation to remove glucose.

The concept of a time-varying, patient-specific insulin sensitivity is preserved in this model. Several clinical studies [Vaucher et al., 1982; Ostertag et al., 1986; Beardsall et al., 2007a] have reported the neonatal response to exogenous insulin and nutrition inputs is highly patient-specific. Thus, a similar approach is taken in this model adaptation to use population constant parameters for the glucose-insulin kinetics and fit insulin sensitivity as a lumped parameter. Thus S_I effectively captures the overall patient response to exogenous nutrition and insulin inputs. This approach, just as in the adult applications of this model, thus minimises the unknown to critical parameters and, as a result, maximises

identifiability. Hence, with its physiologically relevant structure, it sits in the intersection of Figure 2.1.

2.3.1 Glucose kinetic modelling

The model of Equations 2.20 - 2.24 uses a mono-compartmental description of glucose kinetics. Three-compartment models of glucose kinetics have been identified by various dose-response and glycaemic clamp tests with the help of glucose tracers [Insel et al., 1974; Cobelli et al., 1984]. However, the costly nature of multi-tracer experiments limit their use to very specialised research studies and render them impractical for control or clinical use.

As the fastest equilibrating compartment in the 3-compartment model was found to be too fast to identify accurately (time constant 0.6 min, [Cobelli et al., 1984]), it was proposed to combine the 'fast' and 'medium' compartments. Some researchers assume a fixed relationship between glucose compartments [Hovorka et al., 2002]. The neonatal system model will be used to identify patient parameters from measurements spaced 1-4 hours apart, and rapid changes in blood glucose concentration are not a goal of control in this setting. Thus, the main advantage of the glucose compartment structure used here is its identifiability using limited plasma samples, while still accounting for the dominant physiologically relevant dynamics.

The term G_E in Equation 2.20 originated in the minimal model and is defined as the basal glucose level. This term is available in studies such as intravenous and oral glucose tolerance tests, as typically these investigations begin with the patient in a fasted state and thus permit measurements of baseline variables. However, in critical care such baseline measurements are not feasible and, due to the critical illness of the patient, the baseline glucose level may be altered or time-varying due to circulating counter-regulatory hormones. This approach is also not feasible in the preterm neonate with limited endogenous energy stores, who must be fed continuously.

Thus, the term $G(t)$ in Equation 2.20 can be redefined as the total blood glucose concentration. This change creates a constant term ($p_G.G_E$), which represents the endogenous balance between glucose output (eg: from the liver) and

non-insulin mediated glucose uptake (eg: central nervous system). Equation 2.25 shows the glucose compartment model adapted from Equation 2.20. The endogenous glucose production and central nervous system uptake terms are explicitly defined, and nutritional inputs are separated in enteral (P_{EN}) and parenteral (P_{TPN}) pathways to reflect typical NICU nutrition practices:

$$\begin{aligned}\dot{G} &= -p_G G - S_I G\left(\frac{Q}{1+\alpha_G Q}\right) + \frac{P_{TPN}(t)+P_{EN}(t)}{V_{G,frac}\times m_{body}} \\ &\quad + \frac{((EGP_{max} - CNS.m_{brain,frac})\times m_{body})}{V_{G,frac}\times m_{body}}\end{aligned} \tag{2.25}$$

where $G(t)$ [mmol/L] is the total plasma glucose. Patient endogenous glucose clearance and insulin sensitivity are p_G [min^{-1}] and S_I [L/(mU.min)], respectively. Endogenous glucose production is denoted by EGP_{max} [mmol/kg/min] and $V_{G,frac}$ [L/kg] represents the glucose distribution volume per kilogram of body weight. CNS [mmol/kg/min] represents non-insulin mediated glucose uptake by the central nervous system, and $m_{brain,frac}$ represents brain weight as a proportion of body weight. Body weight is denoted by m_{body} [kg]. Michaelis-Menten functions are used to model saturation with α_G [L/mU] used for the saturation of insulin-dependent glucose clearance. $P_{TPN}(t)$ [mmol/min] represents dextrose from parenteral sources and $P_{EN}(t)$ [mmol/min] represents dextrose absorption from enteral sources via the gut.

The parameter CNS represents non-insulin mediated glucose uptake by the central nervous system. In contrast to the adult case, the brain represents a major source of glucose uptake in infants, due to their larger brain-to-body weight ratio [Hertz et al., 1993; Farrag et al., 1997]. Glucose metabolism by the brain is relatively constant [Gruetter et al., 1998] and independent of insulin concentration [Cowett and Farrag, 2004]. Positron Emission Tomography (PET) is used to quantify cerebral glucose uptake, however this technique requires the use of radioactive compounds, and thus is technically and ethically difficult to perform in preterm neonates. The value used for CNS in this study was 8.8μmol/min/100g brain weight (0.088 mmol/min/kg brain weight) based on [Powers et al., 1998]. This study used PET to quantify cerebral glucose uptake in neonates with suspected hypoxic-ischaemic encephalopathy to justify subjecting the patients to

radioactive compounds. The value used for CNS in this study is taken from patients in [Powers et al., 1998] that did not display any long-term neurological deficits, and thus represents an estimate of cerebral glucose uptake in a neonatal brain without any major defects. The average brain weight of the preterm infant at the age used in this cohort was estimated at 14% of body weight [Ho et al., 1981].

The parameter EGP_{max} represents endogenous glucose production, which can be measured in tracer studies [Hertz et al., 1993; Poindexter et al., 1998; Cowett et al., 1983; Sunehag et al., 1999; Tyrala et al., 1994; Van Kempen et al., 2003; Kalhan et al., 1986]. Endogenous glucose production is decreased in the presence of increased blood glucose concentration and increased plasma insulin concentration [Kalhan et al., 1986; Bergman et al., 1985]. Because of the fragile nature of this population, the true fasting rate of glucose production cannot be explicitly determined. In addition, almost all such studies are performed concurrently with parenteral nutrition to avoid underfeeding the low birth weight neonate.

However, Figure 2.4 plots the average endogenous glucose production against blood glucose concentration for the available literature reporting tracer studies in preterm neonates, the details of which are shown in Table 2.2. At $G = 0$, the p_G and S_I terms in Equation 2.25 become zero. Thus, the range of values for EGP_{max} = [0.0172 to 0.0312 mmol/kg/min] suitable for this model formulation were obtained from Figure 2.4 at $G = 0$ (the intercept with the y-axis). This extrapolation of endogenous glucose production to zero glucose is similar to the procedure employed by [Hovorka et al., 2002], and also used by Bergman to evaluate renal uptake [Bergman et al., 1985]. Bootstrapping with replacement (N=1000) was used to determine the mean intercept and the upper and lower 5% of possible intercepts that define this range for the data shown.

The estimates of basal endogenous glucose production used in this study are higher than the values seen in adults [Hertz et al., 1993; Thorell et al., 2004]. The explanation for this difference is that the extra glucose is required in infants for growth and to supply the glucose requirements of the relatively large brain in the infant compared to total body weight [Kalhan, 2003]. In particular, it has been shown that endogenous glucose production (via glycogenolysis and gluconeogenesis, primarily from the liver) may not be suppressed in the preterm infant

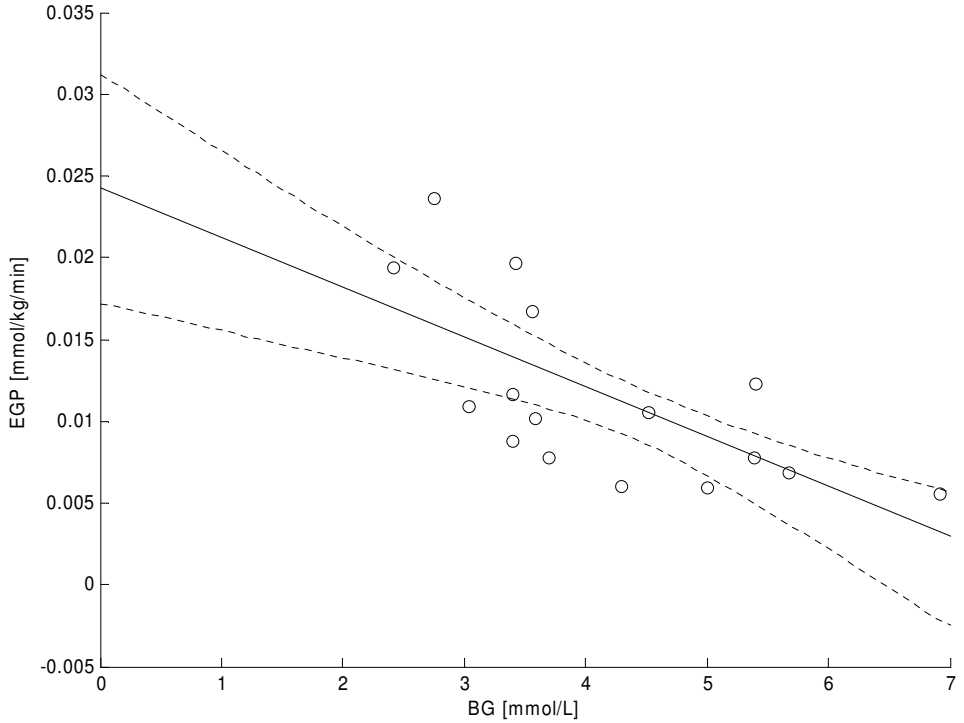

Figure 2.4: Endogenous glucose production (EGP) against steady-state blood glucose concentration. Dashed lines represent the 5%-95% confidence interval range of possible endogenous glucose production (0.0172-0.0312 mmol/kg/min).

by exogenous glucose infusions [Farrag et al., 1997; Cowett et al., 1983]. Specifically, [Farrag et al., 1997] found a maximal suppression of endogenous glucose production of 58% of basal rates. This result is in marked contrast to the healthy adult who can effectively completely suppresses endogenous glucose production. However, it is similar to the critically ill adult [Chase et al., 2006a; McCowen et al., 2001]. In this research, some of this effect is captured by the parameters p_G and S_I, which incorporate contributions of increased insulin concentration [Hertz et al., 1993] and plasma glucose concentration [Farrag and Cowett, 2000] to decreasing net hepatic glucose output.

Several studies have reported that many neonates produce an inadequate glucose raising response to decreases in glucose infusion [Van Kempen et al., 2003] and to a bolus of glucagon [Jackson et al., 2003]. Additionally, it has

Table 2.2: Endogenous glucose production (EGP) measured in preterm neonates.

Gest. age (weeks)	Weight (kg)	EGP (mg/kg/min)	Blood glucose (mmol/L)	Source
34.5	2.1	3	3.6	[Cowett et al., 1983]
34.2	2.0	1.4	5.39	
28.2	1.0	10.9	3.0	[Sunehag et al., 1999]
26.2	0.9	1.0	6.9	[Hertz et al., 1993]
26.3	0.9	1.2	5.7	[Poindexter et al., 1998]
23-28	0.9	12.3	5.4	[Tyrala et al., 1994]
31.0	1.1	6.0	4.3	[Van Kempen et al., 2003]
31.0	1.1	8.8	3.4	
34.5	1.7	7.8	3.7	
34.5	1.7	11.6	3.4	
39.1	3.0	1.1	5.0	[Kalhan et al., 1986]
38.0	2.1	1.8	3.6	
35.5	2.2	1.9	4.5	
38.0	2.1	4.3	2.8	
39.1	3.0	3.5	3.4	
35.5	2.2	3.5	2.4	

been shown that many preterm infants have concentrations of hepatic glucose-6-phosphatase, the rate limiting enzyme in gluconeogenesis, below the limit of normal term infants [Hume et al., 2005]. Glycogen stores in premature infants to produce further glucose for use are also relatively sparse [Mena et al., 2001; Hume et al., 2005]. Therefore, low birth weight infants must be fed adequately to prevent long-term deficiencies in growth and development [Hay et al., 1999].

The majority of exogenous dextrose supply for preterm infants is in the form of parenteral nutrition, typically through pre-made parenteral nutrition formulas or occasionally mixed with other medications such as morphine, insulin and dobutamine. Enteral feedings are often initiated during the first week of life through administration of expressed breast milk (EBM). The P_{EN} term in Equation 2.25 represents the absorption of enteral nutrition through the gut. The uptake of dextrose from enteral sources for neonates uses the same model as Equations 2.23 and 2.24. The parameters k_{pr} and k_{pd} represent the rate of change of dextrose absorption into the bloodstream following a change in the enteral nutrition rate, based on [Wong et al., 2006b], and are set to half-lives of 20 minutes and 100 minutes respectively, similar to the adult case.

Enteral feedings represent a minor source of glucose in this cohort and its

administration is highly dependent upon clinical condition. Many preterm infants with insulin infusions receive less than 5-10% of total daily glucose via the enteral route based on retrospective data, and in many cases infants receive no enteral nutrition. Thus, the values used for k_{pr} and k_{pd} are assumed to have a small effect on model dynamics. EBM is modelled with an effective glucose concentration of approximately 7% [Anderson et al., 1983].

In normal, healthy subjects most glucose filtered through the kidney is re-absorbed and very little is lost through urine. In diabetic subjects, high blood glucose concentrations exceed the renal threshold for glucose reabsorption and renal losses account for a measurable amount of glucose disposal. Coulthard and Hey [1999] showed that in ventilated preterm neonates renal glucose excretion showed a less well-defined threshold value than in adults, and that the amount of renal excretion was related to the amount of filtered glucose and hence blood glucose concentration. Thus, in the model presented here, this effect is assumed to be largely captured in the p_G term of Equation 2.25.

With respect to saturation effects [Farrag et al., 1997] found no plateau in the rate of glucose uptake at several increasing levels of insulin infusion during clamp tests, and that the neonatal glucose response to insulin far exceeded the maximal response reported in the adult [Rizza et al., 1981]. This result suggests that insulin mediated glucose uptake does not saturate at the insulin delivery rates typically encountered in neonatal intensive care. Therefore, the parameter representing saturation of insulin mediated glucose uptake, α_G, was set to zero in this study. This lack of saturation effect is significantly different to the adult case, where the significant glucose uptake saturation can occur [Wong et al., 2006a; Prigeon et al., 1996; Chase et al., 2004; Natali et al., 2000].

The distribution of fluids in the neonatal body is markedly different from children and adults. In particular, the extra-cellular fluid compartment is a much higher percentage of total body weight [Lorenz et al., 1995; Hartnoll et al., 2000; Simpson and Stephenson, 1993]. It can also change over time as very preterm neonates can pass through a diuretic stage in the first few days of life [Lorenz et al., 1995; Bidiwala et al., 1988], and the body fluid compartments redistribute over the first few weeks of life to approach adult proportions, as shown in Table 2.3. Hence, a population-based, time-varying volume of glucose distribution as a proportion of body weight was created for the parameter $V_{G,frac}$ based on

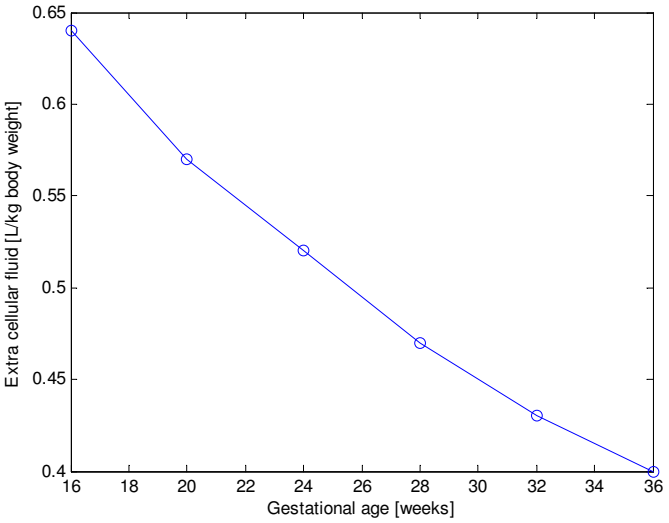

Figure 2.5: Proportion of body weight used to estimate V_G. Adapted from [Avery et al., 1994].

Table 2.3: Body water distribution in preterm infants and adults. All values are expressed as percentage of body weight. Adapted from [Avery et al., 1994].

	Gestation(weeks)					Adult
	24	28	32	36	40	
Total body water	86%	84%	82%	80%	78%	60%
Intra-cellular fluid	27%	28%	30%	32%	34%	40%
Extra-cellular fluid	59%	56%	52%	48%	44%	20%

the clinical data shown in Figure 2.5 [Avery et al., 1994; Cassady, 1966].

2.3.2 Insulin kinetic modelling

The two-compartment insulin model of Equations 2.21 and 2.22 upon which this model is based allows 'delay' in insulin action and 'memory' effects of previously infused insulin to be captured, similar to the Hovorka model of Equations 2.13-2.15 [Hovorka et al., 2002]. These effects are accounted for via physical insulin transport in the I and Q compartments, as opposed to remote insulin-action compartments, which allows model calibration using plasma insulin measurements. The insulin compartments used in this model are thus defined:

$$\dot{Q} = -kQ + kI \tag{2.26}$$

$$\dot{I} = \frac{-nI}{1 + \alpha_I I} + \frac{u_{ex}(t)}{V_{I,frac} * m_{body}} + I_B e^{-\left(k_I \frac{u_{ex}(t)}{V_{I,frac} * m_{body}}\right)} \tag{2.27}$$

where $I(t)$ [mU/L] is the plasma insulin, exogenous insulin input is represented by $u_{ex}(t)$ [mU/min] and basal endogenous insulin secretion I_B [mU/L/min], with k_I [min^{-1}] representing the suppression of basal insulin secretion in the presence of exogenous insulin. The effect of previously infused insulin being utilized over time is represented by $Q(t)$ [mU/L], with k [L/(mU.min)] accounting for the effective life of insulin in the system. The parameter $V_{I,frac}$ [L/kg] is the insulin distribution volume per kilogram body weight and n [1/min] is the constant first order decay rate for insulin from plasma. Michaelis-Menten functions are used to model saturation, with α_I [L/mU] used for the saturation of plasma insulin disappearance.

2.3.2.1 Plasma insulin compartment (I)

The distribution volume for insulin, $V_{I,frac}$, was set to a neonatal plasma volume of approximately 4.5% of the body weight expressed in kilograms [Leipala et al., 2003; Cassady, 1966]. The parameter I_B represents basal insulin secretion in the presence of no exogenous insulin input. This parameter provides an estimate of basal insulin secretion to better model the actual physiological situation. It also makes the model robust in the sometimes frequent periods where no exogenous insulin is administered. It is assumed that exogenous insulin administration suppresses endogenous insulin secretion and the parameter k_I broadly captures this suppression effect.

The parameter I_B was set to a population constant of 10 mU/L/min to achieve steady state basal insulin concentrations of approximately 12 mU/L (ie: the concentration I for which $\dot{I}$ in Equation 2.27 is equal to zero). This value is very similar to the reported clinical results shown in Table 2.4.

Table 2.4: Basal plasma insulin concentration in preterm neonates. N indicates number of patients in each study.

Basal plasma insulin	Source
7 mU/L (N=11) 14 mU/L (N=8)	[Pildes et al., 1969]
15 mU/L (N=11) 18 mU/L (N=12) 6 mU/L (N=11) 16 mU/L (N=12)	[Andronikou and Hanning, 1987]
13.9 mU/L (N=14) 11.9 mU/L (N=12)	[Poindexter et al., 1998]
4 - 9 mU/L (N=30)	[Farrag et al., 1997]

The parameter k_I was set to 0.1 to produce a suppression of endogenous insulin that matched data reported in [Farrag et al., 1997], who found plasma insulin concentration was relatively insensitive to rate of insulin infusion for low insulin infusion rates, and a proportional increase in plasma insulin concentration for higher rates of insulin infusion. Figure 2.6 shows the modelled appearance rate of insulin into the plasma compartment against rate of exogenous insulin infusion. The appearance of insulin is dominated by the endogenous insulin production estimate at low exogenous insulin infusion rates, and matches exogenous insulin infusion at higher rates.

The parameter n represents the disappearance of insulin from plasma. Factors influencing this parameter include transport into the interstitial space and removal by the liver and kidneys. Data shown in Table 2.5 are adapted from studies that achieved a steady state of insulin infusion. The values of n in Table 2.5 were obtained by numerically solving Equation 2.27 using the constant insulin infusion rate documented for each study until steady-state was reached. The resulting concentrations were compared to the reported literature study, and the parameter n was adjusted until the simulated and reported plasma insulin concentrations matched. In this study, a value of $n = 0.9\text{min}^{-1}$ was used, compared to 0.16 min^{-1} in adults [Hann et al., 2005]. The values and range from these studies are presented in Table 2.5. This result matches observations that the rate of insulin clearance was much higher in neonates compared to healthy adults [Farrag et al., 1997].

Table 2.5: Steady state insulin concentration from constant insulin infusions. N indicates number of patients in each study.

Insulin infusion (U/kg/hr)	Weight (kg)	Steady state insulin (mU/L)	n min^{-1}	Reference
0.012	2.024 (N=6)	12 ± 2	0.49	[Farrag et al., 1997]
0.03	1.977 (N=6)	9 ± 2	1.30	
0.06	2.046 (N=6)	19 ± 2	1.21	
0.12	1.841 (N=6)	54 ± 12	0.90	
0.24	1.822 (N=6)	89 ± 22	1.15	
0.6	3.43 ± 0.73 (N=4)	407 ± 103	0.92	[Agus et al., 2004]
0.6	3.30 ± 0.96 (N=12)	447	0.87	[Agus et al., 2006]
0.05	0.894 (N=4)	79	0.28	[Poindexter et al., 1998]
0.025	0.790 ± 0.26 (N=8)	14.1	0.79	[Beardsall et al., 2007a]

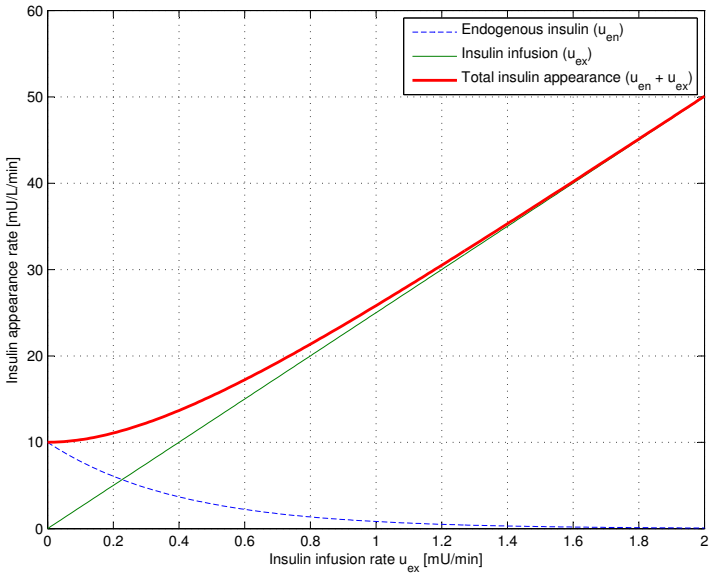

Figure 2.6: Endogenous and exogenous components of the rate of appearance of insulin into the plasma compartment against rate of exogenous insulin infusion. u_{en} represents the endogenous insulin production term and u_{ex} represents exogenous insulin infusion.

Figure 2.7 shows the plasma insulin model and population constants are valid for a wide range of reported insulin concentrations from steady exogenous insulin infusions. Typical insulin infusion rates expected in neonatal control scenarios would occupy the left half of the range shown in Figure 2.7, below 0.3 U/kg/hr. Agus et al [2006; 2004] used supra-physiological concentrations of insulin to determine the effects of insulin on protein breakdown. Thus, they provide further data points but at clinically irrelevant values.

Typical steady state insulin concentrations for the adult insulin model of Equation 2.22 for similar weight-based rates of insulin infusion are shown in Figure 2.7. Neonatal plasma insulin concentrations are significantly lower than adults for similar weight-adjusted rates of exogenous insulin infusion [Farrag et al., 1997]. This result may represent a much higher metabolic clearance rate of insulin in the neonate. To date, the specific mechanisms that create a higher metabolic clearance rate in neonates remain as open questions. The goal of this study was to generate a model designed for control purposes that matches observable insulin kinetics in the neonate and further investigation of physiological mechanisms of insulin transport is outside the scope of this research.

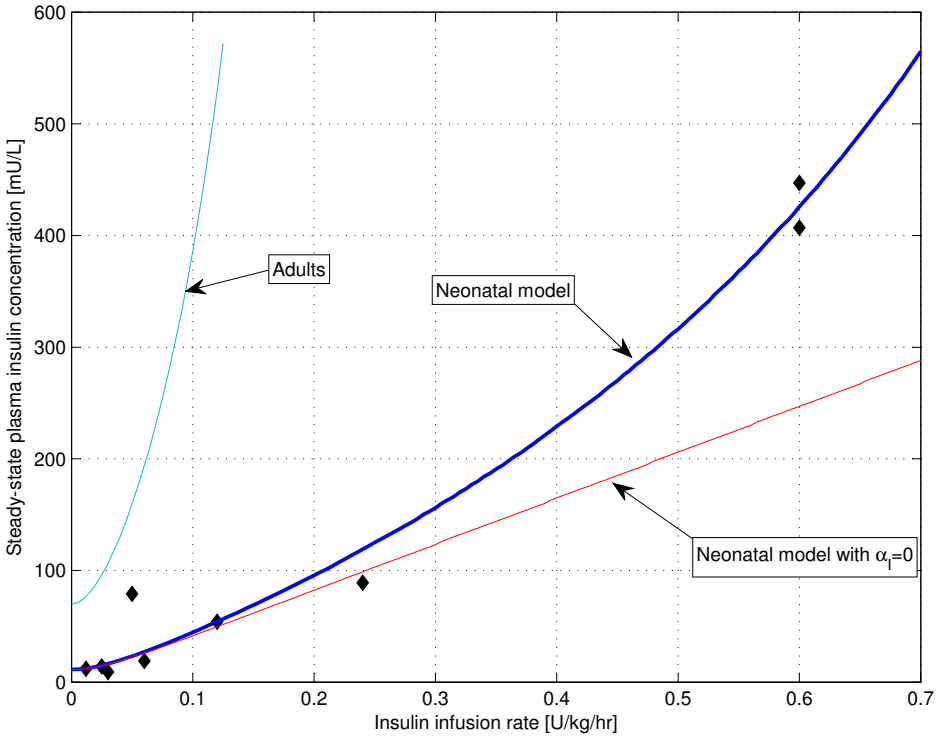

Figure 2.7: Modelled and measured steady-state plasma insulin concentration against insulin infusion rate. The neonatal model used for this study neglecting insulin disposal saturation and the model used for adults are shown for comparison. The discrete points represent individual studies as presented in Table 2.5

Published data was not available to directly estimate the insulin removal saturation parameter α_I, so this parameter was held at the same value as the adult case. Figure 2.7 shows that the effect of α_I is only relevant at very high insulin infusion rates, and that the value employed provides a good fit to the supra-physiological results of [Agus et al., 2004, 2006]. The insulin model in adults exhibits instability for insulin infusion rates greater than approximately 18 U/hr for a typical 70kg adult due to the insulin removal saturation term α_I. The adult model was designed for use for insulin in the range of 0 - 8 U/hr (0 - 0.11 U/kg/hr). The dynamics of the neonatal model allow stability for a insulin infusion rates up to 1.4 U/hr for a typical 1kg infant, and represents an infusion rate approximately 3x - 9x higher than would be used for control.

2.3.2.2 Insulin delay compartment (Q)

The Q compartment reflects accumulation dynamics of insulin [Doran, 2004]. This compartment can be pictured in terms of a delay in the action of insulin due to transport of insulin through the interstitium to the site of action. Given the 1-3 hour window between BG measurements and insulin interventions, and that the sole method of insulin delivery to be used in neonates is via infusion (as opposed to bolus), the effects of any extra non-linear dynamics that could be introduced using a bolus-based regime are minimized. Thus, the I compartment to Q compartment transport is likely to play less importance in neonatal control compared to adults. The ratio of extra-cellular fluid (ECF) to plasma is higher in neonates compared to adults, as shown in Table 2.3. Thus, it is possible that the model may over-estimate the accumulated insulin 'on-board' as a conservative assumption to minimise a model-based controller over-infusing insulin.

The effective life of insulin, k was assumed not to differ significantly from adults [Hann et al., 2005], and that passive diffusion can explain the major transport phenomenon between plasma and the interstitium [Castillo et al., 1994; Rasio et al., 1967; Sjostrand et al., 1999; Yang et al., 1989; Steil et al., 1996]. It should also be noted that a constant excretion would be expected in the presence of relatively constant nutritional infusions.

Finally, Figure 2.8 shows a typical response of the I and Q compartments developed in this section to a typical insulin infusion regime from clinical data. The plasma insulin concentration (I) closely follows the insulin infusion rate due to the relatively short effective half-life of insulin in this compartment. The response of the Q compartment demonstrates the overall smoothing effect to create a physiologically likely insulin effect response.

2.3.2.3 Comparison with adult model

The response of the individual compartments of the insulin kinetics model to typical insulin infusions in neonates and adults are compared in Figure 2.9. The data points in Figure 2.9 are generated by comparing the hourly average concentration in the specific compartment, I or Q, with the average rate of exogenous insulin administration over the hour. Polynomial curves are fitted to the data to

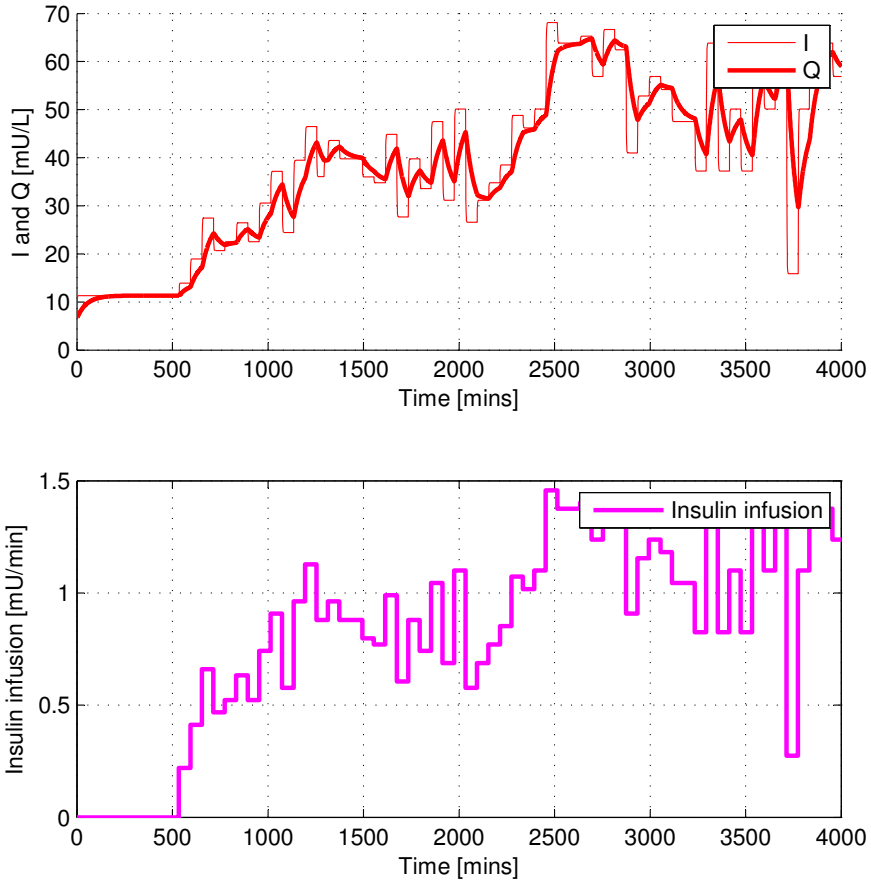

Figure 2.8: Plasma insulin (I) and insulin accumulation (Q) compartment response to a typical insulin infusion profile from retrospective neonatal data.

generate curves that represent the 95% prediction bounds for comparison. The data for the NICU analysis was obtained from the retrospective cohort described more fully in Section 3.2. The data for the adult ICU analysis was obtained from the SPRINT study [Chase et al., 2008b]. SPRINT primarily uses boluses as the insulin delivery route, discretised to 1U increments, which creates the vertical banding effect in Figures 2.9b and 2.9d. Also note the scales are different between cohorts.

The response of the plasma insulin compartment is much tighter in neonates compared to adults, as evidenced by the tighter 95% prediction bounds in Figure 2.9a versus Figure 2.9b. This result is a consequence of the significantly higher insulin clearance rate in neonates. The modelled plasma insulin concentrations are generally lower than adults, as a result.

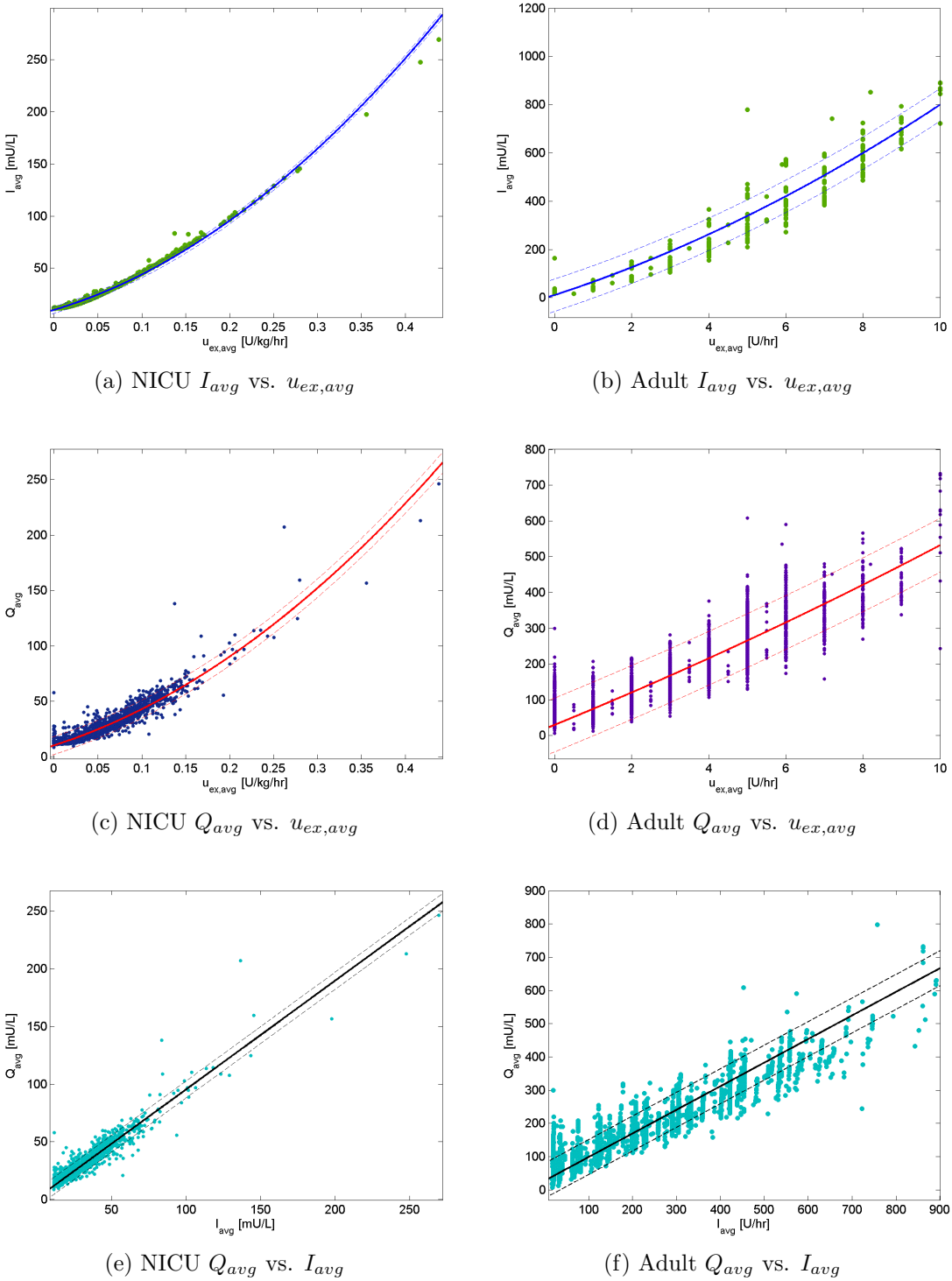

(a) NICU I_{avg} vs. $u_{ex,avg}$

(b) Adult I_{avg} vs. $u_{ex,avg}$

(c) NICU Q_{avg} vs. $u_{ex,avg}$

(d) Adult Q_{avg} vs. $u_{ex,avg}$

(e) NICU Q_{avg} vs. I_{avg}

(f) Adult Q_{avg} vs. I_{avg}

Figure 2.9: Comparison of average values of I and Q compartment with exogenous insulin infusion rate. Dashed lines represent 95% prediction bands.

The insulin delay compartment, Q, shows a similar difference between adults and neonates. The averaged modelled concentrations in the I and Q compart-

ments shows a near 1:1 ratio in neonates (Figure 2.9e), reflecting the use of infusions and the typical longer time period between infusion rate changes that allows both compartments to equilibrate. The ratio of concentrations is lower than 1:1 in adults suggesting that transport between the insulin compartments plays a more significant role.

A primary reason for the shallower slope in Figure 2.9f is the bolus method of delivery for the adult data. A bolus of insulin is effectively a very high insulin infusion rate over a relatively very short amount of time. The effectively high infusion rate leads to a high plasma insulin concentration that saturates the modelled insulin clearance mechanisms, determined by the value of α_I, and creates non-linear effects. Thus, clinical considerations, such as the method of insulin delivery, play a role in determining the relative importance of model parameters.

Any and all of the insulin clearance pathways could be feasibly altered in the neonate. More detailed insulin kinetics models exist for the adult case that incorporate separate liver and kidney insulin clearances with separate saturation mechanics, tissue insulin breakdown and back-flow transport of insulin from the interstitial compartment to the plasma compartment [Lotz et al., 2006; Sherwin et al., 1974]. The model presented here uses lumped parameters to broadly capture these effects to create a system that may be useful for control and reflects the compromise required to make use of limited clinical data.

The cohort for control and the method of insulin delivery can influence the model BG response. As a simulated example, Figure 2.10 shows two virtual trials of an adult patient for a sliding-scale protocol using the same absolute amount of insulin per hour, delivered as a bolus on the hour for the 'Bolus' method, and a constant infusion for the 'Infusion' method. Virtual trial methodology will be covered in detail in Chapter 6. The bolus method resulted in a lower simulated BG response. This result is due to the non-linear clearance of insulin. Thus, more insulin is available to bind with tissue receptors and stimulate glucose uptake in the bolus case, causing an overall lower BG response. Therefore, the saturation of plasma insulin clearance would be an important parameter for control of glycaemia in a bolus-based scheme. However, neonatal glucose control is entirely infusion based. Thus, the plasma insulin clearance saturation mechanisms carry a lower weighting in creating a model designed for glycaemic control in neonates.

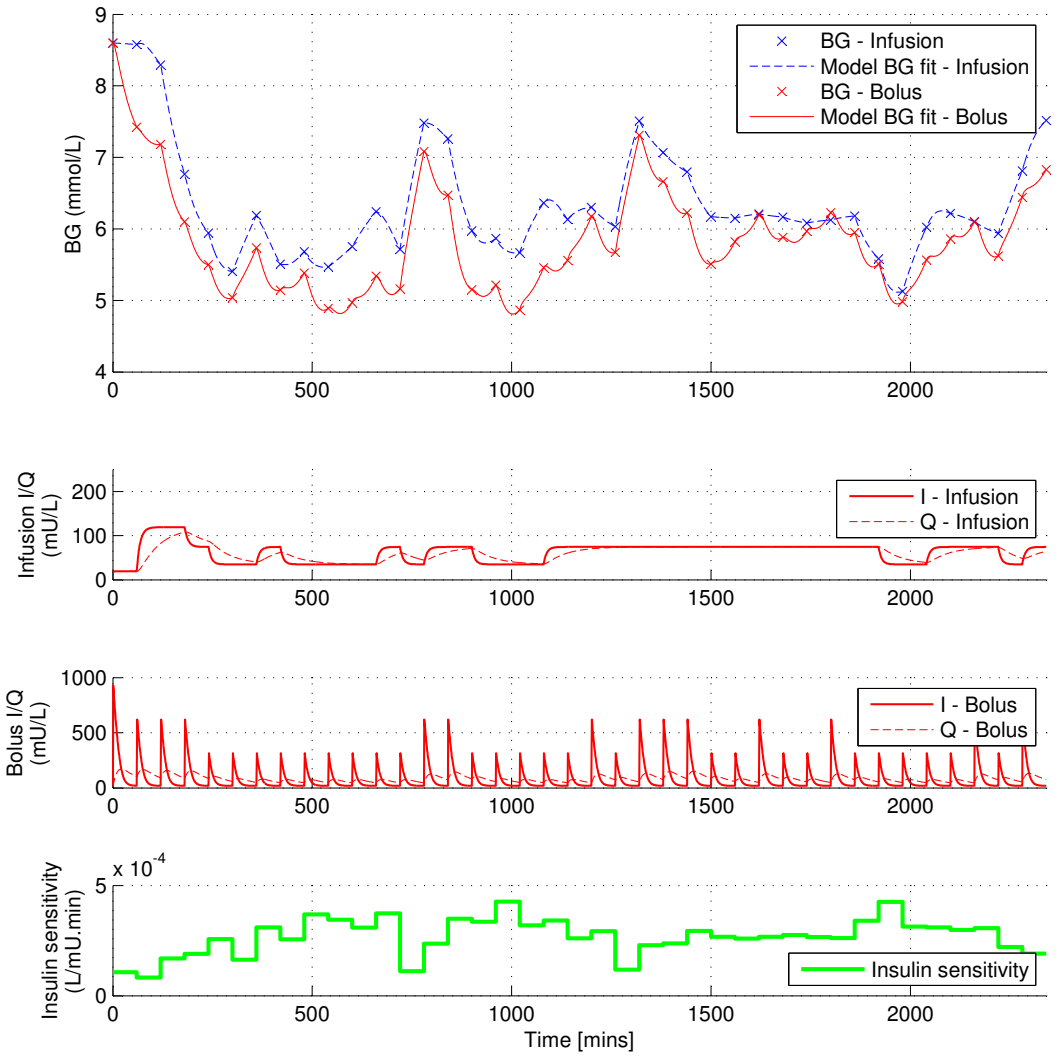

Figure 2.10: Virtual trial BG response for bolus and infusion insulin delivery methods. The top panel shows simulated blood glucose concentration. The middle panels show the concentrations in the I and Q compartments for infusion and bolus insulin delivery methods. Model-fitted insulin sensitivity is displayed in the bottom panel. The bolus method of insulin delivery resulted in a generally lower blood glucose profile.

2.4 Model summary

In summary, the overall model used in this work is defined:

$$\dot{G} = -p_G G - S_I G\left(\frac{Q}{1+\alpha_G Q}\right) + \frac{P_{TPN}(t) + P_{EN}(t)}{V_{G,frac} * m_{body}} + \frac{((EGP_{max} - CNS.m_{brain,frac}) * m_{body})}{V_{G,frac} * m_{body}} \tag{2.28}$$

$$\dot{Q} = -kQ + kI \tag{2.29}$$

$$\dot{I} = \frac{-nI}{1+\alpha_I I} + \frac{u_{ex}(t)}{V_{I,frac} * m_{body}} + I_B e^{-\left(k_I \frac{u_{ex}(t)}{V_{I,frac} * m_{body}}\right)} \tag{2.30}$$

$$P_{EN}(t) = \bar{P}_{EN,i+1} + (P_{EN}(t_i) - \bar{P}_{EN,i+1}) e^{-k_p(t-t_i)} \text{ for } t_i < t < t_{i+1} \tag{2.31}$$

where:

$$k_p = \begin{cases} k_{pr} & \text{where } \bar{P}_{EN,i+1} > P_{EN}(t_i) \\ k_{pd} & \text{where } \bar{P}_{EN,i+1} < P_{EN}(t_i) \end{cases}$$

where $G(t)$ [mmol/L] is the total plasma glucose and $I(t)$ [mU/L] is the plasma insulin, exogenous insulin input is represented by $u_{ex}(t)$ [mU/min] and basal endogenous insulin secretion I_B [mU/L/min], with k_I [L/(mU.min)] representing the suppression of basal insulin secretion in the presence of exogenous insulin. The effect of previously infused insulin being utilized over time is represented by $Q(t)$ [mU/L], with k [min^{-1}] accounting for the effective life of insulin in the system. Body weight and fractional brain weight are denoted by m_{body} [kg] and $m_{brain,frac}$ respectively. Patient endogenous glucose clearance and insulin sensitivity are p_G [min^{-1}] and S_I [L/(mU.min)], respectively. The parameter $V_{I,frac}$ [L/kg] is the insulin distribution volume per kilogram body weight and n [min^{-1}] is the constant first order decay rate for insulin from plasma. Endogenous glucose production is denoted by EGP_{max} [mmol/kg/min] and $V_{G,frac}$ [L/kg] represents the

Table 2.6: Constant model parameter values

Parameter	Value
k	0.0086 min^{-1}
n	0.90 min^{-1}
α_I	1.70 x 10^{-3} L/mU
α_G	0 L/mU
CNS	0.088 mmol/min/kg brain weight
m_{brain}	0.14 * m_{body} kg
I_B	10 mU/L/min
$V_{I,frac}$	0.045 L/kg
$V_{G,frac}$	ECF proportion[a] L/kg
EGP_{max}	0.02838 mmol/kg/min
p_G	0.003 min^{-1}

[a] ECF proportion derived from Figure 2.5

glucose distribution volume per kilogram of body weight. CNS [mmol/kg/min] represents non-insulin mediated glucose uptake by the central nervous system. Michaelis-Menten functions are used to model saturation, with α_I [L/mU] used for the saturation of plasma insulin disappearance, and α_G [L/mU] for the saturation of insulin-dependent glucose clearance. $P_{TPN}(t)$ [mmol/min] represents dextrose from parenteral sources and $P_{EN}(t)$ [mmol/min] represents dextrose absorption from enteral sources via the gut due to set exogenous dextrose rates $\bar{P}_{EN}$. The parameters k_{pr} [min^{-1}] and k_{pd} [min^{-1}] are the effective half lives of glucose transport from gut to plasma for both increasing (k_{pr}) and decreasing (k_{pd}) feed rates respectively.

Table 2.6 summarises the parameters used in this model. For this study, k, n, α_I, α_G, CNS, I_B and $V_{I,frac}$ are set to generic population values based on reported data, as described in this chapter. Prior clinical and model sensitivity studies with the similar adult model [Hann et al., 2005; Wong et al., 2006a] have shown this choice to be robust with respect to prediction of response to clinical interventions. The specific values for EGP_{max} and p_G are determined from parameter sensitivity studies presented in Section 3.3.

2.5 Summary

Glucose-insulin system dynamics are described by models designed for applications from interpreting detailed tracer studies and quantifying human physiology, to control system models that capture patient dynamics and variability based on the limited data available in critical care. The model presented in this section is developed for ready clinical control applicability. The focus of development in this case is more a robust, adaptable model, rather than being metabolically correct in every detail.

While glucose-insulin dynamics in neonates has not to date been extensively modelled, the rich history of model-based methods in adults helps guide the adaptation of the model to the neonatal case. Differences in both neonatal physiology and aspects of routine neonatal care can be quantified and explored in a model-based environment.

Finally, the model developed in this section provides an overall measure of a critically ill patient's sensitivity to exogenous insulin and nutrition inputs. The following chapter uses retrospective hospital data to validate the model against a cross-section of typical preterm neonatal patients to explore model robustness and performance metrics.

Chapter 3

Parameter identification and sensitivity analysis

This chapter presents the parameter identification methods used to identify critical model parameters. It thus also presents a sensitivity analysis on several model parameters to ensure the choices of population constant parameter values and identified parameters are robust. Thus, it implicitly presents a limited model validation analysis in its evaluation of model parameters and model performance versus retrospective clinical data. A full, complete validation of the model, while partly overlapping some results, is left for Chapter 4.

3.1 Fitting methods

The insulin sensitivity parameter S_I is the critical time-varying, patient-specific parameter to be identified from either retrospective data in simulation-based virtual patient studies, or in clinical real-time. The fitting procedure must be able to account for significant patient variation over time. It must also be computationally simple enough to be performed in clinical real-time of 1-5 minutes, or preferably faster. Finally, fitting the patient specific parameters in any of the models presented typically presents a non-convex optimisation problem, due primarily to the series of non-linear differential equations involved [Carson and Cobelli, 2001].

The most commonly used method for fitting parameters in these types of compartment models is non-linear recursive least squares (NRLS) [Carson and Cobelli, 2001; Marquardt, 1979]. Given the non-convex nature of the problem this method will produce results that are starting point dependent, and thus require a

range of initial values to generate optimal results. NRLS is also computationally intense [Carson and Cobelli, 2001], particularly where longer periods of data are being fit than those encountered in short 30-300 minute physiological research studies.

Iterative, Bayesian and gradient descent based methods have also been used in a variety of forms [Vicini and Cobelli, 2001; Hovorka et al., 2002; Erichsen et al., 2004; Zheng and Zhao, 2005]. Given the non-convex and non-linear models involved, these methods are all specific to the exact model and methods employed. In addition, they still rely on a core optimisation problem that is non-convex, computationally intensive and not necessarily robust to noise in the data. Thus, they are essentially problem specific and not necessarily generalisable to broader situations.

Overall, a variety of fitting methods are available. Traditional methods, such as NRLS, offer results with some potential limitations depending on the specific problems. However, these methods also require repeated re-simulation to generate gradients for each variable to be fit, resulting in significantly added computation.

An emerging method that simplifies many of these problems is the integral method of [Hann et al., 2005]. Integrating the differential model equations converts the problem to one of matching areas under curves. Parameterising unknown, time-varying patient specific parameters as piecewise constant, or higher order, functions recreates the problem in terms of unknown constants that are more readily identified. Using measured data and numerical integration, the problem can thus be converted into a convex linear least squares problem to obtain these constants. The numerical integration further low-pass filters the data making it robust to noise. Finally, it does not require gradients or, thus, re-simulation of the model saving significant computational effort. The integral method has been used in a variety of clinical glycaemic control studies [Wong et al., 2006a,b; Hann et al., 2005; Chase et al., 2005b] and in other similar biomedical models [Hann et al., 2006; Lotz et al., 2006], providing significant in-silico and clinical validation.

The integral-based method is used to identify S_I in the neonatal model. For this study, the form of the insulin sensitivity function is chosen to be piecewise constant, with a new value determined every hour, which has been shown to

adequately capture the variation in S_I [Lin et al., 2006, 2008]. Equation 2.28 defines the glucose kinetics for this model, and is repeated below:

$$\begin{aligned}\dot{G} &= -p_G G - S_I G\left(\frac{Q}{1+\alpha_G Q}\right) + \frac{P_{TPN}(t)+P_{EN}(t)}{V_{G,frac} * m_{body}} \\ &\quad + \frac{(EGP_{max} - CNS * m_{brain,frac}) * m_{body}}{V_{G,frac} * m_{body}}\end{aligned} \tag{3.1}$$

The integral-based method fits insulin sensitivity by first integrating both sides of the glucose compartment equation between the limits t_a and t_b, defined as the fitting start and end time respectively:

$$\begin{aligned}\int_{t_a}^{t_b} \dot{G}(t)dt &= \int_{t_a}^{t_b} \left\{ -p_G G - S_I G\left(\frac{Q}{1+\alpha_G Q}\right) + \frac{P_{TPN}(t)+P_{EN}(t)}{V_{G,frac} * m_{body}} \right. \\ &\quad \left. + \frac{(EGP_{max} - CNS * m_{brain,frac}) * m_{body}}{V_{G,frac} * m_{body}} \right\} dt\end{aligned} \tag{3.2}$$

All values except insulin sensitivity (S_I) are known, measured or approximated population constants. A linear piece-wise polynomial fit to the BG measurements is used to approximate $G(t)$ between measured values. Insulin sensitivity is assumed constant over the fitting window t_a to t_b. This interval is typically 1 hour, but can be made any convenient length. Additionally, it may be allowed to vary more or less frequently than the measurement rate [Hann et al., 2005]. Thus, Equation 3.2 can be rearranged:

$$\begin{aligned}&G(t_b) - G(t_a) = \\ &-S_I \int_{t_a}^{t_b} \left\{ G\left(\frac{Q}{1+\alpha_G Q}\right) \right\} dt \\ &+ \int_{t_a}^{t_b} \left\{ -p_G G + \frac{P_{TPN}(t)+P_{EN}(t)+(EGP_{max} - CNS * m_{brain,frac}) * m_{body}}{V_{G,frac} * m_{body}} \right\} dt\end{aligned} \tag{3.3}$$

Table 3.1: Time segments used to generate a system of equations for a fitting window of [0 60] minutes

$t_{a,i}$ (mins)	$t_{b,i}$ (mins)
0	15
15	30
30	45
45	60
0	30
15	45
30	60
0	45
15	60
0	60

Rearranging terms yields:

$$\begin{aligned} &S_I \int_{t_a}^{t_b} \left\{ G \left(\frac{Q}{1+\alpha_G Q} \right) \right\} dt = \\ &\quad -\left(G(t_b) - G(t_a)\right) \\ &\quad + \int_{t_a}^{t_b} \left\{ -p_G G + \frac{P_{TPN}(t) + P_{EN}(t) + (EGP_{max} - CNS * m_{brain,frac}) * m_{body}}{V_{G,frac} * m_{body}} \right\} dt \end{aligned} \tag{3.4}$$

Equation 3.4 can be used to generate a system of linear equations that can be solved by linear least-squares methods. The system of equations is generated by splitting the fitting window (t_a, t_b) into a set of time segments, which allows more accurate area-fitting of the non-linear model in a least-squares sense. Table 3.1 shows an example of splitting the fitting period into 10 segments, although any number might be used [Hann et al., 2005] to allow higher fitting higher order functions for the insulin sensitivity parameter S_I. Equations can be generated by integrating between different pairs of time segments.

The use of several time segments creates an over-determined system that can be solved using the method of least squares. The resulting set of equations can be arranged into a standard linear-algebra form (for k time segments):

$$Ax = b \tag{3.5}$$

where

$$A = \begin{bmatrix} \int_{t_{a,1}}^{t_{b,1}} \left\{ G\left(\frac{Q}{1+\alpha_G Q}\right) \right\} dt \\ \cdots \\ \cdots \\ \int_{t_{a,k}}^{t_{b,k}} \left\{ G\left(\frac{Q}{1+\alpha_G Q}\right) \right\} dt \end{bmatrix} \tag{3.6}$$

$$x = S_I \tag{3.7}$$

$$b = \begin{bmatrix} -\left(G(t_{b,1}) - G(t_{a,1})\right) \\ + \int_{t_{a,1}}^{t_{b,1}} \left\{ -p_G + \frac{P_{TPN}(t) + P_{EN}(t) + \left(EGP_{max} - CNS * m_{brain,frac}\right) * m_{body}}{V_{G,frac} * m_{body}} \right\} dt \\ \cdots \\ \cdots \\ -\left(G(t_{b,k}) - G(t_{a,k})\right) \\ + \int_{t_{a,k}}^{t_{b,k}} \left\{ -p_G + \frac{P_{TPN}(t) + P_{EN}(t) + \left(EGP_{max} - CNS * m_{brain,frac}\right) * m_{body}}{V_{G,frac} * m_{body}} \right\} dt \end{bmatrix} \tag{3.8}$$

Finally, solving Equation 3.5 yields the value of S_I over the time window $[t_a, t_b]$. Further details and analysis of the integral-based fitting method are available in [Hann et al., 2005].

Overall, the integral-based method has several merits specific to the estimation of insulin sensitivity in glycaemic control:

- Ability to fit entire patient record and multiple measurements all at once to generate virtual patient insulin sensitivity profiles.
- Hour-to-hour measurements may be fitted in real-time for model-based control.
- Requires no re-simulation and is 10-100 times faster than NRLS [Hann et al., 2005].

A caveat of the integral-based method is that relatively 'dense' blood glucose measurements are required for accurate identification. The method has been successfully used to identify insulin sensitivity using retrospective BG measurement data with measurement intervals of up to 3-4 hours [Hann et al., 2005; Doran, 2004].

3.2 Retrospective data

Retrospective data from 25 episodes of insulin therapy treatment in Christchurch Women's Neonatal Intensive Care Unit was used in the study for model validation. Ethics approval for the collection and publication of data was obtained from the Upper South A Ethics Committee. The 25 episodes of insulin usage comprised 21 individual patients representing 3,567 hours of patient data. Gestational age at birth ranged from 23 to 28.9 weeks, and birth weight ranged from 600 to 1,280 grams. Inclusion criteria were birth weight less than 1,500 grams and a period of treatment with insulin of at least 12 hours. The clinical details of the retrospective cohort are presented in Table 3.2. Data was collected during episodes of insulin infusions, and includes periods around the times of insulin usage where blood glucose was actively monitored even though no insulin was infused.

The retrospective cohort contained 14 female and 7 male patients. Five patients were of Maori ethnicity, which tend to be over-represented in the population of preterm neonates in New Zealand [Mantell et al., 2004]. Two patients died in-hospital and represent the mortality of this cohort.

Table 3.3 summarises the major glycaemic control information for each retrospective patient.

The distribution of blood glucose measurements, insulin infusion rates and dextrose administration are shown in Figure 3.1. In particular, 31% of blood glucose measurements were within the 4 - 7 mmol/L range, with median insulin usage of 0.032 U/kg/hr. The majority of dextrose infusion rates spanned a 3-fold range of approximately 5 - 15 mg/kg/min.

Patients 1, 12 and 23 had low minimum BG measurements ($\leq$ 2.6 mmol/L). Several of these cases were not associated with insulin infusions, and thus rep-

Table 3.2: Patients selected for long-term data collection. Cohort summaries are presented as median [IQR]. All patients are of NZ European descent unless otherwise specified.

Patient	Length of fitting (days)	Gestational age at birth (weeks)	Age at start of data (days)	Weight at birth (grams)	Gender	Notes
1	12.7	23	< 1	600	F	Mortality, Maori
2	13.9	24.4	4	650	F	
3	8.8	23.7	< 1	625	M	
4	12	25.4	< 1	800	F	Several sepsis episodes
5	5.9	26.6	7	840	F	Twin of patient 8
6	3.9	25	< 1	900	F	
7	4.6	26.3	7	810	M	
8	4.3	26.6	6	825	F	Twin of patient 5
9	3.8	26.6	3	915	M	Maori
10	2.7	27.9	3	1280	F	Metabolic acidosis
11	4.9	28.1	< 1	1275	F	Maori, persistent metabolic acidosis
12	1.4	28.6	< 1	845	F	Maternal IDDM, Maori/Russian
13	2.4	27.7	< 1	860	F	Mortality
14	7.6	24.9	3	735	M	
15	8.6	26.9	2	880	F	Maori
16	1.8	29.9	< 1	865	F	
17	1.9	26.4	7	990	M	
18	3.8	26.6	3	920	M	Other European
19	1.8	28.6	4	930	M	
20	4.7	26.6	4	860	F	Sepsis + NEC
21 [a]	5.8		20			
22	11.8	25.4	2	800	F	Severe CLD
23 [b]	12.7		22			
24 [b]	5.9		41			
25 [b]	1.3		56			
Cohort	4.7 [2.6 - 8.7]	26.6 [25.4 - 27.1]	3.0 [1.0 - 7.0]	845 [800 - 904]		

[a] Second episode of insulin usage for Patient 20

[b] Subsequent episodes of insulin usage for Patient 22

Table 3.3: Glycaemic variables in retrospective cohort. Cohort summaries are presented as median [IQR].

Patient	Median dextrose rate[a]		Median insulin[a]	$BG^{b}_{mean,geo}$	$BG^{b}_{SD,geo}$	Max. BG	Min. BG	Measurement
	mg/kg/min	kcal/kg/day	U/kg/hr	mmol/L		mmol/L	mmol/L	period, hours
1	8.9	51.2	0.091	6.8	1.30	19.1	1.7	2.8
2	10.4	59.7	0.053	7.8	1.12	12.4	4.0	4.4
3	9.0	51.6	0.050	7.5	1.18	14.6	3.5	4.0
4	8.2	47.5	0.026	7.6	1.15	11.7	3.3	4.4
5	10.5	60.6	0.037	8.0	1.17	16.3	3.2	3.9
6	4.9	28.1	0.037	7.3	1.20	15.2	2.8	2.2
7	11.8	68.0	0.092	7.9	1.13	10.5	3.5	4.5
8	10.7	61.4	0.031	7.7	1.13	10.8	4.7	4.9
9	9.7	56.1	0.026	8.5	1.11	12.6	6.0	4.0
10	9.9	56.9	0.025	6.9	1.18	12.2	3.6	3.5
11	5.9	34.2	0.047	9.1	1.25	19.6	4.1	3.2
12	5.3	30.3	0.047	6.2	1.36	13.8	1.5	2.3
13	4.0	23.1	0.025	5.6	1.33	31.2	2.9	2.3
14	10.0	57.7	0.029	8.9	1.13	13.4	3.2	3.4
15	9.2	52.8	0.053	7.9	1.17	12.7	3.2	3.6
16	5.0	28.6	0.040	8.2	1.17	12.7	4.3	2.6
17	11.4	65.4	0.059	6.3	1.21	9.2	3.4	4.1
18	8.3	47.5	0.025	7.7	1.10	11.2	5.3	4.4
19	11.3	65.2	0.050	8.3	1.20	14.4	5.6	2.1
20	14.1	81.4	0.030	8.4	1.14	13.0	4.8	4.0
21	10.3	59.5	0.022	9.3	1.21	20.0	3.7	3.0
22	8.5	49.2	0.027	7.5	1.15	15.4	3.9	2.4
23	8.8	50.6	0.077	8.2	1.24	20.3	2.6	2.6
24	10.0	57.6	0.017	8.0	1.25	15.8	3.3	3.0
25	9.6	55.1	0.030	9.6	1.14	14.9	5.9	3.4
Cohort	9.6 [8.3 - 10.4]	55.1 [47.5 - 59.7]	0.037 [0.026 - 0.050]	7.9 [7.5 - 8.3]	1.17 [1.14 - 1.21]	13.8 [12.4 - 15.8]	3.5 [3.2 - 4.3]	3.4 [2.6 - 4]

[a] Infusion rates averaged over 60-minute window

[b] $BG_{mean,geo}$ = geometric BG mean (lognormal); $BG_{SD,geo}$ = geometric BG standard deviation (lognormal)

resent other causes of neonatal hypoglycaemia. Such causes would include low endogenous stores of nutritional substrates, and reduced expression of key elements involved in gluconeogensis, such as glucose-6-phosphatase [Van Kempen et al., 2003; Diderholm et al., 2007]. These events were close to the initiation of insulin therapy, and were thus included in the retrospective data.

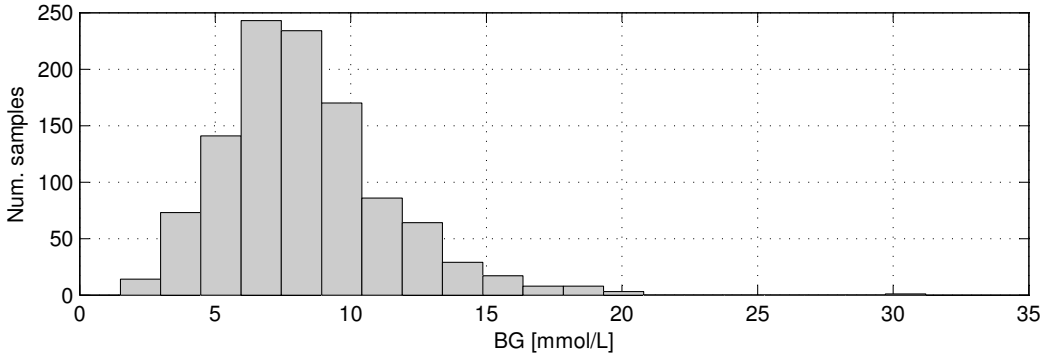

(a) Blood glucose measurements in retrospective patients, with $\hat{\mu}_{geo} = 7.9$ mmol/L and $\hat{\sigma}_{geo} = 1.17$.

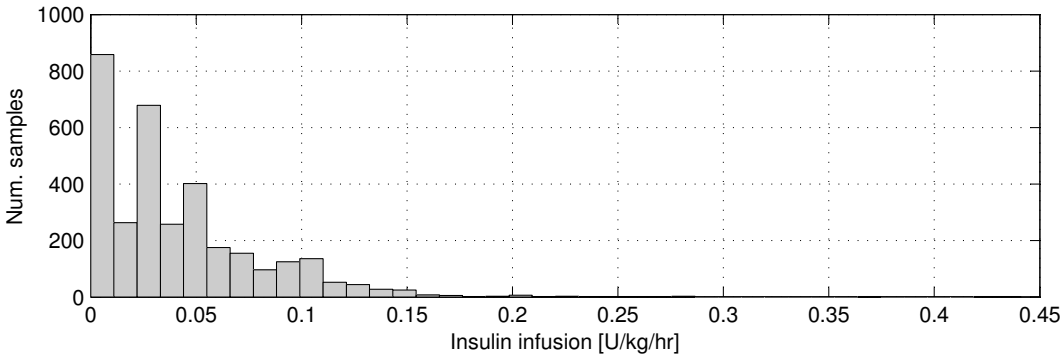

(b) Insulin infusions (hourly average) in retrospective patients. Median rate [IQR] = 0.037 [0.026 - 0.050] U/kg/hr.

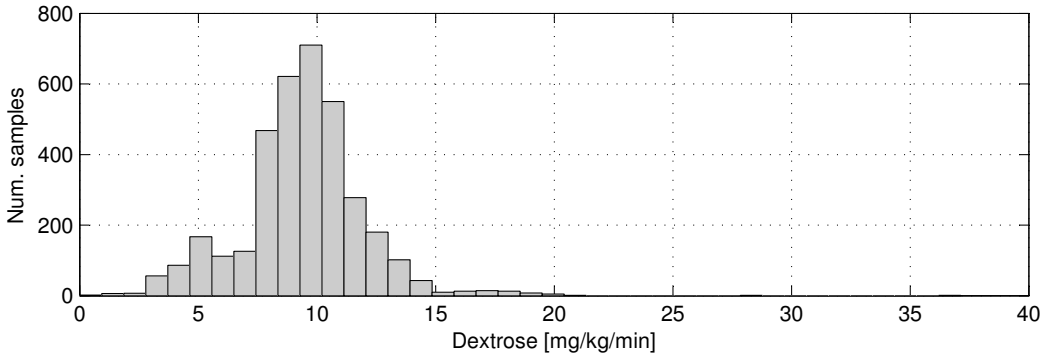

(c) Dextrose infusion rates (enteral and parenteral) in retrospective patients. Median rate [IQR] = 9.6 [8.3 - 10.4] mg/kg/min.

Figure 3.1: Distribution of glycaemic variables in retrospective cohort.

Also evident in Figure 3.1a is the right-skewed spread of blood glucose measurements resembling a lognormal distribution. Thus, the summary metrics in Table 3.3 are reported using lognormal statistics. For a given set of BG measurements the lognormal distribution parameters for the sample, $\hat{\mu}$ and $\hat{\sigma}$, are fitted using maximum likelihood parameter estimation. The geometric mean and geometric standard deviation are given by $\mu_{geo} = e^{\hat{\mu}}$ and $\sigma_{geo} = e^{\hat{\sigma}}$ respectively, and are quoted in Table 3.3. Upper and lower bounds for confidence intervals for the data are given by multiplying and dividing the geometric mean by the geometric standard deviation. For example, the 2σ confidence interval is given by $\left[\mu_{geo}/\sigma_{geo}^2, \mu_{geo}.\sigma_{geo}^2\right]$.

3.3 Parameter identification and sensitivity analysis

3.3.1 Endogenous glucose production and glucose uptake parameters

The parameters EGP_{max}, p_G and S_I are the remaining parameters to explicitly determine from the data. As a result of using EGP_{max} at $G = 0$, the parameters p_G and S_I incorporate the effects of insulin and blood glucose concentration to inhibit endogenous glucose production. Finally, the range of EGP_{max} in Figure 2.4 delimits the acceptable values for this parameter, but not a specific population or patient-specific value.

A grid search was performed to determine the optimal population values of EGP_{max} and p_G for this cohort. In particular, p_G was found to be relatively constant in an adult intensive care population [Hann et al., 2005], and is initially assumed so here. However, no such indication exists for EGP_{max}.

To this end, the time-varying parameter S_I was fitted to the clinical data using several values of EGP_{max} held constant within the range of [0.01442 - 0.03396] mmol/kg/min, based on Figure 2.4. The range of EGP_{max} assessed in simulation extends beyond the 5%-95% range shown in Figure 2.4 to more fully observe the effect of this model parameter. The value of p_G was also held constant within the range [0.0005 - 0.02] min^{-1}. This range of p_G is based on a wide range of adult results [Doran, 2004] with no further data or indication available for the neonate.

The time-varying S_I profile found for each (p_G, EGP_{max}) pair for values is smoothed using a 3-point moving average to reduce any effects of sensor noise. The smoothed insulin sensitivity profile was then used to generate a model derived BG curve to compare to the clinical data and thus assess the model. A total of 2,000 such assessments were made over the ranges of p_G and EGP_{max} for the 25 patient cohort with S_I identified for each (p_G, EGP_{max}) set of values.

The median and IQR of absolute fitting error and prediction error were the metrics used to compare the ability of the model to fit the data for any set of parameters. Fitting error was assessed by analyzing the absolute percentage difference between measured blood glucose concentration and identified model generated blood glucose concentration. Prediction error is clinically more important and was assessed over 1, 2, 3 and 4-hour intervals. Predictions were generated at each blood glucose measurement by holding all parameter values constant over the prediction interval. Prediction error was analyzed by comparing the error between the predicted blood glucose concentration and its measured value, or where a measurement was not available the prediction was compared to a linearly interpolated value between two appropriate blood glucose measurements. The optimal or best (p_G, EGP_{max}) values are thus those that provide the best outcomes in these fitting and prediction metrics.

Hence, the goal of this model is to provide a vehicle for real-time blood glucose control. It is therefore desirable to minimise the number of patient-specific parameters to be identified to avoid identifiability issues with limited (glucose only) measurements. This issue is particularly important in this neonatal case where real-time tracer studies are not viable and control must be based upon a very minimal number and volume of blood samples compared to the adult case. This latter point is a salient difference from the critically ill adult case where the blood sampling frequency used is primarily a question of clinical burden. Therefore, the model must provide better longer term prediction performance at 2 or more hours forward, which is dependent on good identification.

Figure 3.2 shows that median fit and prediction errors, comparing model and measured glucose values, plateau at minimum levels. These results suggest that a range of values for p_G and EGP_{max} will provide robust fitting and prediction performance. In particular, Figure 3.2 also shows the 1, 2, 3 and 4-hour prediction errors over these same ranges result in similar plateaus of minimal error for p_G

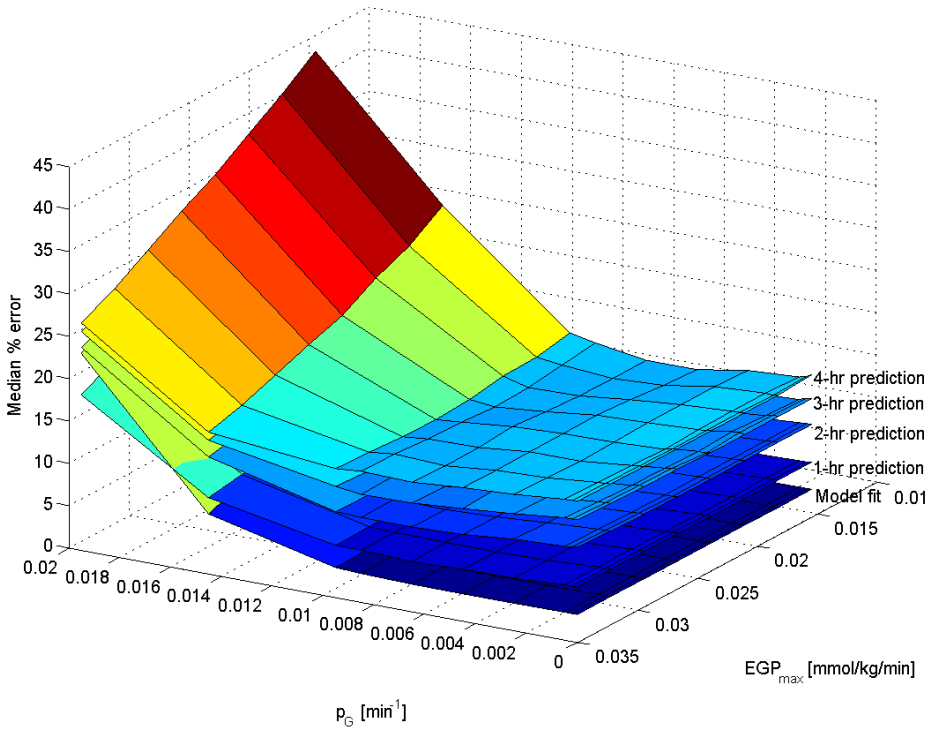

Figure 3.2: Median cohort percentage fit error and model prediction error for several values of endogenous glucose production (EGP_{max}) and endogenous glucose clearance (p_G). Fit and prediction quality is very robust to the value of p_G and EGP_{max} utilised.

< 0.01 min^{-1} and $EGP_{max} > 0.02$ mmol/kg/min.

Maximum per-patient fitting error acts as a more sensitive additional assessment metric. This provides more weight to areas of poor fit and prediction instead of overall fit quality. This aspect is important from a safety standpoint, as it is more likely that isolated cases of poor model fit and/or prediction will compromise safety and it is thus very important that these instances are highlighted.

The sum of the maximum five BG fitting errors per patient profile was used to choose the optimum values of p_G and EGP_{max} within the plateau region of Figure 3.2. The combination of $p_G = 0.003$ min^{-1} and $EGP_{max} = 0.02838$ mmol/kg/min provided the smallest sum of maximum fitting errors across the entire cohort.

3.3.2 Parameter sensitivity

A parameter sensitivity analysis was performed on the model and retrospective data to determine the effect of assumed population constants on the model fit and prediction performance. Population parameters in this model are estimated from literature data, or adapted from adult data where no information on the parameter in neonates was available. The model parameters p_G and EGP_{max} are robust to reasonable estimation errors as shown in the Section 3.3.1. The robustness of the model to the variations in the remaining population constant parameters is assessed in this section.

This parameter analysis explores two effects stemming from using population constants in the model:

Model sensitivity to errors in population constants: This sensitivity is assessed by comparing the model fit and prediction performance for variations in population constants over the whole cohort.

Appropriateness of using a particular population-based constant: This aspect is assessed by comparing model fit and prediction errors on a per-patient basis for variations in population constants to determine whether significantly different or better performance is achieved.

The constants α_I, CNS, k, k_{pr}, k_{pd}, n, V_G and V_I were varied by -50%, -10%, +10% and +50%. The retrospective cohort data was re-fitted for each parameter variation. BG fit and prediction analyses were performed to assess performance to address the questions above.

A model sensitivity analysis was performed for the adult ICU case by [Hann et al., 2005], and found relatively little difference in insulin sensitivity and model performance for up to 20% variation in the parameters n, k, α_G, and α_I. Additionally, p_G was shown to exhibit little variation, compared to insulin sensitivity. However, differences between adult and neonatal physiology, as well as clinical practices may weight the sensitivity of the model to variations in these parameters differently. Such differences, if they exist, may also provide unique insight.

The results in Table 3.4 and Figure 3.3 show that the model performance is

Table 3.4: Sensitivity of model BG fit and prediction to variations in population parameters within retrospective cohort. Values are presented as medians across retrospective cohort.

(a) Model BG fit error.

	Parameter variation			
	-50%	-10%	+10%	+50%
α_I	2.2%	2.2%	2.2%	2.2%
CNS	2.3%	2.2%	2.2%	2.2%
k	2.1%	2.2%	2.2%	2.3%
k_{pd}	2.2%	2.2%	2.2%	2.2%
k_{pr}	2.2%	2.2%	2.2%	2.2%
n	2.2%	2.2%	2.2%	2.2%
V_G	2.8%	2.3%	2.2%	1.9%
V_I	2.2%	2.2%	2.2%	2.2%

(b) 1-hr absolute BG prediction error.

	Parameter variation			
	-50%	-10%	+10%	+50%
α_I	5.0%	5.0%	5.1%	5.0%
CNS	5.1%	5.0%	5.0%	5.0%
k	5.1%	5.0%	5.0%	5.0%
k_{pd}	5.0%	5.1%	5.0%	5.1%
k_{pr}	5.0%	5.1%	5.1%	5.0%
n	4.9%	5.0%	5.0%	5.0%
V_G	6.3%	5.2%	4.9%	4.7%
V_I	5.1%	5.0%	5.0%	4.9%

(c) 2-hr absolute BG prediction error.

	Parameter variation			
	-50%	-10%	+10%	+50%
α_I	8.8%	8.8%	8.8%	8.9%
CNS	9.0%	8.8%	8.8%	8.9%
k	8.9%	8.8%	8.9%	8.9%
k_{pd}	8.9%	8.8%	8.8%	8.8%
k_{pr}	8.8%	8.8%	8.8%	8.9%
n	8.7%	8.8%	8.8%	8.9%
V_G	10.3%	9.1%	8.7%	8.3%
V_I	9.3%	8.9%	8.7%	8.6%

(d) 3-hr absolute BG prediction error.

	Parameter variation			
	-50%	-10%	+10%	+50%
α_I	11.4%	11.4%	11.4%	11.4%
CNS	11.3%	11.4%	11.4%	11.4%
k	11.4%	11.4%	11.3%	11.2%
k_{pd}	11.4%	11.4%	11.4%	11.3%
k_{pr}	11.3%	11.4%	11.4%	11.4%
n	11.2%	11.4%	11.4%	11.5%
V_G	12.4%	11.6%	11.2%	10.8%
V_I	11.6%	11.4%	11.4%	11.4%

(e) 4-hr absolute BG prediction error.

	Parameter variation			
	-50%	-10%	+10%	+50%
α_I	13.1%	13.1%	13.1%	13.2%
CNS	13.2%	13.1%	13.1%	12.9%
k	13.%	13.0%	13.2%	13.3%
k_{pd}	13.1%	13.1%	13.1%	13.0%
k_{pr}	13.%	13.1%	13.1%	13.2%
n	13.1%	13.1%	13.2%	13.3%
V_G	14.5%	13.2%	13.1%	13.0%
V_I	13.6%	13.2%	13.2%	13.1%

relatively insensitive to the variations in population constants introduced here. The volume of glucose distribution, V_G, created the greatest effect on model performance at -50% of the population value used here, which is a very large change for a typically well known or understood parameter. A reduction of V_G of 50% brings this volume closer to the value used for adults in proportion to body weight. Thus, recognising the increased proportion of body weight taken up as extra-cellular fluid in neonates is seen to be relevant to accurate glucose control. This last result provides a further model validation, in that good model performance requires accurate neonatal physiology where such differences to adults are known to exist.

The applicability of constant population parameter values for this model was tested by assessing the per-patient fit and prediction errors for each population constant parameter. The BG fit and 1-hour prediction errors are presented for the parameter V_G in Tables 3.5 and 3.6, which are also the worst-case scenario based on the whole-cohort results of Table 3.4 and Figure 3.3. Variation in the other population parameters produced similar inter-patient variations in model performance, but decreased in absolute magnitude.

Thus, the model is overall robust to moderate errors in population parameters. Additionally, the choice of population parameters appears appropriate for the cohort as a whole, as no particular patients exhibited significantly better model fit or prediction performance when variations in population constants were introduced. The maximum difference in fit and prediction performance results are presented in Tables 3.5 and 3.6 for each patient to identify any individual patient records that are particularly sensitive to the parameter changes.

The median per-patient model fit errors showed largely little inter-patient variation. The maximum difference in fit performance was less than 2% for 24 of 25 patients. Similarly, the maximum difference in 1-hr prediction performance was less than 4.2% for 24 of 25 patients. The greatest contributor to this metric was the 50% reduction in glucose distribution volume, V_G. If the results for this parameter reduction are neglected, the maximum difference between results per-patient drops to $< 2.7\%$ for all patients.

The largest error results belongs to Patient 13. This patient spent a large amount of time off insulin, and thus provides a ‘stress-test’ for the model to

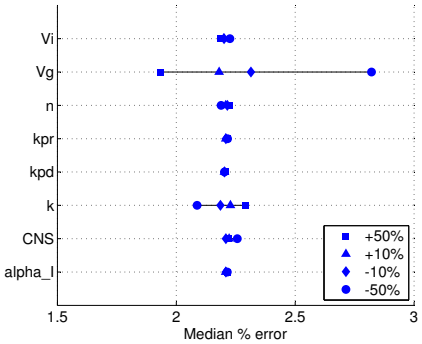

(a) Model BG fit error.

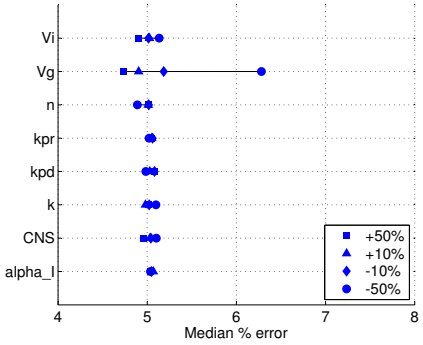

(b) 1-hr BG prediction error.

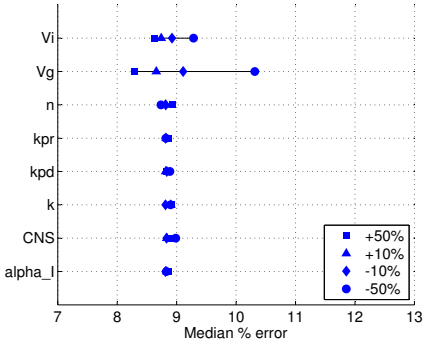

(c) 2-hr BG prediction error.

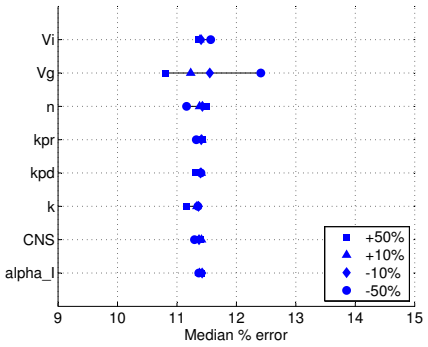

(d) 3-hr BG prediction error.

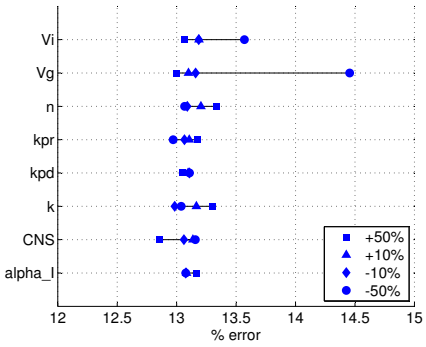

(e) 4-hr BG prediction error.

Figure 3.3: Model fit and prediction sensitivity to population parameters.

handle the clinically likely periods off insulin. The relatively large maximum errors in fit and prediction result from increased errors when simulating a 50% reduction in the glucose volume of distribution. This outlying result further supports the use of a volume of glucose distribution, V_G, that is more compatible with the body fluid compartment proportions reported in neonatal literature. This result also highlights that periods without insulin infusions in particular are more sensitive to variations in the assumed glucose volume of distribution, likely due to the significant variability in observed endogenous insulin production (I_B

Table 3.5: Per-patient model fit performance sensitivity to variations in V_G. Max. diff. indicates the maximum difference in performance between results for any two values of V_G.

Patient	-50%	-10%	+10%	+50%	Max. diff.
1	3.0%	2.5%	2.4%	2.3%	0.6%
2	2.9%	1.9%	1.8%	1.5%	1.4%
3	3.4%	2.3%	2.1%	1.8%	1.6%
4	2.1%	1.5%	1.3%	1.3%	0.8%
5	3.7%	2.8%	2.5%	2.0%	1.8%
6	3.7%	3.5%	3.4%	4.9%	1.5%
7	2.8%	1.5%	1.2%	1.3%	1.6%
8	2.4%	1.6%	1.2%	1.0%	1.4%
9	1.1%	1.1%	1.2%	1.2%	0.1%
10	3.7%	2.5%	2.3%	2.0%	1.7%
11	1.4%	1.2%	1.2%	1.3%	0.2%
12	0.6%	0.6%	0.7%	0.7%	0.2%
13	5.3%	2.1%	2.2%	2.6%	3.3%
14	1.9%	1.2%	1.0%	1.3%	0.9%
15	2.4%	2.1%	1.7%	1.6%	0.8%
16	2.6%	1.7%	1.7%	1.4%	1.2%
17	3.9%	3.4%	3.0%	2.1%	1.9%
18	1.8%	1.4%	1.3%	1.4%	0.5%
19	2.7%	2.1%	2.1%	2.3%	0.6%
20	3.1%	2.2%	2.0%	1.6%	1.5%
21	2.7%	2.2%	2.1%	2.0%	0.7%
22	2.6%	2.3%	2.3%	2.0%	0.6%
23	5.9%	5.9%	6.1%	5.8%	0.2%
24	3.4%	3.1%	3.0%	3.0%	0.5%
25	1.4%	0.6%	0.7%	1.0%	0.8%

in the model) and efficacy in neonatal cohorts [Mitanchez-Mokhtari et al., 2004; Meetze et al., 1998; Farrag and Cowett, 2000].

Overall, the population parameter that appeared to have the most influence on model fit and prediction errors was the glucose volume of distribution, V_G. Outside this parameter, the low sensitivity of model performance to the remaining parameters is similar to the adult case [Hann et al., 2005]. This result may imply that, with the right neonatal parameters, neonates and adults exhibit 'similar' metabolic dynamics, which may be unexpected given the differing external clinical management of metabolism in these patient groups.

Table 3.6: Per-patient model 1-hr prediction performance sensitivity to variations in V_G. Max. diff. indicates the maximum difference in performance between results for any two values of V_G.

Patient	-50%	-10%	+10%	+50%	Max. diff.
1	8.4%	7.1%	6.0%	6.1%	2.3%
2	4.9%	3.8%	4.0%	3.3%	1.6%
3	6.5%	4.2%	3.2%	2.8%	3.6%
4	3.9%	3.7%	3.5%	3.5%	0.4%
5	4.9%	3.5%	3.5%	3.3%	1.6%
6	6.3%	5.9%	5.8%	5.4%	1.0%
7	4.8%	3.5%	3.0%	2.6%	2.3%
8	5.5%	3.2%	3.4%	2.6%	3.0%
9	5.3%	4.6%	4.3%	3.6%	1.7%
10	7.8%	6.3%	6.5%	7.8%	1.5%
11	4.9%	5.0%	4.8%	3.7%	1.2%
12	8.1%	5.4%	5.5%	5.5%	2.7%
13	12.9%	7.4%	6.9%	4.8%	8.2%
14	3.4%	5.0%	5.1%	4.8%	1.7%
15	4.4%	4.0%	4.5%	4.7%	0.7%
16	5.0%	3.1%	3.1%	3.5%	2.0%
17	6.0%	4.8%	6.9%	6.8%	2.1%
18	5.6%	5.0%	4.8%	4.9%	0.8%
19	7.7%	4.4%	4.0%	3.5%	4.2%
20	8.2%	5.8%	4.9%	4.3%	3.9%
21	5.6%	5.3%	4.9%	4.8%	0.8%
22	5.7%	4.7%	4.3%	4.4%	1.4%
23	11.4%	10.9%	11.0%	11.3%	0.5%
24	7.1%	6.1%	5.2%	5.4%	1.8%
25	5.5%	5.3%	5.5%	5.4%	0.2%

3.3.3 The impact of assuming constant values for EGP_{max} and p_G

Population values were chosen for the parameters p_G and EGP_{max} based upon model fitting and prediction performance in Section 3.3.1. In this section, the parameter sensitivity analysis is extended to explore the effects of holding these variables as population constants using a 'fit-predict' method. More specifically, should they be constant or time-varying and what is therefore the impact of holding them constant?

The parameters to be tested were held piecewise-constant over a period of

time, and re-evaluated at the end of each period. In this case, periods of 1 and 6 hours were used. At the end of each period, the model is re-simulated several times over the previous 1 or 6 hours of data using a different value of the parameter each time to determine which value would have, in retrospect, given the best 1-hour prediction performance. This best performing parameter value is then used over the next 1-hour or 6-hour period.

In an additional analysis, both p_G and S_I were fitted simultaneously using the integral-based fitting method. These simulations would thus generate parameters that produce an optimal fit on a per-patient basis, and track any potential changes in this parameter over time. CDF plots of p_G, EGP_{max} and S_I were used to examine the behaviour and interaction of these parameters.

The fit and prediction results are shown in Table 3.7. Allowing variations in the endogenous glucose production parameter, EGP_{max}, overall produced fit and prediction results similar to holding the parameter constant, with slightly worse prediction performance. The CDF of EGP_{max} values selected by the fit-predict method showed values tended towards the upper limit of the allowable EGP range. In contrast, the fit-predict method selected p_G values at either the upper or lower limit of the allowable range. These results created greater variability in fitted insulin sensitivity, as shown by a flatter CDF. Thus, these effects combine to create significantly worse fit and prediction results.

Finally, using the integral-based method to fit p_G generated slightly better BG fit results, however prediction performance was significantly weakened. Additionally, the resulting shape of the insulin sensitivity distribution was different to all other results. All these results highlight parameters trading-off with each other when fitting multiple parameters to serial BG measurements.

3.3.4 Effect of enteral feed on model prediction

The enteral feed model used in this study was adapted from the similar model used successfully in adult intensive care. This model accounts for delays in the appearance of glucose in the bloodstream from changes in the enteral infusion rate, and accounts for differing rates due to increases and decreases in feed rates.

Table 3.7: Fitting and prediction errors using the fit-predict parameter selection method. All fit and prediction errors are quoted as Median [IQR]. Cumulative distribution functions over the cohort of the parameter values selected by the fit-predict method are shown. Vertical lines indicate the parameter was held constant for the set of simulations.

	Constant	**Fit and predict method**				**Fitted**
	Constant EGP_{max}, p_G	EGP hourly	EGP 6-hourly	pG hourly	pG 6-hourly	pG fitted
Fit error	2.50% [1.0% - 5.3%]	3.00% [1.1%-6.3%]	2.50% [1% - 5.5%]	5.60% [2.3%-10.6%]	3.30% [1.3%-7.1%]	2.30% [1.0%-5.0%]
1-hr prediction	5.80% [2.6%-11.2%]	6.40% [3.0%-12.2%]	6.80% [3.0%-12.5%]	9.80% [4.6%-17.1%]	12.80% [4.6%-25.2%]	11.60% [4.6%-21.6%]
2-hr prediction	9.90% [4.5%-19.3%]	11.30% [5.1%-20.5%]	11.50% [5.1%-20.7%]	15.50% [7.3%-26.7%]	19.40% [7.5%-36.2%]	17.50% [7.5%-34.3%]
3-hr prediction	12.40% [5.5%-23.8%]	13.10% [6.0%-24.9%]	14.10% [6.2%-25.4%]	18.20% [8.8%-31.9%]	22.40% [9.2%-43.0%]	20.80% [8.5%-41.3%]
4-hr prediction	14.50% [6.3%-27.2%]	15.30% [7.3%-28.0%]	15.90% [7.3%-29.1%]	19.40% [9.8%-35.2%]	24.10% [10.8%-46.5%]	22.90% [9.5%-45.9%]
p_G	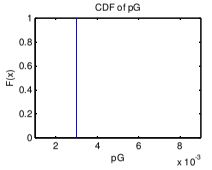	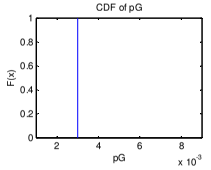	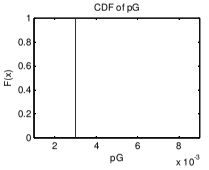	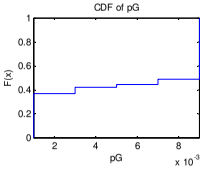	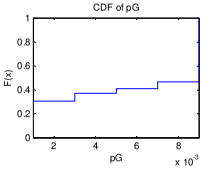	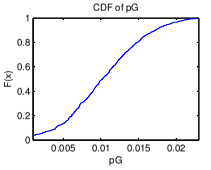
EGP_{max}	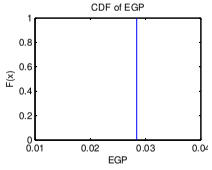	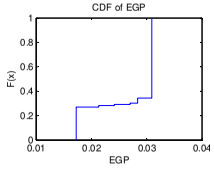	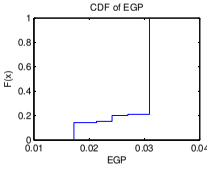	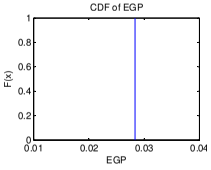	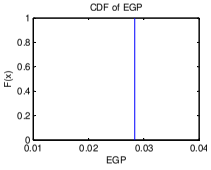	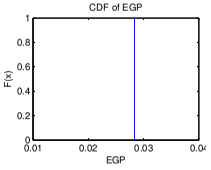
S_I	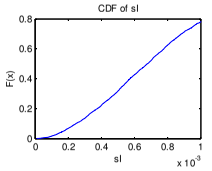	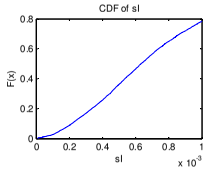	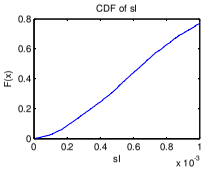	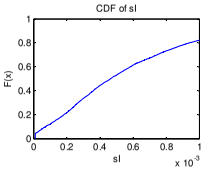	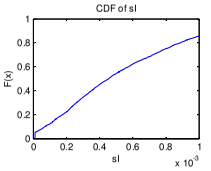	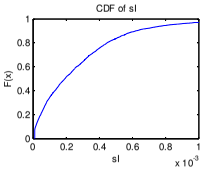

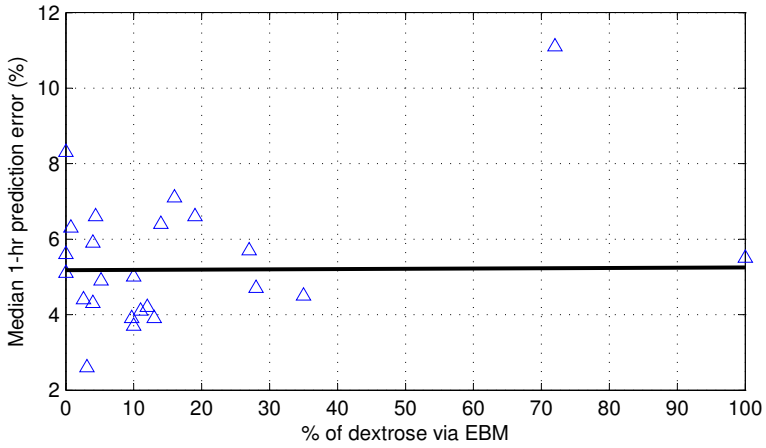

Figure 3.4: Model 1-hr prediction error against proportion of dextrose fed via enteral route. Each individual point represents a single retrospective patient. The fitted line shows the correlation neglecting the outlying Patient 23 ($R^2 = 2.2\text{x}10^{-4}$, $p = 0.94$). EBM = Expressed Breast Milk.

Enteral feeding represents a minority route for dextrose into the body for these patients. Over half of the retrospective cohort had at least 90% of dextrose administered via the intravenous parenteral route or TPN. Figure 3.4 shows the effect of the proportion of dextrose fed via EBM against the median 1-hour model prediction error. The outlying point belongs to Patient 23, who, as will be described in Section 4.2, experienced much more rapid swings in glucose control compared to other patients despite relatively constant nutritional inputs. Neglecting this outlying point there is no significant correlation between proportion of dextrose via EBM and model prediction performance ($p = 0.94$).

3.3.5 Insulin pump and tubing adsorption errors in model

Daily fluid balances are a critical component of neonatal intensive care. The small volume of the neonate necessitates very low pump flow rates for infusions. These flow rates are often near the limit of accuracy for many pumps. Additionally, adsorption of insulin to the walls of the plastic tubing from the pump to the patient has been shown to alter the net amount of insulin delivered to the patient in laboratory studies [Hewson et al., 2000; Fuloria et al., 1998; Zahid et al., 2008]. Christchurch Women's Neonatal Department flushes all insulin tubing with insulin solution prior to use to saturate the tube binding sites and minimize

this latter delivery variation.

To explore these effects on the model prediction performance, four case scenarios were simulated to assess the impact. These scenarios adjusted the insulin input into the model ($u_{ex}(t)$ in Equation 2.30) to simulate typically reported effects:

- Baseline model. No change to retrospectively recorded insulin rates.
- Pump error model. When pump rate increases, 40% of the change occurs immediately, and the remaining 60% occurs after 5 - 60 minutes, depending on the new pump rate. Assumes decreases/stoppages are instant. Data for this scenario model was adapted from the Alaris CC pump instruction manual [Cardinal Health, 2008].
- Tubular adsorption model. When insulin is started from zero-rate, assume 60% is available instantly, up to 85% after 2 hours. Data adapted from [Hewson et al., 2000].
- Smoothed insulin. Insulin rate is smoothed using 3-point moving average if infusion rate of zero is not present.

An example of the pump error model, tubular adsorption model and smoothed insulin is shown in Figure 3.5. The effect of the insulin delivery models on 1-hour prediction performance are shown in Table 3.8.

Overall, the insulin delivery models present a relatively small impact to the overall performance of the model both in a whole-cohort and per-patient sense. The tubular adsorption and pump models have a relatively small impact on the insulin delivery rate for typical-to-worst-case values reported in the literature and technical documentation. In particular, no individual patient shows dramatic changes in prediction performance accounting for the various errors.

More specifically, the insulin smoothing model accounts for errors during the data recording and collection process. Infusions in the Christchurch Women's Hospital Neonatal Department are recorded as a cumulative amount for the day to aid in assessing daily fluid balances. Thus, pump flow rates are obtained by taking the first difference of the recorded data. This process is thus susceptible

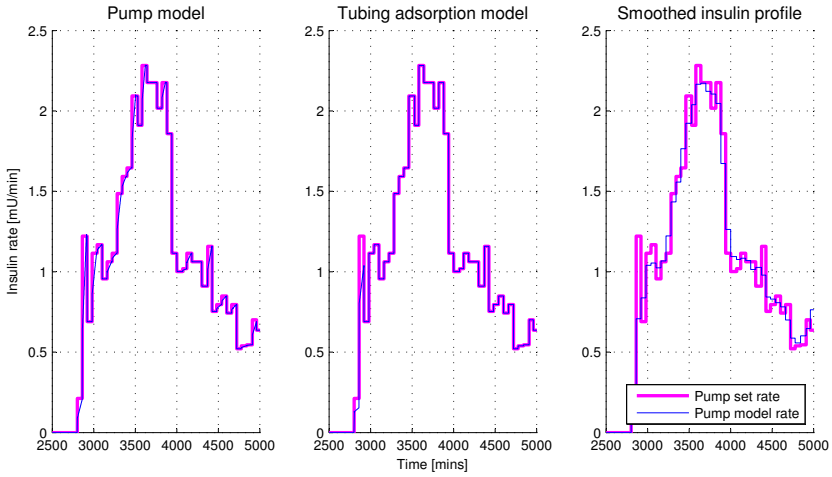

Figure 3.5: Effect of tubular adsorption models and pump error models on net insulin flow rate. The pump set rate represents the intended flow rate as set at the pump. The pump model rate represents the net rate of insulin reaching the patient.

to noise from errors in the time the observation was recorded. Additionally, pump displays typically report in units of 0.1 or 0.01 mL, and this rounding may introduce a relatively large error given the very low flow rates. However, the insensitivity of model prediction performance to smoothed and un-smoothed insulin data suggests these errors are minor and relatively evenly dispersed, as well as that they may provide both reductions and increases in errors that effectively cancel in summary. This last result would imply that these effects are thus inside the effective model resolution, which, given the generally low prediction errors compared to measurement errors, means they have little impact.

3.4 Summary

A model of the glucose regulatory system has been adapted from adult critical care to the neonatal case. Model fit and prediction performance was found to be robust to a range of values for endogenous glucose production and non-insulin mediated glucose clearance parameter values. Further parameter sensitivity analysis found model performance, when known neonatal physiology was accounted for, was insensitive to relatively large deviations in population-constant parameters. Finally, the integral-based fitting method was presented as an efficient parameter estimation procedure for both *in-silico* and real-time clinical utility.

Table 3.8: Tubular absorption and insulin pump model effects on 1-hour BG prediction performance. Values are median 1-hr prediction error (%) and [Average of largest 5 errors (%)]

Patient	Baseline model	Pump-model	Tubing model	Smoothing insulin
1	6.6% [48.0%]	7.9% [43.6%]	8.0% [44.5%]	6.8% [44.0%]
2	4.2% [23.7%]	4.8% [23.2%]	4.5% [24.0%]	4.0% [24.6%]
3	4.2% [19.6%]	5.0% [25.0%]	5.3% [25.1%]	3.2% [23.2%]
4	3.7% [24.6%]	4.2% [22.5%]	4.4% [23.0%]	4.1% [23.0%]
5	3.9% [16.0%]	4.7% [17.9%]	4.2% [17.8%]	2.8% [16.6%]
6	6.3% [21.6%]	6.3% [23.2%]	6.3% [23.4%]	6.3% [23.9%]
7	3.9% [15.3%]	3.7% [16.7%]	3.7% [17.4%]	3.1% [14.8%]
8	4.5% [12.2%]	5.5% [11.8%]	5.0% [12.2%]	4.6% [12.3%]
9	4.3% [11.6%]	5.1% [11.2%]	5.2% [11.2%]	4.9% [10.4%]
10	6.4% [22.2%]	5.9% [25.4%]	5.5% [28.9%]	6.6% [21.8%]
11	4.9% [18.4%]	4.8% [19.6%]	5.2% [19.4%]	5.3% [19.3%]
12	5.6% [12.8%]	5.7% [11.1%]	5.7% [11.1%]	5.7% [10.4%]
13	8.3% [22.4%]	8.3% [18.6%]	7.4% [14.0%]	7.4% [18.6%]
14	5.0% [17.3%]	5.1% [19.6%]	5.3% [19.8%]	4.4% [18.4%]
15	4.1% [22.8%]	5.0% [23.2%]	4.5% [22.8%]	3.3% [22.4%]
16	2.6% [13.5%]	3.6% [12.9%]	3.5% [12.3%]	3.6% [13.6%]
17	7.1% [16.7%]	7.6% [16.7%]	8.7% [18.0%]	5.2% [15.3%]
18	4.7% [8.6%]	5.1% [9.0%]	5.1% [9.2%]	4.8% [9.0%]
19	5.1% [14.3%]	6.0% [10.8%]	4.3% [12.8%]	4.6% [12.7%]
20	6.6% [21.0%]	8.1% [22.0%]	8.1% [22.4%]	6.9% [20.0%]
21	5.9% [12.4%]	6.2% [17.2%]	6.7% [17.1%]	5.9% [17.1%]
22	4.4% [31.5%]	4.9% [31.8%]	4.7% [31.8%]	4.0% [32.7%]
23	11.1% [44.1%]	10.8% [44.5%]	10.8% [43.9%]	11.1% [46.4%]
24	5.7% [28.8%]	7.9% [32.4%]	8.8% [32.5%]	7.8% [33.1%]
25	5.5% [13.5%]	4.6% [11.3%]	4.6% [10.5%]	6.0% [12.5%]
Cohort	5.2% [25.8%]	5.8% [26.4%]	5.8% [26.5%]	5.2% [26.3%]

Chapter 4

Model validation on retrospective clinical data

This chapter presents the overall and complete validation of the model on retrospective clinical data using the final parameter values selected in Chapter 3. Model validation was assessed through ability to fit the data and capture patient dynamics, as well as its ability to provide predictions for future blood glucose concentration. Thus, there is some overlap between Chapters 3 and 4, which is repeated here for completeness of this critical part of the study. Finally, the variation in fitted insulin sensitivity in neonates is compared to adult critical care patients and the influence of several clinical variables on insulin sensitivity is investigated, as well as a brief analysis of these distributions and their potential impact on control.

4.1 Model fit to clinical data

The ability of the model to fit clinical data with a given identified set of physiologically relevant parameters validates whether the mathematically modelled dynamics are able to capture the clinical dynamics observed in the data.

Table 4.1 shows the median and IQR for absolute percentage model fit error and absolute fit error in mmol/L for the 3,567 hours of patient data over 25 patient episodes described previously in Table 3.2. The median absolute cohort model fit error was 2.4% or 0.2 mmol/L. The median non-absolute model fitting error was 0.2% indicating no significant tendency for the model fits to over-shoot or under-shoot BG concentration. The insulin sensitivity smoothing process results in a more physiological profile at the expense of a potentially greater fit error. Two

Table 4.1: Relative and absolute model fitting error for NICU cohort for $p_G = 0.003$ min^{-1} and $EGP_{max} = 0.02838$ mmol/kg/min.

Patient	Length of fit [hours]	Percentage fit error		Absolute fit error [mmol/L]	
		Median	IQR	Median	IQR
1	305	2.6%	[1.3%-5.4%]	0.2	[0.1-0.4]
2	334	2.0%	[1.0%-3.8%]	0.2	[0.1-0.3]
3	211	2.7%	[0.6%-5.1%]	0.2	[0.1-0.3]
4	288	1.5%	[0.5%-3.6%]	0.1	[0.0-0.3]
5	142	3.0%	[1.2%-5.2%]	0.2	[0.1-0.3]
6	94	3.6%	[1.8%-5.3%]	0.3	[0.1-0.4]
7	110	2.1%	[0.6%-2.9%]	0.2	[0.0-0.2]
8	103	1.6%	[0.9%-1.9%]	0.1	[0.1-0.2]
9	91	1.0%	[0.3%-2.9%]	0.1	[0.0-0.2]
10	65	2.6%	[1.2%-4.5%]	0.1	[0.1-0.3]
11	118	1.3%	[0.8%-2.3%]	0.1	[0.1-0.2]
12	34	0.6%	[0.1%-1.8%]	0.0	[0.0-0.1]
13	58	2.1%	[1.0%-5.0%]	0.2	[0.0-0.4]
14	182	1.3%	[0.6%-4.4%]	0.1	[0.1-0.3]
15	206	2.1%	[0.8%-4.7%]	0.2	[0.1-0.3]
16	43	1.8%	[0.9%-4.0%]	0.2	[0.1-0.3]
17	46	4.5%	[1.4%-7.4%]	0.3	[0.1-0.4]
18	91	1.5%	[0.5%-2.8%]	0.1	[0.0-0.2]
19	43	2.4%	[1.0%-3.6%]	0.2	[0.1-0.2]
20	113	2.3%	[1.2%-3.8%]	0.2	[0.1-0.4]
21	139	2.2%	[1.2%-4.1%]	0.2	[0.1-0.4]
22	283	2.2%	[0.8%-4.9%]	0.2	[0.1-0.4]
23	305	6.2%	[2.9%-11.5%]	0.6	[0.2-1.1]
24	142	3.1%	[1.3%-6.6%]	0.3	[0.1-0.6]
25	31	0.6%	[0.4%-6.2%]	0.1	[0.0-0.5]
Cohort		2.4%	[0.9% - 4.8%]	0.2	[0.1 - 0.4]

of the 25 resulting parameter identifications are presented in Figures 4.1 - 4.2, including measurement error bars to provide context for the fit error.

Table 4.2 shows the median fitting error for all patients, as well as repeating the retrospective lognormal geometric blood glucose mean, geometric standard deviation, median insulin rate and median dextrose delivered. The results show a relatively constant level of fitting error spanning a range of cases of relatively unstable blood glucose, indicated by a higher standard deviation and/or higher mean blood glucose. They also show varying levels of insulin and glucose administration over these same results. Thus, there is no apparent bias in fitting error with respect to glucose level, glucose variability, or intervention.

Table 4.2: Quality of fit per-patient compared to model inputs. $BG_{geo,mean}$ and $BG_{geo,SD}$ represent the lognormal geometric mean and standard deviation respectively.

Patient	Median fit error	$BG_{geo,mean}$ [mmol/L]	$BG_{geo,SD}$	Median insulin [U/kg/hr]	Median dextrose rate	
					[mg/kg/min]	[kcal/kg/day]
1	2.6%	6.8	1.30	0.091	8.9	51.2
2	2.0%	7.8	1.12	0.053	10.4	59.7
3	2.7%	7.5	1.18	0.050	9.0	51.6
4	1.5%	7.6	1.15	0.026	8.2	47.5
5	3.0%	8.0	1.17	0.037	10.5	60.6
6	3.6%	7.3	1.20	0.037	4.9	28.1
7	2.1%	7.9	1.13	0.092	11.8	68.0
8	1.6%	7.7	1.13	0.031	10.7	61.4
9	1.0%	8.5	1.11	0.026	9.7	56.1
10	2.6%	6.9	1.18	0.025	9.9	56.9
11	1.3%	9.1	1.25	0.047	5.9	34.2
12	0.6%	6.2	1.36	0.047	5.3	30.3
13	2.1%	5.6	1.33	0.025	4.0	23.1
14	1.3%	8.9	1.13	0.029	10.0	57.7
15	2.1%	7.9	1.17	0.053	9.2	52.8
16	1.8%	8.2	1.17	0.040	5.0	28.6
17	4.5%	6.3	1.21	0.059	11.4	65.4
18	1.5%	7.7	1.10	0.025	8.3	47.5
19	2.4%	8.3	1.20	0.050	11.3	65.2
20	2.3%	8.4	1.14	0.030	14.1	81.4
21	2.2%	9.3	1.21	0.022	10.3	59.5
22	2.2%	7.5	1.15	0.027	8.5	49.2
23	6.2%	8.2	1.24	0.077	8.8	50.6
24	3.1%	8.0	1.25	0.017	10.0	57.6
25	0.6%	9.6	1.14	0.030	9.6	55.1

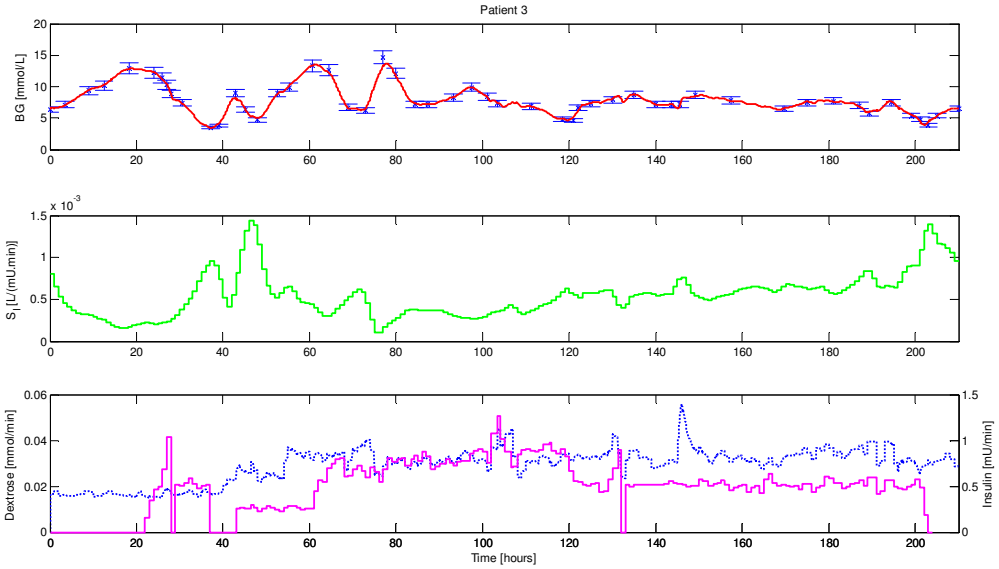

Figure 4.1: Patient 3 blood glucose data fit (top panel, solid line), measured BG concentration (top panel, crosses), corresponding insulin sensitivity S_I (middle panel), and insulin (solid line) and dextrose (dashed line) inputs (bottom panel).

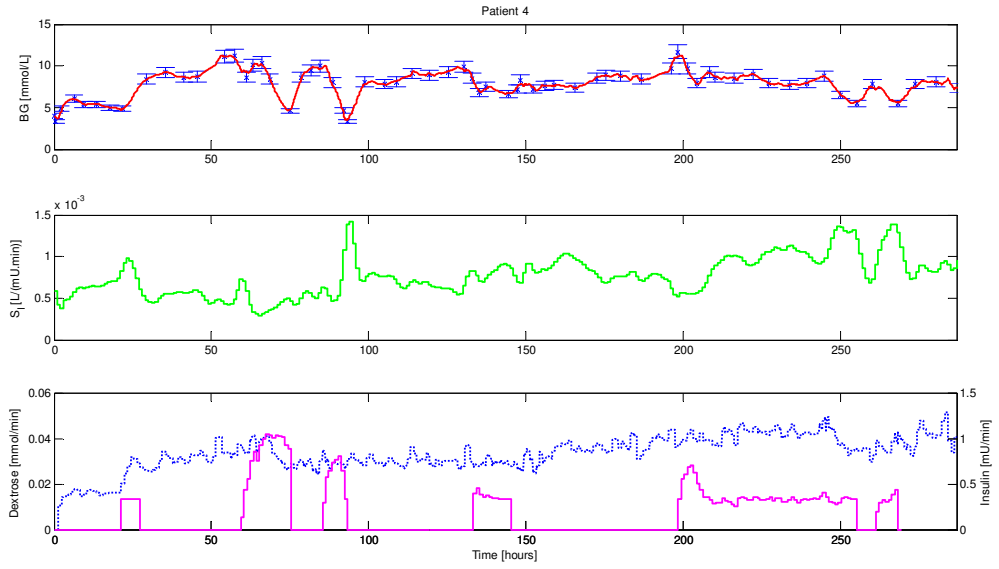

Figure 4.2: Patient 4 blood glucose data fit (top panel, solid line), measured BG concentration (top panel, crosses), corresponding insulin sensitivity S_I (middle panel), and insulin (solid line) and dextrose (dashed line) inputs (bottom panel).

4.2 Model prediction validation

It is imperative that a model used for glycaemic control is able to accurately predict the response to a given clinical intervention. This capability is not the same as being able to fit the data, as in Section 4.1. Many glycaemic control models in the literature do not use or present any form of prediction validation, despite its importance.

Table 4.3 shows the median absolute percentage prediction error for 1, 2, 3 and 4-hour prediction intervals using the final parameter values selected in Section 3.3.1, Chapter 3. The predictions are generated by holding insulin sensitivity constant at the most recent fitted value, and simulating the blood glucose response using this value of S_I over the 1-4 hour prediction interval. Results are compared to blood glucose measurements or linearly interpolated between retrospective measurements where none are available for a given interval.

The cohort median absolute prediction error was 5.2% at 1 hour, 9.4% at 2 hours, 11.9% at 3 hours and 13.6% at 4 hours. This result also emphasizes the importance of frequent blood glucose measurement to provide tighter continuous control and is similar to adult analyses [Hann et al., 2005]. The non-absolute prediction errors for the cohort were -0.2% at 1-hour, -0.3% at 2-hours and -0.8% at 3 and 4 hours. The spread of prediction errors is thus relatively symmetrical about 0%. Figure 4.3 shows the distribution of absolute blood glucose prediction error, with increasing variance as the prediction interval increases. Figure 4.4 summarises these percentage blood glucose prediction results. In particular, 85% of 1-hour predictions and 67% of 2-hour predictions were within ±15% of the linearly interpolated target.

In all these prediction analyses BG is compared to a linearly interpolated value as BG was not always measured at a constant interval or exact hour. Thus, some error may be introduced due to this approximation. In addition, insulin sensitivity was assumed constant over the entire prediction interval, and thus ignores any hour-to-hour changes, which might be significant [Lin et al., 2008]. Thus, this prediction analysis provides an indication of the model ability to broadly capture patient dynamics for prediction in a clinical control scenario. A typical prediction profile is shown in Figure 4.5, where larger discrepancies between model BG value and prediction are evident at longer prediction intervals, as ex-

Table 4.3: Median prediction errors compared to linearly interpolated BG value. Abs. Avg. BG slope is the average of absolute BG slope expressed in [mmol/L/hr].

Patient	1-hour		2-hours		3-hours		4-hours		Avg BG
	Median	IQR	Median	IQR	Median	IQR	Median	IQR	slope
1	6.6%	[3.3%-12.7%]	12.5%	[6.2%-20.9%]	15.6%	[9.2%-27.6%]	22.8%	[8.0%-38.0%]	0.59
2	4.2%	[1.5%-8.8%]	7.9%	[4.0%-14.0%]	11.1%	[3.5%-18.6%]	11.5%	[6.3%-20.1%]	0.33
3	4.2%	[2.2%-7.1%]	6.9%	[3.3%-16.4%]	10.0%	[3.1%-23.7%]	11.9%	[5.9%-26.1%]	0.5
4	3.7%	[1.5%-6.7%]	5.5%	[2.3%-13.1%]	8.5%	[3.5%-15.3%]	8.9%	[4.3%-15.9%]	0.35
5	3.9%	[1.1%-9.3%]	7.7%	[1.9%-12.8%]	6.6%	[3.4%-11.1%]	7.0%	[3.4%-9.9%]	0.73
6	6.3%	[2.8%-10.7%]	12.5%	[8.7%-20.9%]	19.1%	[9.3%-27.4%]	21.9%	[12.9%-34.5%]	0.72
7	3.9%	[1.4%-9.2%]	6.3%	[3.4%-11.1%]	5.1%	[2.9%-10.5%]	6.1%	[4.9%-12.9%]	0.26
8	4.5%	[2.3%-6.8%]	10.9%	[5.1%-18.6%]	13.5%	[7.3%-20.4%]	12.3%	[6.0%-18.8%]	0.35
9	4.3%	[2.1%-7.9%]	4.2%	[1.3%-9.3%]	6.4%	[1.8%-12.8%]	5.2%	[3.1%-14.0%]	0.49
10	6.4%	[3.2%-15.7%]	13.7%	[3.7%-29.1%]	13.3%	[5.7%-24.5%]	21.4%	[12.3%-30.0%]	0.62
11	4.9%	[2.1%-7.9%]	7.5%	[2.6%-16.6%]	13.6%	[6.6%-30.3%]	19.6%	[8.5%-35.1%]	0.64
12	5.6%	[3.1%-9.7%]	10.0%	[6.3%-20.7%]	15.3%	[7.9%-31.5%]	21.0%	[10.3%-38.8%]	0.69
13	8.3%	[4.3%-14.0%]	12.7%	[6.9%-29.3%]	16.7%	[10.6%-56.7%]	16.6%	[9.8%-65.6%]	1.96
14	5.0%	[1.6%-8.6%]	8.1%	[1.9%-14.9%]	7.8%	[3.3%-18.4%]	12.7%	[5.7%-19.8%]	0.55
15	4.1%	[2.3%-9.3%]	8.5%	[3.1%-15.7%]	12.3%	[5.9%-21.2%]	13.0%	[6.1%-22.8%]	0.46
16	2.6%	[1.7%-8.8%]	6.8%	[2.7%-9.9%]	11.2%	[5.2%-25.8%]	12.4%	[4.4%-24.2%]	0.57
17	7.1%	[2.2%-8.3%]	8.8%	[4.0%-17.2%]	15.9%	[7.9%-25.2%]	11.3%	[10.4%-23.9%]	0.56
18	4.7%	[4.3%-6.8%]	6.2%	[4.2%-9.6%]	5.9%	[2.8%-9.8%]	6.7%	[5.0%-11.5%]	0.31
19	5.1%	[2.9%-10.3%]	11.5%	[6.8%-15.1%]	14.3%	[4.7%-29.4%]	18.2%	[10.0%-42.2%]	0.39
20	6.6%	[2.6%-10.1%]	9.7%	[3.9%-18.3%]	14.3%	[5.0%-26.6%]	15.4%	[6.3%-29.4%]	0.56
21	5.9%	[4.1%-8.3%]	11.6%	[6.4%-17.7%]	14.3%	[7.5%-23.8%]	18.5%	[6.5%-29.7%]	0.66
22	4.4%	[2.2%-10.0%]	7.2%	[3.8%-16.7%]	8.9%	[4.1%-18.5%]	10.8%	[4.5%-23.0%]	0.58
23	11.1%	[4.9%-19.3%]	17.4%	[7.3%-34.2%]	17.3%	[7.8%-35.5%]	18.7%	[10.0%-38.3%]	1.41
24	5.7%	[2.5%-15.0%]	10.4%	[5.2%-25.7%]	13.7%	[6.7%-31.3%]	17.7%	[6.4%-34.6%]	0.94
25	5.5%	[3.2%-11.7%]	10.9%	[8.5%-18.7%]	12.8%	[8.0%-24.2%]	11.8%	[7.1%-22.5%]	0.89
Cohort	5.2%	[2.5%-10.3%]	9.4%	[4.5%-18.4%]	11.9%	[5.1%-23.7%]	13.6%	[6.3%-27.6%]	

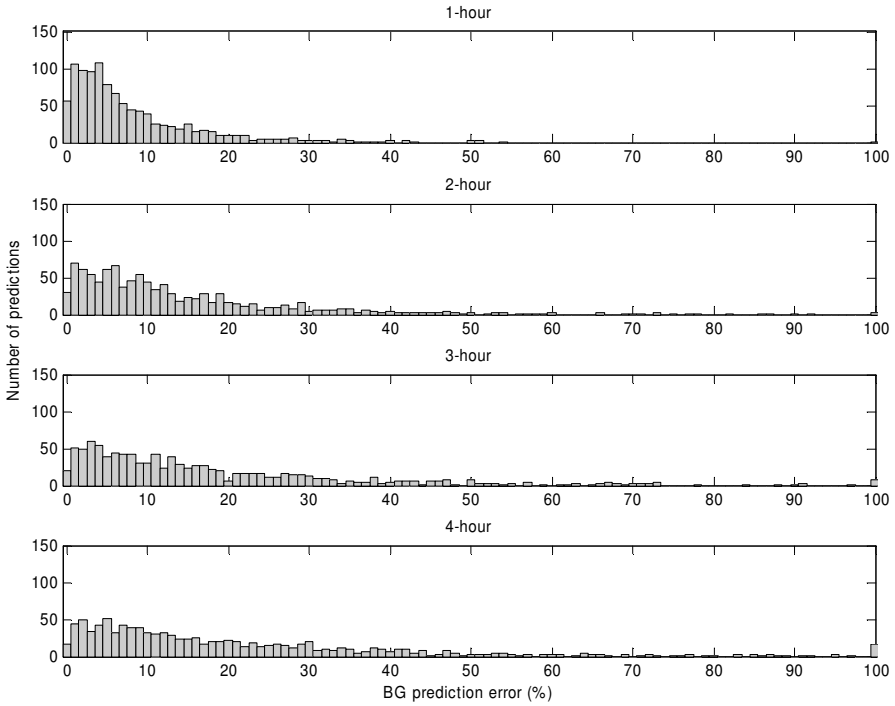

Figure 4.3: Distribution of blood glucose prediction errors at 1, 2, 3 and 4-hour prediction intervals. Summary statistics are presented in Table 4.3.

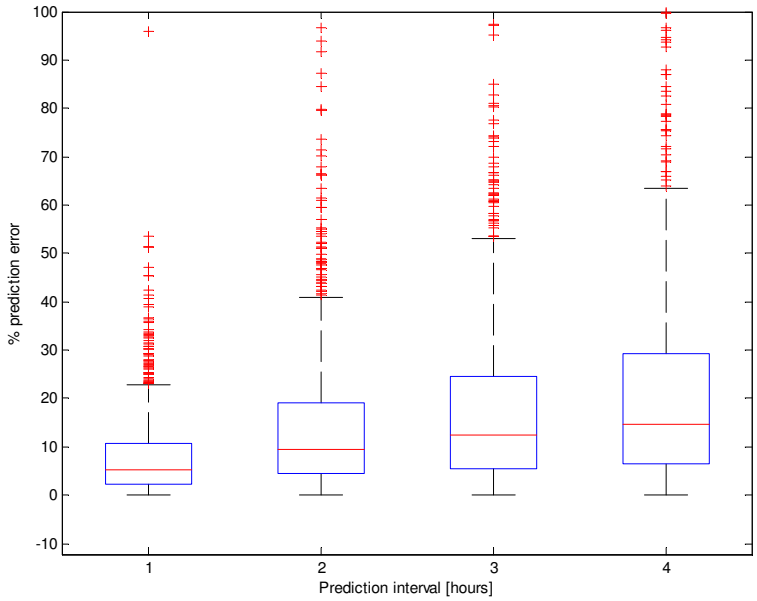

Figure 4.4: Box and whisker plot showing percentage BG prediction error. The boxes represent the inter-quartile range and are intersected by the median. The whiskers represent 1.5* IQR limit, and crosses represent outlying measurements.

pected. Insulin sensitivity forecasting models, covered in Chapter 5, can provide more detailed estimates of prediction performance.

Figure 4.6 shows that there is no strong relationship between proportion of time on exogenous insulin and the model fitting error. This result suggests that the model can adequately handle the, generally brief, periods off insulin that are interspersed within episodes of insulin usage. Whilst this result also suggests that the population values used to estimate endogenous insulin secretion are appropriate, it should be noted this model is primarily designed to handle the case of exogenous insulin administration.

Figure 4.7 shows part of the record for Patient 13. This episode is dominated by the BG measurement of 31.2 mmol/L at 7 hours, a change of 25.7 mmol/L from the measurement 1.5 hours prior. The gradual decrease in BG over the next 11 hours suggests this measurement was not due to error in the measuring device. This patient had severe metabolic imbalances, was relatively clinically unstable, and did not survive intensive care. A glucose/insulin mixture was administered for clinical reasons at 6 hours that contained 0.26U insulin in 8mL/kg of 50% dextrose. The 0.26U is approximately 9.4x the 0.034 U/kg/hr average dose given in Table 3.3 to the cohort for this 860g infant, and is thus very large. Interestingly, the model was able to account for this relatively extreme intervention and the resulting deviation in blood glucose concentration, and accurately captured the impact of this sudden large amount of added dextrose on BG concentration, as well as its long term clearance and impact.

It should be noted that the frequency of measurement of retrospective data can influence the accuracy of blood glucose predictions, where some dynamics may be missed by sparse data collection. This issue is especially evident in the relatively poor prediction results for Patient 23. The average absolute BG slope for these patients shown in Table 4.3 indicates that this patient experienced much more rapid swings in blood glucose compared to the rest of the cohort by a factor of approximately 2x. Figure 4.8 shows a part of the record for Patient 23, highlighting a period of rapid change in blood glucose. This period of glycaemic instability coincided with steroid and antibiotic administration, very unstable respiratory periods requiring resuscitation, a number of new IV lines, and some BG measurements taken using a GlucoCard glucometer, rather than the typical blood gas analyser. In general, more frequent blood glucose measurements would

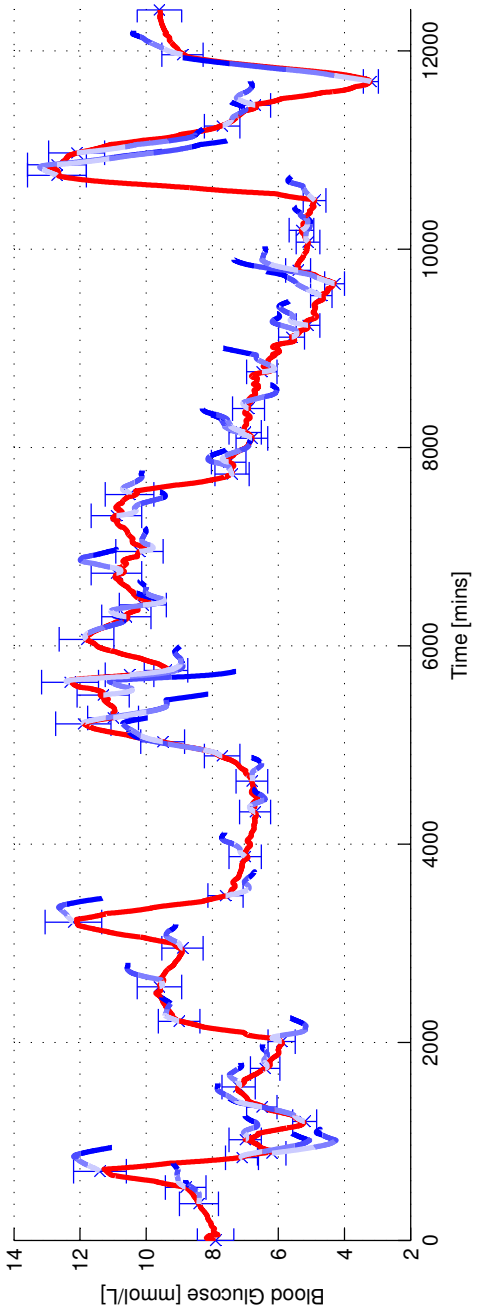

Figure 4.5: Example of model generated blood glucose response over a 1-4 hour prediction interval for Patient 15. Predictions are generated after each recorded BG measurement assuming a constant insulin sensitivity over the prediction interval.

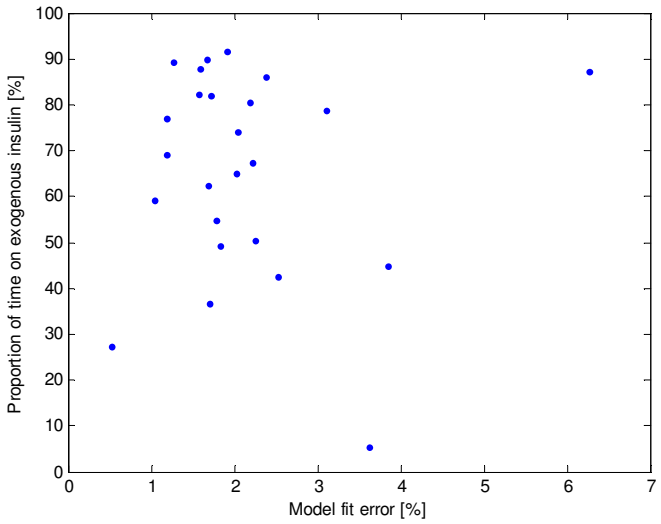

Figure 4.6: Correlation of model fit error with proportion of patient time receiving exogenous insulin.

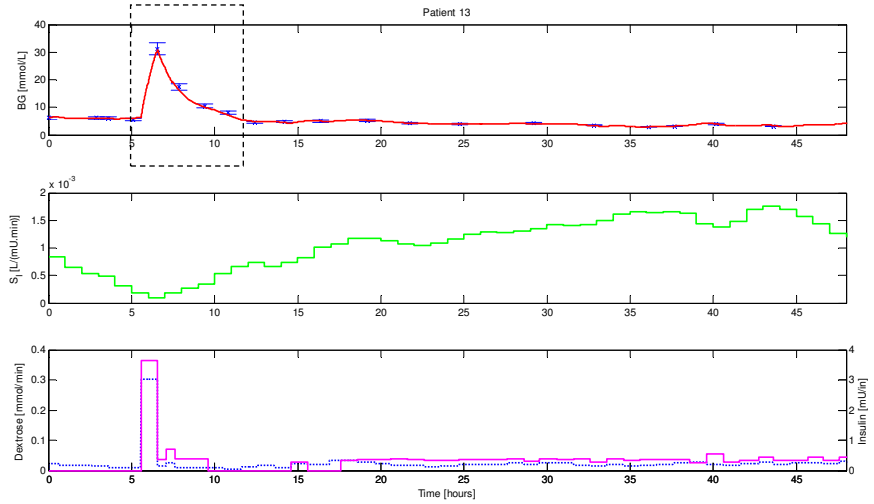

Figure 4.7: Model-generated fit for Patient 13, highlighting extreme rise in blood glucose. The top panel shows the blood glucose data fit (solid line) and measured BG concentration (crosses), the middle panel shows the corresponding insulin sensitivity S_I, and the bottom panel shows insulin (solid line) and dextrose (dashed line) infusions.

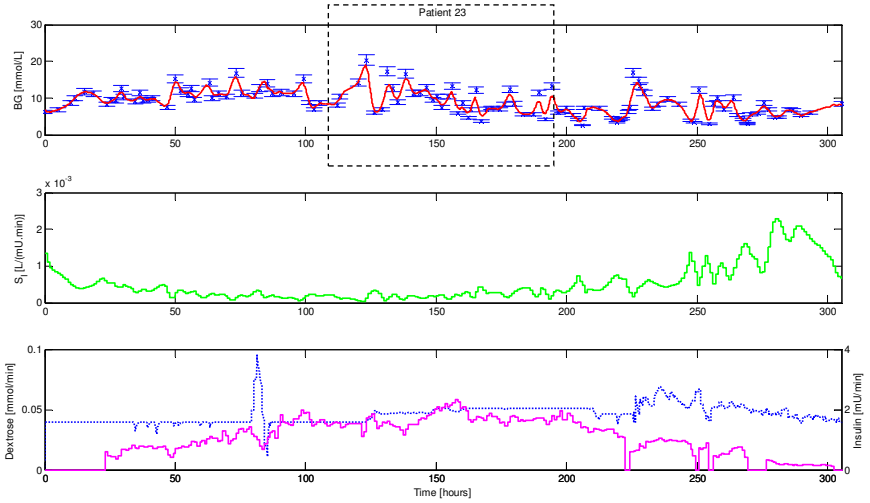

Figure 4.8: Model generated fit for Patient 23, highlighting area of large swings in blood glucose concentration.

enable the model to more accurately capture such periods of rapid change in glucose concentration, as well as provide insight into the relative contributions to the observed unstable glucose due to patient condition, intervention therapy, and noise from measurement devices.

The predictive ability presented is similar to other studies that have successfully applied similar models to control glycaemia in adult intensive care patients [Hann et al., 2005]. The model sufficiently captures the varied dynamics observed in the neonatal cohort. This outcome suggests that adults and neonates are not dissimilar in metabolic dynamics, even though fundamental parameter values representing specific physiological differences may vary.

4.2.1 Clarke Error Grid Analysis

The Clarke Error Grid Analysis (EGA) is often considered a "gold-standard", or at least well-accepted, method to compare the accuracy of blood glucose sensors to a reference method [Clarke, 2005]. EGA was performed on the 1-4 hour blood glucose prediction intervals. This analysis allows a more detailed comparison of the prediction ability of the model with reported data for typical blood glucose sensors, as well as putting it into a clinical decision-making context.

The EGA method categorises the differences between reference BG concentration and a test method into five divisions labelled 'A' to 'E'. 'A' represents the highest correlation between the test and the reference method, and 'E' represents significant deviation likely to cause harm. The ranges reflect typical adult values for a Type I diabetic. The main discriminator is whether the error from the reference method would result in a difference clinical intervention ('A' = no), and how harmful that different intervention might be ('B' to 'E'). Whilst neonatal BG targets are typically lower, the adult ranges provide a reasonable comparison. Figure 4.9 presents the BG model prediction against the "reference" method of linear-interpolated BG from the retrospective clinical data.

Overall, 93% of 1-hour predictions were in zone A and a further 6% of 1-hour predictions were in zone B. The proportion of 2-hour predictions in zone A was 80%, with 18% in zone B. The performance of 1-hour predictions compares well with [Hovorka et al., 2004], which achieved 95% of 1,674 predictions in zone A and 5% in zone B for a prediction horizon of 15-60 min (0.25 - 1.0 hours) on 15 adult patients with Type I diabetes, shown in Figure 4.9e.

Greater variations are introduced with longer prediction intervals, as expected. This analysis provides further evidence of the model to predict BG over a clinically useful 1-2 hour window, and further emphasises the importance of measuring frequently to obtain good control. Additionally, it quantifies the increase in risk of providing an inappropriate or harmful treatment when measurement periods are extended from a more optimal 1-3 hours for glycaemic control to the 4-6 hour measurement period reported in some studies [Beardsall et al., 2008], clearly illustrating a major factor in the success or failure of control.

More specifically, these predictions and EGA analysis indicate the tradeoff of tight control and measurement frequency. Similar to adult studies [Hann et al., 2005; Lonergan et al., 2006b; Chase et al., 2007, 2008b], a 1-2 hour interval provides a relatively optimal result compared to clinical or *in-silico* results at longer intervals. Thus, a first main result of this research would be that anything longer than 3 hours (1-2 hours preferred) will not be able to provide tight glucose control.

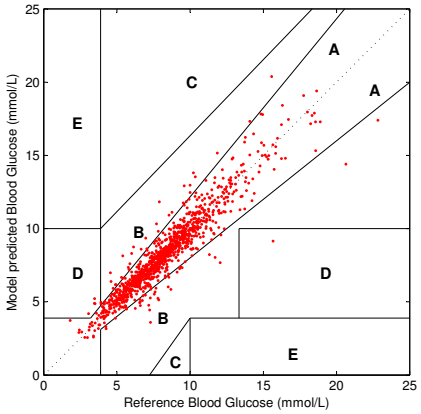

(a) CEGA for 1-hr predictions.

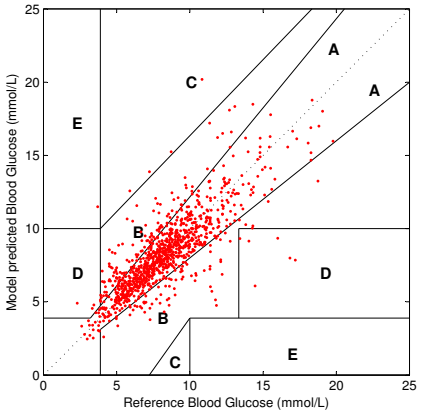

(b) CEGA for 2-hr predictions.

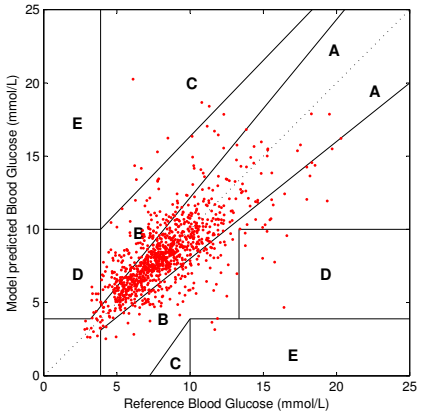

(c) CEGA for 3-hr predictions.

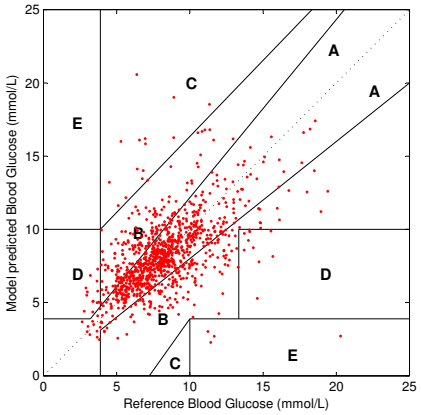

(d) CEGA for 4-hr predictions.

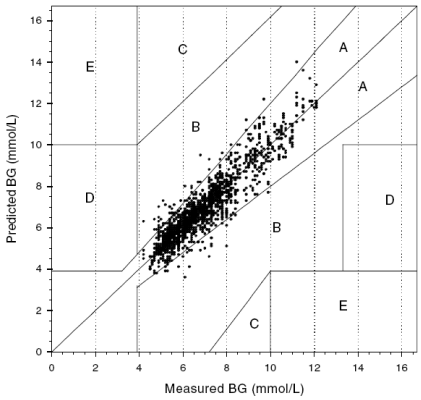

(e) Clarke Error Grid analysis for Hovorka model. Adapted from [Hovorka et al., 2004].

Figure 4.9: Clarke Error Grid analysis of model BG prediction performance.

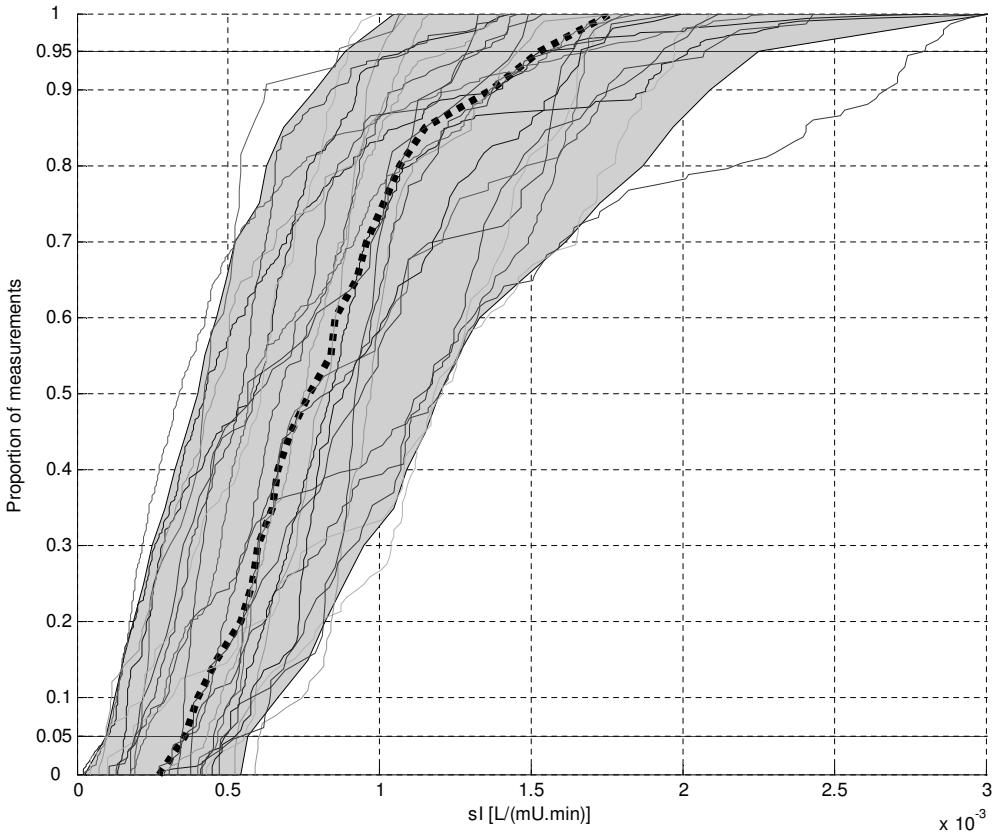

Figure 4.10: Per patient empirical cumulative distribution of insulin sensitivity. The overlaid dashed line shows the median and the shaded region represents the 5%-95% range of per-patient insulin sensitivity. Each line represents a fitted insulin sensitivity profile for one of the 25 retrospective patient data sets.

4.3 Insulin sensitivity variation

The model can be seen to account for a range of different patient responses, which include a range of insulin sensitivity values. This variation indicates that these patients can be highly dynamic metabolically. Figure 4.10 shows that each patient's insulin sensitivity distribution is unique, as well as showing there are also no significantly outlying patient profiles.

Figure 4.11 compares histograms of the empirical probability distribution functions of model-fitted insulin sensitivity for the neonatal cohort of this research to 393 adult intensive care patients totalling 44,386 hours of fitted data from the SPRINT study [Chase et al., 2008b]. The median insulin sensitivity for neonates was 0.68×10^{-3} L/(mU.min), compared to 0.24×10^{-3} L/(mU.min) for adults, and

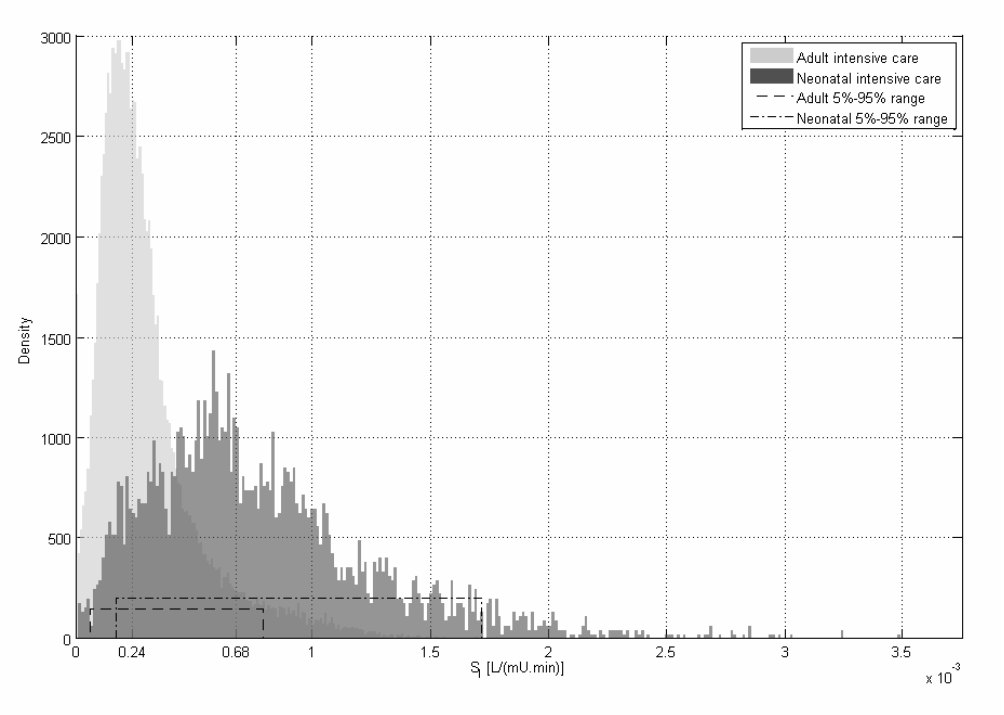

Figure 4.11: Empirical probability distribution function of model-fitted insulin sensitivity in adult critical care (light grey) and neonatal (dark grey) cohorts. The shaded area of each plot is equal to 1.0. The 5%-95% rage of insulin sensitivity for adult and neonatal cohorts are shown by the dashed and dash-dot lines respectively.

the 5%-95% data interval was [0.17 - 1.70]x10^{-3} L/(mU.min) for neonates and [0.06 - 0.79]x10^{-3} L/(mU.min) for adults respectively. The range and variation of model-fitted insulin sensitivity has been studied in adult critical care populations using similar models [Lin et al., 2006, 2008]. However, this research is the first time this form of modelling and analysis has been applied to a neonatal cohort.

Two reasons for the higher median insulin sensitivity are higher rates of glucose turnover and higher metabolic clearance of insulin resulting in lower plasma insulin concentrations. More specifically, [Farrag et al., 1997] found greater peripheral sensitivity to insulin compared to adult controls. In addition, [Hertz et al., 1993] found their estimate of non-insulin mediated glucose uptake to be similar to that of normal adults. Thus, the lower insulin concentrations normally found in infants require a higher value of S_I to account for the remaining glucose uptake, and matches the relatively sparse clinical evidence available.

The model-fitted insulin sensitivity and its hour-to-hour changes are also quantified for neonates. These results can then be compared to model-fitted insulin sensitivity for adults. Thus, a similar model is used for neonates as in adult critical care, with the results shown in Figure 4.12.

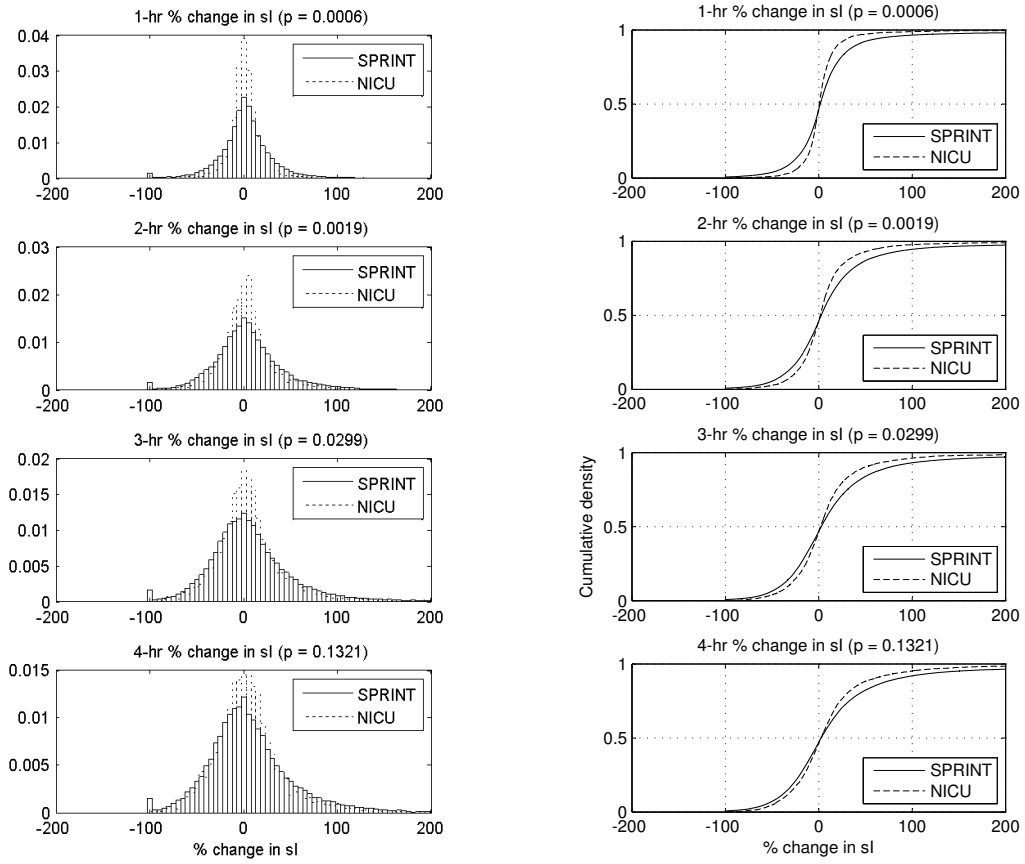

(a) Distribution of change in insulin sensitivity for 1-4 hour intervals

(b) Cumulative density functions for change in insulin sensitivity for 1-4 hour intervals

Figure 4.12: Temporal variation in insulin sensitivity for adult and neonatal cohorts. 'SPRINT' represents adult intensive care data from patients on the SPRINT protocol.

The distributions of insulin sensitivity variation between adults and neonates in Figure 4.12 is significantly different for intervals of 1-3 hours ($p < 0.05$, Mann-Whitney test). NICU patients show significantly less variation in insulin sensitivity over 1-hourly and 2-hourly periods compared to adult critical care patients. Thus, noting the wider spread in Figure 4.11, NICU patients exhibit less intra-patient variation and higher inter-patient variation compared to adults.

More specifically, Figure 4.10 shows that each patient has a uniquely identified

insulin sensitivity profile. The intra-patient variability of response to exogenous insulin is heightened in the neonate, increasing the importance of accurate identification for control. Thus, an adaptive control scheme must be able to dose insulin appropriately to the unique identified patient state. As a result, it can be seen that such an adaptive method will be required to provide tight control for all patients, rather than fixed clinical protocols.

4.4 Secondary insulin sensitivity markers

4.4.1 Influence of age and weight on insulin sensitivity

The literature is conflicting with regard to the relationship between indicators of the maturity of the glucose regulatory system and infant age, weight, and whether a particular infant is small or appropriate weight for gestational age [Van Kempen et al., 2003; Sunehag et al., 1999; Diderholm et al., 2007]. Model-fitted insulin sensitivity was compared to gestational age at birth, birth weight and the ratio of birth weight to gestational age as a measure of size for gestational age, shown in Figure 4.13. Hourly insulin sensitivity, S_I, was also compared to post-birth age and total age (gestational age + post-birth age) in Figure 4.14 to see if there was any impact on variability of these factors.

As shown in Figures 4.13 and 4.14, there is no evident relationship between model-fitted insulin sensitivity and variables related to weight and gestational age. However, it should be noted that the model already accounts for weight in endogenous glucose production and central nervous system uptake parameters. It also accounts for both weight and age in the compartment volume parameters. Thus, age and weight appear to exert no strong influence on sensitivity to insulin, perhaps because they are already a part of the model structure.

4.4.2 Influence of indicators of clinical condition

Insulin sensitivity may be related to clinical condition, and could be used as a marker of the severity of illness, or to provide information on the time course

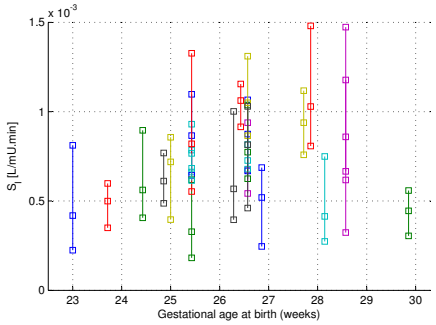

(a) Influence of gestational age at birth on S_I.

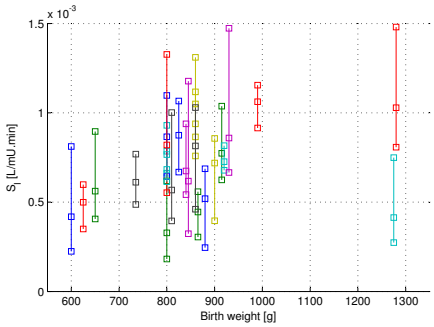

(b) Influence of birth weight on S_I.

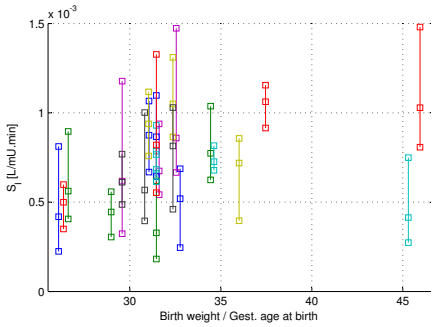

(c) Influence of birth weight/gestational age on S_I

Figure 4.13: Impact of age and weight on insulin sensitivity. Results are plotted as median and IQR values

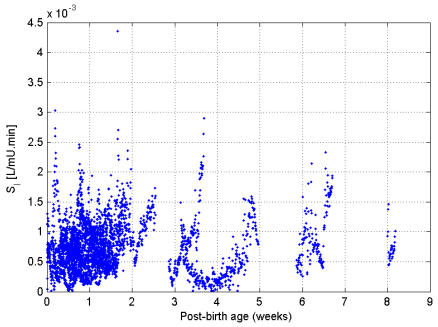

(a) Influence of post-birth age on S_I.

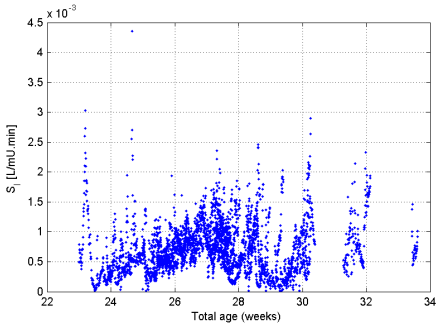

(b) Influence of total age on S_I

Figure 4.14: Impact of age on hourly insulin sensitivity. Hourly model-fitted insulin sensitivity is plotted against patient age.

of conditions such as sepsis [Blakemore et al., 2008]. The model-fitted insulin sensitivity of the retrospective cohort was thus compared to several commonly measured clinical variables indicative of patient condition to establish any relationships. The correlation of model-fitted insulin sensitivity with sodium concentration, blood pH, pCO_2, urea, lactate and creatinine concentrations, as well

as lipid administration rate was assessed. In all cases, each clinical variable explained less than 7% of the variability in insulin sensitivity.

While it is physiologically reasonable that many of the clinical indicators tested here will have some impact on the body's processing of insulin and glucose, confounding physical effects and noise associated with other perturbations or interventions in patient condition leave no easily identifiable relationship within the retrospective data.

The effect of insulin syringe changes, red cell transfusions and transfusions of other blood products on insulin sensitivity was also assessed by comparing the average model-fitted insulin sensitivity value for two hours before and after the time of the event. Each of these events may feasibly create a change in apparent insulin sensitivity through tubing adsorption effects in the case of insulin syringe changes, and changes in plasma volume in the case of the transfusions. However, as shown in Figure 4.15, there is also no clear effect of these events on model-fitted insulin sensitivity.

4.5 Summary

A model of the glucose regulatory system has been adapted from adult critical care to the neonatal case and validated on retrospective clinical data. Model fits of insulin sensitivity were generated for 25 patient records and 3,587 hours of retrospective data. Adaptation of several physiological model parameters, including insulin clearance rate, endogenous production rate and volumes of distribution, resulted in an average fitting error of 2.10%. The predictive ability of the model was assessed by assuming insulin sensitivity was constant over the interval. Median prediction errors at 1, 2 and 4-hour intervals were 5.2%, 9.5% and 14.7% respectively. The model performance is within variations that would also account for dynamic patient evolution. The model thus provides a first in-silico result for modelling the metabolic dynamics of the low-birth weight preterm infant. It also creates a platform towards better metabolic clinical management of glycaemia in neonates.

The major assumption used in the predictions made in this study is that the insulin sensitivity parameter S_I is constant over the prediction interval. Hence,

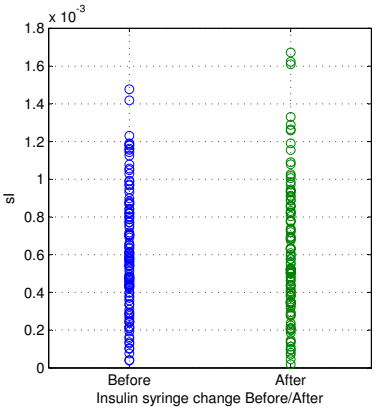

(a) Insulin sensitivity averaged over 2 hours before and after an insulin syringe change.

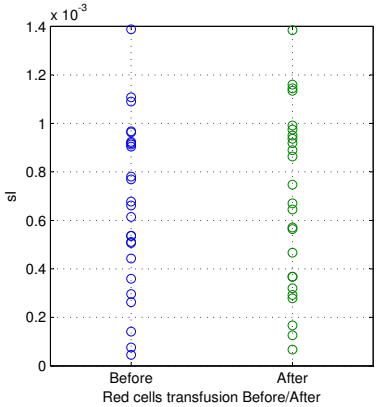

(b) Insulin sensitivity averaged over 2 hours before and after transfusions of red blood cells.

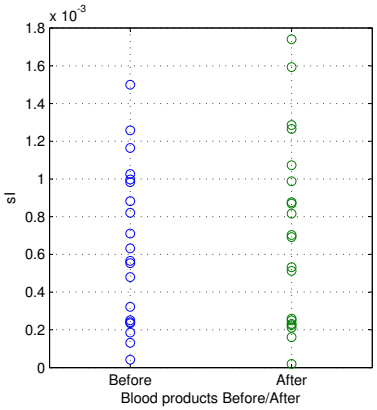

(c) Insulin sensitivity averaged over 2 hours before and after transfusions of blood products.

Figure 4.15: Effect of insulin syringe change and transfusion events on model-fitted insulin sensitivity.

longer intervals will subsequently show potentially greater variation as patient condition has a longer time and thus more opportunity to evolve. Thus, the increasing likelihood of changes over time in insulin sensitivity S_I are evident, as seen previously in the adult population [Hann et al., 2005; Lin et al., 2006, 2008]. Stochastic modelling of insulin sensitivity, as applied in adult critical care patients [Lin et al., 2006], could provide a more accurate forecast of future S_I values and thus create confidence intervals for predicted blood glucose concentrations that account for this variation and would thus provide better clinical guidance.

Chapter 5

Insulin sensitivity variation forecasting

Model-based methods allow information about the fundamental metabolic state of the patient, insulin sensitivity in this case, to be inferred from serial blood glucose measurements and records of nutrition and insulin administration. Once the current insulin sensitivity of the infant has been identified, prediction of future insulin sensitivity ranges or variation is possible. Knowing or estimating these variations would allow accurate predictions of the range of outcome blood glucose concentrations for an intended clinical intervention.

Stochastic models provide a means to quantify this probability of a future insulin sensitivity [Lin et al., 2006, 2008]. Thus, the resulting distribution of blood glucose concentrations that would result from a given intervention can be determined. This information can then be used to guide dosing to avoid or minimise the risk of low blood sugar concentrations, improve overall glycaemic control, and identify periods of potential high glucose variability that may be indicative of emerging clinical events, such as infection [Blakemore et al., 2008].

This chapter presents the adaptation of a stochastic model for insulin sensitivity prediction from adult critical care to the unique clinical and physiological case of the neonate. Several modifications to the initial kernel density estimation model are used to explore the relationship between the model and the underlying data set. In addition, the stochastic modelling approach is extended to include more than just the prior hour values to determine if improved prediction can be obtained in this neonatal case. Finally, a time-series model that provides patient-specific insulin sensitivity forecasts is developed and compared to the whole-cohort stochastic model.

5.1 Hourly insulin sensitivity variation in neonates

Figure 5.1 shows the distribution of hourly variation in insulin sensitivity for the 3,567 hours of patient data. Approximately 92% of data values are below 1.5x10^{-3} L/(mU.min). The fitted insulin sensitivity values presented in Figure 5.1 are unsmoothed to avoid introducing any artificial temporal effects and to develop the model to accurately emulate actual clinical usage. It is clear that the variability of insulin sensitivity over any given fitting time frame is dependent on its present value, and that the stochastic behaviour or distribution of these variations also depends on their current state. These distributions are thus a vertical slice at any $x = S_{I,n}$ value in Figure 5.1 and thus particularly useful where data is dense.

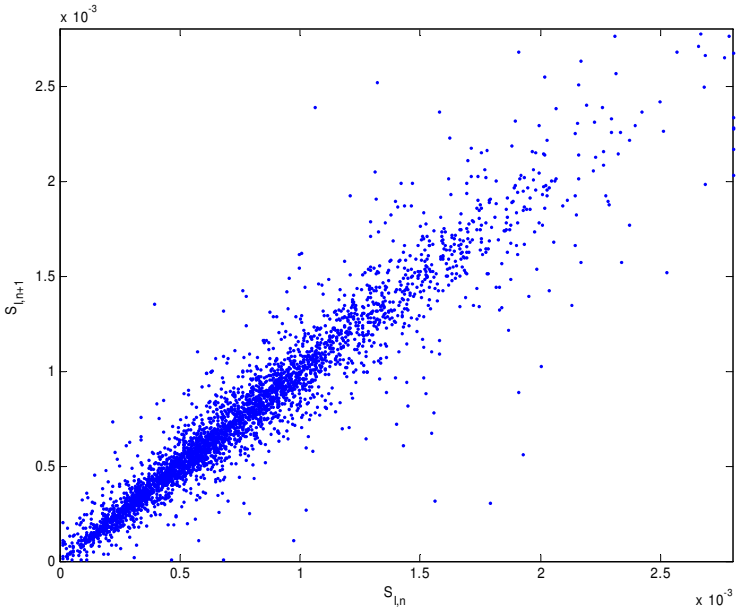

Figure 5.1: Variation of fitted insulin sensitivity from hour n to hour $n+1$ for 3,567 hours of fitted data. The distribution of $S_{I,n+1}$ changes based on the value of $S_{I,n}$ and cannot be described by a simple statistical distribution.

5.2 Stochastic model (Lag-1)

5.2.1 Model development

A two-dimensional kernel density estimation method is used to construct the stochastic model that describes the hourly transition of insulin sensitivity. This method has the advantage of producing a smooth, continuous function across the parameter range, and automatically accounts for any possible multi-modality. The overall result is a bivariate probability density function for the potential parameter values. The goal of this statistical model is to quantify the range of insulin sensitivity one hour ahead in time ($S_{I,n+1}$) based on available data ($S_{I,n}$, $S_{I,n-1}$, $S_{I,n-2}$, ..., $S_{I,0}$) to guide real-time clinical control. Thus, it is important that the model formulation is computationally feasible for real-time applications on typical hardware.

The two-dimensional kernel density method is chosen for creating the stochastic model because the distribution of $S_{I,n+1}$ varies with $S_{I,n}$, as shown in Figure 5.1, and cannot be simply described with a standard statistical distribution. Thus, the variations in S_I can be treated as a Markov process. A Markov process has the property that the conditional probability density function of future states of the process, given the current state, depends only upon the current state. Therefore, using the Markov property of the stochastic behaviour of S_I, the conditional probability density of $S_{I,n+1}$ taking on a value y can be calculated by knowing $S_{I,n} = x$:

$$p\left(S_{I,n+1} = y \,|\, S_{I,n} = x\right) = \frac{p\left(S_{I,n+1} = y, S_{I,n} = x\right)}{p\left(S_{I,n} = x\right)} \tag{5.1}$$

Considering the fitted S_I in a 2D space, as shown in Figure 5.1, the joint probability density function across the x-y ($S_{I,n}$ - $S_{I,n+1}$) plane is defined by the fitted values shown by the dots whose coordinates are x_i and y_i, and is defined using Normal distributions:

$$p\left(x, y\right) = \frac{1}{n} \sum_{i=1}^{n} \frac{\phi\left(x; x_i, \sigma_{x_i}^2\right)}{p_{x_i}} \frac{\phi\left(y; y_i, \sigma_{y_i}^2\right)}{p_{y_i}} \tag{5.2}$$

where:

$$p_{x_i} = \int_{S_{I,lower}}^{S_{I,upper}} \phi\left(x; x_i, \sigma_{x_i}^2\right) dx \tag{5.3}$$

$$p_{y_i} = \int_{S_{I,lower}}^{S_{I,upper}} \phi\left(y; y_i, \sigma_{y_i}^2\right) dy \tag{5.4}$$

Effectively, this joint 2D probability density function is the normalised summation of all the Normal or Gaussian probability density functions that describe the data and are centred at individual data points.

In Equations 5.2 - 5.4, the variances σ_{x_i} and σ_{y_i} at each data point are functions of the local data density in a centred and orthonormalised space of $x = S_{I,n}$ and $y = S_{I,n-1}$. Putting Equations 5.3 and 5.4 into Equation 5.2 normalises each $\phi\left(x; x_i, \sigma_{x_i}^2\right)$ and $\phi\left(y; y_i, \sigma_{y_i}^2\right)$ in the positive domain, effectively putting boundaries along the $x = S_{I,lower}$, $x = S_{I,upper}$, $y = S_{I,lower}$ and $y = S_{I,upper}$ lines and thus enforcing physiological validity in S_I values. For the neonatal case, the boundary values $S_{I,lower}$ and $S_{I,upper}$ were set to 1x10^{-5} L/(mU.min) and 2.8x10^{-3} L/(mU.min) respectively to define the computation domain based on the observed distribution of S_I found in fitting the model to the data.

The right hand side denominator of Equation 5.1, $p\left(S_{I,n} = x\right)$ can be calculated by integrating Equation 5.2 with respect to y. Hence, Equation 5.1 can be rewritten:

$$\begin{aligned} p\left(S_{I,n+1} = y \,|\, S_{I,n} = x\right) &= \frac{\sum_{i=1}^{n} \frac{\phi\left(x; x_i, \sigma_{x_i}^2\right)}{p_{x_i}} \frac{\phi\left(y; y_i, \sigma_{y_i}^2\right)}{p_{y_i}}}{\sum_{i=1}^{n} \frac{\phi\left(x; x_i, \sigma_{x_i}^2\right)}{p_{x_i}}} \\ &= \sum_{i=1}^{n} w_i(x) \frac{\phi\left(y; y_i, \sigma_{y_i}^2\right)}{p_{y_i}} \end{aligned} \tag{5.5}$$

where:

$$w_i(x) = \frac{\frac{\phi\left(x;x_i,\sigma_{x_i}^2\right)}{p_{x_i}}}{\sum_{i=1}^{n} \frac{\phi\left(x;x_i,\sigma_{x_i}^2\right)}{p_{x_i}}} \tag{5.6}$$

Thus, knowing $S_{I,n} = x$ at hour n, the probability of $S_{I,n+1} = y$ at hour $n+1$ can be calculated using Equations 5.5 - 5.6 across the x-y plane. Where there is a higher density of data, more certainty can be drawn on the "true" behavioural pattern. Note that Equation 5.6 makes use of the local data variances ($\sigma_{x_i}^2$, $\sigma_{y_i}^2$). Further details of the general modelling approach, theoretical background and specific computations, including formulation of the local data variance estimator, are available in [Lin et al., 2006, 2008; Lin, 2007].

5.2.2 Model analysis

Figure 5.2 shows the conditional probability plot for the lag-1 model, where the forecast probability bounds depend on the current insulin sensitivity value only. Figure 5.3 shows the 5$^{\text{th}}$, 25$^{\text{th}}$, 50$^{\text{th}}$, 75$^{\text{th}}$ and 95$^{\text{th}}$ percentile probability bounds, overlaid on the raw data. The probability bounds of $S_{I,n+1}$ for a given $S_{I,n} = x$ are found by integrating the conditional probability function shown in Figure 5.2 along the line $x = S_{I,n}$, an example of which is shown in Figure 5.3, using Equation 5.5.

In particular, the 25$^{\text{th}}$ to 75$^{\text{th}}$ percentile prediction bound is found by determining the intersection of the 25$^{\text{th}}$ percentile and 75$^{\text{th}}$ percentile of the resulting cumulative density function with the line $x = S_{I,n} = 1\text{x}10^{-3}$. These probability bounds can then be sequentially substituted for S_I into Equation 2.28 to produce blood glucose concentration forecasts based on the 25$^{\text{th}}$ to 75$^{\text{th}}$ percentile range of likely future S_I, or any other probability bound. The 5% to 95% probability interval can be found in a similar manner. Finally, note that the median or 50$^{\text{th}}$ percentile line in Figure 5.3 lies largely along the $S_{I,n+1} = S_{I,n}$ line indicating no change hour to hour.

Table 5.1 shows the per-patient in-sample results for the lag-1 model. The

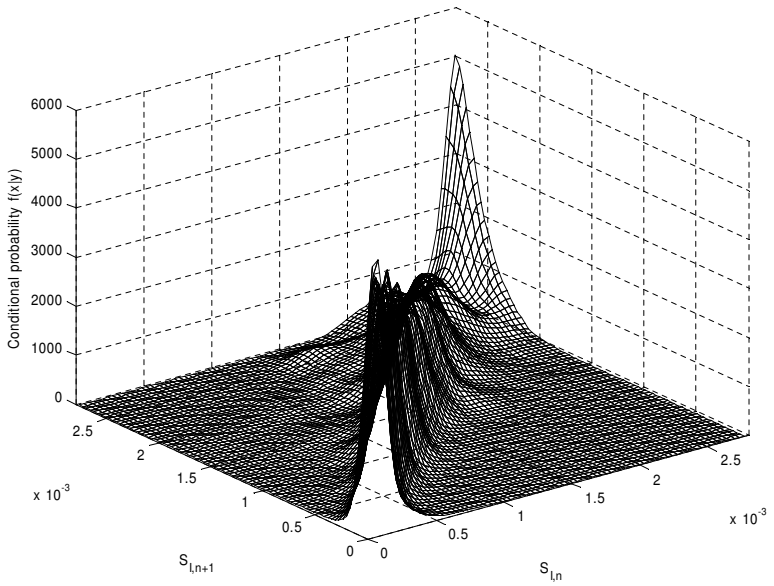

Figure 5.2: Conditional probability density function for $S_{I,n+1}$ knowing $S_{I,n}$. The structure of the plot is largely unimodal in the region $S_{I,n} < 1.5\text{x}10^{-3}$ and $S_{I,n+1} < 1.5\text{x}10^{-3}$, corresponding to the region of densest data.

Table 5.1: In-sample results for stochastic model prediction widths. Data are expressed as cohort medians (n=3,530 predictions).

% S_I within prediction interval	[25$^{\text{th}}$ - 75$^{\text{th}}$]	62.6%
	[5$^{\text{th}}$ - 95$^{\text{th}}$]	93.4%
% BG within prediction interval	[25$^{\text{th}}$ - 75$^{\text{th}}$]	59.1%
	[5$^{\text{th}}$ - 95$^{\text{th}}$]	92.2%
% BG prediction interval width	[25$^{\text{th}}$ - 75$^{\text{th}}$]	0.78 mmol/L
	[5$^{\text{th}}$ - 95$^{\text{th}}$]	2.32 mmol/L
Median absolute % BG point prediction error		4.3%
Median absolute BG point prediction error		0.34 mmol/L

overall median per-patient 1-hour point prediction error comparing BG based on the 50$^{\text{th}}$ percentile of predicted S_I to the interpolated value from retrospective data is 4.3%, corresponding to an average BG error of 0.34 mmol/L. The width of the [25$^{\text{th}}$ - 75$^{\text{th}}$] BG probability interval is 0.78 mmol/L. Similarly, the [5$^{\text{th}}$ - 95$^{\text{th}}$] BG probability interval width is 2.32 mmol/L. The prediction intervals for insulin sensitivity and BG concentration are shown graphically for Patient 8 in Figure 5.4.

Overall, 62.6% of $S_{I,n+1}$ predictions were within the [25$^{\text{th}}$ - 75$^{\text{th}}$] probability

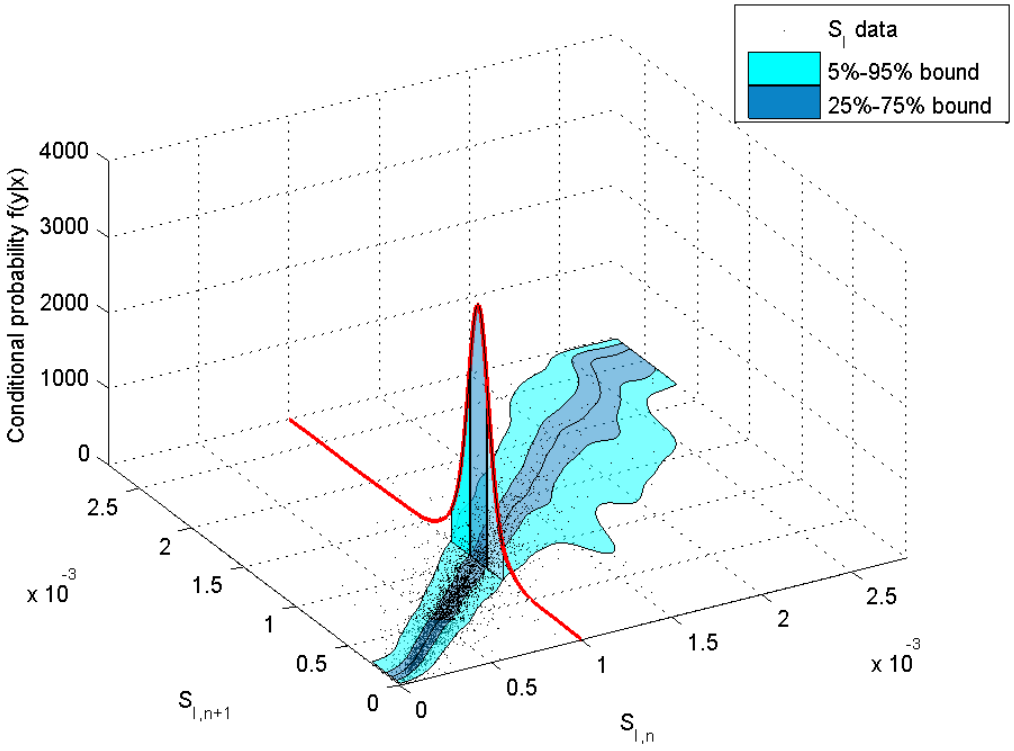

Figure 5.3: Hourly insulin sensitivity variation data with probability bounds. The bounds are computed using an equal-tailed method approximation. An example curve showing the computation of probability bounds for $S_{I,n}$ = 1x10^{-3} L/(mU.min) is displayed.

intervals, corresponding to 59.1% of BG predictions. A total of 93.4% of $S_{I,n+1}$ predictions were within the [5$^{\text{th}}$ - 95$^{\text{th}}$] probability intervals, corresponding to 92.2% of BG predictions. The proportion of fitted insulin sensitivity that fell within the [25$^{\text{th}}$ - 75$^{\text{th}}$] and [5$^{\text{th}}$ - 95$^{\text{th}}$] probability intervals was higher than the expected 50% and 90%. Thus, the cohort model conservatively captures variation but the process of fitting the kernel estimator does not capture all of it exactly.

5.2.3 Cross-validation

The lag-1 model was cross-validated by splitting the 25 patient NICU cohort into 5 groups, each containing 5 patients. For each group the model was fitted on or defined using data from the remaining 20 patients of the cohort representing

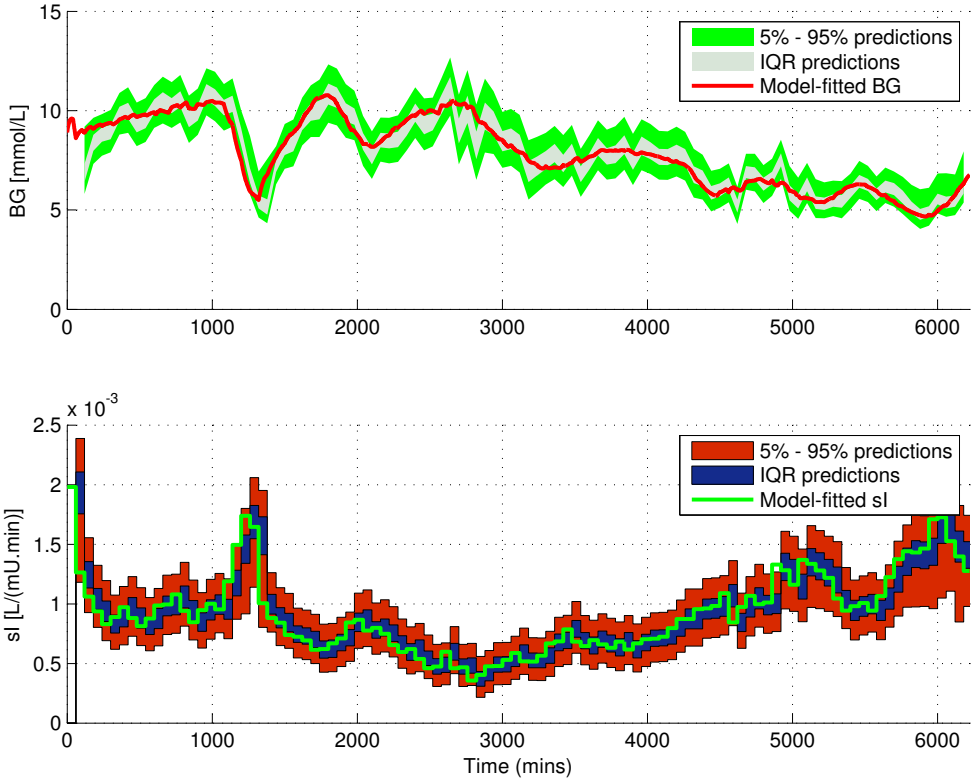

Figure 5.4: Patient 8 with BG forecasts (top panel) and S_I parameter forecasts (bottom panel). The IQR and 5% - 95% prediction bounds for both variables are displayed as shaded areas, and the model fitted BG and S_I are overlaid.

approximately 2,800 hours of data. Out-of-sample insulin sensitivity predictions were then generated for the 5 patients of the group not used to create the model and compared to the proportion of fitted insulin sensitivity that fell within the probability bounds.

Table 5.2 shows the results of this out-of-sample cross-validation of the model. The results are generally consistent between groups, suggesting the overall model contains sufficient data to account for the range of dynamics observed in this cohort. Table 5.2 shows the model consistently over-estimates the probability bounds, with the proportion of insulin sensitivity within the bounds higher than expected from the specific bandwidth.

The lag-1 stochastic model presented here has been employed on a cohort of adult intensive care patients [Lin et al., 2006, 2008]. The results of [Lin et al.,

Table 5.2: Cross-validation comparison study for the 25 patient cohort. Each group contained 5 patients, with each model generated from approximately 2,800 hours of data.

Group	Groups used to create model	% S_I within interval		% BG within interval		BG interval width (mmol/L)		BG point prediction error	
		[25th - 75th]	[5th - 95th]	[25th - 75th]	[5th - 95th]	[25th - 75th]	[5th - 95th]	[%]	[mmol/L]
Group 1:	[-, 2, 3, 4, 5]	57.4%	92.2%	56.4%	90.9%	0.71	2.06	4.2%	0.32
Group 2:	[1, -, 3, 4, 5]	68.7%	92.1%	64.3%	91.5%	0.75	2.17	3.7%	0.28
Group 3:	[1, 2, -, 4, 5]	67.0%	94.8%	62.4%	94.0%	0.91	2.61	4.6%	0.36
Group 4:	[1, 2, 3, -, 5]	59.2%	91.8%	56.2%	90.8%	0.87	2.48	4.8%	0.41
Group 5:	[1, 2, 3, 4, -]	61.7%	95.6%	57.1%	92.7%	0.85	2.53	5.2%	0.38
Overall	[1, 2, 3, 4, 5]	62.6%	93.4%	59.1%	92.2%	0.78	2.32	4.3%	0.34

2006] also show the model produces conservative probability bounds. However, their result of 54.0% within the [25$^{\text{th}}$ - 75$^{\text{th}}$] percentile bound is closer to the ideal 50%. The results of Tables 5.1 and 5.2 suggest the model prediction coverage is moderately over-conservative. Therefore, a lag-2 model was developed to investigate whether these effects could be mitigated by incorporating S_I information from two previous hours, in effect evaluating whether the stochastic model needed further dynamics not in the lag-1 model.

5.3 Stochastic model (Lag-2)

5.3.1 Model development

The lag-2 model produces probability intervals for $S_{I,n+1} = z$ at hour $n+1$ given the insulin sensitivity for the previous two hours: $S_{I,n-1} = x$ and $S_{I,n} = y$. The derivation of the model is similar to that of the lag-1 case, and the conditional probability estimator is defined:

$$p\left(S_{I,n+1} = z \,|S_{I,n-1} = x, S_{I,n} = y\right) = \frac{\sum_{i=1}^{n} \frac{\phi\left(x;x_i,\sigma_{x_i}^2\right)}{p_{x_i}} \frac{\phi\left(y;y_i,\sigma_{y_i}^2\right)}{p_{y_i}} \frac{\phi\left(z;z_i,\sigma_{z_i}^2\right)}{p_{z_i}}}{\sum_{i=1}^{n} \frac{\phi\left(x;x_i,\sigma_{x_i}^2\right)}{p_{x_i}} \frac{\phi\left(y;y_i,\sigma_{y_i}^2\right)}{p_{y_i}}}$$

$$= \sum_{i=1}^{n} w_i(x,y) \frac{\phi\left(z;z_i,\sigma_{z_i}^2\right)}{p_{z_i}} \tag{5.7}$$

where:

$$w_i(x,y) = \frac{\frac{\phi\left(x;x_i,\sigma^2_{x_i}\right)}{p_{x_i}}\frac{\phi\left(y;y_i,\sigma^2_{y_i}\right)}{p_{y_i}}}{\sum_{i=1}^{n}\frac{\phi\left(x;x_i,\sigma^2_{x_i}\right)}{p_{x_i}}\frac{\phi\left(y;y_i,\sigma^2_{y_i}\right)}{p_{y_i}}} \tag{5.8}$$

$$p_{z_i} = \int_{S_{i,lower}}^{S_{I,upper}} \phi\left(z;z_i,\sigma^2_{z_i}\right) \tag{5.9}$$

where all terms are similar to those used previously and computed with the same fundamental methods or approach.

5.3.2 Model analysis

Figure 5.5 shows the insulin sensitivity data in the x, y, z coordinate space. The probability bounds for the lag-2 model are shown in Figure 5.6, together with slices of probability bound surfaces along several values of $S_{I,n-1}$. The surface sliced curves appear smooth around the value of $S_{I,n-1}$ and less smooth away from that value. This outcome shape highlights the (expected) result that sudden, large changes over two hours of patient data are less common, and the less-smooth regions of the curves are caused by lower data density. Thus, the hour-to-hour variation observed in the S_I data does not show any further temporal dependence in this analysis.

Table 5.3 compares the coverage proportions for the lag-1 and lag-2 models. Here, 61.3% of S_I fell within the [25$^{\text{th}}$ - 75$^{\text{th}}$] percentile interval for the lag-2 model, similar to the 62.6% result for the lag-1 case. Similarly, 94.6% of S_I fell within the lag-2 [5$^{\text{th}}$ - 95$^{\text{th}}$] interval compared to 93.4% for the lag-1 model. These results further suggest that lag-2 effects do not play a major role in the evolution of insulin sensitivity in this NICU cohort compared to the simpler lag-1 model case.

Clinically, the small influence of lag-2 effects is interesting. It says that variation is largely hour-to-hour in these neonates and effectively random over that period with little build-up. A second clinical outcome or interpretation is that major changes in the neonate's condition are not likely over that long a period

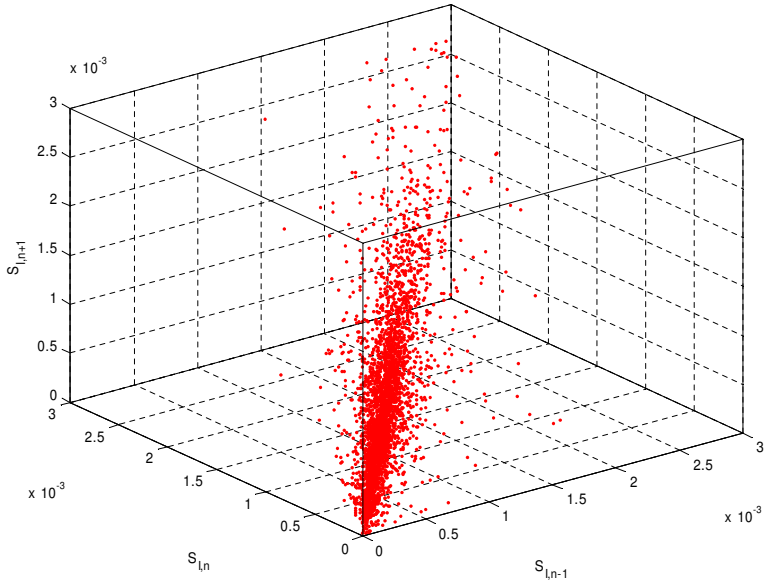

Figure 5.5: Insulin sensitivity data for lag-2 model. The S_I parameter for the upcoming hour is plotted against S_I one and two hours previously.

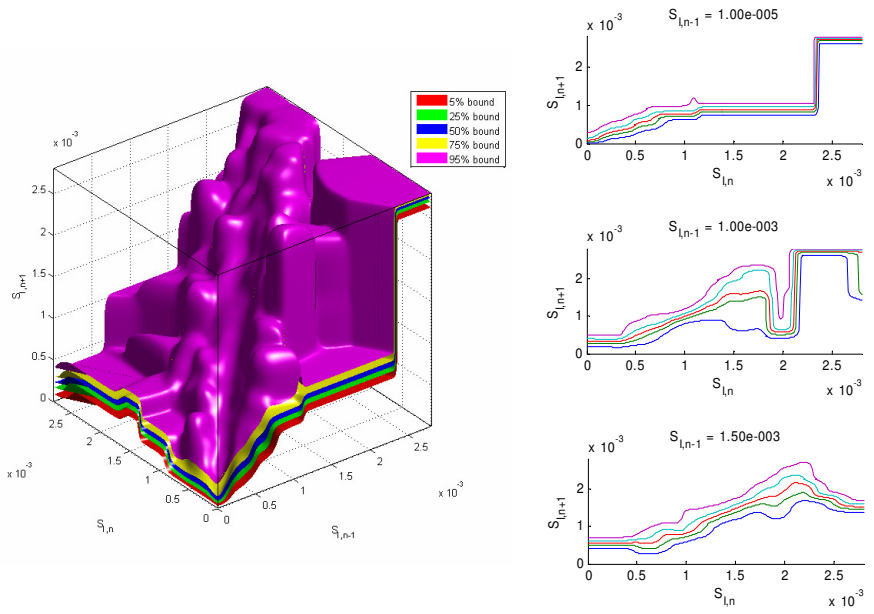

Figure 5.6: Lag-2 stochastic model probability bounds. The surfaces on the 3D plot represent the 5%, 25%, 50%, 75% and 95% bounds for $S_{I,n+1}$ given $S_{I,n}$ and $S_{I,n-1}$. Three slices of the probability bound distribution are presented for $S_{I,n-1}$ at 0.5x10^{-3}, 1.0x10^{-3} and 1.5x10^{-3} L/(mU.min).

of time (2 hours), and are thus more acute in nature. They thus appear random over the 1-hour interval used because no finer measurement resolution is available in this cohort.

5.4 Model bias-variance trade-off

The kernel density estimator method employed in this stochastic model produces a smooth distribution and, in this case, a conservative model. This conservatism can provide a layer of safety, as wider probability bounds would be more likely to capture dynamics and changes not observed in the cohort used to fit the model. However, wider coverage bands may also impact glycaemic control performance as wide probability bands used to reduce the risk of hypoglycaemia may needlessly force a controller to maintain a mildly hyperglycaemic state.

The overall BG width of the [5^{th} - 95^{th}] percentile probability band was 2.32 mmol/L. This 2.32 mmol/L range would severely impact performance for a controller targeting a typical 4-7 mmol/L target range, as it is almost 50% of a 6 mmol/L target.

Therefore, a trade-off between model bias and variance is required. The cross-validation showed consistent results. This outcome suggests that the cohort data set is large enough to satisfy the assumption that the model contains enough data points to reasonably reflect the vast majority of target patients presented in the Christchurch Women's Hospital NICU.

Figure 5.7 shows the proportion of in-sample predictions within the 25% to 75% probability bound grouped by location along the $x = S_{I,n}$ axis. Also plotted on Figure 5.7 is the number of data points (=number of in-sample predictions) for each group. The 25^{th} to 75^{th} percentile bounds would be expected to contain approximately 50% of the data. However, Figure 5.7 shows that the coverage

Table 5.3: Comparison of in-sample insulin sensitivity coverage prediction proportions for lag-1 and lag-2 stochastic models.

	Lag-1	Lag-2
% within 25^{th} - 75^{th} percentile	62.6%	61.3%
% within 5^{th} - 95^{th} percentile	93.4%	94.6%

often exceeds this expectation. This coverage discrepancy is highest where the data density is greatest. This apparently contrary result suggests that the local data density variance estimators (σ_x, σ_y) are conservative for this data set and/or cohort, and may be a source of over-estimation.

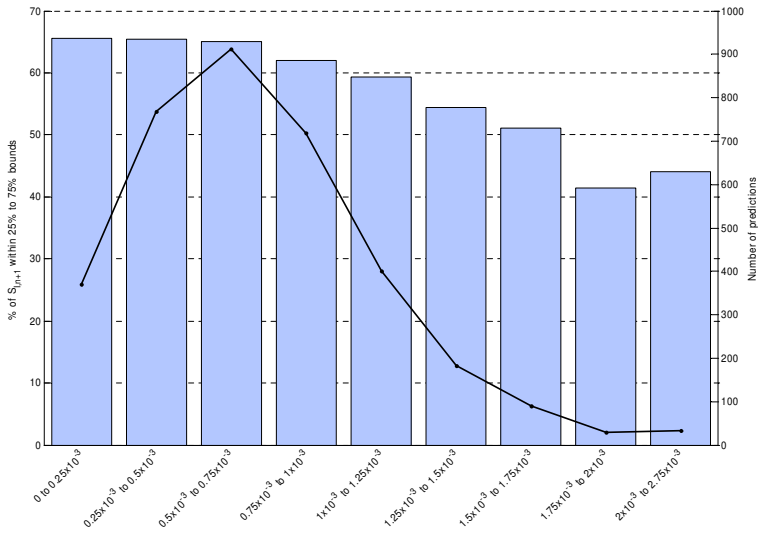

Figure 5.7: Proportion of in-sample predicted insulin sensitivity within the 25%-75% prediction bounds (bars) and number of predictions (line) grouped by insulin sensitivity range.

A modification to the model is to multiply the variance estimators by a constant c (ie: $c\sigma_x$, $c\sigma_y$) to explore the model bias-variance trade-off for this data. The effect of this modification is to tighten the distributions used in Equation 5.2 by reducing the variance. The overall effect on forecast performance for several values of c is shown in Table 5.4. Reductions of the variance estimators to approximately 10% - 50% ($c = 0.1$ - 0.5) of their original value yield coverage widths that contain numbers closer to the approximately expected proportion of in-sample data values.

Figure 5.8 shows probability plots for c=1.0, c=0.5 and c=0.1. As expected, the probability distribution becomes less smooth. In particular, it does so for lower values of c, which is further enhanced for higher values of S_I where data is less dense. Additionally, for lower values of c the [25$^{\text{th}}$ - 75$^{\text{th}}$] and [5$^{\text{th}}$ - 95$^{\text{th}}$] percentile probability bounds for $S_{I,n+1}$ are essentially equal for some regions of $S_{I,n}$ due to sparse data, which may contribute to the increase in coverage proportion for c less than 0.1, and show the model possibly over-fitting the data.

Table 5.4: Comparison of probability bounds for modifications of kernel density estimator ($\sigma'_x = c\sigma_x$ and $\sigma'_y = c\sigma_y$).

c	% of S_I within prediction bounds		% of BG within prediction bounds	
0.05	50.8%	90.5%	45.2%	86.2%
0.08	50.8%	90.6%	45.9%	87.1%
0.1	50.7%	90.9%	46.2%	87.5%
0.2	51.7%	90.8%	46.8%	88.3%
0.3	52.2%	90.6%	48.0%	88.8%
0.5	54.7%	90.9%	50.8%	89.5%
1.0	62.6%	93.4%	59.1%	92.2%
2.0	75.4%	96.9%	72.5%	96.4%
Ideal	50%	90%	50%	90%

The value of c=0.5 provides a balance between prediction coverage and over-modelling the data.

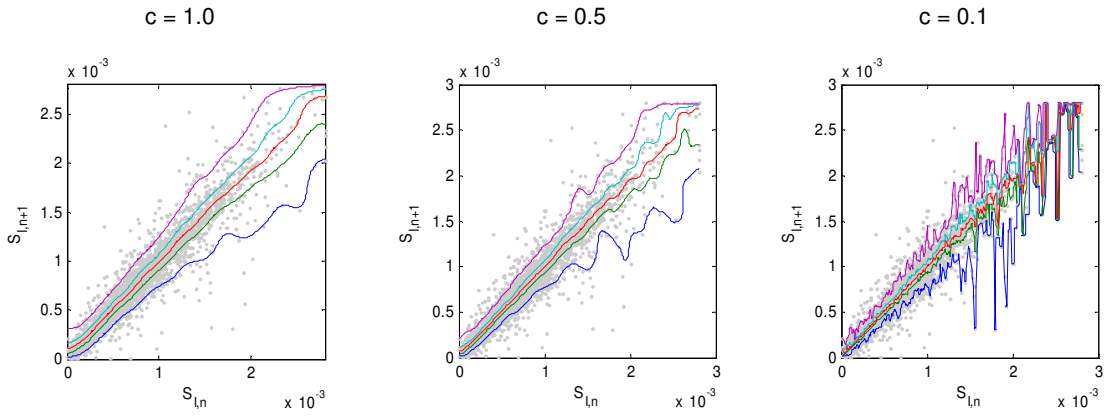

Figure 5.8: Probability bound determination using local variance estimator modified by a constant c. The lower values of c produce a less smooth probability distribution particularly at higher insulin sensitivity. The individual points represent raw insulin sensitivity data. The solid lines represent the 5%, 25%, 50%, 75% and 95% probability bounds.

Despite the over-estimation of the prediction band widths, the 50$^{\text{th}}$ percentile of the fitted probability distribution represents the centre of the data reasonably well with 49.1% and 50.9% of in-sample predictions above and below the 50$^{\text{th}}$ percentile limit respectively. Thus, the probability bands are well centred on the data. This result indicates that the median, and likely nearby, variations are

accurately captured.

Probability bounds for the [50−a, 50+a] percentile limits can be compared to the ideal prediction coverage, as shown in Figure 5.9. Thus, for example, for $a = 10$ the proportion of predictions within the [40$^{\text{th}}$, 60$^{\text{th}}$] percentile limits of the model distribution can be compared to the ideal value of (2a)% = 20%. This analysis would thus determine over what centred percentile range the model prediction is most accurate.

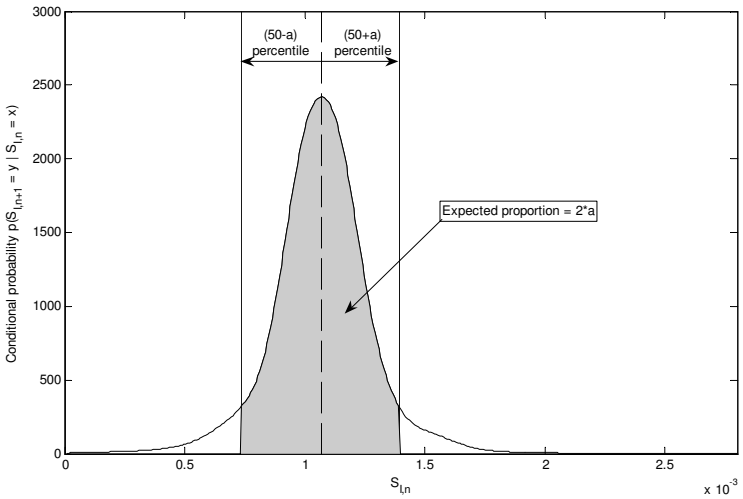

Figure 5.9: Comparison of integrated area under probability curve with ideal prediction coverage. The dashed line represents the 50$^{\text{th}}$ percentile of the distribution, and the shaded area represents the probability interval of width 2a centred on the 50$^{\text{th}}$ percentile.

Figure 5.10 shows the extent of the model coverage over-estimation across the range of prediction bounds for $c = 0.5$ and 1.0. In particular, for $c = 1.0$, 50% of the data lies between the 31$^{\text{st}}$ and 69$^{\text{th}}$ percentiles of the model where the expected coverage is 38%. A total of 90% of the data for $c = 1.0$ lies between the 7$^{\text{th}}$ and 93$^{\text{rd}}$ percentiles where the expected coverage is 86%. It is clear from Figure 5.10 that these average estimations improve for the $c = 0.5$ line.

Finally, the variance estimator employed here is aligned with the cardinal axes. The major and minor axes of the ellipse that forms from the contours of each individual distribution in Equation 5.5 are aligned with the x and y directions. A further modification may incorporate a rotation of the distribution such that the variance in each distribution is described by three parameters (σ_x,

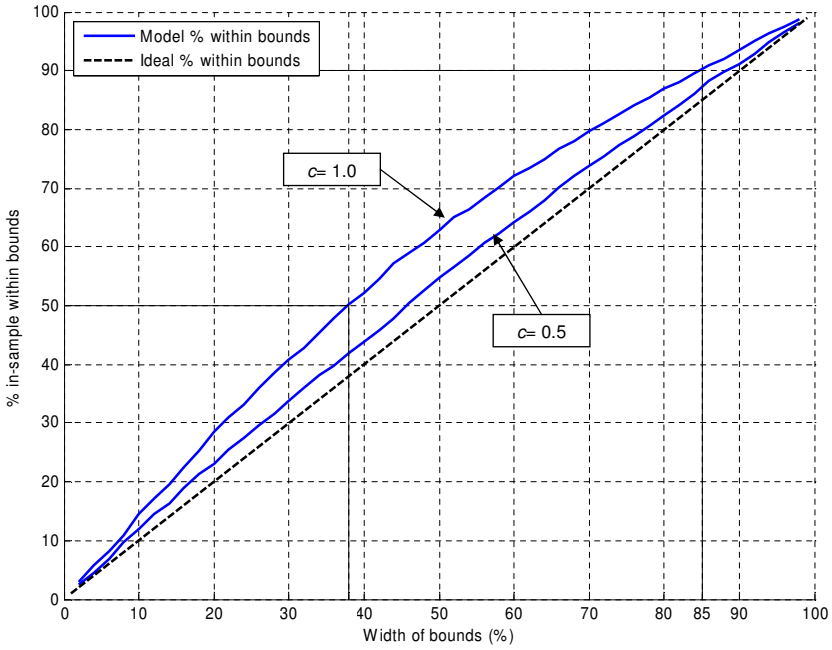

Figure 5.10: Comparison of in-sample predicted insulin sensitivity within arbitrary probability bounds ($2a$) against ideal proportion of predictions within bounds ($y = x$ line) for c=1.0 and c=0.5, where the ideal IQR is the $2a = 50\%$ case.

σ_y, θ) to represent scaling in the x and y directions and rotation respectively [Kern et al., 2003]. However, the meaning of a rotation is unclear in physiological or control system terms, and thus not pursued here.

In summary, modifying the local data density variance estimator showed that less variance ($c < 1.0$) resulted in distributions that more accurately reflected the observed data prediction coverage. The ideal value of the adjustment parameter c was found to be in the range of 0.1 to 0.5. However, Figure 5.8 shows that the probability bounds of the distribution for small c are not smooth, suggesting that this particular distribution is over-modelling the data, where a smoother variation is physiologically more realistic. The method shown in Figure 5.9 provides a means to produce smooth probability bounds with a customisable trade-off between glycaemic control performance and hypoglycaemic protection. Overall, c=0.5 appeared to provide the most suitable trade-off between model bias and

variance for this cohort, as shown in Table 5.4 and Figure 5.10.

5.5 Measurement density

The cohort data represents 3,567 hours of fitted insulin sensitivity data over 25 patients. Blood glucose measurement density for these patients was typically 2-4 hourly, thus there may be some effect introduced by interpolating between BG measurements to fit insulin sensitivity. However, a stochastic model produced by only taking the data closest to each BG measurement still yielded 64.0% of predicted insulin sensitivity within the 25^{th} to 75^{th} percentiles, over-shooting the 50% expected by a similar value as obtained using the full model. This result suggests that the blood glucose interpolation is not playing a significant role in this data set.

Higher blood glucose measurement density may reveal more dynamics that could be used to refine the blood glucose system model and, subsequently, the stochastic model. However, such greater measurement density is ethically difficult in the very low-blood-volume NICU population [Cowett and Farrag, 2004]. Hence, it is difficult to do more than speculate further on this aspect.

5.6 Probability bound calculation

The non-parametric formulation of the kernel density model automatically accounts for multi-modality. The probability bounds are computed by integrating the area under the conditional probability curve to create a cumulative density function which is then used to determine the probability limits. However, an equal-tailed assumption is used to find the bounds. For a multi-modal distribution this equal-tailed assumption may lead to regions of lower probability being included within the percentile bounds.

An alternative method to compute the probability bounds is to use the highest regions of the conditional probability curve to compute the required area, as shown in Figure 5.11. A comparison of the bounds computed using the two methods is shown in Figure 5.12. The probability distribution is largely uni-

modal in regions of high data density and the bounds computed using the two methods largely correspond within this region. For higher insulin sensitivity the two methods diverge slightly. However, there is generally little difference between the percentile points for either method. These results suggest that the equal-tailed assumption does not have a large effect on the bounds. This conclusion is reflected by the proportion of in-sample predictions within the probability bounds at 62.6% within the [25^{th} - 75^{th}] and 93.4% within the [5^{th} to 95^{th}] percentile bounds compared to 62.8% within the [25^{th} to 75^{th}] and 93.6% within the [5^{th} to 95^{th}] percentile bounds for the equal-tailed and highest-probability methods respectively.

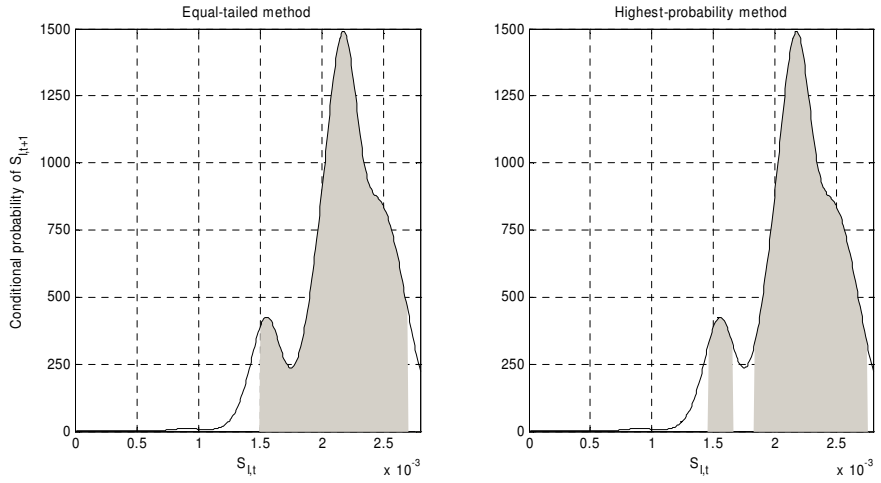

Figure 5.11: Comparison of probability bound determination using equal-tailed and highest-probability methods. This forecast ranges are shown as the shaded areas under the curves. The highest-probability method can produce discontinuous probability bounds.

The discontinuous probability bounds for regions of higher insulin sensitivity suggest that intermediate changes in patient metabolic state are less likely during periods of high insulin sensitivity. They also reveal the clinical possibility for dramatic change in condition to a lower value at this state. Clinically, such a sudden or large change could be due to a sudden worsening of condition. Thus, the multi-modal model may provide some measure of estimating the risk of sudden significant change (for the worse) at higher insulin sensitivity, which might offer some significant clinical benefit.

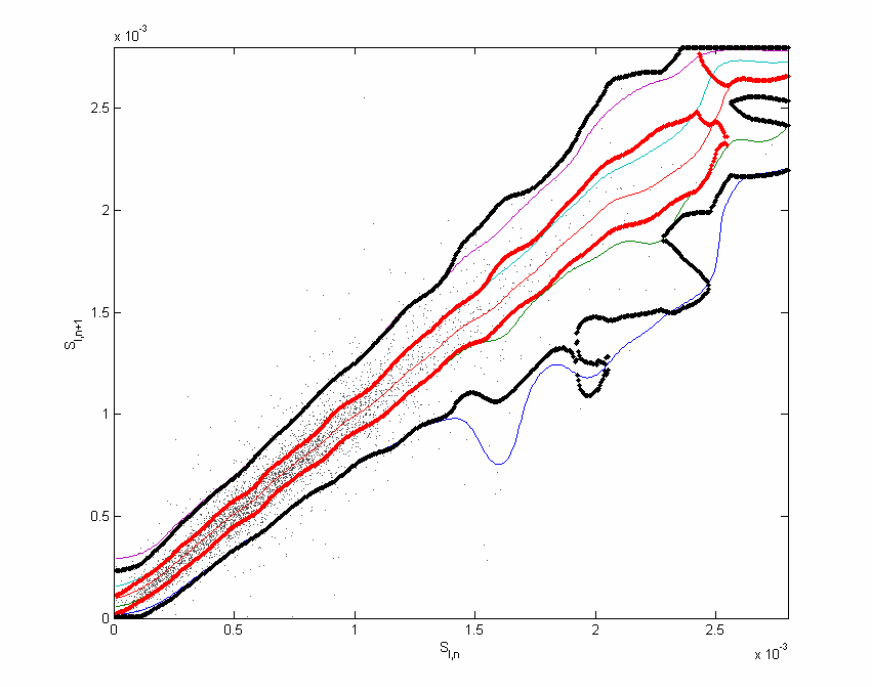

Figure 5.12: Comparison of probability bounds from equal-tailed and highest-probability methods. The thin bounds represent the IQR and [5^{th} - 95^{th}] bounds from the equal-tailed method. The thick lines represent the corresponding bounds from the highest-probability method.

5.7 Insulin sensitivity in the positive domain

The insulin sensitivity parameter, S_I, is constrained to the positive domain for physiological validity. Normal probability distributions are used in Equation 5.2 to describe the data. There may be some degree of skewness as S_I cannot be negative and the Normal probability function spans the domain of $[-\infty, \infty]$. Figure 5.13 shows the joint probability density for six pairs of insulin sensitivity data extracted from Figure 5.1. The tightness of the peaks is related to the variance estimator based on local data density, where tighter peaks are generated in regions of higher concentrations of data and wider peaks are present in regions of lower data density. In all cases however, the influence of the chosen Normal distributions is small close to the positive/negative interface shown in Figure 5.13, demonstrating the use of a Normal probability distribution to have a minor effect with respect to the requirement of a non-negative S_I value.

The quantities p_{x_i} and p_{y_i} in Equation 5.2 provide a renormalisation to allow

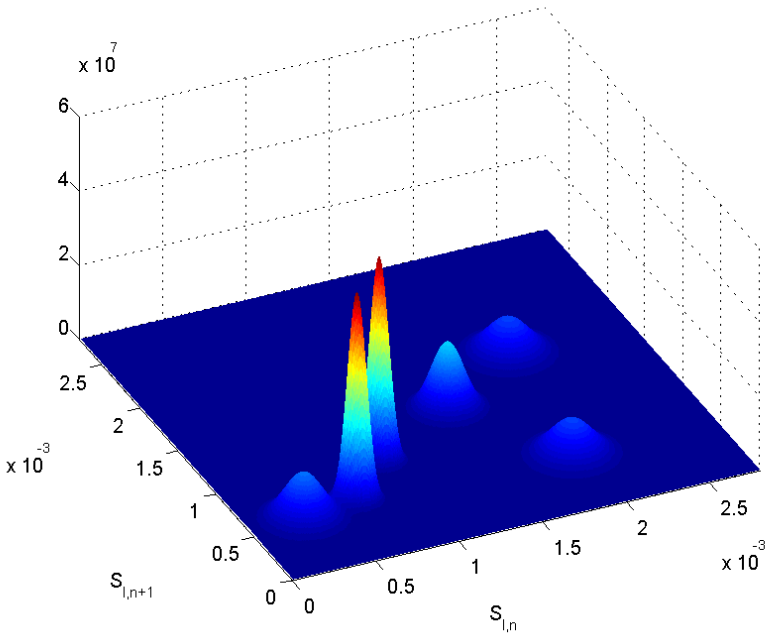

Figure 5.13: Joint probability density for six pairs of $[S_I,\ S_{I,n+1}]$ data. The shapes of the peaks are described by Normal probability density functions, and the tightness of the peaks is related to the local data density variance estimator.

for truncation of the domain of the distributions. The truncation effect is greatest at the extreme low and high end of the S_I domain, as shown in Figure 5.14 where the percentile bounds are curved in the ranges of $S_I < 0.2\text{x}10^{-3}$ L/[mU.min] and $S_I > 2.5\text{x}10^{-3}$ L/[mU.min]. The majority of the data lies outside these ranges, and the probability bounds in this region is not influenced by truncation effects. Figure 5.14 highlights the 50^{th} and 95^{th} probability bounds, which are used by model-based controllers for targeted control and hypoglycaemia prevention respectively, as will be discussed in Chapter 6.

The truncation effect skews insulin sensitivity higher in the low S_I range, thus a controller would subsequently use less insulin for control. The reverse applies for the high S_I range. However, higher insulin sensitivity generally corresponds with lower overall insulin requirements for glycaemic control. The net result is that truncation effects in this case create a more conservative control approach when stochastic forecasts are used to drive model-based control.

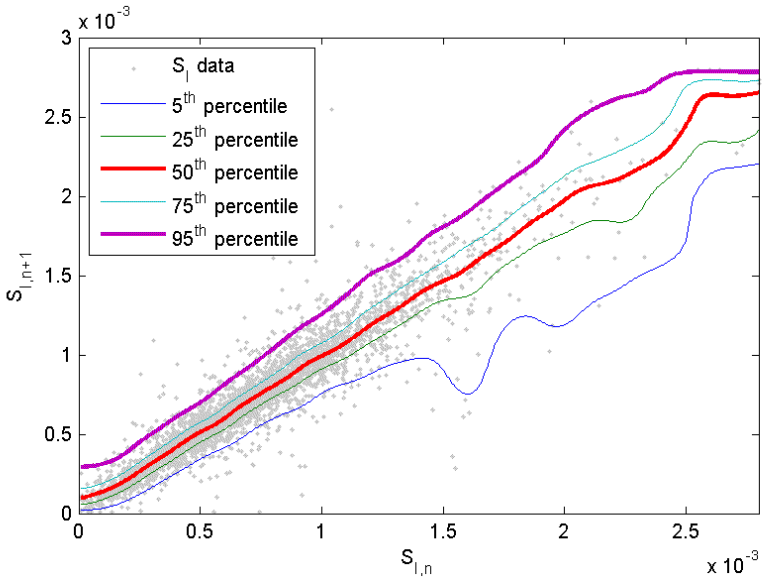

Figure 5.14: Insulin sensitivity percentile probability bounds overlaid on the raw insulin sensitivity variation data. The 50^{th} and 95^{th} bounds are highlighted.

5.8 Time series modelling for patient-specific forecasting

Overall, the stochastic method provides predictions based on a cohort-wide data set. The prediction bounds for less dynamic patients would typically be more conservative than necessary to account for more dynamic patients that make up the patient population. Thus, the probability bounds are optimised in a cohort sense, but not necessarily on a per-patient basis. Time-series methods, such as ARIMA modelling, may provide enhanced prediction performance by customising the model to the individual patient in real-time. These methods provide the opportunity to optimise insulin sensitivity forecasting in a per-patient sense for more optimal control.

This section presents the development of auto-regressive time series models for insulin sensitivity forecasting. A bootstrap method is used to generate probability bounds, and the prediction performance of the time-series models are compared to the stochastic method. The overall approach is thus patient-specific in contrast to the stochastic cohort-specific model presented in Sections 5.2 - 5.6.

5.8.1 Cyclic variation in insulin sensitivity

It is unknown whether neonates exhibit any significant diurnal variations in insulin sensitivity. Circadian rhythmicity has a profound and independent effect on glucose tolerance in man, as reviewed by [Van Cauter et al., 1997]. In normal, non-critically ill subjects diurnal patterns in glucose tolerance exist and are balanced by insulin secretion throughout the course of a day. The exact mechanisms of diurnal glucose tolerance are still under debate, but reduced effective insulin sensitivity appears to be a major factor [Bolli et al., 1986].

Capturing any diurnal, or similar, rhythms that exist in neonatal insulin sensitivity would improve model predictions, and hence controller performance. Rhythms in metabolism may also appear in critical care linked to daily medication dosing regimens or other routines in clinical practice.

The piecewise constant insulin sensitivity profile obtained from clinical data (see Section 3.1) can be considered as a discrete time series. A discrete fourier transform (DFT) was performed on the insulin sensitivity profile generated for each retrospective patient. Figure 5.15 shows the distribution of the two strongest frequencies for each patient.

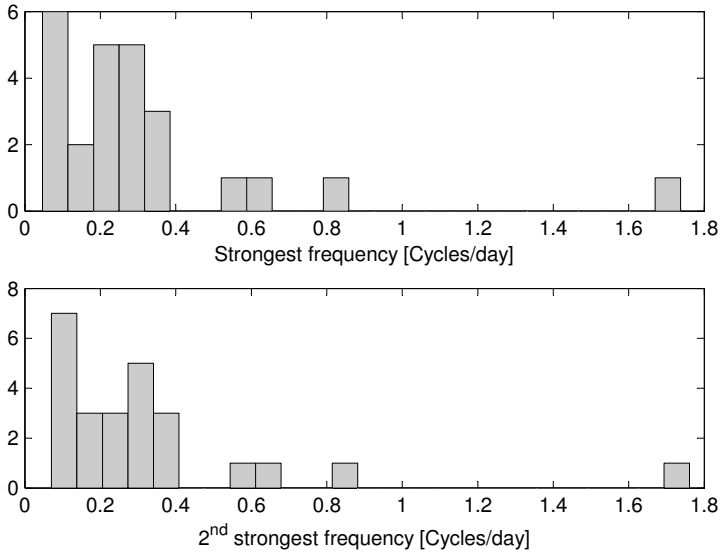

Figure 5.15: Histogram of the two strongest identified frequencies via DFT for the retrospective cohort.

The strongest frequencies for most patients was below 0.4 cycles per day, or 2.5 days per cycle, which is very close to the minimum detectable frequencies for a number of patients. This result suggests critically ill neonates appear to exhibit no significant periodicity in effective insulin sensitivity that could be linked to diurnal cycles. Rather, the data suggests more gradual evolutions in insulin sensitivity, characterised by non-cyclic trends and higher frequency noise.

5.8.2 Model specification

The structure of the autocorrelation (ACF) and partial-autocorrelation functions (PACF) allow the order of the time-series model to be inferred from available data. The relatively strong low frequency periods shown in Figure 5.15 suggest that the mean value of insulin sensitivity may gradually evolve for a patient, as suggested in the example profile presented in the top panel of Figure 5.16. Thus, a first difference was applied to the insulin sensitivity data $S_{I,t}$ to obtain a time series x_t with stable mean:

$$x_t = S_{I,t} - S_{I,t-1} \tag{5.10}$$

A sample ACF and PACF are shown in Figure 5.16. From observation of the ACF and PACF, the structure of the model that appeared most appropriate for neonatal patients was AR(1) or AR(2). This outcome agrees with the observed results for the lag-1 and lag-2 stochastic models that showed little performance improvements with higher lags. Both AR(1) and AR(2) models were assessed in simulation.

The AR(1) and AR(2) models are of the form:

$$x_t = \delta + \alpha_1 x_{t-1} + a_t \tag{5.11}$$

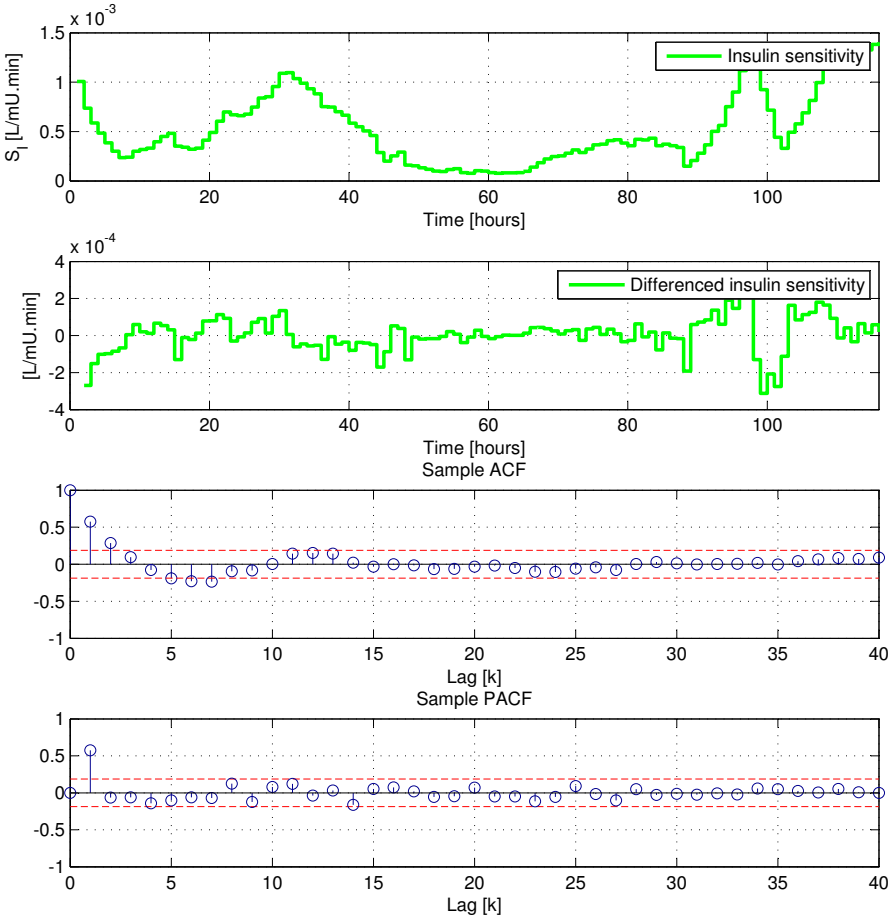

Figure 5.16: Example sample autocorrelation functions for Patient 11. The top panel shows the raw model-fitted insulin sensitivity series. The second panel shows the first difference of the insulin sensitivity series. The bottom two panels show the sample autocorrelation function and partial autocorrelation function of the differenced series respectively.

for AR(1), and for AR(2):

$$x_t = \delta + \alpha_1 x_{t-1} + \alpha_2 x_{t-2} + a_t \tag{5.12}$$

where a_t is a zero-mean, independent random process with common distribution function F_a, with $E[a^2] = \sigma_a^2$, and δ, α_1, α_2 are constants. The parameters α_1 and α_2 may be estimated as $\hat{\alpha}_1$ and $\hat{\alpha}_2$ with least squares minimization of the

Yule-Walker equations [Chatfield, 2004]:

$$\bar{A}\{\hat{\alpha}\}^T = \bar{b} \tag{5.13}$$

where, for the AR(1) case:

$$\{\hat{\alpha}\} = \{\hat{\alpha}_1\}, \bar{A} = (1), \bar{b} = r_1 \tag{5.14}$$

and for the AR(2) case:

$$\{\hat{\alpha}\} = \{\hat{\alpha}_1, \hat{\alpha}_2\}, \bar{A} = \begin{pmatrix} 1 & r_1 \\ r_1 & 1 \end{pmatrix}, \bar{b}^T = \begin{pmatrix} r_1 & r_2 \end{pmatrix} \tag{5.15}$$

The term r_k in Equations 5.14-5.15 is the sample autocorrelation, where c_k is the sample autocovariance function at lag k, both of which are defined:

$$r_k = \frac{c_k}{c_0} \tag{5.16}$$

$$c_k = \frac{1}{N} \sum_{t=1}^{N-k} (x_t - \bar{x})(x_{t+k} - \bar{x}) \tag{5.17}$$

where $\bar{x}$ is the sample mean.

The parameter δ of Equations 5.11 and 5.12 may be estimated as $\hat{\delta}$:

$$\hat{\delta} = \bar{x}\left(1 - \sum_{i=1}^{p} \hat{\alpha}_i\right) \tag{5.18}$$

Further information on the AR methods in this study and their derivation can be found in [Chatfield, 2000, 2004] and [Bloomfield, 2000] and several other fundamental texts on this topic.

5.8.3 Bootstrap prediction intervals

For prediction bands, the AR bootstrap method of Thombs and Schucany [1990] is used in this study. This non-parametric resampling method is chosen given that the parameter S_I is forced to account for many complex, non-random effects.

The Thombs and Schucany [1990] method is outlined briefly here for clarity. Given a data set $x_t = x_1, \ldots, x_N$, the ith residual or error of an AR(p) model with n data samples is defined:

$$\begin{aligned} \hat{a}_i &= x_i - \hat{\delta} - \hat{\alpha_1} x_{i-1} - \cdots - \hat{\alpha_p} x_{i-p}, \\ & \qquad i = t, t-1, \ldots, t-n+p+1 \end{aligned} \tag{5.19}$$

where $\hat{a}_i$ replaces the true errors a_i of Equation 5.12 in the generation of bootstrap replicates. The *backward representation* of the AR series is used to generate conditional bootstrap replicates that have the same last p values and have the same correlation structure as the series being predicted:

$$x_t = \delta + \alpha_1 x_{t+1} + \cdots + \alpha_p x_{t+p} + e_t \tag{5.20}$$

where e_t is a sequence of random variables with a common distribution function F_e. It can be shown that the true error distributions F_a and F_e of the forward and backward models are the same when they are normal [Box and Jenkins, 1976]. To obtain a bootstrap replicate, $\mathbf{x}^*$, the last p values of the replicate are defined:

$$\begin{aligned} x^*_{t-j+1} &= x_{t-j+1}, \\ & \qquad j = 1, \ldots, p \end{aligned} \tag{5.21}$$

The remainder of $\mathbf{x}^*$ are generated by the recursive equations:

$$\begin{aligned} x_j^* &= \hat{\delta} + \hat{\alpha_1} y_{j+1}^* + \cdots + \hat{\alpha_p} y_{j+p}^* + e_j^* \\ & \qquad j = t-p, \ldots, t-n+1 \end{aligned} \tag{5.22}$$

where $\hat{e}_j^*$ is a random draw from the estimated error distribution function $\hat{F}_e$.

Hence a typical bootstrap replicate is $\left(x_{t-n+1}^*, x_{t-n+2}^*, \ldots, x_{t-p}^*, x_{t-p+1}, \ldots, x_t\right)$. Figure 5.17 shows six bootstrap replicates generated from an AR(2) process ($p = 2$), which means that each bootstrap replicate has the same last two values x_{t-1} and x_t.

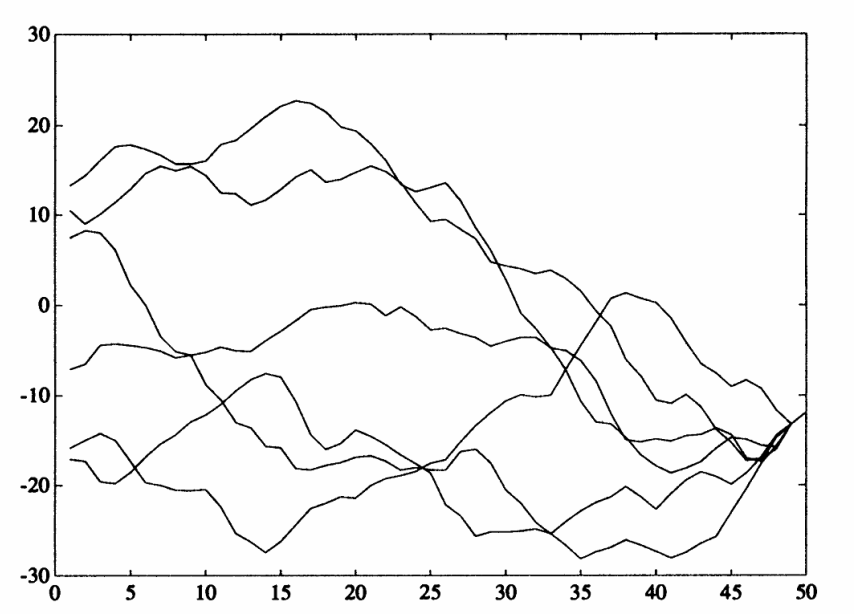

Figure 5.17: Six bootstrap replicates from an AR(2) process ($\delta = 0$, $\alpha_1 = 1.75$, $\alpha_2 =$ -0.76) of length $n = 50$, conditional on having the last p values x_{49} and x_{50}. Adapted from [Thombs and Schucany, 1990].

The bootstrap procedure for a $100\beta\%$ prediction interval begins by calculating a bootstrap future value X_{t+k}^* for each of the B replicates. For a single replicate, X_{t+k}^* is obtained from:

$$X_{t+k}^* = \hat{\delta}^* + \hat{\alpha_1}^* y_{t+k-1}^* + \cdots + \hat{\alpha_p} y_{t+k-p}^* + \hat{a}_{t+k}^* \tag{5.23}$$

where $\left(\hat{\delta}^*, \hat{\alpha}^*\right)$ are the least squares estimates based on the specific bootstrap replicate, and $\hat{a}^*_{t+k}$ is a random draw from $\hat{F}_a$.

Having obtained the set of B bootstrap future values, the prediction limits are defined as the quantiles of the bootstrap CDF of X^*_{t+k}. A summary of the procedure is a follows:

1. Compute residuals from Equation 5.19. Let $\hat{F}_a$ be the empirical CDF of the residuals.

2. Generate bootstrap replicate using Equations 5.21 and 5.22.

3. Compute AR model paramater estimates $\hat{\delta}^*$ and $\hat{\alpha}^*_i$, $i = 1, \ldots, p$ from the bootstrap replicate. Compute a bootstrap point prediction as in Equation 5.23 for lag k, using $\hat{a}^*_{t+k}$, a random draw from $\hat{F}_a$.

4. Repeat Steps 2 and 3 for B bootstrap replicates.

5. Calculate the required prediction band from the quantiles of the bootstrap CDF.

5.8.4 AR model bootstrap prediction results

Bootstrap windows of 12, 24 and 48 hours for both AR(1) and AR(2) models were evaluated to determine the performance of the forecasting procedure. Table 5.5 shows the median forecast IQR width over the cohort, together with the 25^{th} and 75^{th} percentiles, for S_I and BG. The summary statistics are also reported for the 5% - 95% forecast interval width. All forecasts were for 1-hour prediction intervals. The stochastic model results provided for comparison were generated with a variance modifier of $c = 0.5$ (see Section 5.4). Several patients were excluded from the 24 and 48 hour window analyses due to insufficient retrospective data. A comparison of insulin sensitivity forecasts for the bootstrap procedure and the stochastic model is shown in Figure 5.18.

The AR models of both orders gave similar performance across the assessed range of bootstrap windows. In all cases, the width of the prediction forecast

Table 5.5: Insulin sensitivity and BG forecast performance for AR model with bootstrap prediction method. Stochastic model results with constant variance modifier $c = 0.5$ are presented for comparison. All forecasts are for 1-hour prediction intervals.

(a) Insulin sensitivity forecast performance

		Num. forecasts	S_I IQR width (x10^{-3})		% in band	S_I 5% - 95% width (x10^{-3})		% in band
			Median	IQR		Median	IQR	
AR(1)	12 hour	3252	0.106	[0.091 - 0.130]	50.7%	0.327	[0.267 - 0.414]	86.7%
	24 hour	2952	0.098	[0.084 - 0.119]	48.6%	0.315	[0.256 - 0.396]	86.3%
	48 hour	2399	0.092	[0.080 - 0.110]	48.4%	0.302	[0.253 - 0.375]	86.2%
AR(2)	12 hour	3252	0.104	[0.088 - 0.126]	50.0%	0.316	[0.260 - 0.390]	86.4%
	24 hour	2952	0.097	[0.081 - 0.117]	48.3%	0.304	[0.249 - 0.371]	85.8%
	48 hour	2399	0.092	[0.078 - 0.109]	47.9%	0.298	[0.249 - 0.355]	86.3%
Stochastic		3530	0.109	[0.097 - 0.141]	54.7%	0.357	[0.287 - 0.447]	90.9%

(b) BG forecast performance

		BG IQR width		% in band	BG 5% - 95%		% in band
		Median	IQR		Median	IQR	
AR(1)	12 hour	0.6	[0.4 - 1.0]	48.8%	1.9	[1.3 - 3.2]	84.9%
	24 hour	0.6	[0.4 - 0.9]	47.8%	1.8	[1.2 - 3.0]	85.1%
	48 hour	0.5	[0.4 - 0.9]	47.8%	1.7	[1.2 - 3.0]	85.3%
AR(2)	12 hour	0.6	[0.4 - 1.0]	49.4%	1.8	[1.2 - 2.9]	84.4%
	24 hour	0.6	[0.4 - 0.9]	48.6%	1.7	[1.1 - 2.8]	85.4%
	48 hour	0.5	[0.4 - 0.9]	49.5%	1.7	[1.1 - 2.9]	85.8%
Stochastic		0.6	[0.5 - 0.9]	50.8%	2.0	[1.7 - 2.6]	89.5%

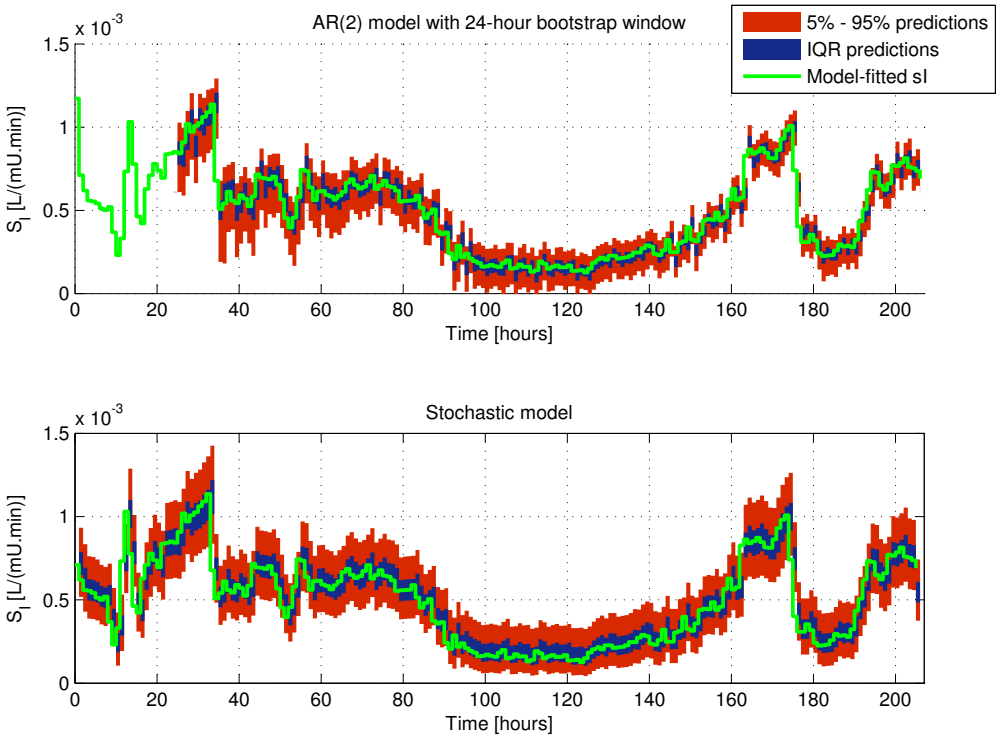

Figure 5.18: Comparison of insulin sensitivity forecasts using the bootstrap method for an AR(2) model with 24-hour bootstrap window (top panel) and stochastic model (bottom panel). The AR model shows tighter probability band widths compared to the stochastic model for periods of relatively stable S_I.

intervals tightened for longer bootstrap data windows. The 25^{th} and 75^{th} percentiles of the IQR and 5% - 95% prediction widths show greater variation for all forms of the AR model compared to the stochastic model. This result highlights the AR model bootstrap prediction intervals adapting to less variable periods by tightening the prediction forecast interval, indicating a more patient-specific adaptation potentially useful for control.

The proportion of insulin sensitivity and BG values within the forecasted band was close to the desired 50% and 90% for all AR models, compared to the relatively conservative result of the stochastic model. Whilst the stochastic model captures insulin sensitivity variability for an entire cohort of patients, the AR model will only capture insulin sensitivity variability in a single patient up to the current time. Thus, there is a possibility that the AR model could miss a sudden change in insulin sensitivity that is not unlikely in terms of the

whole cohort, but had not yet been observed in the particular patient. This possibility suggests that whilst the tighter insulin sensitivity prediction intervals may encourage more aggressive insulin usage, maintaining global limits on insulin rates would be prudent to minimise risk due to sudden changes in condition.

Adequate data is required to adequately estimate the error distribution $\hat{F}_a$. Thus, an AR method would not be applicable until at least 12-24 hours of data had been collected for the patient. This aspect is of particular concern for the neonate as hyperglycaemia often requires treatment within the first day of life. In contrast, the stochastic method is able to generate forecasts from the 2$^{\text{nd}}$ BG measurement during clinical usage.

Figure 5.18 shows that the prediction bounds tighten during periods of relative stability in the insulin sensitivity profile for the AR model case, compared to a relatively constant prediction interval width for the stochastic model case. Thus, the AR model identifies periods of stable insulin sensitivity as a tighter prediction interval. However, it is important that this result should not be interpreted as a reason for less intensive BG monitoring. Due to the clinical fragility of this patient group sudden changes in overall patient condition are not uncommon, such as the onset of a new infection. Such changes have the undesirable effect of increasing the variability in insulin sensitivity. In particular, the NIRTURE trial [Beardsall et al., 2008] found most hypoglycaemia was in infants deemed relatively healthy and concluded that these infants were probably monitored less intensively, thus missing changes in metabolic condition.

The AR bootstrap procedure can be naturally extended to generate prediction intervals for longer lags. Equation 5.23 can be applied recursively to generate prediction intervals for lags greater than 1 hour. A comparison of the insulin sensitivity prediction performance for an AR(2) model with 24-hour bootstrap window over lags of 1-4 hours is presented in Table 5.6.

The IQR and 5% - 95% prediction interval widths presented in Table 5.6 increase with longer lags. The prediction performance as assessed by proportion of values within prediction bounds decreases dramatically over longer time periods. This is expected as for lags less than the order of the model p, prediction error variance is due to variability due to the residual term and variability due to parameter estimation [Thombs and Schucany, 1990]. For longer lags, future

Table 5.6: Insulin sensitivity forecast performance for AR model with bootstrap prediction interval method for lags 1-4 hours.

	Num. forecasts	S_I IQR width (x10^{-3})			S_I 5% - 95% width (x10^{-3})		
		Median	IQR	% in band	Median	IQR	% in band
Lag 1	2952	0.097	[0.081 - 0.117]	48.3%	0.304	[0.249 - 0.371]	85.8%
Lag 2	2902	0.107	[0.092 - 0.128]	37.8%	0.319	[0.264 - 0.401]	74.7%
Lag 3	2852	0.109	[0.093 - 0.130]	33.5%	0.326	[0.271 - 0.406]	68.5%
Lag 4	2802	0.110	[0.093 - 0.130]	30.4%	0.329	[0.271 - 0.404]	64.7%

values will vary with each bootstrap replicate, thus increasing the variance of the set of future values. Clinically, these changes would also be expected.

The bootstrap method of Thombs and Schucany requires iteration, whereas the Markov model can be stored as a look-up table, or set of piecewise polynomials to allow interpolation. Thus, the AR approach is a computationally more expensive routine. For example, a single forecast using the stochastic model requires < 0.1 seconds of computation time, however it takes approximately 5.4 seconds to 18.6 seconds for each prediction generated by the AR bootstrap method for 12-hour and 48-hour bootstrap windows respectively. The bootstrapping routine lends itself well to parallel processing, so execution time may be reduced on modern multi-core computer processors. This computational speed difference becomes a relevant factor for Monte-Carlo analyses, and an increase in simulation time of up to 18 seconds for the 48-hour window case may cause a noticeable delay for clinical staff using the system in real-time.

5.9 Summary

A stochastic model to provide insulin sensitivity predictions is developed from a set of insulin sensitivity data for a neonatal intensive care cohort. The model provided conservative prediction estimators that provided greater coverage than expected from the probability bounds. Incorporating lag-2 effects did not improve the coverage proportion, and greater coverage over-estimation in regions of higher data density pointed to the variance estimator based on local data density as a possible source of over-estimation. Modifying the data density estimator by introducing a constant scaling factor showed appropriate coverage was obtained at approximately 10-50% of the original value. However, at low values of the scaling factor the probability bounds were no longer smooth or physiologically realistic. Smooth probability bounds containing the appropriate proportion of prediction coverage could be obtained by choosing the probability bounds to obtain the desired prediction performance.

AR models are able to generate a patient-specific model to allow for tighter prediction intervals during periods of relative stability in insulin sensitivity. However, such models require substantial individualised patient data (eg: 12 - 48

hours) which may not be available at the commencement of real-time glycaemic control. Thus, the cohort wide model presented here may be employed to provide prediction bounds until a suitable amount of data is generated to employ a patient-specific model.

The analyses in this chapter established forecasting performance is influenced by trade-offs between methods and within methods. The stochastic model uses a kernel estimator based on the Normal probability distribution. A kernel based on a different probability distribution may prove more ideal for this data, or alternatively the ideal kernel for this data may not resemble any commonly used distribution. Thus, modifying the variance estimator effectively shifts the trade-off between conservatism and control applicability. A similar trade-off exists between the stochastic and AR forecast methods. AR models may allow for tighter control when patients are stable, however stochastic models can provide a higher level of safety during periods of greater variability. A combination of forecasting techniques may provide the best of both worlds, and the balance between these trade-offs can be adjusted based on the qualities of control desired in a particular clinical application.

Chapter 6

Virtual trials

Several design parameters must be considered in developing a safe, effective and optimal neonatal glycaemic control algorithm. Virtual trials offer the opportunity to explore control strategies in simulation before pilot clinical trials. In particular, the proposed control algorithm needs to reduce elevated blood glucose level in a controlled, predictable manner accounting for external nutrition. The controller must also account for inter-patient variability and varying physiological condition. Hence, it must be adaptive and/or able to identify changes in patient dynamics, particularly with respect to insulin sensitivity. The protocol should require only infrequent sensor measurements to minimise labour and comply with existing medical protocols on the treatment of neonatal hyperglycaemia to ensure the method developed could be readily implemented in a clinical environment. Finally, the controller must be robust to sensor errors, and other clinical events that may impact the transition from the simulation environment to clinical practice.

This chapter will introduce the methodology behind virtual trials and model-based targeted glycaemic controllers. Several control variables related to controller implementation specifics will be assessed in simulation to determine their impact on BG control performance. Finally, effects including missed BG measurements, delays in implementing controller recommendations and BG sensor noise are simulated to test the robustness of the controller.

6.1 Virtual trial methods

The insulin sensitivity parameter, S_I, drives the dynamics of the blood glucose model and is assumed independent of exogenous insulin and nutrition administration [Bergman et al., 1981]. Once a patient-specific profile of time-varying insulin sensitivity is generated, it can be used to predict blood glucose concentration based on different insulin and nutrition control schemes by solving the set of differential equations representing the system over the future time period of interest. Such analyses are effectively *in-silico* or virtual trials and have been used extensively in protocol design for adult critical care [Chase et al., 2007; Lonergan et al., 2006b; Wilinska et al., 2008] and Type I diabetes [Wong et al., 2008].

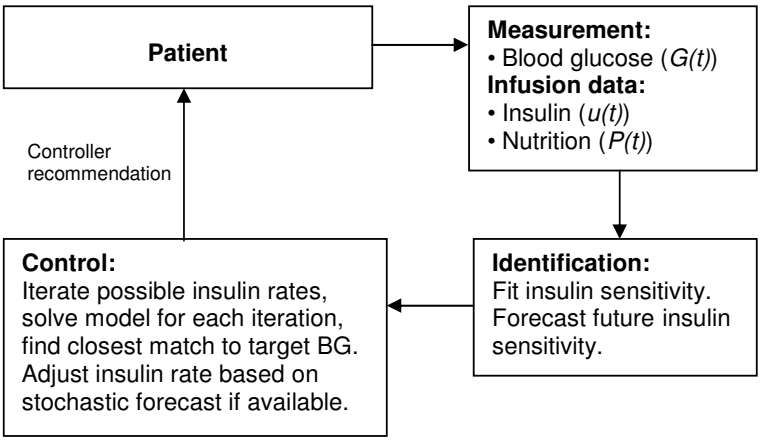

Figure 6.1: Controller implementation schematic

The clinical implementation procedure for the model-based controller in a clinical environment is shown in Figure 6.1. A BG measurement and subsequent controller intervention represents one cycle of the loop in Figure 6.1. Typically, this process is repeated every 1-2 hours in adult critical care. The virtual trial procedure replaces the 'Patient' in Figure 6.1 with a forward solution of the model using an insulin sensitivity profile generated from retrospective data, and adds sensor noise and other variations as required.

The blood glucose history, along with insulin and nutrition history, are used to

fit the patient's insulin sensitivity profile in real-time. A forecast for future insulin sensitivity is then generated using a statistical method or other technique. This S_I profile is then used by the controller to solve Equations 2.28-2.30 (Chapter 2) to predict blood glucose concentration based on insulin and nutrition rates. Several combinations of infusion rates can be simulated to select the dosage that will most likely meet the target BG concentration, as shown in Figure 6.2. Thus, the controller adapts to the current metabolic state of the neonate in real-time. The controller employed in this research uses a bisection algorithm, shown in Figure 6.3 to determine the insulin infusion rate that will bring the BG closest to a target BG, if the target is physiologically possible with safety. Thus, every BG measurement is followed by a controller intervention to alter the insulin infusion rate.

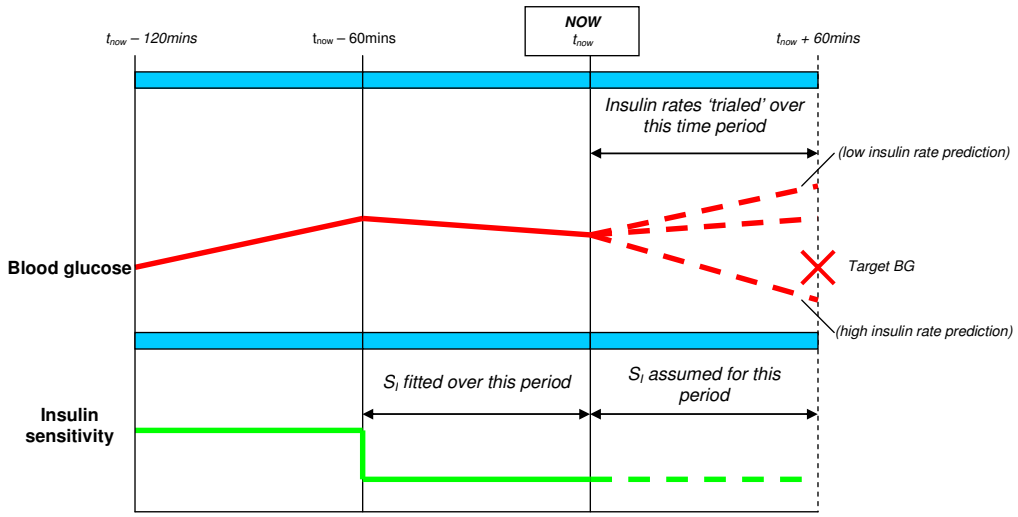

Figure 6.2: Insulin sensitivity period and BG prediction period used by the model-based controller.

6.1.1 Controller development

Controllers using 1 - 4 hourly BG measurement and intervention intervals were examined and compared to the retrospective hospital control clinical data and simulations using a typical insulin sliding scale shown in Table 6.1. All initial

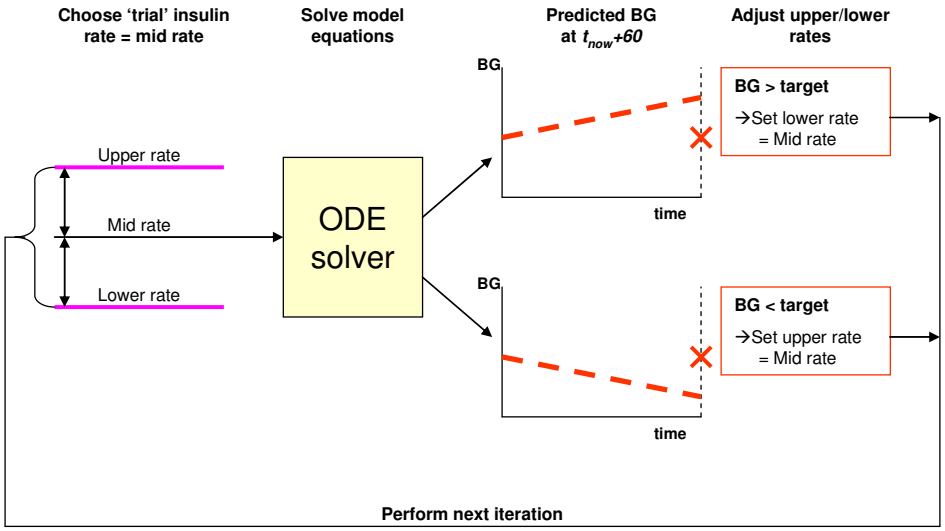

Figure 6.3: Iterative bisection method used by the model-based controller to select an insulin infusion rate.

Table 6.1: Typical insulin sliding scale used in simulation.

Blood glucose	Insulin rate
$>$ 20 mmol/L	0.100 U/kg/hr
15 - 20 mmol/L	0.075 U/kg/hr
10 - 15 mmol/L	0.050 U/kg/hr
5 - 10 mmol/L	0.025 U/kg/hr
$<$ 5 mmol/L	STOP

simulations were performed with uniformly distributed 7% measurement error, which is a conservatively large choice [Peet et al., 2002; Chen et al., 2003]. The insulin sensitivity profiles fitted to the 25-patient retrospective cohort provided the virtual patients for simulation. The blood glucose target is 6.0 mmol/L or a 15% reduction per hour from the current BG concentration, whichever is the greater value. The controllers developed modulated only the insulin infusion rate and used the retrospective parenteral dextrose and enteral nutrition infusion profiles. Controllers that modulate both insulin and nutrition are investigated in Section 6.4.

Crucially, blood volumes in neonates are small [Cassady, 1966; Leipala et al., 2003], which restricts the frequency of BG sampling. This restriction provides an

additional challenge for model-based control in the neonatal setting compared to the adult case. Thus, it is important to optimise the number of BG measurements required for control. Clinically, volume restrictions mean most neonates will not be sampled more than 2-hourly (12 per day) as a maximum rate overall.

The metabolic status of a critically ill neonatal patient can change rapidly. This change is reflected by sudden rises and drops in insulin sensitivity. Additionally, sudden changes in apparent insulin sensitivity may be caused by sensor noise and/or measurement error [Chase et al., 2008b]. Thus, for example, a balance is required between the speed at which a controller reacts to correct blood glucose rises due to sudden changes in metabolic state, and the risk of running higher insulin infusion rates when a sudden apparent rise in blood glucose resolves quickly, or was due to measurement error.

To explore the balance between speed of control response and robustness against either real sudden metabolic changes or large sensor errors (false changes), two sets of controller schemes were evaluated. Scheme 'A' controllers set a relatively high upper limit of 0.5 U/kg/hr for the maximum controller insulin infusion rate, and limited the maximum increase in insulin infusion rate permitted from one intervention to the next. Scheme 'B' controllers used a lower maximum insulin infusion rate of 0.1-0.5 U/kg/hr based on reported trials of insulin infusion in neonates [Collins et al., 1991; Kanarek et al., 1991; Meetze et al., 1998], but no limit on the ability to increase the insulin infusion rate (up to the maximum allowable rate). Note that both schemes have no limit on decreasing the infusion rate to allow the protocol to 'back-off' quickly.

Performance was measured as more BG measurements within a clinically recommended target 4 - 7 mmol/L band, while minimizing or eliminating measurements lower than 2.6 mmol/L. The LBG-P (Low BG to Performance) ratio provides a measure of the increased risk of low BG measurements under tight glycaemic control compared to the increase in measurements within the target BG band. The LBG-P ratio is defined as:

$$\frac{\%\text{ measurements} < 2.6\text{ mmol/L}}{\%\text{ measurements within 4-7 mmol/L band}} * 100 \tag{6.1}$$

Both insulin rate control schemes were tested with 1, 2, 3 and 4 hour BG

measurement intervals to assess the robustness of each scheme to increasing measurement interval length. The best performing controller was subjected to further analysis, including simulated BG sensor error and clinical delays.

6.2 Controller analysis

6.2.1 Controller limits

A comparison of controller rules on insulin infusion for several combinations of maximum insulin infusion rate and maximum increase in insulin infusion rate per intervention is presented in Table 6.2. Interestingly, despite the targeted BG controller using model-based BG forecasts to implement insulin dosage, the implementation of limits on maximum insulin rate and rate of change of insulin infusions produced noticeable variations in controller quality, as evidenced by the spread of times in relevant glycaemic bands and the LBG-P ratio. This result highlights the dynamic, evolving nature of the neonatal patient and emphasises the importance of relatively frequent BG measurement and control cycles.

Scheme 'A' with a 0.01 U/kg/hr limit on insulin infusion rate increases had a median BG greater than 6.0 mmol/L for all measurement interval cases, as well as a relatively low proportion of measurements within the 4 - 7 mmol/L range. Thus, this scheme does not react to changes in metabolic state fast enough for optimal control. The results for Scheme 'A' simulations with allowable insulin infusion rate increases of 0.03 and 0.05 U/kg/hr per intervention show a similar level of performance. The 0.05 U/kg/hr increase limit achieved a higher percentage of measurements within the target BG band. However, the 0.03 U/kg/hr increase limit achieved a lower LBG-P ratio for 2-4 hourly measurement intervals.

Scheme 'B' with the lower upper insulin rate of 0.1 U/kg/hr yielded a lower percentage of measurements within the 4 - 7 mmol/L range across all measurement frequencies compared to the higher-performing Scheme 'A' results, suggesting that 0.1U/kg/hr is too low for a maximum insulin infusion rate for most patients. The results for Scheme 'B' simulations with 0.3 U/kg/hr and 0.5 U/kg/hr upper insulin rate limits showed little difference in measurements within the 4 - 7 mmol/L band despite the availability of higher insulin infusion rates. However,

Table 6.2: Effect of controller rules for insulin infusion rate increases on BG control and hypoglycaemia. The LBG-P ratio compares Low-BG to Performance, which is defined as the ratio of the percentage of measurements < 2.6 mmol/L and the percentage of measurements within the 4-7 mmol/L range.

Controller scheme	Max insulin rate	Max increase in insulin per intervention	Measurement interval	% of measurements within range 4-7 mmol/L	> 4 mmol/L	< 2.6 mmol/L	BG median (mmol/L)	LBG-P ratio
A	0.5 U/kg/hr	0.01 U/kg/hr	1hr	65.9	1.6	0.1	6.4	0.21
			2hr	63.5	2.5	0.3	6.4	0.44
			3hr	56.9	3.1	0.3	6.5	0.60
			4hr	54.9	3.3	0.5	6.6	0.83
		0.03 U/kg/hr	1hr	81.7	1.7	0.2	6.1	0.28
			2hr	76.1	3.4	0.5	6.0	0.59
			3hr	69.3	5.8	0.6	6.1	0.86
			4hr	64.6	7.1	0.9	6.1	1.41
		0.05 U/kg/hr	1hr	85.7	1.8	0.2	6.0	0.26
			2hr	80.0	3.7	0.7	5.9	0.85
			3hr	71.9	6.7	0.9	6.0	1.30
			4hr	68.8	7.3	1.4	5.9	1.98
B	0.1 U/kg/hr		1hr	77.1	1.7	0.1	6.1	0.18
			2hr	71.4	3.4	0.3	6.1	0.40
			3hr	65.6	5.9	0.9	6.2	1.43
			4hr	62.9	6.1	0.9	6.1	1.45
	0.15 U/kg/hr		1hr	83.9	1.8	0.2	6.0	0.27
			2hr	77.9	4.1	0.4	5.9	0.51
			3hr	70.6	6.9	1.1	6.0	1.57
			4hr	67.0	7.8	1.5	5.9	2.21
	0.3 U/kg/hr		1hr	89.0	2.5	0.2	5.9	0.25
			2hr	79.2	5.8	1.0	5.9	1.21
			3hr	72.3	9.1	1.4	5.9	2.00
			4hr	68.9	9.4	1.8	5.8	2.64
	0.5 U/kg/hr		1hr	88.5	3.0	0.4	5.9	0.45
			2hr	80.4	6.0	1.1	5.9	1.40
			3hr	72.3	8.9	2.0	5.9	2.71
			4hr	68.5	10.0	2.7	5.8	3.99

these two control schemes recorded the highest percentage of measurements less than 2.6 mmol/L, and the high LBG-P ratio reflects that the increased risk of low BG measurements was greater than the possible increase in measurements in the target BG band compared to the other insulin schemes.

Thus, Scheme 'A' with a 0.03 U/kg/hr allowable insulin infusion increase rate and Scheme 'B' with an upper limit of 0.15 U/kg/hr of insulin represent the best performing versions of each control scheme. The Scheme 'B' simulation achieved a higher proportion of measurements within the target band across all measurement frequencies. However, the Scheme 'B' simulation showed a higher proportion of measurements below 2.6 mmol/L for longer measurements intervals than the Scheme 'A' counterpart, a result emphasised by the higher LBG-P ratio. Thus, Scheme 'A' with a maximum increase in insulin rate of 0.03 U/kg/hr, highlighted in Table 6.2, provides an effective compromise between controller performance and robustness to increased times between measurements, and was chosen as the controller for the remaining simulations in this study.

6.2.2 Comparison with retrospective and sliding-scale control

The impact of constant measurement frequency with different measurement periods was investigated for the model-based controller and the sliding scale of Table 6.1. The results were also compared to hospital control in the retrospective clinical data. Clinical implementation requires efficient use of clinical staff time and hospital resources. Measurement frequency is often a balance between nursing burden and accuracy of control [Chase et al., 2008a; Mackenzie et al., 2005]. An additional aspect to more frequent blood glucose measurement specific to the neonatal case is that the doors to the incubator are open more often, which may negatively affect the infant's hydration status [Hartnoll, 2003].

Table 6.3 compares blood glucose performance metrics, along with insulin intake, between the actual retrospective NICU control, and simulated sliding scale and targeted control. The median BG for all model-based control cases presented in Table 6.3 is at, or close, to the target BG. The percentage of measurements within the 4 - 7 mmol/L and 4 - 8 mmol/L ranges are [65% - 82%] and [76% -

Table 6.3: Comparison of glycaemic control performance between retrospective control, typical sliding scale control and targeted model-based control with increasing BG measurement interval.

Control scheme	Measurement frequency	Total measurements	Median BG (mmol/L)	BG IQR (mmol/L)	% of measurements within range 4-7 mmol/L	4-8 mmol/L	< 2.6 mmol/L	Avg. insulin (U/kg/hr)
Model-based controller	1-hourly	3555	6.1	[5.6-6.6]	82%	90%	0.23%	0.054
	2-hourly	1771	6.0	[5.4-6.8]	76%	86%	0.45%	0.056
	3-hourly	1175	6.0	[5.3-7.0]	69%	81%	0.60%	0.057
	4-hourly	879	6.1	[5.2-7.2]	65%	76%	0.91%	0.055
Retrospective		1091	8.0	[6.3-9.9]	31%	46%	0.73%	0.034
Sliding scale	1-hourly	3555	8.6	[6.8-10.4]	26%	40%	0.20%	0.029
	2-hourly	1771	8.6	[6.9-10.5]	25%	39%	0.34%	0.029
	3-hourly	1175	8.5	[6.8-10.6]	25%	41%	0.34%	0.030
	4-hourly	879	8.5	[6.9-10.8]	24%	41%	0.57%	0.030

90%] which is [103% - 161%] and [61% - 91%] higher than retrospective hospital control respectively. The sliding scale results showed higher median BG than either model-based control or retrospective results.

The length of time between blood glucose measurements reduces the quality of model-based control, dropping from 82% to 65% of BG measurements within the 4 - 7 mmol/L band for 1-hour to 4-hour measurement intervals. The proportion of simulated measurements below 2.6 mmol/L is less than retrospective control for 1 - 3 hourly measurements, but slightly greater for 4-hourly measurements. The width of the IQR for retrospective control was 3.6 mmol/L and for sliding scale control was 3.6 - 3.9 mmol/L, in contrast to a much tighter 1.0 - 2.2 mmol/L for 1 and 4-hour simulations.

The results for the sliding scale protocol showed very little variation over the 1 to 4 hourly measurement intervals simulated. This result may be due to the very discrete nature of the sliding scale used, and perhaps highlights that more frequent measurement must be combined with a more refined protocol in order to safely achieve glycaemic reductions and control with this type of approach.

Table 6.3 shows that time in a relevant glycaemic band is a clearer indication of control performance when comparing control protocols than a median value. The median blood glucose did not change significantly within protocols. However, time in band decreased dramatically in the presence of longer measurement intervals out to 4 hours for the model-based controller, indicating increased glycaemic variability and thus potentially worse outcomes [Egi et al., 2006; Krinsley, 2008]. The BG IQR width also showed the changes in BG variability. However, time in band provides an easy-to-visualise method of comparison.

Cumulative distribution functions provide not only the means to compare protocols, but also obtain time in any glycaemic band preferred. Figure 6.4 shows the empirical cumulative distribution functions (CDF) for BG measurement between simulated trials and retrospective control. The results for 1 - 4 hour measurement frequencies all intersect the 50^{th} percentile area at approximately the target value of 6.0 mmol/L. The major difference in control quality between the simulations lies within the slope of the lines, where more frequent BG measurement and controller intervention results in a steeper slope, and thus a tighter BG distribution.

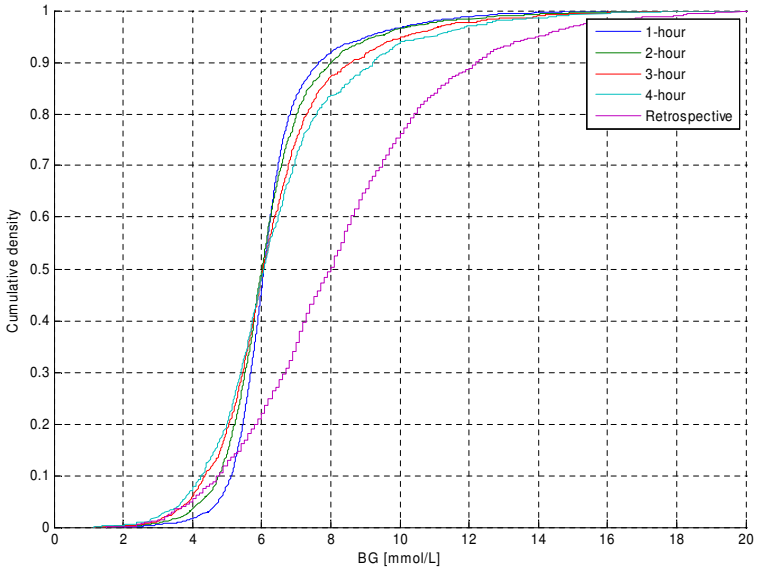

Figure 6.4: Empirical cumulative distribution functions of BG measurements for retrospective hospital control versus simulated model-based control trials of 1, 2, 3 and 4-hour measurement and intervention frequency.

Finally, it is equally interesting to note that higher (or lower) insulin usage is also not associated with an increase (or decrease) in hypoglycaemia. In this case, the model-based controller used more insulin, but had the least hypoglycaemia. Hence, it is not the amount of insulin used, but how it is used, that results in variability and hypoglycaemic risks.

Insulin usage between the measurement frequencies was similar for model-based control, and 65% - 74% higher than hospital control. It is interesting to note in Table 6.3 that higher average insulin rates did not necessarily correspond with greater proportion of measurements within target BG ranges. The highest proportion of measurements within the target band was for the 1-hour control, yet this measurement frequency used the least insulin of all simulated trials.

All model-based controller results are significantly different from the retrospective BG measurement distribution. It is important to note the curves presented in Figure 6.4 are not symmetrical - the slope at lower BG ranges is steeper. Thus, BG results when not within the target range are skewed towards the upper BG range, as mild hyperglycaemia is considered safer than an increased risk of hypoglycaemia.

Figure 6.5 shows the median CDF and 5% - 95% range of CDFs of the per-patient control results for the model-based controller with 2-hourly measurement frequency and those for the retrospective data. The inter-patient variation in BG control with the model-based controller is much tighter compared to retrospective control. Thus, the model-based controller better modulates insulin to account for each individual patient's glycaemic response.

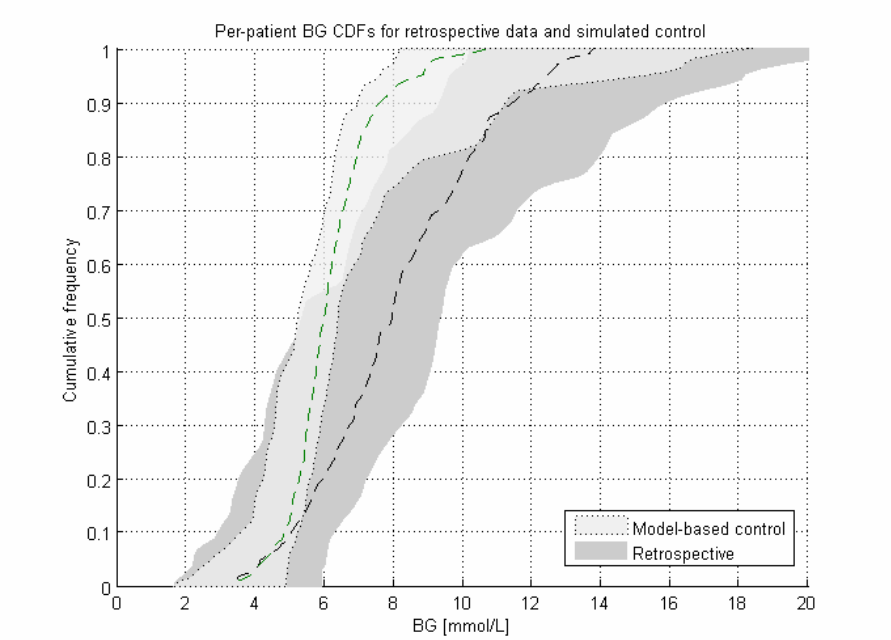

Figure 6.5: Median and 5%-95% interval of per-patient BG CDFs.

Figure 6.6 compares the proportion of BG measurements within the target 4 - 7 mmol/L band for retrospective and simulated model-based control. Only one patient retrospectively had greater than 50% of BG measurements within the target band under hospital control. All patients had greater than 50% of BG measurements within the target band in simulation. The 45° line in Figure 6.6 represents the line of no-change in performance. All results are above this line indicating that the model-based controller achieved more BG measurements within the target band than retrospective control for a range of preterm neonates. The distance from the line is a measure of the increase in BG measurements within the target band per-patient.

Figures 6.7a, 6.7b and 6.8 compare retrospective control and simulated model-based control for three typical patients. The bottom panel of Figures 6.7a, 6.7b and 6.8 show the model's ability to track the insulin sensitivity profile in real-

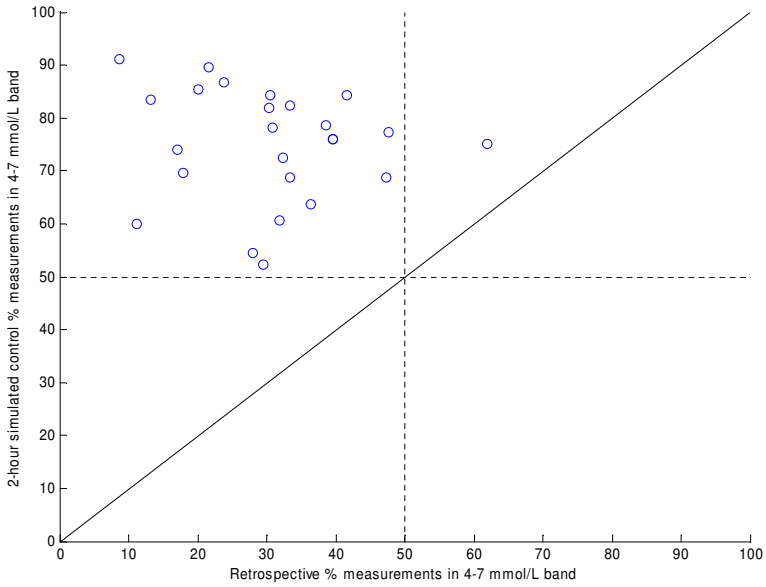

Figure 6.6: Comparison of percentage of BG measurements within the 4 - 7 mmol/L BG range for retrospective and 2-hour simulated control. Each circle represents one of the 25 patient profiles.

time based on data available at the bedside. This tracking is achieved through the integral-based fitting method and through the independence of insulin sensitivity as a model parameter.

6.2.3 BG-based measurement scheme

A BG measurement timing scheme based on current BG concentration was tested. In particular, a high BG concentration carries little risk of hypoglycaemia and may thus require less frequent BG sampling compared to periods at lower concentrations. Thus, a BG-concentration derived measurement scheme was simulated where measurements were taken every 3 hours if BG $>$ 8 mmol/L and any decrease in BG since the last measurement was less than 2 mmol/L/hr. A measurement period of 3 hours was also used if the last 4 hours have been within the 4-8 mmol/L band, as a response to relative glycaemic stability. Measurements were otherwise taken 2-hourly if BG was within the 4-8 mmol/L range, and hourly if BG was less than 4 mmol/L.

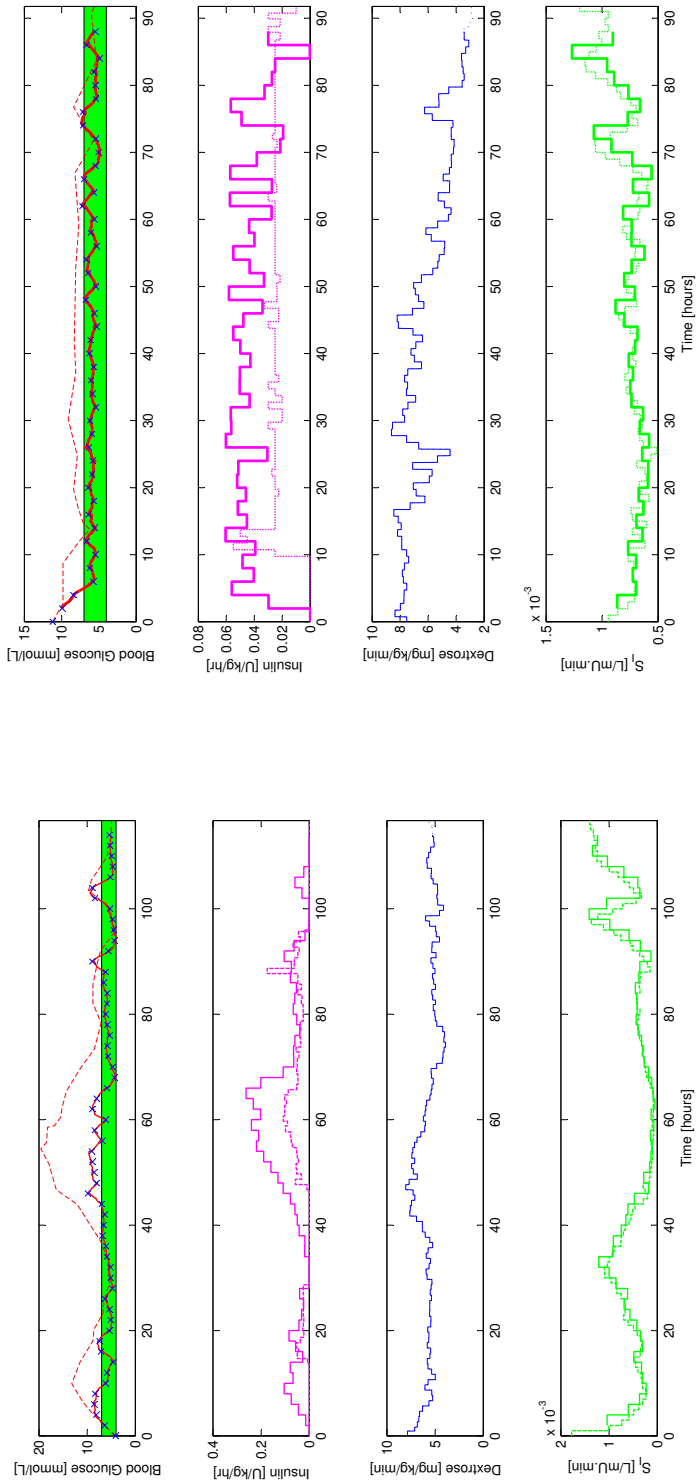

(a) Patient 11

(b) Patient 18

Figure 6.7: Comparison of blood glucose, insulin, nutrition and S_I profiles for Patients 11 and 18 under retrospective control (dashed) and simulated model-based control (solid).

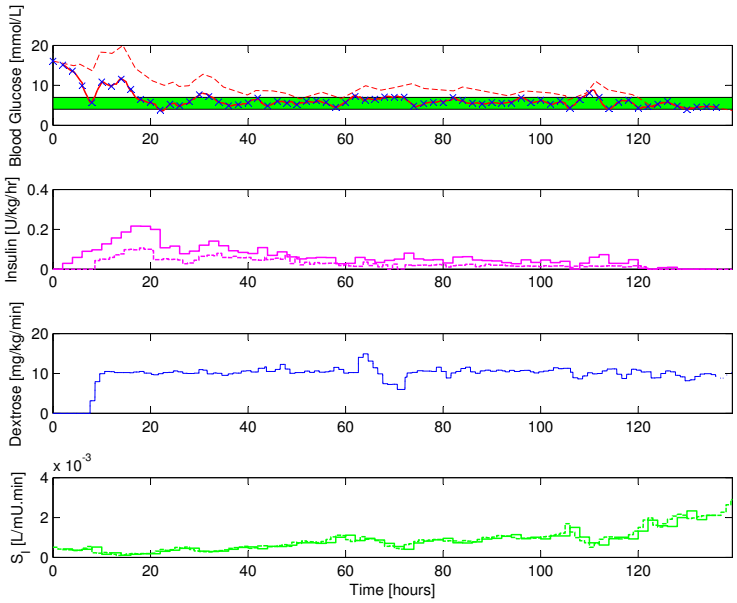

Figure 6.8: Comparison of blood glucose, insulin, nutrition and S_I profiles for Patient 21 under retrospective control (dashed) and simulated model-based control (solid).

Table 6.4 shows BG control performance metrics for the BG concentration-based variable measurement frequency scheme. A total of 1,446 simulated measurements were used across the cohort, representing an average measurement frequency of 2.4 hours. The summary BG control metrics for the BG-based measurement scheme in Table 6.4 were computed using the model-fitted BG concentration at 2.4 hour intervals to remove bias introduced by different measurement frequencies at different BG concentrations. The BG-based measurement scheme resulted in lower time in target BG band, higher median BG and wider BG interquartile range when compared to 2- and 3-hour constant measurement frequency schemes. Interestingly, this result is not necessarily expected. The primary basic course is a delay in response to changes in patient condition after periods of relative glycaemic stability, slowing the response to hyperglycaemia as shown by the higher BG upper quartile result for the BG-based scheme.

Figure 6.9 shows a simulated trial using the BG-based measurement and intervention scheme. This timing scheme demonstrates the effects of non-symmetrical control rules. The controller has limitations on increases in insulin infusion rates, whereas there is no limit on decreases in insulin infusion rates. Thus, as fewer BG measurements are taken at higher BG concentrations under this timing scheme, there are fewer iterations of the control cycle and thus a slower increase of insulin

Table 6.4: BG controller performance for BG-based measurement interval scheme.

	Measurement scheme		
	BG-based	2-hour	3-hour
Num. measurements	1,446	1,771	1,175
% measurements within 4 - 7 mmo/L	63.6%	76%	69%
% measurements < 2.6 mmol/L	0.45%	0.45%	0.60%
BG median [mmol/L]	6.2	6.0	6.0
BG IQR [mmol/L]	[5.3 - 7.5]	[5.4 - 6.8]	[5.3 - 7.0]

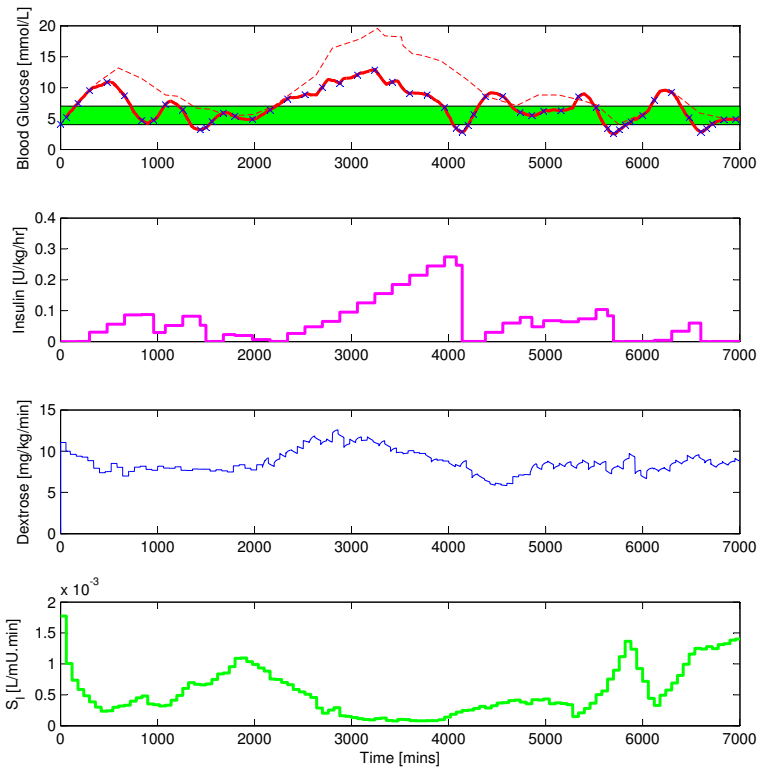

Figure 6.9: Patient 11 simulated control using a BG-based measurement and intervention timing scheme. The dashed line in the top panel represents the retrospective blood glucose concentration under hospital control.

infusion rate in response to higher BG levels. As more measurement/control cycles are performed at lower BG concentrations, there is a higher chance the insulin infusion may be stopped.

Several examples of this effect are shown for Patient 11 in Figure 6.9 at 4,000, 5,500 and 6,500 minutes. The insulin infusion is stopped during periods of frequent BG measurement. Subsequent BG measurements do not cause a

Table 6.5: Glucose control performance and frequency of measurement for insulin volume-based BG measurement scheme.

Insulin volume	Num. measure-ments	BG (mmol/L)		% of measurements within range		
		Median	IQR	4-7 mmol/L	< 4 mmol/L	< 2.6 mmol/L
0.4 mL	2,239	6.1	[5.6 - 6.8]	76.6	2.0	0.2
0.5 mL	1,845	6.1	[5.5 - 7.0]	73.0	2.4	0.3
0.6 mL	1,612	6.1	[5.5 - 7.1]	70.6	3.6	0.4
0.7 mL	1,429	6.2	[5.4 - 7.1]	68.5	4.2	0.3

change in the insulin infusion rate - these measurements act as 'confirmation' measurements rather than 'control' measurements. Thus, the BG-based scheme makes less efficient use of BG measurements for control purposes compared to constant measurement schemes due to anti-symmetry in the control rules, and highlights the use of virtual trials as an iterative design tool to develop optimised protocols.

6.2.4 Infusion-volume based measurement scheme

A novel BG measurement and controller intervention timing scheme based on the rate of insulin infusion was investigated. Standard insulin delivery pumps used in neonatal intensive care can be programmed to deliver a set amount of insulin at a specified rate, and then cease infusions. This feature can provide a safeguard against over-infusion of insulin, and provides a natural reminder for the nursing staff to take another BG measurement. Simulations were performed with BG measurements spaced by the amount of time taken for a set volume of insulin to be infused into the patient. Thus, higher rates of insulin infusion will incur more frequent BG measurements. Insulin concentrations of 0.25 U/kg/mL, as used in the Neonatal Department of Christchurch Women's Hospital, were assumed in the simulations. Measurement timings based on insulin volumes for 0.4 - 0.7 mL were investigated, as shown in Table 6.5 and Figure 6.10.

The insulin volume cutoffs presented in Table 6.5 equate to measurement frequencies of 1.6 - 2.6 hours. While median BG was relatively constant between simulations, glycaemic control performance steadily decreased with higher volumes of infused insulin between BG measurements, as expected given the results of Table 6.3. However, the distribution of BG shown in Figure 6.10 displays little

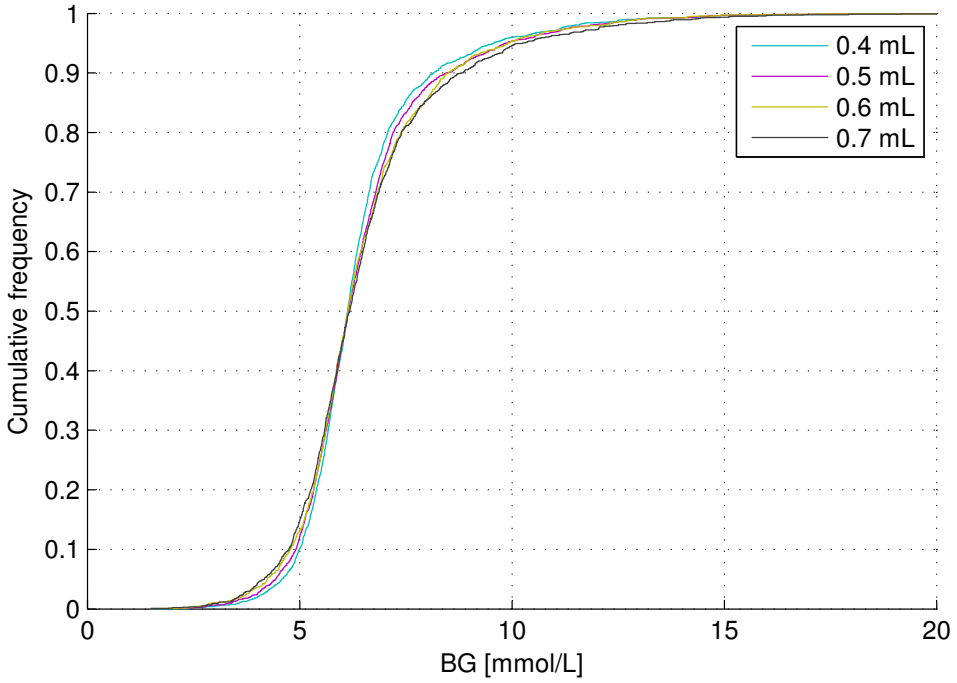

Figure 6.10: Empirical CDFs of model-based controller results for insulin-volume based BG measurement scheme.

overall difference in BG control.

6.2.5 Comparison of measurement schemes

BG and control intervention timing schemes have been investigated in simulation for three cases: constant frequency, BG-concentration based and insulin volume based measurement schemes. Figure 6.11 compares the glycaemic control performance, as measured as percentage of BG measurements within the 4 - 7 mmol/L band compared to the total number of BG measurements. The effectiveness of glucose control with respect to frequency of blood glucose measurement is compared, which has implications for both nursing burden and blood volume requirements.

The line of best fit through the constant measurement frequency results provide a cut-off for comparing performance. Results above the line indicate higher

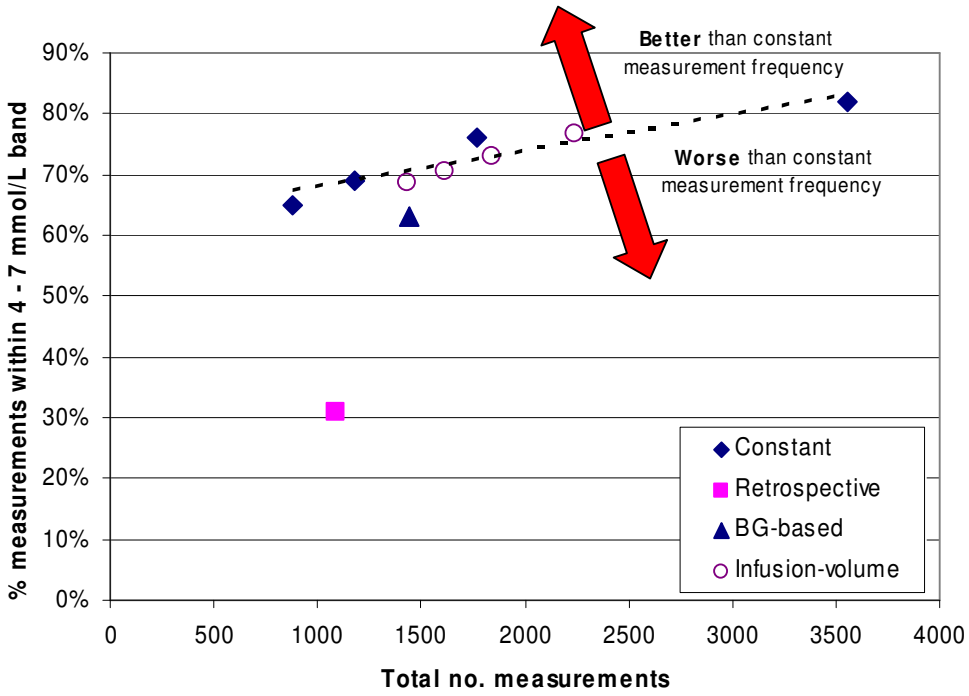

Figure 6.11: Comparison of BG control performance with different measurement and control timing schemes. The dashed line represents a line of best fit through the constant measurement frequency results.

control performance per BG measurement, and below the line indicate less control performance per BG measurement. Constant measurement frequency showed the best performance results, with the insulin-volume measurement scheme achieving a similar level of performance. The BG-based measurement scheme resulted in a similar level of performance for an equivalent number of BG measurements, and retrospective control had the lowest overall percentage of BG measurements within the target band. Thus, these measurement frequency schemes and protocols do not make a more optimal use of the measurements available compared to the clinically easier regular measurement frequency.

6.2.6 Stochastic model

Stochastic modelling of the insulin sensitivity parameter can provide bands of forecasted BG probability for a given intervention. These bands can delimit the 5%-95% confidence interval for future BG concentration based on current

insulin sensitivity for a particular patient and observed changes in insulin sensitivity within the retrospective patient cohort used to generate the stochastic model. The forecast bands can be used to provide further protection against hypoglycaemia by providing a statistical measure of confidence against low BG concentrations.

The stochastic model developed in Chapter 5 was incorporated into the controller to provide safety against hypoglycaemia. The median forecasted insulin sensitivity was used by the controller to select an insulin infusion rate that will produce a forecasted BG concentration closest to target. The 95^{th} percentile of forecasted insulin sensitivity corresponds to the lower 5% limit of forecasted BG concentration for a given insulin intervention. This outlying value was used to adjust the the insulin infusion rate so that the lower 5% bound of forecasted BG was always greater than 4 mmol/L. This adjustment resets the target to provide a guaranteed maximum risk of 5% for a BG measurement less than 4 mmol/L.

Table 6.6: BG controller performance incorporating cohort-wide stochastic model.

	No stochastic forecasts	Stochastic model
% measurements within 4 - 7 mmo/L	76%	76%
% measurements $<$ 4 mmol/L	3.4%	3.2%
% measurements $<$ 2.6 mmol/L	0.45%	0.34%
BG median	6.0	6.0
BG IQR	[5.4 - 6.8]	[5.4 - 6.8]
LBG-P ratio	0.59	0.44

Table 6.6 shows the effect of the stochastic model with 7% simulated BG sensor error on BG performance results for the 2-hourly controller. The lower 5% limit of the forecast bound was set to 4 mmol/L. The stochastic model resulted in a reduction in BG measurements less than 4 mmol/L and 2.6 mmol/L, and a reduction in the LBG-P ratio, thus lessening the risk and extent of hypoglycaemia.

Interestingly, incorporating the stochastic model resulted in a relatively small control improvement as shown in Table 6.6. While it appears the stochastic model was not able to prevent a period of hypoglycaemia, it did significantly limit the length of time spent at hypoglycaemic BG concentrations. The stochastic modelling approach employed here was originally developed for adult critical care, which used a lower target BG concentration of 5 mmol/L [Lin et al., 2006, 2008], compared to the 6 mmol/L used in this study. Thus, the higher target

for this initial neonatal controller will also avoid some hypoglycaemia, and it is expected the incorporation of the stochastic model would have a greater effect on control performance for lower target BG concentrations.

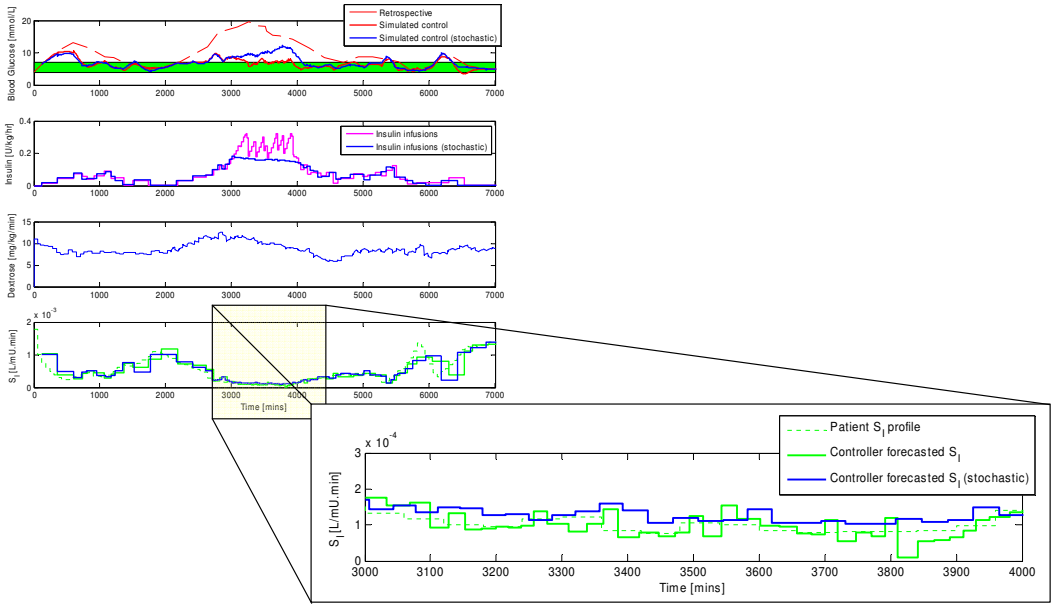

Figure 6.12: Comparison of glycaemic control performance for model-based controller with and without stochastic model insulin sensitivity forecasts, highlighting the effect of skewed probability bounds at low insulin sensitivity.

Figure 6.12 shows simulations of model-based control for Patient 11 with and without stochastic insulin sensitivity forecasts. A main feature of this patient's insulin sensitivity record is a period of very low insulin sensitivity between 3,000 and 4,000 minutes. As discussed in Section 5.7, the physiological requirement that S_I must be positive creates truncation effects at the extreme low region of the insulin sensitivity domain. Figure 6.12 shows the stochastic model forecasted insulin sensitivity is consistently higher than the patient S_I profile during this period. The controller selects lower insulin infusion rates as a conservative response during this period of resistance to insulin, and consequently the simulated BG concentration is higher compared to a controller that did not use stochastic forecasting.

Whilst the stochastic model in this study is derived from a patient cohort that would represent a typical case-mix of patients in a typical NICU, one cannot be certain that all types of patients are covered in the initial 25 patient episode

data set. Thus, the combination of stochastic model and limits on the controller provide a very safety-conscious control system that is aware of possible limitations in both information about clinical condition and model fit/prediction ability. However, the model validation on retrospective data and the evidenced robustness of the controller to errors and delays suggests that these errors will have a rather small impact on overall controller performance.

6.2.7 Clinical BG targets

The ideal range for blood glucose concentration in neonatal intensive care is under debate. Unlike adults, a major proportion of energy for brain metabolism is provided by fuels other than glucose (eg: ketones) [Avery et al., 1994]. Thus, the neonatal brain may be more resistant to hypoglycaemia compared to the adult. However, persistent low blood glucose concentration (< 2.6 mmol/L) can reduce cerebral development and lead to long term neurological deficiencies [Lucas et al., 1988]. Likewise, the upper limit for clinically desirable blood glucose concentration is also subject to debate [Cowett and Farrag, 2004]. For this study, the range of 4 - 7 mmol/L, as used in several adult studies, was targeted. However, to date, no outcome based study has provided a specific insight or result in this regard. Thus, glucose management goals vary widely between intensive care units [Alsweiler et al., 2007], targets for glucose control have varied between insulin therapy studies [Beardsall et al., 2008; Vlasselaers et al., 2009], and it is likely that the desired target for glucose control may change in the future.

The model-based controller was tested on the retrospective cohort with targets of 4 mmol/L, 5 mmol/L, 7 mmol/L and 8 mmol/L, which represent a range of target glucose concentrations likely to be encountered in neonatal critical care. All simulations used a constant 2 hour period between BG measurements and a 7% BG sensor error. The stochastic model was employed to limit the risk of undesired low BG concentrations. For the 4 mmol/L and 5 mmol/L targets the lower bound for the stochastic model forecast was set to 3 mmol/L and 3.5 mmol/L respectively. A comparison of overall control performance for different BG targets is presented in Table 6.7, and the cumulative distribution functions for BG concentration are presented in Figure 6.13.

The controller achieved a median BG close to target for the 6, 7 and 8 mmol/L

Table 6.7: Glucose control performance for different BG targets for the model-based controller.

Target BG	BG (mmol/L)		% of measurements within range		
	Median	IQR	4-7 mmol/L	< 4 mmol/L	< 2.6 mmol/L
4 mmol/L	5.3	[4.8 - 6.3]	78.7	6.7	0.6
5 mmol/L	5.4	[4.8 - 6.3]	77.9	6.9	0.6
6 mmol/L	6.0	[5.4 - 6.8]	75.6	3.2	0.3
7 mmol/L	7.0	[6.2 - 7.8]	48.4	1.5	0.3
8 mmol/L	7.9	[7.0 - 8.7]	23.7	1.5	0.3

targets. The stochastic model prevented lower BG targets from being achieved despite reducing the prescribed lower bound for forecasted BG concentration. This result is largely due to the use of higher simulated insulin infusions to achieve the lower targets, which thus also widens the forecast band for a specific value of insulin sensitivity, and effectively cancels the effect of the reduced lower forecast bound. This result is highlighted in Figure 6.13, where the 4 mmol/L and 5 mmol/L results largely correspond. Relaxing the stochastic safety constraints may have allowed a slightly lower median in the 4 mmol/L and 5 mmol/L target

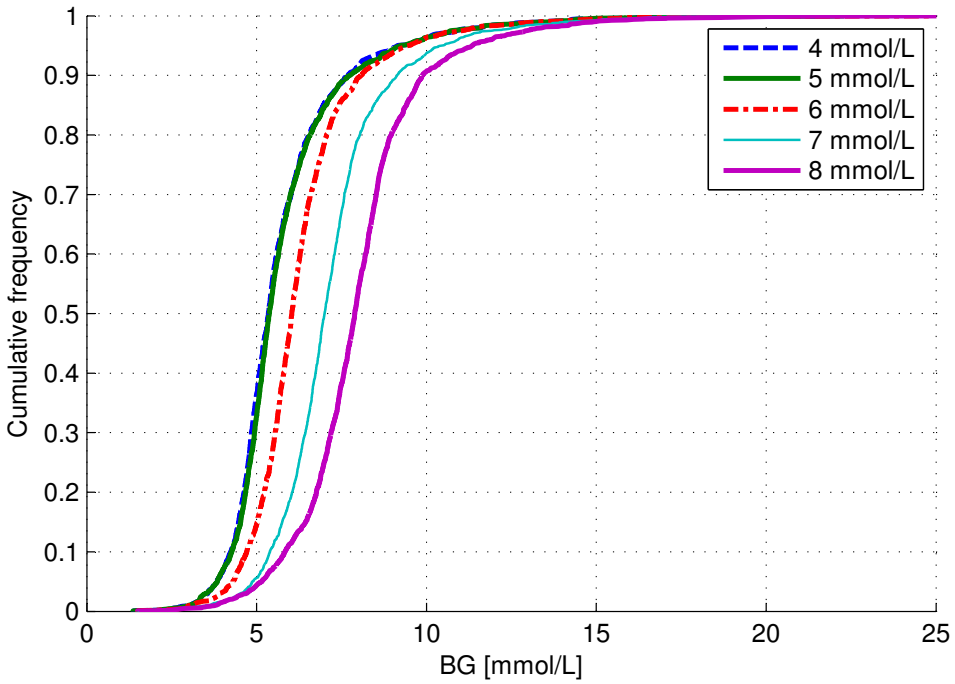

Figure 6.13: Empirical CDFs of model-based controller results incorporating BG targets of 4 - 8 mmol/L. The results for 4 mmol/L and 5 mmol/L are essentially overlaid.

cases, but a corresponding rise in hypoglycaemia events.

Figure 6.13 shows the different distributions of simulated BG measurements have largely the same shape, but are shifted for the different targets. They are particularly different when compared to the retrospective control results presented in Figure 6.4. More specifically, the model-based controllers are steeper and thus tighter in performance.

Model-based control can be set to target a specific glucose concentration relatively easily. This ease and directness in setting a target is in contrast with fixed sliding scale or similar control approaches that must be completely re-calibrated. This target setting feature may be useful in research settings outside of routine critical care to elucidate the specific effects of glucose control to a range of targets on patient outcome.

Thus, the control targets are customisable to within a reasonable range. Very low targets run higher risks of hypoglycaemic measurements, and very high targets cannot be achieved without increasing dextrose infusions. Clinicians may also select a BG target on a per-patient basis, or change the level of glucose control in the future based on emerging research in this field.

6.3 Clinical implementation testing

Clinical implementation of any control system requires a transfer of technology from the precise, exact simulation environment to the busy clinical setting where, despite best training practices, the potential for errors and mistakes remain. The BG measurement input may contain errors due to sensor noise. Human errors can include missed BG measurements and delays in implementing controller recommendations. These effects were introduced into the simulation environment to stress-test the controller against a range of possible clinical complications.

Table 6.8: Comparison of glycaemic control performance with increasing simulated BG sensor error for 2-hourly measurement interval.

Sensor error	BG (mmol/L)		% of measurements within range		
	Median	IQR	4-7 mmol/L	< 4 mmol/L	< 2.6 mmol/L
2%	6.0	[5.4 - 6.7]	78%	3.2%	0.40%
5%	6.0	[5.4 - 6.7]	77%	3.3%	0.34%
7%	6.0	[5.4 - 6.8]	76%	3.4%	0.45%
10%	6.1	[5.3 - 6.8]	75%	3.1%	0.40%
15%	6.1	[5.3 - 7.0]	69%	4.8%	0.51%
20%	6.1	[5.2 - 7.3]	65%	5.3%	0.40%

6.3.1 BG sensor error

Glycaemic control performance was tested with simulated uniformly distributed BG measurement errors of 2%, 5%, 7%, 10%, 15% and 20%, representing the range (and beyond) seen in clinical practice depending on the BG measurement device/analyser used [Peet et al., 2002; Chen et al., 2003]. Table 6.8 shows most accurate control was achieved, as expected, with the minimum amount of measurement noise with 78% versus 65% time in the 4-7 mmol/L band for ±2% versus ±20% measurement error, for a 2-hourly BG measurement interval. Decreases in time in glycaemic control bands showed a similar pattern for other measurement frequencies simulated. Figure 6.14 shows the percentage of measurements within the 4 - 7 mmol/L band and less than 4 mmol/L for 1-4 hour measurement frequencies. Absolute time in band decreased 7% - 17% for an 18% absolute increase in simulated sensor error, and a corresponding absolute increase of 1.0% - 2.6% for measurements less than 4 mmol/L. The effect of sensor error on overall BG control is shown in Figure 6.15. Increased measurement error results in a less steep CDF. However, even with 20% simulated sensor error Figure 6.15 shows significantly increased tightness of BG control compared to retrospective clinical results.

As much as possible, accurate, safe glycaemic control requires a complete and accurate knowledge of the model inputs. The integral-based fitting method provides robustness by effectively acting as a low-pass filter to reduce the effect of noise in blood glucose concentration sensing, as shown by the relative robust results of Table 6.8. As well as blood glucose concentration, the history of insulin and nutrition administration needs to be accurate to effectively determine patient-

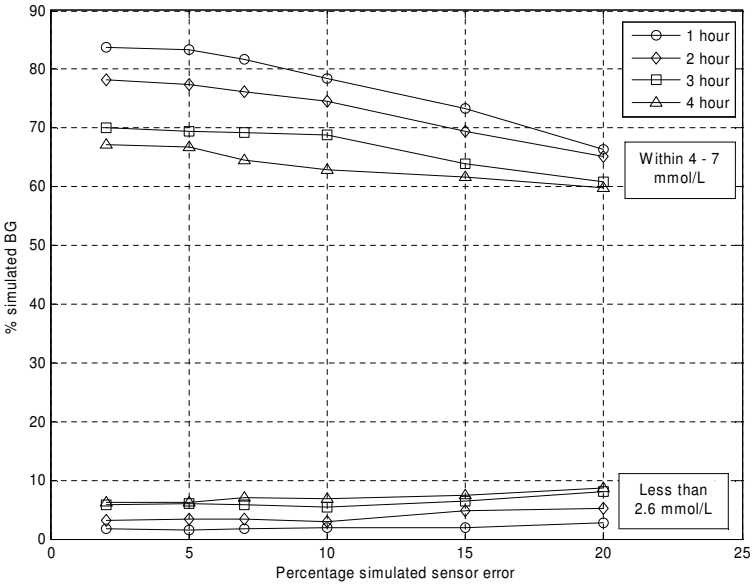

Figure 6.14: Effect of simulated BG sensor error on BG control.

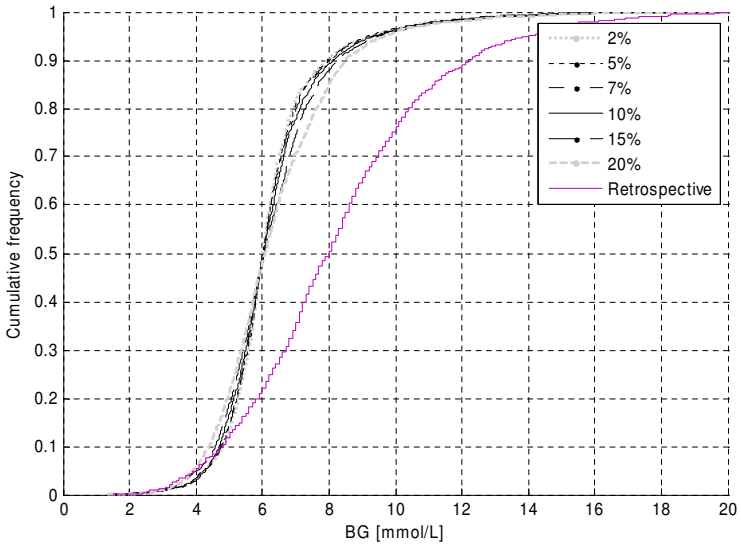

Figure 6.15: Empirical CDFs of model-based controller results incorporating sensor error compared to retrospective hospital control. The main group of CDFs represent 2% - 20% sensor error for the model-based controller as summarised in Table 6.8.

specific and/or time-varying parameters. Thus, efficient data flow is an important design concern to minimise time consuming and error-prone bedside data entry.

Table 6.9: Glucose control performance for delays between BG measurement and insulin infusion rate change.

Delay	BG (mmol/L)		% of measurements within range		
	Median	IQR	4-7 mmol/L	< 4 mmol/L	< 2.6 mmol/L
None	6.0	[5.4 - 6.8]	75.6	3.2	0.3
10 min	6.1	[5.5 - 6.9]	74.0	2.9	0.4
20 min	6.1	[5.5 - 6.9]	73.7	2.7	0.3
30 min	6.2	[5.5 - 7.0]	73.0	2.4	0.3
40 min	6.2	[5.5 - 7.1]	71.0	2.7	0.5

6.3.2 Clinical intervention delays

A common source of delay is a lag between the time of BG measurement and the time the insulin infusion rate is changed to the amount recommended by the controller. As insulin may cause irreparable damage in extreme circumstances, special precautionary procedures are taken by clinical staff when handling insulin infusions. Typically, any change in rate must be approved and signed by an attending clinician, and the change in rate on the pump must be sighted by at least two members of clinical staff. However, due to the spontaneous nature of emergency child-birth, doctors are often away from the unit assisting with a delivery. Additionally, nursing staff may be unavailable due to clinical instability with either the patient receiving insulin or another patient within the unit that requires immediate attention. Thus, substantial delays can exist between the time of BG measurement and eventual adjustment of insulin infusion rate.

The effect of these delays are modelled by incorporating a lag between the time of the BG measurement and the time of insulin infusion change. Delays of an added 10, 20, 30, and 40 minutes were assessed. The results in Table 6.9 show that the controller is robust to these delays, with the small change in performance tending towards higher BG concentrations.

The results of Figure 6.16 confirm the model-based controller is robust to delays in insulin infusion rate changes, tending towards a marginally higher proportion of hyperglycaemic measurements with longer delays. The stochastic model is a source of protection against significant increases in low BG measurements. Thus, the lower limits of the curves of Figure 6.16 are essentially identical.

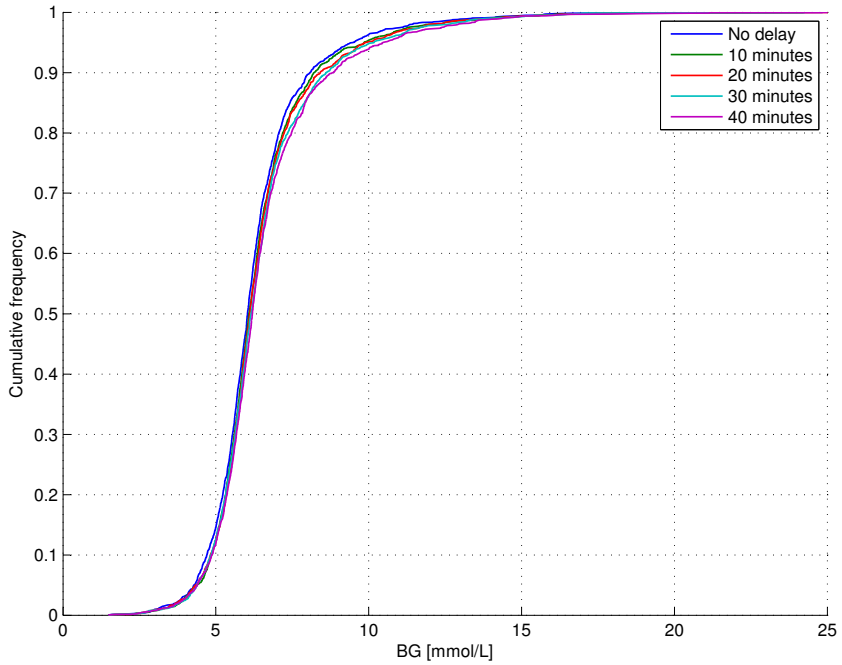

Figure 6.16: Empirical CDFs of model-based controller results incorporating delays between BG measurement and change of insulin infusion rate of 10 to 40 minutes.

The controller attempts to lower BG concentration though steady reductions in BG level per hour, rather than trying to reach the target range as quickly as possible, and the limits on the controller assessed in Section 6.2.1 results in generally gradual changes in insulin infusion rate. Thus, it is likely some measure of the robustness of the controller can be attributed to reduced accumulated errors as the change in insulin infusion rate between successive interventions is generally small.

6.3.3 Missed BG measurements

A missed BG measurement may occur for a number of reasons, many of which are related to clinical workload. A missed BG measurement means both a missed data point and a missed iteration of the control cycle of Figure 6.1. Control simulations were performed with a missed BG measurement chance of 1/3, 1/4, 1/5 and 1/6, from a base measurement frequency of 2 hourly. These proportions

Table 6.10: Glucose control performance and frequency of measurement versus chance of a missed BG measurement.

Chance	Num. measure-ments	BG (mmol/L)		% of measurements within range		
		Median	IQR	4-7 mmol/L	< 4 mmol/L	< 2.6 mmol/L
1/3	1371	6.3	[5.5 - 7.5]	62.1	4.8	0.7
1/4	1453	6.2	[5.5 - 7.4]	66.1	3.7	0.8
1/5	1551	6.2	[5.5 - 7.2]	69.2	3.9	0.6
1/6	1564	6.2	[5.5 - 7.3]	67.4	3.6	0.6
None	1771	6.0	[5.4 - 6.8]	75.6	3.2	0.3

of missed BG measurements (17% to 33% of measurements) are likely to be much higher than typical clinical practice, and thus represent a worst-case scenario test. The resulting BG control performance is presented in Table 6.10, with simulated BG CDFs presented in Figure 6.17.

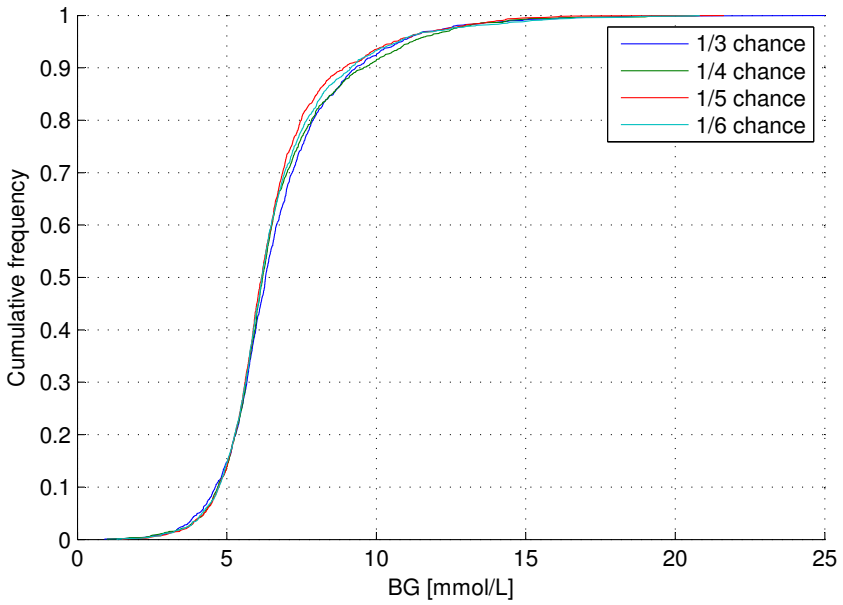

Figure 6.17: Empirical CDFs of model-based controller results for simulated missed BG measurements.

The missed BG measurements extended the average measurement frequency from the base value of 2 hours to 2.3 - 2.6 hours. A general decrease in BG control quality is evident with increasing frequency of missed BG measurements. However, the quality of BG control is relatively consistent across the proportions of missed BG measurements, which may be attributed to the limits placed on the stochastic forecasting method and BG controller to target more gradual changes

in BG concentration.

6.4 Dextrose modulation

The targeted controller can be used to optimise several glycaemic control inputs simultaneously within clinical limits. In the glycaemic control case, both insulin and nutrition inputs may be modulated to adapt control to the infant's changing metabolic condition, as captured by the fitted insulin sensitivity parameter. For example, a constant dextrose infusion rate may be selected, and may be modified during periods of low insulin sensitivity where benefit-to-risk ratio for insulin infusions is lower.

To provide an example for comparison, simulations were performed over the virtual patient cohort with a controller that targeted a 10 mg/kg/min parenteral dextrose infusion rate for all patients. The dextrose rate was lowered in steps of 20% only if the maximum allowable insulin rate would result in a predicted BG concentration higher than target. The dextrose rate was raised in steps of 20% if the forecasted BG concentration was below target with zero insulin input. The stochastic model was employed to minimise the risk of hypoglycaemia and constant 2-hourly BG and measurement intervals were used. Enteral feeds, a minor source of nutrition, were not altered from retrospective data. The target BG concentration was 6 mmol/L.

The simulation results are presented in Table 6.11 and Figure 6.18. Dextrose rate data is presented as an average per-hour on a whole-cohort basis (n=3,492 data points).

The BG control performance again showed lower, tighter control compared to retrospective clinical data, while the distribution of dextrose infusions was simultaneously increased. Thus, both lower, tighter glycaemia *and* higher rates of dextrose administration may be achieved with a patient-specific adaptive controller. While the median and IQR of dextrose infusions were close to target, patients spent approximately 30% of the time with a dextrose infusion rate less than the target of 10 mg/kg/min. These lowered rates coincide with periods of relatively low insulin sensitivity. Thus, the controller uses reduced dextrose rates as a tool to control glycaemia during periods when insulin infusions alone would

Table 6.11: Glucose control performance and parenteral dextrose infusions for model-based controller modulating both insulin and dextrose compared to retrospective hospital control.

	Dextrose modulation	Retrospective
Median BG (mmol/L)	6.1	8.0
BG IQR (mmol/L)	[5.4 - 6.8]	[6.3 - 9.9]
Median dextrose (mg/kg/min)	10.0	8.2
Dextrose IQR (mg/kg/min)	[8.7 - 10.0]	[5.6 - 9.5]
% measurements within 4 - 7 mmol/L	75.4	30.9
% measurements < 4 mmol/L	3.3	4.9
% measurements < 2.6 mmol/L	0.5	0.7

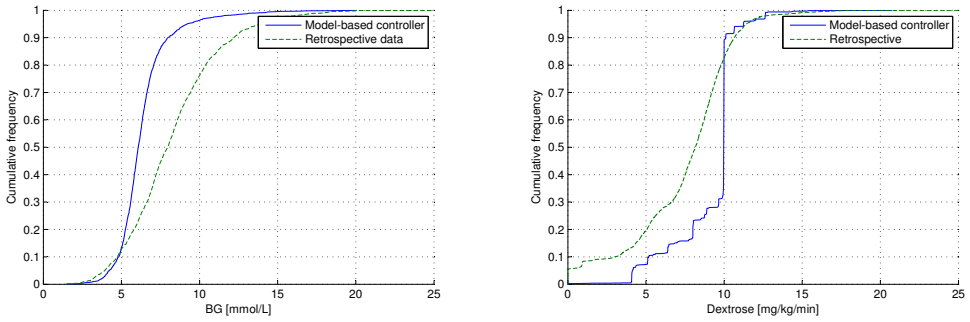

(a) BG concentration (b) Dextrose rate

Figure 6.18: Empirical CDFs of BG concentration and parenteral dextrose infusion rate for controller modulating both insulin and dextrose, compared to retrospective data.

provide limited efficacy. An example is presented in Figure 6.19, where the insulin sensitivity is relatively low between 90 and 130 hours. The controller lowers the dextrose infusion rate to approximately 5 mg/kg/min to maintain glucose control instead of increasing an already high insulin infusion rate. Hence, where the risk of adding more insulin is high, safety from hypoglycaemia limits what can be achieved. Reducing dextrose infusions thus provides a safe avenue of control for these periods of a patient's stay.

Higher dextrose infusions generally require higher overall insulin infusions, increasing both sides of the glucose-insulin balance. This may magnify the patient glycaemic response to changes in patient condition, which may result in more dramatic changes in glycaemia for changes in insulin sensitivity. Additionally, whilst it may be possible to feed significantly higher dextrose by using high

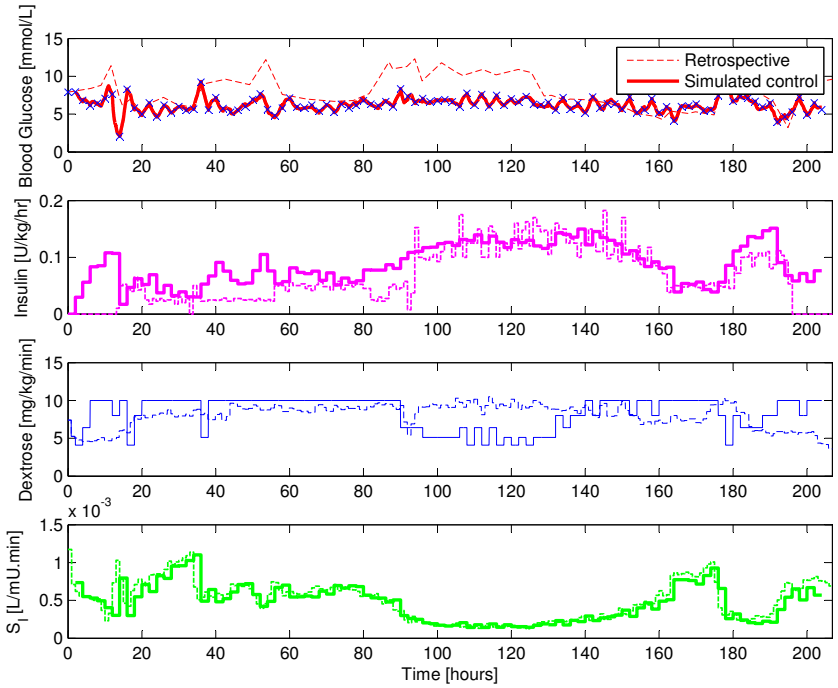

Figure 6.19: Controller simulation for Patient 15 incorporating modulation to the parenteral dextrose infusion rate. Dashed lines represent retrospective data, and solid lines represent simulation results. The top panel shows blood glucose concentration. The second and third panels display the rate of insulin and parenteral dextrose infusion respectively. The bottom panel shows model-fitted insulin sensitivity.

insulin rates, over-aggressive feeding may lead to non-productive somatic growth, and could have negative implications for metabolism in later life such as insulin resistance, obesity and diabetes [Hay, 2006].

A paper-based protocol that uses both insulin and nutrition inputs for control has also been used on 394 adult intensive care patients in large-scale clinical implementation [Chase et al., 2008b]. SPRINT uses 1-2 hourly measurements, and modulates both insulin and nutrition to achieve tight glycaemic control. SPRINT targets a 4.0 - 6.1 mmol/L BG band, and achieved 79% of measurements within the 4 - 7 mmol/L band, which is similar to the 82% and 76% of simulated measurements in this study within same band using 1-hour and 2-hour measurement frequencies. The addition of nutrition modulation provides another pathway for BG reduction that can be effective during periods of very low insulin sensitivity, particularly as adults appear to exhibit greater insulin effect saturation than preterm neonates [Rizza et al., 1981]. In contrast, extremely preterm infants

lack substantial endogenous stores of energy, and thus must be fed constantly to maintain basal energy expenditure and provide excess for growth [Hume et al., 2005]. Given the relatively new practice of tight glycaemic control using insulin in neonates, any similar system for neonates would likely be initially an 'insulin-only' controller or one that sought to maximise nutritional inputs.

Further improvements to the model could incorporate daily nutritional and fluid volume goals that can be set by clinicians with model-based targeted control taking care of glycaemia - thus relieving clinical staff from estimation and ad-hoc decision making. The ideal content and composition of nutritional regimes for preterm infants is still under debate [Hay et al., 1999]. The appropriate proportions of dextrose, protein and lipids given in the NICU may be different to what an infant receives in-utero. While the relevant major organs express many of the biological mechanisms responsible for glucose regulation from a relatively early age, the foetus depends upon the mother to control energy supply. Thus, the controller is essentially attempting to replicate some of the mother's functions, as well as account for the synchronised processes that regulate foetal growth that are perturbed by premature birth and life outside the womb. This outcome may also highlight the model-based controller as an investigative tool to help clinicians test different nutrition intakes and their effect on indicators of infant health.

6.5 Impact of controller technologies

The simulation studies in this chapter aimed to explore the impact of controller design and clinical variables on control quality. The results were used to create an optimum controller suitable for long-term clinical glycaemic control, which was piloted in clinical trials as described in Chapter 7.

A detailed example demonstrating the control impact of the technologies developed in this research is presented in this section for a typical real-life control scenario. Figure 6.20 shows one of the pilot clinical trials that used the model-based controller. This clinical study will be presented in full in Chapter 7. The model-based controller utilised in the clinical trial used 2-hourly BG measurements and employed stochastic model forecasts to aid intervention selection. Overlaid on the clinical BG results are re-simulations using the sliding scale con-

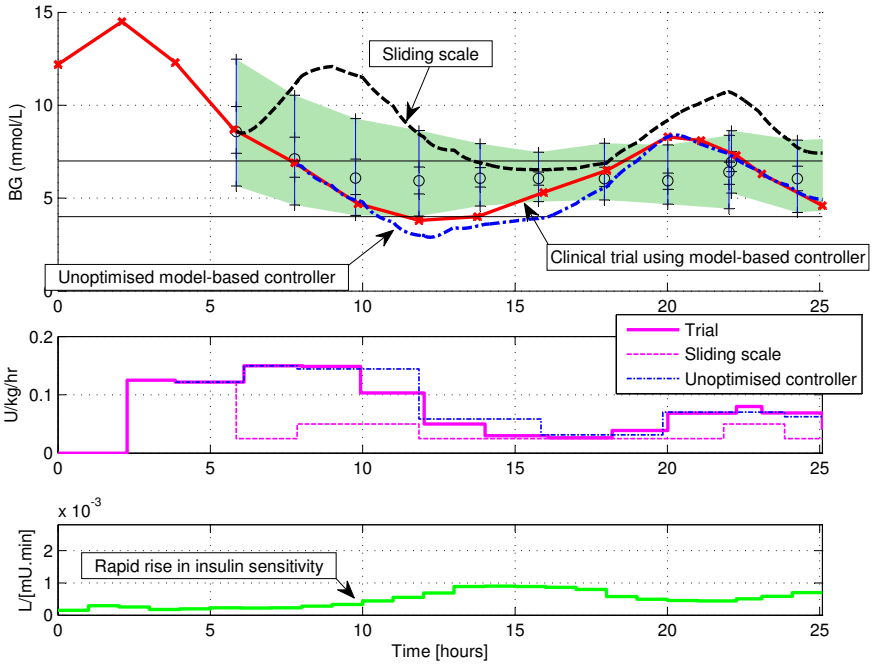

Figure 6.20: Patient F clinical trial with re-simulated controllers. The top panel shows the BG concentration as measured during the clinical trial, as well as the simulated response for sliding scale and unoptimised model-based controllers. The shaded area indicates the stochastic model forecast bounds generated during the clinical trial. The second panels shows the insulin infusion rate during the clinical trial and for the two simulated controllers. The bottom panel shows the identified insulin sensitivity profile.

troller of Table 6.1 and an unoptimised model-based controller with no stochastic model and 4-hour BG measurement intervals.

The identified insulin sensitivity profile for this clinical trial patient is shown in the bottom panel. This patient began the trial with low insulin sensitivity, which underwent a rapid increase at 10 hours into the trial. Thus, this patient profile provides a benchmark to compare how different controllers react to this example of intra-patient variability.

The model-based controllers both achieved tight BG control compared to the sliding scale controller, which fails to adapt to changing patient condition. Due to a longer BG measurement interval, and no stochastic forecasting, the unoptimised model-based controller misses the rapid rise in insulin sensitivity. Thus, this controller causes a period of mild hypoglycaemia in this case. The

clinical model-based controller, optimised through simulations on virtual patients and using interventions guided by stochastic forecasts, responds adequately to rise in insulin sensitivity to maintain a safe level of control.

Thus, this result demonstrates the complementary nature of the technologies developed in this and previous chapters. The parameter identification methods allows the identification of insulin sensitivity in clinical real-time. This information is used by model-based controllers to provide adaptive, targeted BG control. The controllers are optimised based on virtual simulation results that highlight the importance of frequent BG measurements on control quality, explore the effects of speed of controller response, and assess robustness to clinical implementation variables. The stochastic model provides forecasts of future insulin sensitivity to adjust interventions for a guaranteed level of safety from hypoglycaemia. Finally, the virtual trial framework creates an environment where different protocols can be compared in simulation to aid clinical decision-making. Thus, the suite of technologies combine to create a system that can respond adequately to the dynamic critically ill neonate.

6.6 Summary

An adaptive, model-based predictive controller designed to incorporate the unique metabolic state of the neonate was presented. The controller was developed in simulation on a 25 patient cohort and results were compared to retrospective hospital control. Time in the target 4 - 7 mmol/L band was increased by up to 161%. The effects of measurement frequency schemes were evaluated, and a stochastic model provided further protection against the risk of hypoglycaemia.

Bringing a control system from the perfectly-compliant environment of computerised simulation to implementation in a busy, spontaneous critical care environment requires assessing the robustness of the control scheme to real-life situations. In this chapter missed measurements, errors in the measurement devices and delays in implementing the controller actions were tested. In all cases, the controller proved robust, and thus suitable for initial pilot trials and further longer-term nurse-driven usage.

The studies presented here highlight the flexibility of the virtual patient simu-

lation environment. Controllers can be developed to handle the evolving critically ill patient, as well as the evolving field of glycaemic control in critical care.

Chapter 7

Clinical trials

All reported insulin infusion trials in neonates have used either protocols that fixed insulin dosing to weight or other factors [Beardsall et al., 2007b], or clinician judgment to determine insulin infusion rates. Additionally, it is well known that neonatal response to insulin and glucose infusions exhibits significant inter-patient variations [Cowett and Farrag, 2004], which would render such fixed protocols ineffective because they do not adapt well to different patients or to the dynamic changes within a patient's stay as their condition evolves. Model-based blood glucose control can provide more optimised care by adapting in real-time to identified parameters representing the current metabolic state of the infant, and use this information to drive insulin dosing. Succinctly, clinically derived fixed or largely fixed protocols cannot offer the patient-specific adaptation necessary to manage the clinically observed inter- and intra- patient variations.

This chapter presents the pilot trials of the first model-based blood glucose control system in preterm neonates. The main goals of the pilot trials were to assess the efficacy and safety of model-based control of blood glucose using insulin infusions in neonates. The ability to accurately forecast blood glucose concentrations in real-time to reduce hyperglycaemia in a controlled manner was assessed. The stochastic model is also used to provide a guaranteed pre-specified maximum risk of hypoglycaemia. Overall, these model-based trials assess the ability to successfully translate this model-based control method from a simulation environment into typical clinical practice.

7.1 Study design

7.1.1 Study population

Very low birth weight infants who met eligibility criteria were recruited between August 2008 - February 2009 from the Christchurch Women's Hospital Neonatal Intensive Care Unit. Inclusion criteria included birth weight $<$ 1,500 grams, blood glucose $>$ 10 mmol/L, a clinical decision to commence insulin infusions, and an in-situ arterial line. Infants that were severely moribund or not expected to survive for more than 72 hours were excluded. Written parental consent was obtained for each study participant. The study was approved by the Upper South A Regional Ethics Committee, New Zealand.

7.1.2 Clinical protocol

The timing of intervention actions is shown in Figure 7.1. Blood glucose measurements were taken every 1 to 3 hours for up to 24 hours, and the insulin infusion rate was adjusted as determined by the model-based controller after each BG measurement. The study dictated a maximum of 12 BG measurements over the 24 hour period to converse blood volume. Measurements were generally spaced 2-hourly. However, this measurement interval was adjusted as determined by the attending clinician based on factors relating to clinical condition. Occasionally, extra blood gases, which include BG measurement, were taken for some patients. This extra data was used during the trial to update the insulin infusion rate, and did not contribute to the 12 measurements/day limit. All blood was drawn from an in-situ arterial line, to minimise patient discomfort, and analyzed with a Bayer 850 blood gas analyzer (Bayer AG, Leverkusen, Germany).

The blood glucose profile together with the insulin and nutrition administration profiles were used by the computer algorithm to determine insulin infusion rates to reach the target blood glucose range of 4 to 7 mmol/L. Insulin sensitivity was identified from the measured clinical data in real-time to identify the current metabolic state of the infant. The controller used the fitted insulin sensitivity value to iterate through several possible insulin infusion rates and forecast a BG concentration 2 to 3 hours ahead, depending on the anticipated time of

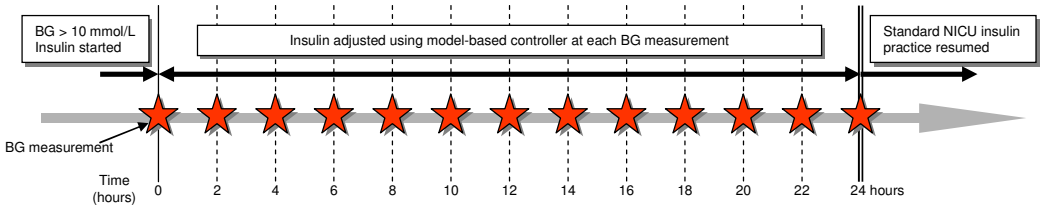

Figure 7.1: Study protocol BG measurement and intervention timing. Each star represents a BG measurement and update of the insulin infusion rate.

the next BG measurement. The insulin infusion rate forecasted to achieve a BG concentration closest to target was selected. The control software accounted for any delays between BG measurement and change in insulin infusion rate. The stochastic model was used to provide confidence bounds on the forecasted BG concentration. For safety, the selected insulin infusion rate was adjusted to ensure that the lower 5% probability bound of forecasted BG was greater than 4 mmol/L providing a guaranteed risk against hypoglycaemia.

The risk of hypoglycaemia is often cited as a barrier to large-scale adoption of glycaemic control via insulin infusions. Most neonatal hypoglycaemia appears to be asymptomatic [Lucas et al., 1988]. Many external signs of low BG (tremors, etc.) are not specific to this condition in neonates. As a result, hypoglycaemic symptoms could only be clearly attributed to low BG in 5 out of 660 clinical cases [Lucas et al., 1988].

Studies in the neonatal rat brain suggest repeated, prolonged exposure to hypoglycaemia resulted in negative neurodevelopment outcomes [Zhou et al., 2008]. Vlasselaers and colleagues [2009] and Beardsall and colleagues [2008] found significantly increased hypoglycaemia in their insulin therapy cohorts compared to controls. As discussed at the beginning of this chapter, such outcomes are, at least, partly due to the protocols control performance and inability to adapt to changes in patient condition or inter-patient variability.

In contrast, SPRINT (developed from a model-based controller) had a hypoglycaemic occurrence similar to retrospective hospital glucose control protocols in adult critical care [Chase et al., 2008b]. Hence, the lower BG forecast limit of 4

mmol/L selected for this study was a relatively conservative choice, reflecting the nature of these pilot trials as the first model-based BG control study performed in preterm neonates.

Infants were mostly fed via parenteral solutions with 10%-12.5% dextrose content. Several infants also received expressed breast milk (EBM), and some infants received morphine and dobutamine infusions prepared using 5% glucose solution. All sources of glucose infusion were reported and considered by the model-based controller algorithm when recommending insulin infusion rates.

Insulin was given via intravenous cannula using Alaris CC pumps (Alaris, San Diego, California, USA) as a continuous infusion. The concentration of insulin was [5*weight (kg)] U made up to 20 mL with 0.9% saline solution to achieve a concentration of 0.25 U/kg/mL. Insulin tubing was flushed with this solution to ensure plastic receptor binding occurs to minimise adsorption to tubing [Hewson et al., 2000]. New insulin infusion rates were determined after every measurement. For additional safety, a neonatal clinician approved every change in insulin infusion rate before adjusting the pump. All patients enrolled into this study were already receiving insulin infusions. Hence, this study only attempted to optimise the insulin infusion rate to more accurately achieve target blood glucose levels. This study is thus a clinical pilot to test the efficacy and safety of this model-based controller.

7.2 Results

7.2.1 Clinical summary

Table 7.1 presents the clinical details of the study population. Six infants were included in the trial with birth weight ranging from 540g to 995g and gestational age at birth of 24.4 to 27.3 weeks. Infants were enrolled at 1 to 9 days of age and had received insulin for 0 to 91.6 hours before the study period began. The intervals between commencement of insulin and the start of the trial were due to obtaining parental consent and ensuring an arterial line was available.

Figure 7.2 presents the blood glucose measurements during the study for

Table 7.1: Clinical details of study population

Patient	Gestational age at birth [weeks]	Age at start of trial [days]	Birth weight [g]	Insulin usage before trial [hours]
A	24.4	7	685	15.3
B	27.3	9	770	15.0
C	25.4	1	720	3.2
D	25.4	7	785	91.6
E	25.9	4	540	2.2
F	27.0	2	900	0.0
G	25.0	6	995	11.5

each of the seven study patients. In each case, the model-based controller reduced blood glucose from hyperglycaemic concentrations towards the target 4-7 mmol/L band, and maintained BG control within the band. The evolution of model-fitted insulin sensitivity is presented for each patient in Figure 7.3. The overall range and variation of insulin sensitivity shown in Figure 7.3 was highly patient-specific. However, Figure 7.2 shows a generally uniform glycaemic response, suggesting the model-based controller is capturing and accounting for these patient-specific dynamics.

Table 7.2 summarises the clinical inputs for blood glucose control during the trials. Infants were fed a median of 4.1 to 9.6 mg/kg/min dextrose via the parenteral route, and up to 11 mL of EBM. Median insulin usage was 0.040 U/kg/hr to 0.191 U/kg/hr. The median BG measurement frequency was 1.7 to 2.5 hours. Finally, the model-fitted insulin sensitivity value showed large inter-patient variation, with medians spanning [0.14 - 1.25]x10^{-3} L/(mU.min).

In particular, several studies have shown that there is no simple relationship between insulin and glucose infusions and level of glycaemia. Great inter-patient heterogeneity is a hallmark of neonatal glucose metabolism making safe, adequate control difficult [Cowett and Farrag, 2004; Collins et al., 1991]. Table 7.2 shows that within this relatively small study population a 2.3x spread of median dextrose infusion rates were used, and an 8.9x spread of insulin sensitivity was computed. In response, the controller used a 7.6x spread of median insulin infusion rates. Thus, fixed insulin protocols may not accurately account for this level of inter-patient variability. In contrast, an adaptive protocol, as presented here, can provide greater benefit.

Table 7.2: Clinical glycaemic variables during trials.

Patient	Median dextrose rate[a]		Median insulin[a]	Total EBM	Max. BG	Min. BG	Median measurement	Median insulin sensitivity
	mg/kg/min	kcal/kg/day	U/kg/hr	mL	mmol/L	mmol/L	period, hours	x10^{-3} L/(mU.min)
A	8.8	50.8	0.047	0.0	7.8	6.9	1.5	0.45
B	9.4	54.4	0.036	5.0	7.4	4.1	1.8	1.25
C	4.1	23.3	0.080	0.0	14.4	5.5	1.8	0.14
D	9.6	55.0	0.056	3.0	7.9	5.0	2.4	0.70
E	6.8	39.1	0.118	11.0	12.6	6.5	2.0	0.20
F	7.9	45.5	0.069	4.5	12.3	3.8	1.6	0.50
G	9.4	54.3	0.195	2.0	9.8	5.3	1.8	0.14

[a] Infusion rates averaged over 60-minute window

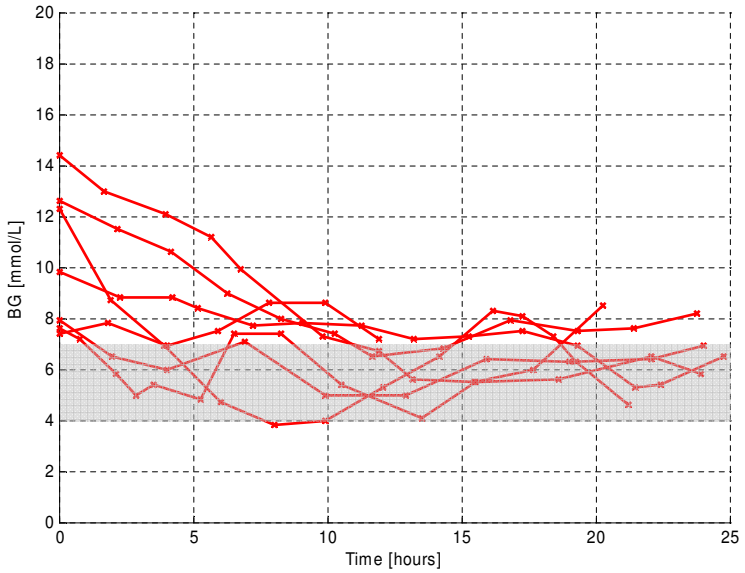

Figure 7.2: BG concentration during computerised insulin dosing. Each line represents blood glucose concentration for one patient while insulin infusion rates were chosen by the computerised controller. The shaded region represents the 4-7 mmol/L target band.

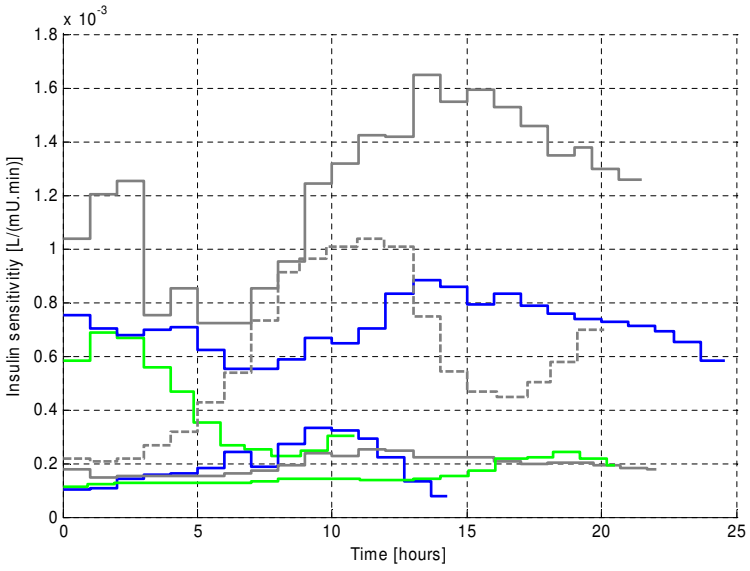

Figure 7.3: Model-fitted insulin sensitivity during trials. Each line represents the evolution of one patient's sensitivity to exogenous insulin fitted as an hourly step-wise function.

The following sections presents the clinical control data for the seven study patients. The BG concentrations presented in each section are compared to the model-predicted values as plotted in Figures 7.4 to 7.9. The shaded areas of each trial plot represent the 5% - 95% BG forecast bound generated by the stochastic model. The insulin and nutrition infusion data during the trial are also shown, where bars represent EBM feedings for those infants receiving EBM. Hourly step-wise model-fitted insulin sensitivity is shown on the bottom panel of each plot.

7.2.2 Patient A

Patient A experienced a four-fold increase in insulin infusion over the 12 hour trial period. However, there was relatively very little change or variation in the glycaemic response. This result may have reflected high insulin resistance due to clinical condition, or could be caused by a technical fault such as an unnoticed blocked line.

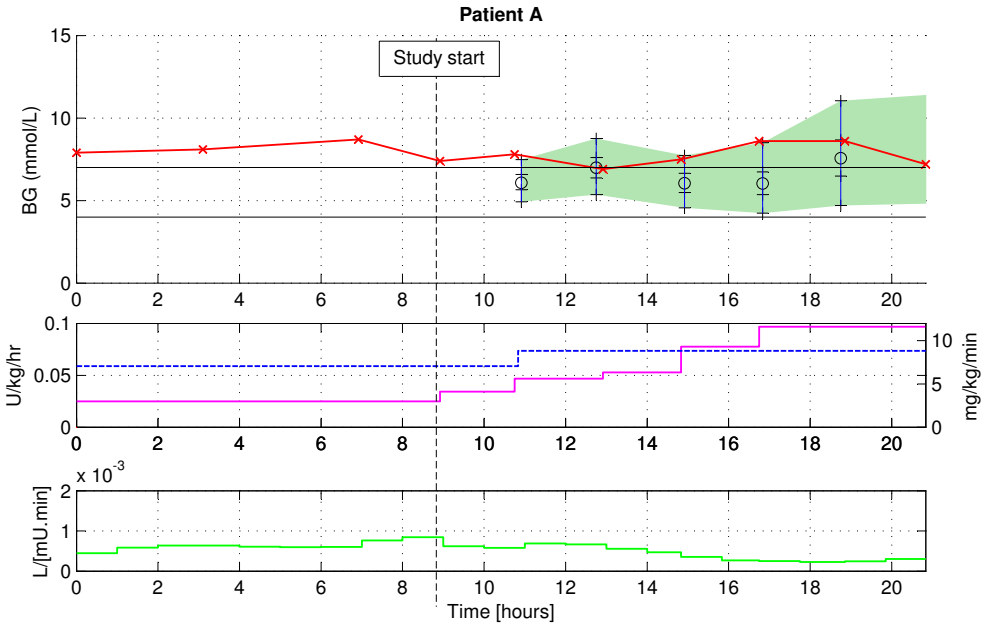

Figure 7.4: BG control during clinical trial for Patient A. The BG measurements are shown in the top panel together with the 5%-95% BG prediction forecast (shaded). The second panel shows insulin infusions (solid line), dextrose infusions (dashed line) and EBM (bars). The third panel shows model-fitted insulin sensitivity.

Patient A was unique as the only infant from an Asian background, whilst the remaining study patients were all Caucasian. Insulin sensitivity differs amongst ethnic groups in adults, where [Chiu et al., 2000] reported Asian-Americans had an ethnic propensity to insulin resistance not related to obesity. It is unknown whether such ethnic differences in insulin sensitivity are also present in preterm neonates.

7.2.3 Patient B

Patient B was on insulin overnight before the study commenced. The controller maintained BG within the target band throughout the majority of the trial. This patient had several extra blood gases taken due to changes in mechanical ventilation settings and strategy, and these measurements were thus also used to adjust the insulin infusion rate that generally steadily increased over the trial. This patient had comparatively high insulin sensitivity, and thus most BG measurements were towards the lower end of the BG forecast range.

7.2.4 Patient C

Patient C received 34%-60% of the total dextrose infused from glucose administered with morphine and dobutamine solutions due to critical illness. The controller achieved a steady decrease in BG from 14.4 mmol/L over 10 hours to the target band. At approximately 27 hours the patient self-extubated and was in a stressed condition, resulting in a sharp rise in BG at the end of the trial. Arterial access was lost soon after this time and the study was therefore stopped after only 20 hours of control.

7.2.5 Patient D

Patient D was the twin of Patient C, and, in contrast to Patient C, had received insulin for several days before the trial commenced. Hence, the starting BG concentration was lower than for most other patients. The controller modulated insulin infusions to maintain glycaemia within the target 4-7 mmol/L band. This

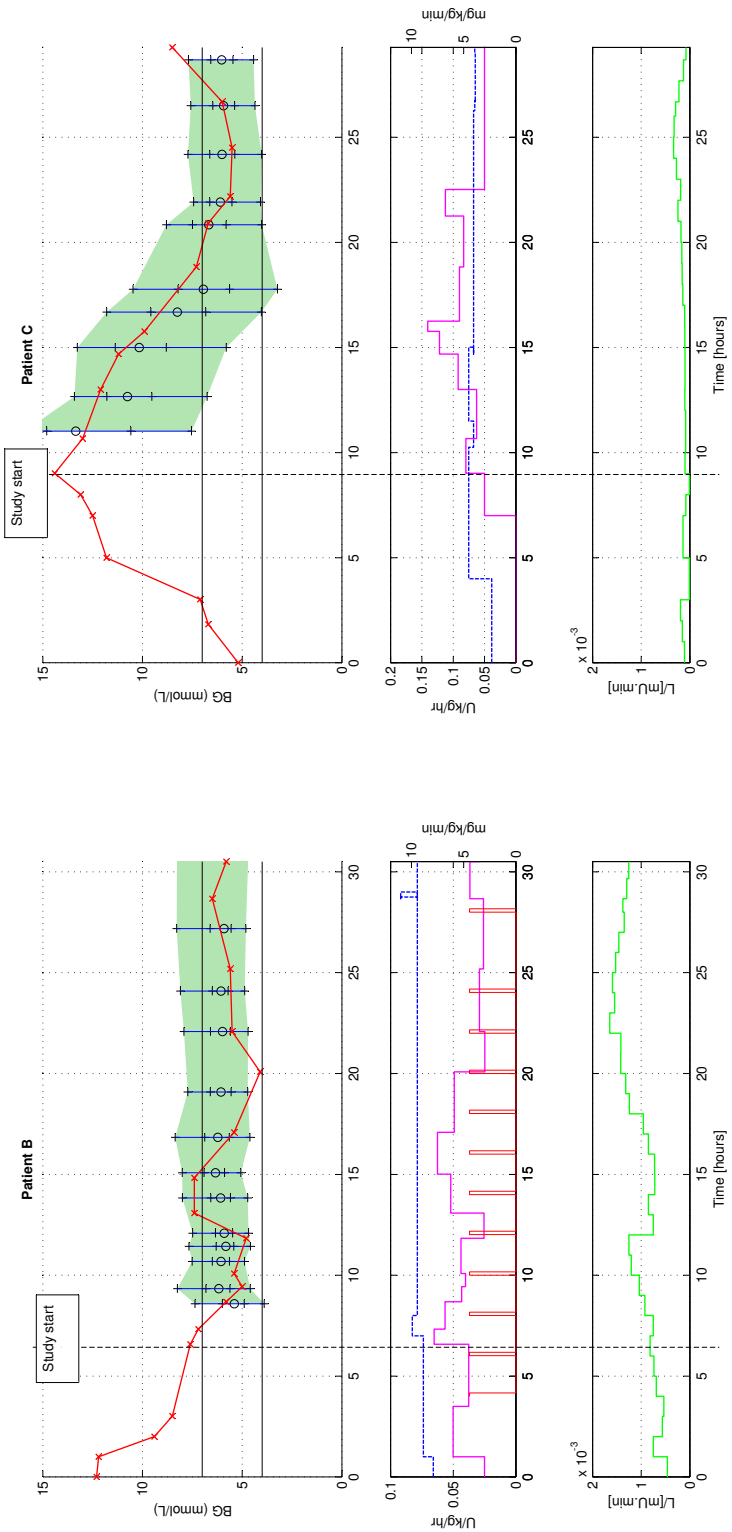

(a) BG control during clinical trial for Patient B.

(b) BG control during clinical trial for Patient C.

Figure 7.5: BG control during clinical trial for Patients B and C. The BG measurements are shown in the top panel together with the 5%-95% BG prediction forecast (shaded). The second panel shows insulin infusions (solid line), dextrose infusions (dashed line) and EBM (bars). The third panel shows model-fitted insulin sensitivity.

patient was metabolically relatively stable over the trial period, as evidenced by the relatively high and stable model-fitted insulin sensitivity, and similarly stable insulin and nutrition interventions.

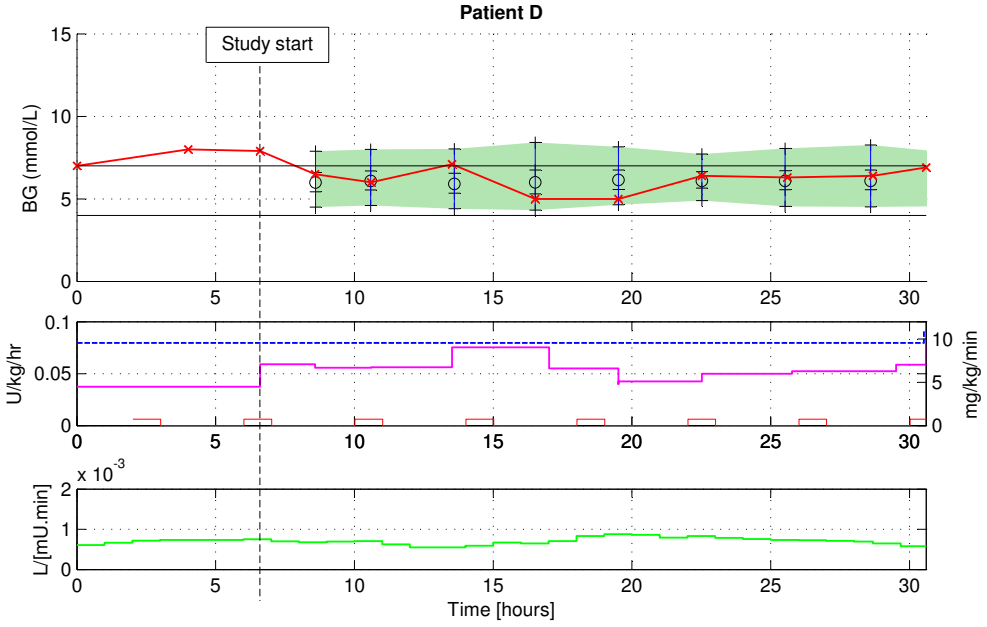

Figure 7.6: BG control during clinical trial for Patient D. The BG measurements are shown in the top panel together with the 5%-95% BG prediction forecast (shaded). The second panel shows insulin infusions (solid line), dextrose infusions (dashed line) and EBM (bars). The third panel shows model-fitted insulin sensitivity.

7.2.6 Patient E

Patient E was the smallest trial subject, with birth weight of 540g. The first 12 hours of the trial showed a controlled decrease of BG from 12.6 mmol/L to 6.5 mmol/L. The lower bound of the forecast band reached the 4 mmol/L limit for much of the trial. This limit indicates how the combination of low birth weight, relatively low insulin sensitivity, and relatively high insulin infusion rate created a risk of low BG. This risk was minimised by adjusting the 50^{th} percentile target, as required. Thus, for several measurements towards the end of the trial the controller targeted a BG concentration slightly over 7 mmol/L to keep the lower bound of the forecast range at 4 mmol/L.

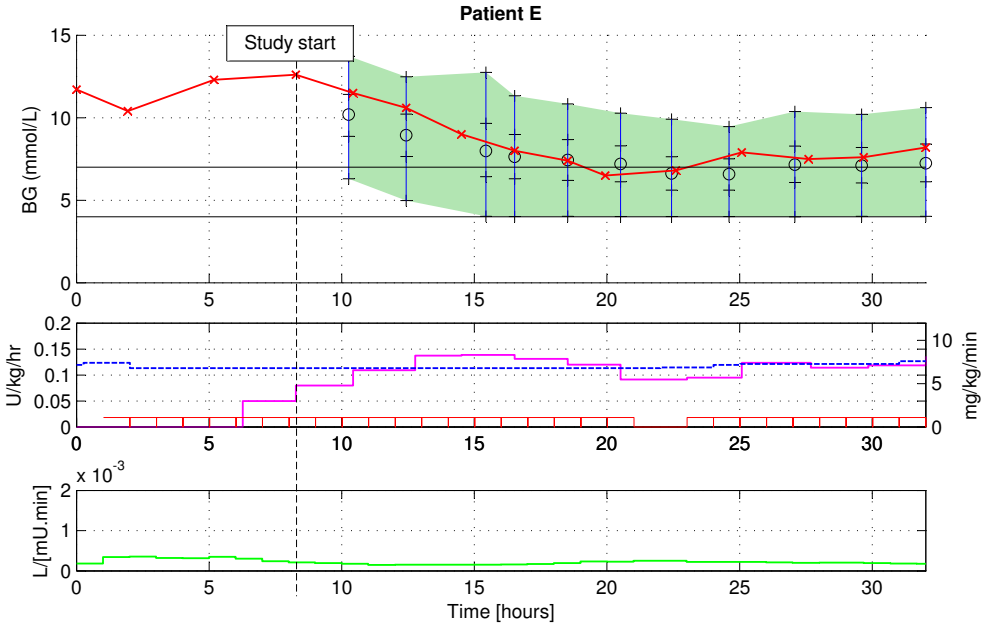

Figure 7.7: BG control during clinical trial for Patient E. The BG measurements are shown in the top panel together with the 5%-95% BG prediction forecast (shaded). The second panel shows insulin infusions (solid line), dextrose infusions (dashed line) and EBM (bars). The third panel shows model-fitted insulin sensitivity.

7.2.7 Patient F

Patient F showed a period of relatively rapid change in insulin sensitivity during the study. Between hours 10 and 13 insulin sensitivity rose 165%. This rise was at the extreme end of observed changes in insulin sensitivity, evidenced by the BG measurement at 14 hours below the 5% BG forecast limit. Between 18 - 20 hours insulin sensitivity decreased relatively rapidly, showing a BG measurement above the 95% BG forecast limit. Post-trial analysis of the clinical data showed no new medications administered over this period or any diagnosed change in condition that could be directly linked to the change in insulin sensitivity.

7.2.8 Patient G

A major feature of the BG control for Patient G was the high rates of insulin infusion employed during the study. The controller reduced the BG concentration

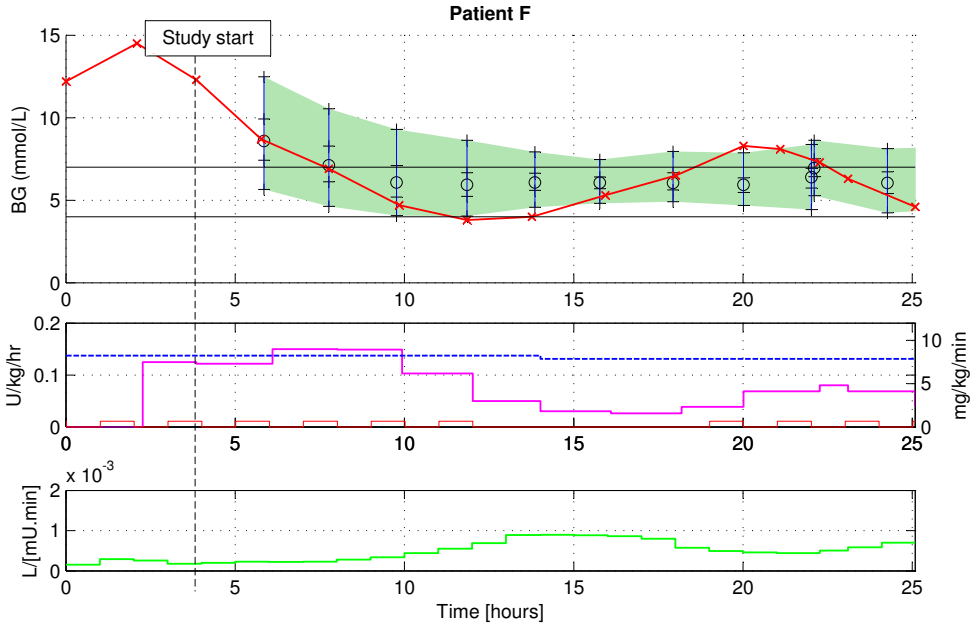

Figure 7.8: BG control during clinical trial for Patient F. The BG measurements are shown in the top panel together with the 5%-95% BG prediction forecast (shaded). The second panel shows insulin infusions (solid line), dextrose infusions (dashed line) and EBM (bars). The third panel shows model-fitted insulin sensitivity.

to < 8 mmol/L over the first seven trial hours. Due to high insulin infusion rates, the stochastic model forecasts drove the controller BG targets. The controller aimed to hold the BG concentration over 7 mmol/L for most of the trial, as dictated by the requirement to maintain the 5% BG forecast bound at no less than 4 mmol/L.

At approximately 32 hours the patient's insulin sensitivity rapidly increased, causing a 1.6 mmol/L drop in BG from the previous measurement. The decrease in BG was adequately contained, avoiding hypoglycaemia. There appeared to be no appreciable change in clinical condition during this time. Thus, the stochastic model directed a period of higher BG, based on the risk of high insulin infusion rates and insulin sensitivity variability observed in retrospective data, to provide an extra buffer that helped avoid hypoglycaemia when a rapid change occurred in insulin sensitivity.

This patient provides a salient example of routine BG measurement and stochastic forecasting providing a layer of safety. Longer BG measurement inter-

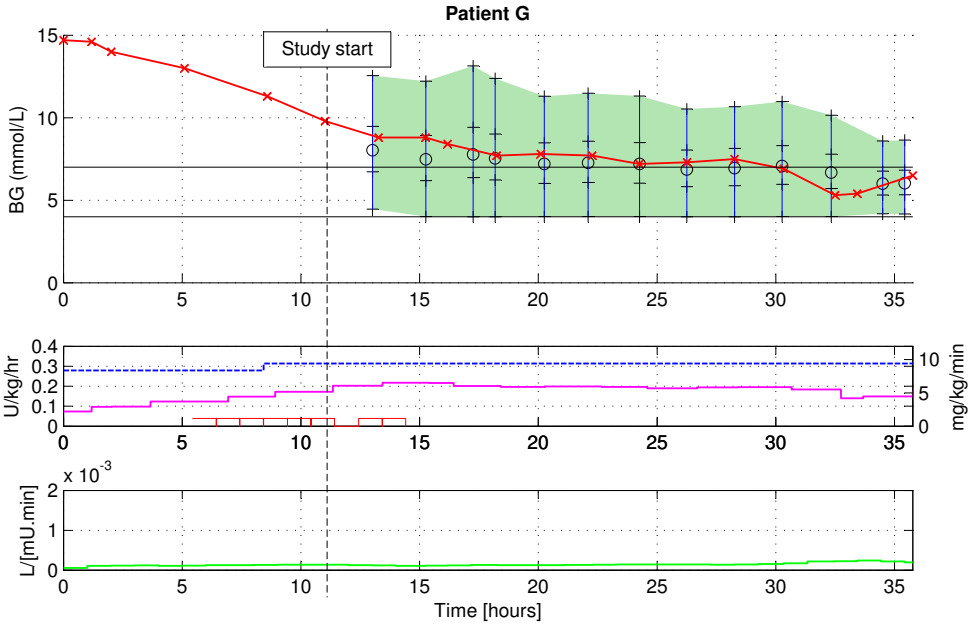

Figure 7.9: BG control during clinical trial for Patient G. The BG measurements are shown in the top panel together with the 5%-95% BG prediction forecast (shaded). The second panel shows insulin infusions (solid line), dextrose infusions (dashed line) and EBM (bars). The third panel shows model-fitted insulin sensitivity.

vals may have likely missed the relatively rapid rise in insulin sensitivity between hours 31-33 of the study. A more aggressive use of insulin may have lead to a hypoglycaemic event in this case.

The patient did not exhibit significant changes in any other routinely measured clinical variable during this time. Thus, it is possible that there was a change in some aspect of glucose metabolism that is not typically measured during neonatal intensive care. This example demonstrates robustness in the controller to account for clinically un-measurable and un-modelled effects.

7.3 Model prediction accuracy

Table 7.3 shows the mean model BG prediction accuracy expressed as a percentage and an absolute concentration. The BG prediction accuracy assessment was generated post-trial by synchronising the forecasted BG concentration with the

Table 7.3: BG prediction accuracy and stochastic model prediction coverage.

Patient	Median BG prediction error (absolute)		BG within forecast range	
	[%]	[mmol/L]	IQR	5% - 95%
A	19.2%	1.47	33%	83%
B	8.6%	0.52	31%	85%
C	7.6%	0.77	80%	90%
D	8.4%	0.53	33%	100%
E	6.4%	0.48	100%	100%
F	8.5%	0.72	50%	83%
G	5.9%	0.44	92%	100%
Cohort	7.6%	0.54	62%	92%

actual time of measurement to account for deviations in measurement frequency experienced in clinical practice. The overall cohort BG prediction error was 7.6% (0.54 mmol/L) over an average measurement interval of 2.1 hours.

The efficacy of the stochastic model was assessed by comparing the percentage of forecasted BG concentrations within the IQR and 5%-95% of prediction bounds. Specifically, 62% of BG predictions were within the forecast IQR and 92% of BG predictions were within the 5%-95% forecast range. These values are slightly higher than those in Chapter 5 for $c = 0.5$ (Table 5.4) for these short-term trials. The distributions of BG prediction errors are shown in Figure 7.10, where 69% and 84% of BG measurements were within $\pm 10\%$ and $\pm 20\%$ of the forecasted concentration, respectively.

The stochastic model employed in this study is built from a whole-cohort perspective using retrospective data from 25 patients as detailed in Chapter 5. Figure 7.3 shows the degree of variability in insulin sensitivity is patient-specific. The amount of patient variability may be linked to other clinical and diagnostic variables. Thus, with further clinical use and data the model may be improved to more clearly identify patients at different stages of development or with different clinical issues. Individualised stochastic models may provide tighter forecast bands by identifying the levels of glycaemic stability per-patient, as discussed in Chapter 5. However, these models require significant data for calibration and were not applicable for these 24-hour pilot trials.

Thus, the glycaemic control problem becomes one of identifying the current (evolving) patient state and managing patient variability in clinical real-time.

Model-based control provides real-time identification of insulin sensitivity, and its evolution with time. However, identification of insulin sensitivity relies on the availability of blood glucose measurements. Thus, two- to three- hourly BG measurements were used in these pilot trials, based on simulation results as presented in Chapter 6 as a compromise between accurate metabolic identification and nursing/patient burden - a factor magnified in preterm neonates with limited blood volumes.

Frequent glucose sampling has been shown to be an important precursor for tight glycaemic control in simulation studies [Lonergan et al., 2006b; Chase et al., 2007]. Some insulin infusion studies in preterm neonates used longer measurement and intervention intervals of up to 6 hours [Beardsall et al., 2008]. These latter studies failed to achieve tight control or safety from hypoglycaemia, and long measurement intervals likely contributed negatively to the level of glycaemic control achieved, as patient condition can evolve significantly over that timeframe as seen in this clinical study.

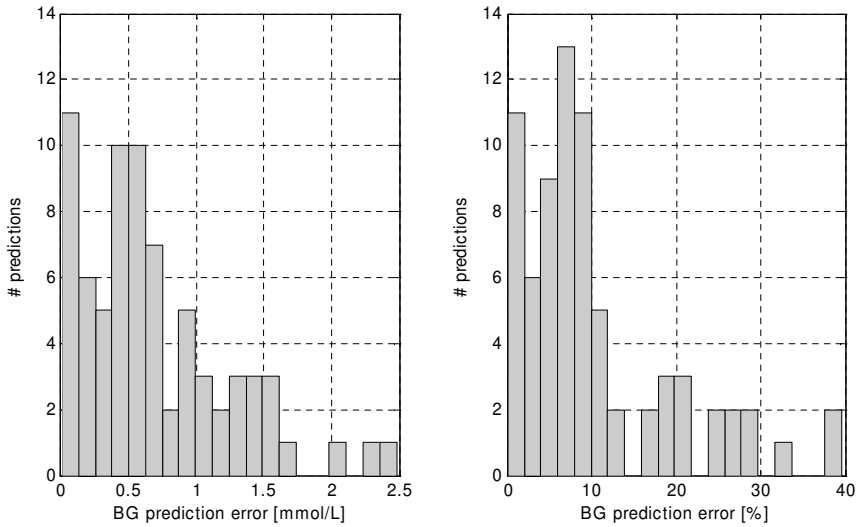

Figure 7.10: Blood glucose prediction errors during trials (expressed as absolute concentration in left panel, and percentage of measured BG concentration in right panel).

7.4 Comparison with retrospective cohort

The control of blood glucose concentrations during clinical trials was compared to simulated 24-hour control trials on the retrospective cohort. The 24-hour control simulation period was selected using the same inclusion criteria as for the clinical trial patients. Simulations were performed on 24 patients from the retrospective cohort, with a total of 312 BG measurements/interventions. Patient 13 was excluded from this analysis as the large spike in glucose for this patient due to a glucose-insulin bolus (see Figure 4.7), a clinically unusual event that would not be expected to occur during the trials.

Figure 7.11a compares CDFs of clinical trial BG measurements and model-fitted S_I to the retrospective cohort simulated 24-hour trials. The BG distributions are close to significantly different ($p = 0.054$, Mann-Whitney test). The insulin sensitivity distributions are significantly different ($p < 0.01$, Mann-Whitney test), where the greatest discrepancy is due to a high proportion of very low insulin sensitivities in the clinical cohort. Figure 7.11b shows the overall range of insulin sensitivity values were similar between cohorts, and highlights the group of 'difficult' or more insulin-resistant patients encountered in the clinical trials.

The BG and S_I distribution analysis was repeated using a subset of patients from the retrospective cohort selected to provide the best possible overall match for gestational age and weight. The details of the matched cohorts are presented in Table 7.4, and the BG and S_I CDFs are presented in Figure 7.12a. The histograms of insulin sensitivity distribution for the two cohorts are presented in Figure 7.12b. The BG distributions in this case are not significantly different ($p = 0.22$, Mann-Whitney test). However, the significant difference in insulin sensitivity remains.

The differences in insulin sensitivity separation effect may be due to small patient numbers, particularly in the clinical trial cohort. There may have also been some bias in the selection of study patients, as the study was a proof-of-concept pilot trial with no randomization. Thus, the presence of the trial may have influenced clinical decisions to commence treatment with insulin. There may also have been selection bias in choosing the periods of trial simulation from the retrospective cohort.

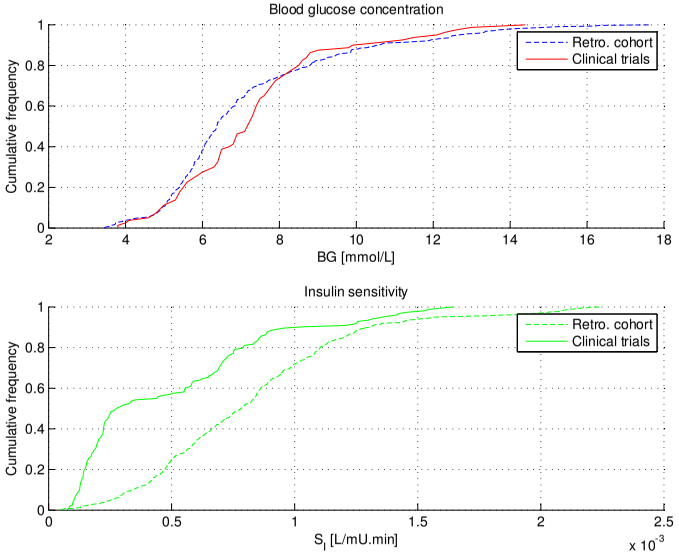

(a) Cumulative distribution of blood glucose (top panel) and insulin sensitivity (bottom panel) for 24-hour trial simulations on retrospective cohort (n=24) and clinical trial patients (n=7).

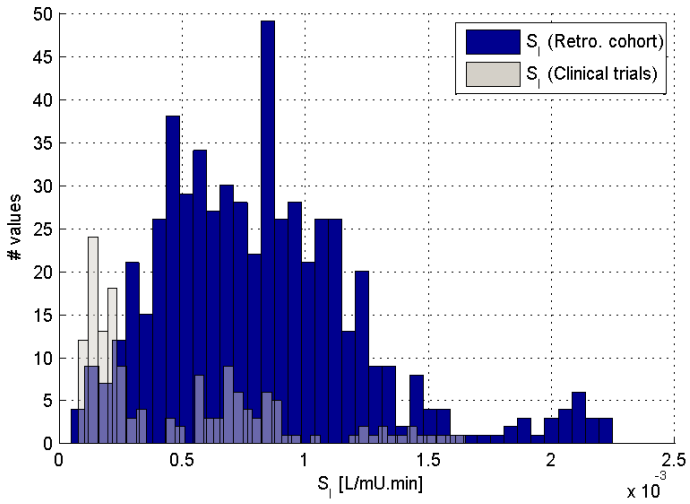

(b) Histogram of insulin sensitivity between 24-hour simulated trials (n=24) and clinical trial patients (n=7).

Figure 7.11: Distribution of blood glucose and insulin sensitivity between trial patients and 24-hour simulated trials.

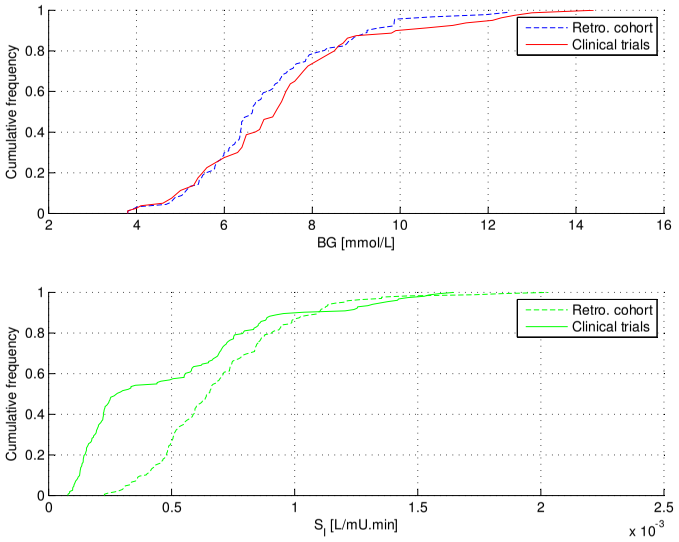

(a) Cumulative distribution of blood glucose (top panel) and insulin sensitivity (bottom panel) for 24-hour trial simulations on *matched* retrospective cohort (n=7) and clinical trial patients (n=7).

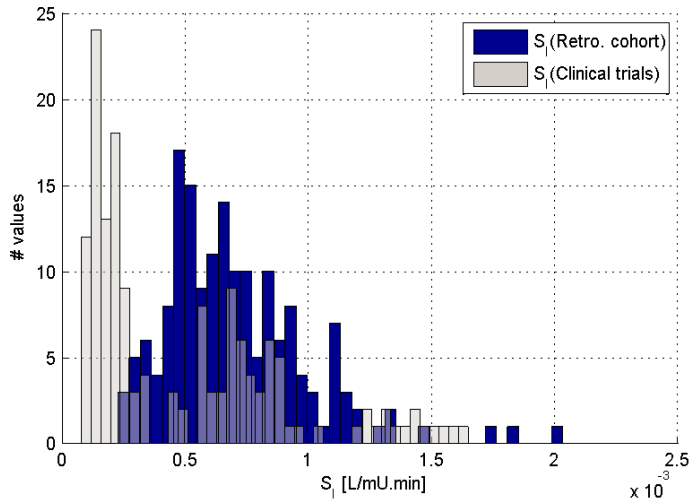

(b) Histogram of insulin sensitivity between *matched* 24-hour simulated trials (n=7) and clinical trial patients (n=7).

Figure 7.12: Distribution of blood glucose and insulin sensitivity between trial patients and matched 24-hour simulated trials.

Table 7.4: Trial patients and matched simulation cohort

Patient match		Trial		Matched Retro.	
Trial	Retro.	Gest. Age	Weight	Gest. Age	Weight
A	14	24.4 wks	685g	24.9 wks	735g
B	8	27.3 wks	770g	26.6 wks	825g
C	4	25.4 wks	720g	23.7 wks	625g
D	7	25.4 wks	785g	26.3 wks	810g
E	2	25.9 wks	540g	24.4 wks	650g
F	15	27.0 wks	900g	26.9 wks	880g
G	6	25.0 wks	995g	25.0 wks	900g

No significant changes in clinical practice had occurred with respect to any likely metabolic input over the period spanning the retrospective cohort data up to the clinical pilot trials. Thus, given the matched cohort results of Figures 7.12a and 7.12b, the only likely clinical difference between retrospective clinical control cohort and the pilot trials cohort was that higher rates of insulin infusion may have been used in the latter. An underestimation of the saturation of the insulin-mediated glucose uptake pathway, represented by α_G in the glucose compartment equation, may manifest itself as an artificially low insulin sensitivity value during periods of greater insulin infusions.

The parameter α_G was set to zero in this study to reflect the reported lack of saturation of the insulin-mediated glucose uptake pathway, within the physiological range of insulin concentrations [Farrag et al., 1996]. Insulin sensitivity was then re-identified for both the retrospective and clinical trial data for two further cases of α_G values:

- $\alpha_G = \frac{1}{65}$: This reflects the value used in adult models [Hann et al., 2005].
- $\alpha_G = \frac{1}{20}$: Given the typical concentrations of insulin in neonates, this value would be likely to cause a significant effect during typical neonatal control situations (if the saturation effect does exist).

Simulation comparisons were performed for both the entire retrospective cohort (n=24) and the matched cohort of Table 7.4. Figure 7.13 presents a comparison of BG and S_I distribution for each value of α_G assessed.

There is little difference in the distribution of both BG and S_I for $\alpha_G = 0$ and $\alpha_G = \frac{1}{65}$, largely due to the lower insulin concentrations in neonates that

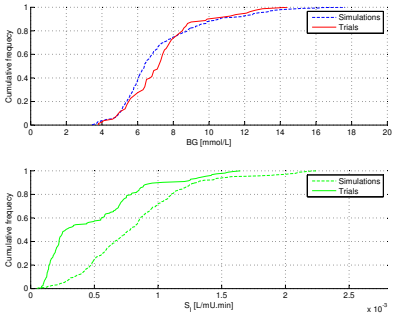

(a) Clinical data (n=7) vs. Retro. cohort (n=24), $\alpha_G = 0$

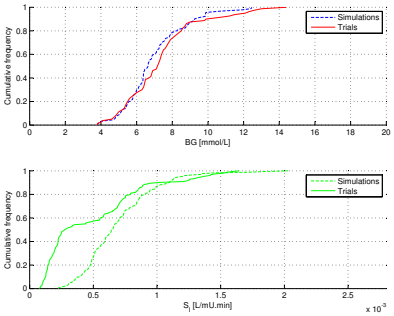

(b) Clinical data (n=7) vs. Matched retro. cohort (n=7), $\alpha_G = 0$

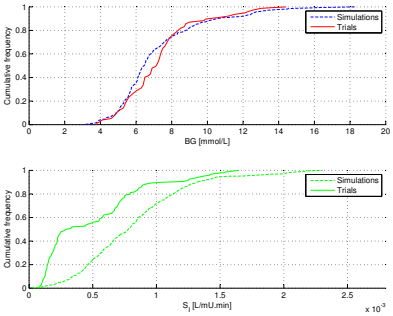

(c) Clinical data (n=7) vs. Retro. cohort (n=24), $\alpha_G = \frac{1}{65}$

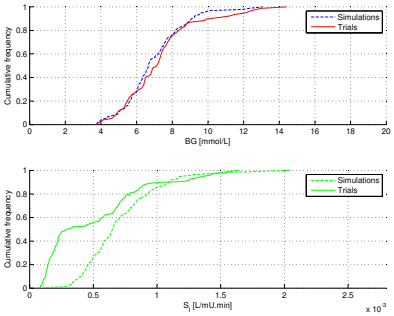

(d) Clinical data (n=7) vs. Matched retro. cohort (n=7), $\alpha_G = \frac{1}{65}$

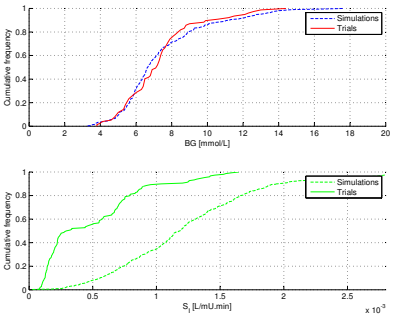

(e) Clinical data (n=7) vs. Retro. cohort (n=24), $\alpha_G = \frac{1}{20}$

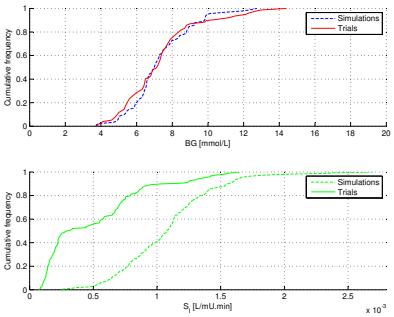

(f) Clinical data (n=7) vs. Matched retro. cohort (n=7), $\alpha_G = \frac{1}{20}$

Figure 7.13: Comparison of BG distribution and insulin sensitivity distribution for clinical pilot trials and 24-hour simulations. Plots in the top row show $\alpha_G = 0$, the middle row $\alpha_G = \frac{1}{65}$, and the bottom row $\alpha_G = \frac{1}{20}$.

prevents most saturation effects for a half-maximum effect concentration of 65 mU/L. The BG distributions are closer for $\alpha_G = \frac{1}{20}$. However, the insulin sensitivity distributions are now separated further. Any increase in differences in model-identified parameters between cohorts is unlikely, given the similar clinical condition of the retrospective and clinical cohorts. Thus, any error in the

estimation of insulin-mediated glucose uptake saturation, an important parameter in adult glucose control, does not appear to explain the difference in insulin sensitivity observed between cohorts in this study.

As a result of this last analysis, these differences may be due to clinical selection bias, small cohort numbers or another un-measured clinical difference. However, despite the differences in insulin sensitivity between the clinical cohort and retrospective counterparts the model-based controller achieved a similar level of glycaemic control performance between groups, highlighting the adaptive ability of the system.

7.5 Clinical trial control compared to overall hospital control

The BG control during the pilot clinical trial study period was compared to the entire record of BG control for each of the study patients. Figure 7.14 highlights the periods of insulin usage and model-based control. The concentration of dextrose solution used to deliver glucose the patient is also shown.

The model-based controller generally assisted in consistently lowering BG to the target band, or maintaining control within the band. There was no clear relationship between the concentration of dextrose solution and level of glycaemic control either within the study or under hospital control. Blood glucose control was generally more variable outside the model-based control period. In particular patients B, E, F and G showed significant rebound hyperglycaemia once insulin infusions were stopped. These results highlight the significant glycaemic variability of critically ill neonates and the necessity for adequate criteria for stopping insulin infusions once a patient is adequately self-regulating. Large scale implementation of the SPRINT protocol [Chase et al., 2008b] used explicitly defined stopping criteria based on a combination of glycaemic stability, low insulin infusion rate and high glucose intake rate. Large-scale implementation of model-based glycaemic control in a neonatal ward would require similar stopping rules.

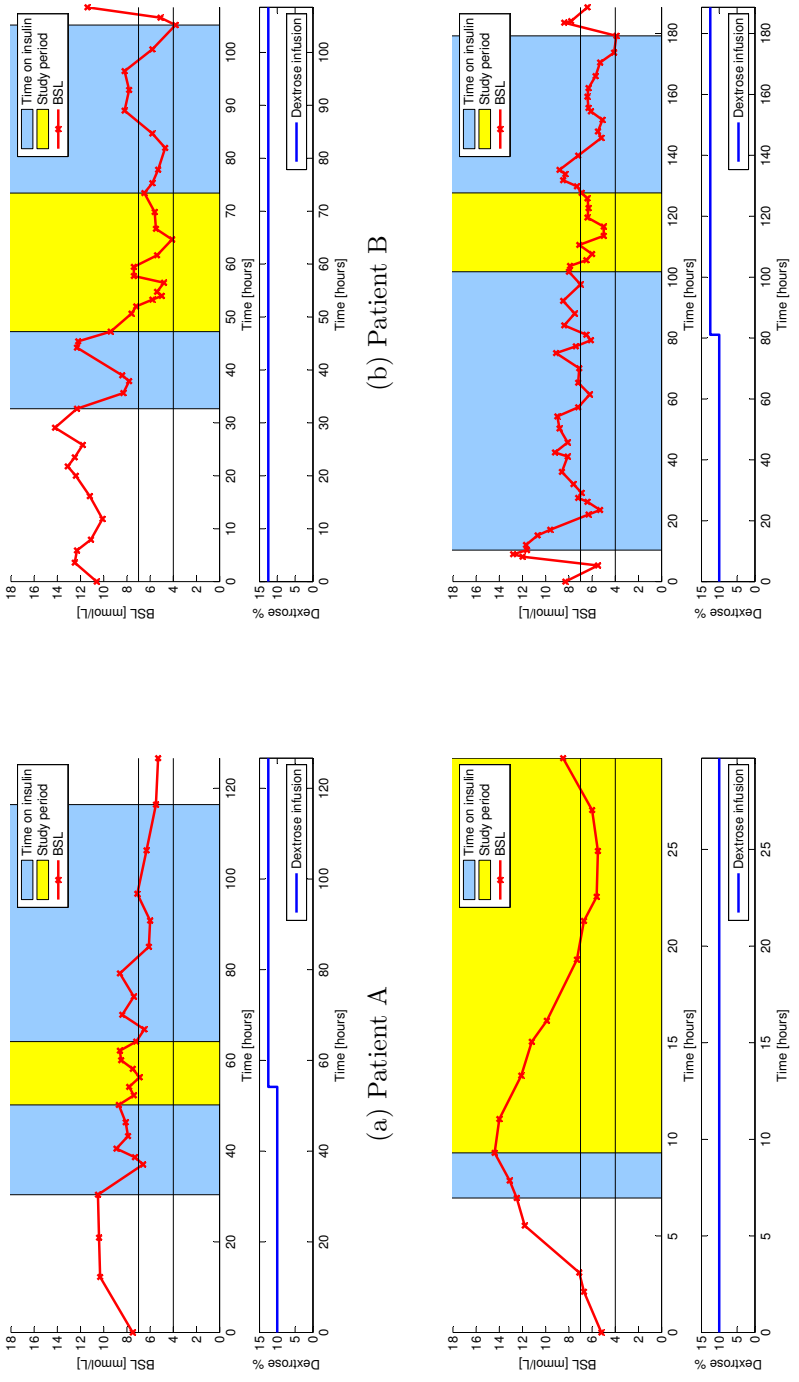

(a) Patient A (b) Patient B

(c) Patient C (d) Patient D

Figure 7.14: Blood glucose control for entire period of insulin usage. Model-based control period and insulin usage are highlighted.

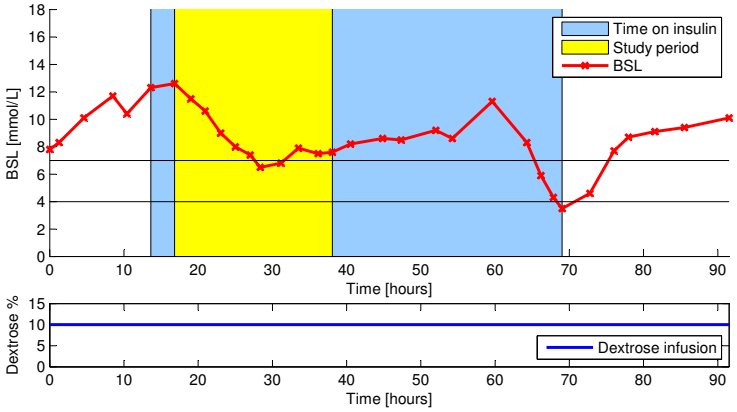

(e) Patient E

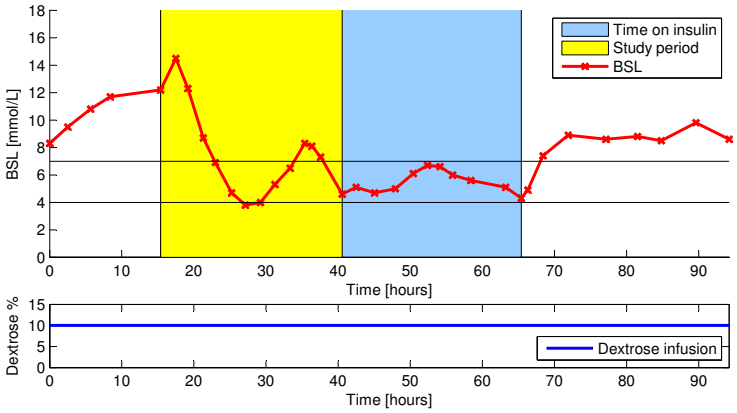

(f) Patient F

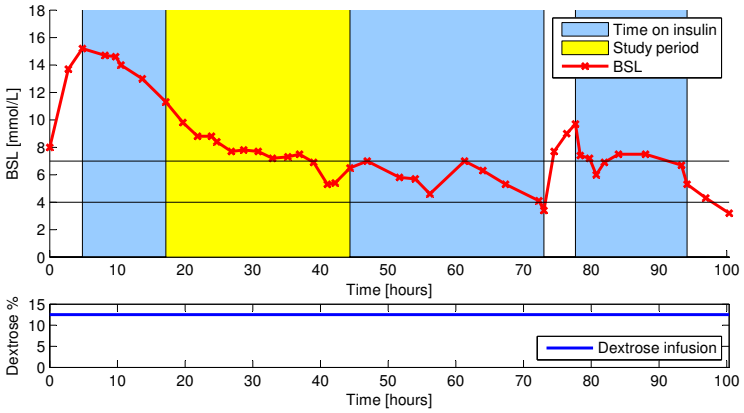

(g) Patient G

Figure 7.14: Blood glucose control for entire period of insulin usage. Model-based control period and insulin usage are highlighted (continued).

7.6 Model-based control effects

The model-based control method provides some insulin dosing recommendations that differ from conventional insulin protocols. Figure 7.15 highlights two specific interventions during clinical trials for Patients C and F where the controller *increased* the insulin infusion rate. What is unique versus any typical clinical practice is that it did so despite a *decrease* in the BG concentration over the previous two measurements, as well as relatively constant nutrition inputs and model-fitted insulin sensitivity over the period.

These controller effects result from the form of the glucose compartment equation, summarised as:

$$\dot{G} = -p_G G - S_I G \frac{Q}{1 + \alpha_G Q} + \text{glucose input} \tag{7.1}$$

By way of example, two similar simplified cases are considered:

- a) A reduction in blood glucose concentration from 9 mmol/L to 8 mmol/L over one hour.
- b) A reduction in blood glucose concentration from 7.5 mmol/L to 6.5 mmol/L over one hour.

In both cases, the left hand side of Equation 7.1, $\dot{G}$, is equal to -1 mmol/L/hr, and the same glucose input and S_I parameter values are assumed for this analysis. The $p_G G$ term is smaller in magnitude for case (b) compared to case (a) due to the lower BG concentration. Thus, to balance the left-hand side of Equation 7.1 the term $S_I G \frac{Q}{1+\alpha_G Q}$ must be larger in magnitude for case (b). As the parameter S_I is constant in this example, and G is lower in case (b), the value of Q must be larger in case (b), relative to case (a). The magnitude of Q, representing the insulin delay compartment, is directly related to the rate of insulin infusion.

Hence, due to the structure of Equation 7.1, a model-based controller would select an increase in the insulin infusion rate for the example presented in (b), despite the lower BG concentration, to maintain a desired constant rate of change

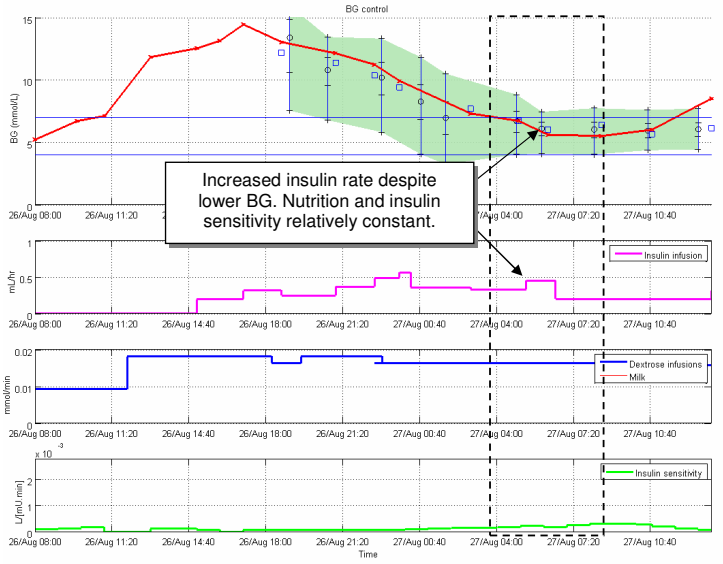

(a) Patient E

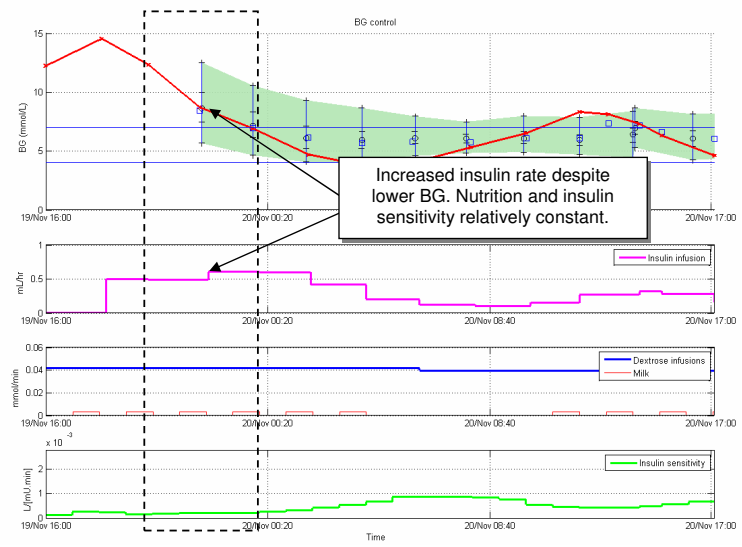

(b) Patient F

Figure 7.15: Clinical model-based control trial results, highlighting controller interventions that increased insulin infusion rate, despite lower BG concentration. The top panel plots BG concentration (with stochastic model forecasts shaded). The second panel plots the insulin infusion rate. The third panel displays nutrition via TPN and EBM, and the bottom panel shows model-fitted insulin sensitivity.

of glucose concentration. This effect is essentially the reverse of a sliding scale approach, and can occur if the desired rate of change of glucose concentration was negative, implying the current BG concentration is above target. In these two simplified cases, the BG was above the target of 6 mmol/L. Hence, one can see an increase in insulin near to the target that one might see well above the target. The model view of this scenario can be pictured in terms glucose transport via facilitated diffusion, as shown in Figure 7.16.

This example highlights how control interventions depend upon the model structure used to approximate the physiological system. The model structure in this case influences control to use a more aggressive insulin dosing response, where a sliding scale approach would have been more conservative. As discussed in Chapter 2, models for control applications must balance physiological validity and real-time identifiability using available clinical data. Thus, under-modelled physiologies may introduce a source of error and impact control performance. Hence, insulin limits are used in the model-based controllers in this research, as developed in Chapter 6, as a response to the balance between dynamics captured well by the model and the effects of a model structure designed for clinical control applicability over total physiological completeness. In the controllers of this thesis, it should be noted that such effects are also mitigated by the stochastic model limits and the use of percentage reductions of BG rather than defined fixed rates of change (e.g. 15% reduction rather than -1 mmol/L per hour).

7.7 Summary

Pilot clinical trials of an adaptive, model-based predictive controller designed to incorporate the unique metabolic state of the neonate showed promise in effectively controlling glycaemia. The controller was used to achieve glycaemic control in seven preterm, low-birth weight neonatal patients during 12-24 hour pilot trials. Significant inter-patient variation in insulin sensitivity was observed in the study cohort, and the controller adequately captured this dynamic variation to regulate blood glucose levels whilst avoiding hypoglycaemia. Comparison to retrospective patient data revealed the model-based controller presented a consistent level of glycaemic control performance for significantly insulin-resistant patients.

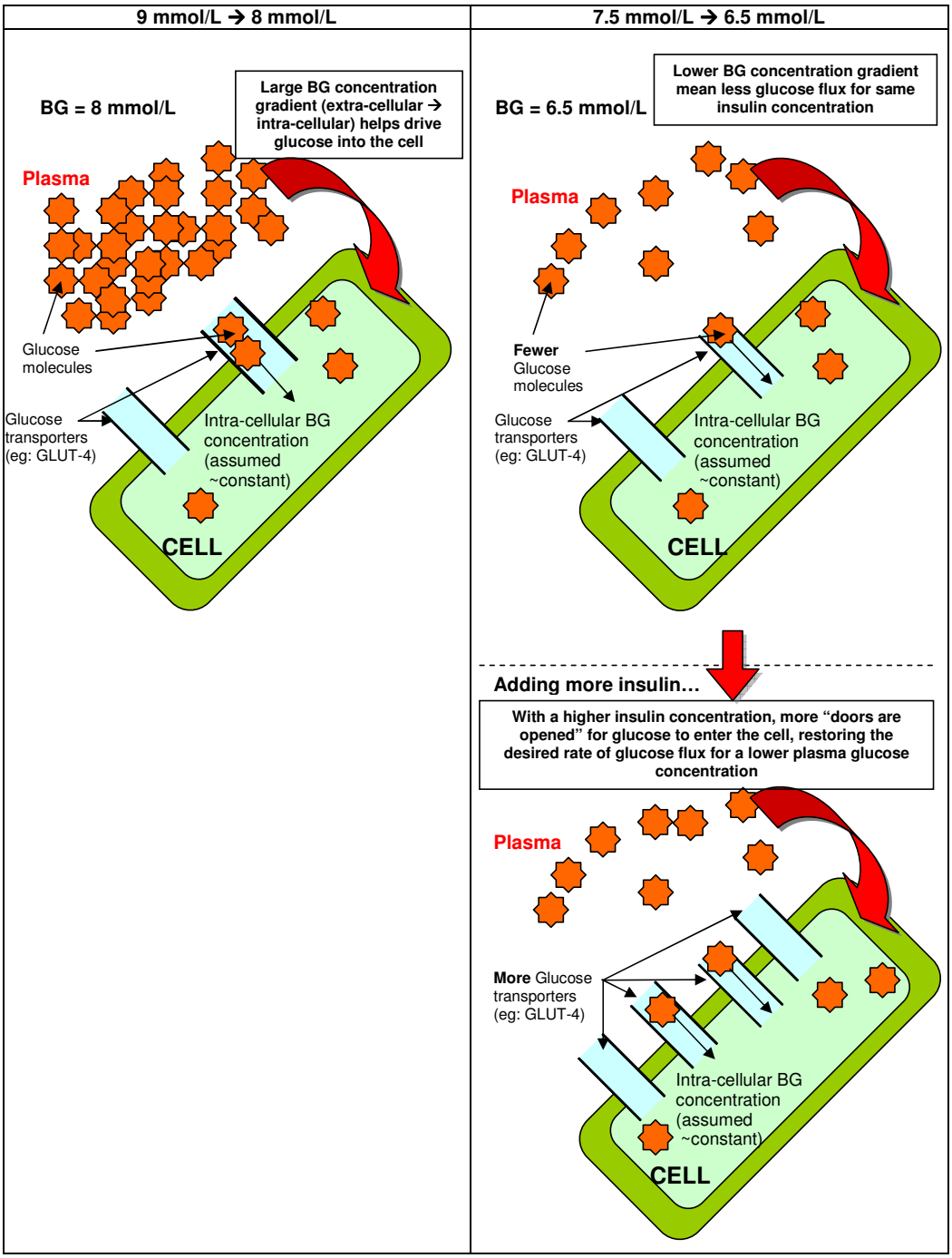

Figure 7.16: Model-based structure effect on controller interventions, based on insulin-mediated glucose transport as a facilitated diffusion process. The 9 mmol/L to 8 mmol/L case is presented in the left panel, and the 7.5 mmol/L to 6.5 mmol/L case is presented in the right panel.

Chapter 8

Conclusions

The work in this thesis presents the development of a complete system for model-based targeted glycaemic control in preterm neonates from initial models through to proof-of-concept clinical pilot trials. A valid, control-applicable physiological system model was developed that incorporated the unique physiology of the neonate. Prediction and control were aided by a stochastic model of insulin sensitivity variation and time-series forecasting methods. A clinical simulation framework built around trials on 'virtual patients' provided an environment to optimise protocol development before clinical implementation. Pilot clinical trials validated the model and control system in a clinical setting and provided tight control of glucose levels on a heterogenous neonatal cohort.

Hyperglycaemia is a common occurrence amongst the youngest and sickest neonates that receive intensive care. A growing body of evidence links the degree of hyperglycaemia to increased morbidity and mortality, and reflects similar findings in the adult critical care case. Recent studies in adults have shown that a 17% - 45% reduction in mortality can be gained if tight glucose regulation is achieved to average levels from 6.0 mmol/L - 7.75 mmol/L [Van den Berghe et al., 2001, 2003; Krinsley, 2003b, 2004; Chase et al., 2008b]. However, such a level of tight control has not yet been achieved for the preterm neonate. The immaturity of the glucose regulatory system in the preterm infant as a cause of hyperglycaemia adds an extra dimension to the stress-induced hyperglycaemia case common to adult critical care. The goals for tight control in neonates emphasise nutrition and growth outcomes in addition to the protective effects of insulin and normoglycaemia.

Significant physiological differences mean there is no simple translation of

adult therapies to the unique neonatal case. Model-based methods can identify patient-specific parameters in real-time and adapt control, and provide a pathway for clinically realistic glycaemic control systems that handle the great heterogeneity that is the hallmark of neonatal glucose metabolism. Glucose-insulin system dynamics are described by models designed for applications from interpreting detailed tracer studies and quantifying human physiology to control system models that capture patient dynamics and variability based on the limited data available in critical care. Whilst the glucose-insulin system dynamics in neonates have not to date been extensively modelled, the rich history of model-based methods in adults helps guide the adaptation of the model to the neonatal case.

A widely validated model of the glucose regulatory system was adapted from adult critical care to the neonatal case. Model fits of insulin sensitivity were generated for 25 patient records and 3,587 hours of retrospective data. Adaptation of several physiological model parameters, including insulin clearance rate, endogenous production rate and volumes of distribution, resulted in an average fitting error of 2.10%. The predictive ability of the model was assessed by assuming insulin sensitivity was constant over the interval. Prediction error at 1, 2 and 4-hour intervals were 5.2%, 9.5% and 14.7% respectively. The model performance was within variations that would also account for dynamic patient evolution. The model thus provided a first in-silico result for modelling the metabolic dynamics of the low-birth weight preterm infant. It also created a platform towards better metabolic clinical management of glycaemia in neonates. The model developed provided an overall measure of a critically ill patient's sensitivity to exogenous insulin and nutrition inputs and allowed comparison of adult and neonatal insulin sensitivity dynamics.

A stochastic model to provide insulin sensitivity predictions was developed from a set of insulin sensitivity data for a neonatal intensive care cohort. The model provided conservative prediction estimators that resulted in greater coverage than expected from the probability bounds. Incorporating lag-2 effects did not improve the coverage proportion, and greater coverage over-estimation in regions of higher data density pointed to the variance estimator based on local data density as a possible source of over-estimation. Modifying the data density estimator by introducing a constant scaling factor showed appropriate coverage was obtained at approximately 10-50% of the original value. However, the probability bounds were no longer smooth or physiologically realistic. Smooth probability

bounds containing the appropriate proportion of prediction coverage could be obtained by choosing the probability bounds to obtain the desired prediction performance.

AR models were able to generate a patient-specific model to allow for tighter prediction intervals during periods of relative stability in insulin sensitivity. However such models require substantial individualised patient data (eg: 12 - 48 hours) which may not be available at the commencement of real-time glycaemic control. Hence, time-series models provide the opportunity for tighter control during periods of patient stability, whereas cohort-wide stochastic models provide extra protection during periods of highly dynamic changes in insulin sensitivity.

An adaptive, model-based predictive controller was designed to leverage metabolic state and forecast information for optimal control. The controller was developed in simulation on a 25 patient cohort and results were compared to retrospective hospital control. Time in the target 4 - 7 mmol/L band was increased by up to 161%, and a range of measurement frequency schemes were evaluated to choose the best compromise between control quality and conservation of the neonate's limited blood supply.

Designing for the transition of a control system from the perfectly-compliant environment of computerised simulation to implementation in a busy, spontaneous critical care ward required assessing the robustness of the control scheme to real-life situations. Missed measurements, errors in the measurement devices and delays in implementing the controller actions were tested. In all cases, the controller proved robust, and thus suitable for initial pilot trials and further longer-term nurse-driven usage.

Pilot clinical trials showed promise in effectively controlling glycaemia, validating the overall targeted model-based control method in neonates. The controller achieved glycaemic control in seven preterm, low-birth weight neonatal patients during 12-24 hour trials. Significant inter-patient variation in insulin sensitivity was observed in the study cohort, and the controller adequately captured this dynamic variation to regulate blood glucose levels whilst avoiding hypoglycaemia. Comparison to retrospective patient data revealed the model-based controller presented a consistent level of glycaemic control performance for significantly insulin-resistant patients.

Chapter 9

Future Work

The models and control methods presented in this thesis provide a framework for glucose control in neonatal critical care. These developments open the doors for wider use of tight glucose control as a treatment in neonatal care, as well as in older pediatric cases, plus related further research opportunities.

9.1 Further clinical validation

The pilot trials presented in this thesis provided an initial validation of the model-based control techniques in this unique patient group. Longer trials and the incorporation of the model-based system as a standard treatment modality for hyperglycaemia in a neonatal intensive care ward would provide validation of long-term control performance. Additionally, longer trials would allow the use of time-series based insulin sensitivity forecasting, as presented in Chapter 5, providing a vehicle for clinical validation of the prediction method. Nutrition modulation may be included to pilot tight glycaemic control with goal nutrition rates in neonatal care.

Long-term follow-up of hyperglycaemic infants with subsequently controlled glucose levels would allow the benefits of tight glycaemic control to be evaluated. Outcome variables such as mortality and in-hospital infections can be evaluated over the course of weeks to months. Overall physical, mental and metabolic development may be assessed over the course of years. Theories of 'metabolic programming' suggest that early post-natal nutrition patterns may have a significant impact on later insulin resistance, obesity and risk of diabetes [Hay, 2006].

Finally, the model-based system can target a range of physiologically sound levels of glycaemia, as well as account for any nutrition and/or insulin infusion rate desired by the clinical. Thus, model-based control may prove useful as a tool in research to compare effects of a range of glucose levels, glucose infusion rates or levels of insulin infusion. Research variables may include concentrations of insulin-like growth factors, rates of proteolysis or other markers of metabolic state across a range of clinical conditions. Such information is not generally available in detail in the neonatal literature.

9.2 Investigation of stochastic behaviours

The stochastic models presented in this thesis are created using general neonatal intensive care data for 25 episodes of insulin usage over 21 patients. Further data over a range of infants of gestational age, birth weight and level of critical illness may isolate some particular characteristics of a specific patient group in the resulting stochastic model. Otherwise, it can help by confirming that insulin sensitivity variation, as modelled, is generic across critically ill neonates.

Observations of stochastic behaviour between patient characteristics can further help the development of different protocols for different patient groups. The overall result would be more tailored control. In addition, identifying such differences may bring to light a deeper understanding of the ontogeny of neonatal glucose metabolism. This point is particularly relevant given the number of hormonal control mechanisms that are still poorly understood in the preterm infant, and the difficulty in performing many intensive pharmacokinetic and pharmacodynamic studies.

9.3 Insulin sensitivity as a marker of illness

Timely diagnosis and treatment of sepsis in critical illness requires significant clinical effort, experience and resources. Insulin sensitivity is known to decrease with worsening condition and could thus be used to aid diagnosis. Initial studies in adults have shown insulin sensitivity provides a negative predictive diagnostic for sepsis [Blakemore et al., 2008]. Premature newborns are at much higher risk

of sepsis than children and adults because of their immature immune system. Accurate and timely diagnosis of early onset neonatal sepsis remains challenging to the clinician and the laboratory. Thus, real-time, model-fitted insulin sensitivity may provide a novel marker of sepsis in this cohort.

9.4 Clinical implementation

Long-term implementation of model-based glycaemic control in neonatal intensive care would require developing robust, verified software. Critical care nursing is a highly technical profession, and staff are typically proficient with computerised technology. Any system needs to operate using terminology and workflow patterns familiar to clinical staff to reduce training time and ease implementation.

A computerised protocol, provided through an easily used graphical user interface, is a standard implementation modality for model-based control. The software may be stored on dedicated bedside computers, or accessed through intranet- or web-based means. An further embodiment of the software would include its incorporation into standard hospital and laboratory information systems, or implemented on programmable infusion pumps.

The metabolic information provided by model-based control relies on accurate knowledge of inputs into the system. New generations of pumps are able to transmit infusion details to hospital information systems, which can be queried by glucose control software. This approach would ensure accurate information is used for control recommendations, reducing double-entry by nurses of infusion information into both the hospital record information system and glucose control software, and move one step along the path to more automated control.

References

Agus, M. S., Javid, P. J., Piper, H. G., Wypij, D., Duggan, C. P., Ryan, D. P., and Jaksic, T. M. (2006). The effect of insulin infusion upon protein metabolism in neonates on extracorporeal life support. *Annals of Surgery Scientific Papers of the 126th Annual Meeting of the American Surgical Association*, 244(4):536–544.

Agus, M. S., Javid, P. J., Ryan, D. P., and Jaksic, T. (2004). Intravenous insulin decreases protein breakdown in infants on extracorporeal membrane oxygenation. *J Pediatr Surg*, 39(6):839–44.

Alaedeen, D. I., Walsh, M. C., and Chwals, W. J. (2006). Total parenteral nutrition-associated hyperglycemia correlates with prolonged mechanical ventilation and hospital stay in septic infants. *J Pediatr Surg*, 41(1):239–44.

Alsweiler, J. M., Kuschel, C. A., and Bloomfield, F. H. (2007). Survey of the management of neonatal hyperglycaemia in Australasia. *Journal of Paediatrics and Child Health*, 43(9):632–635.

Anderson, D. M., Williams, F. H., Merkatz, R. B., Schulman, P. K., Kerr, D. S., and Pittard, W. B. (1983). Length of gestation and nutritional composition of human milk. *Am J Clin Nutr*, 37(5):810–4.

Andronikou, S. and Hanning, I. (1987). Parenteral nutrition effect on serum insulin in the preterm infant. *Pediatrics*, 80(5):693.

Avery, G. B., Fletcher, M. A., and MacDonald, M. G. (1994). *Neonatology : pathophysiology and management of the newborn.* Philadelphia : Lippincott, c1994., 4th edition.

Barker, D. P. and Rutter, N. (1996). Stress, severity of illness, and outcome in ventilated preterm infants. *Archives of disease in childhood*, 75(3):F187–90.

Beardsall, K., Ogilvy-Stuart, A. L., Frystyk, J., Chen, J. W., Thompson, M., Ahluwalia, J., Ong, K. K., and Dunger, D. B. (2007a). Early elective insulin therapy can reduce hyperglycemia and increase insulin-like growth factor-I levels in very low birth weight infants. *The Journal of pediatrics*, 151(6):611–7, 617 e1.

Beardsall, K., Vanhaesebrouck, S., Ogilvy-Stuart, A. L., Ahluwalia, J. S., Vanhole, C., Palmer, C., Midgley, P., Thompson, M., Cornette, L., Weissenbruch, M., Thio, M., de Zegher, F., and Dunger, D. (2007b). A randomised controlled trial of early insulin therapy in very low birth weight infants, "NIRTURE" (neonatal insulin replacement therapy in Europe). *BMC pediatrics*, 7:29.

Beardsall, K., Vanhaesebrouck, S., Ogilvy-Stuart, A. L., Vanhole, C., Palmer, C. R., van Weissenbruch, M., Midgley, P., Thompson, M., Thio, M., Cornette, L., Ossuetta, I., Iglesias, I., Theyskens, C., de Jong, M., Ahluwalia, J. S., de Zegher, F., and Dunger, D. B. (2008). Early insulin therapy in very-low-birth-weight infants. *N Engl J Med*, 359(18):1873–1884.

Bellomo, R. and Egi, M. (2005). Glycemic control in the intensive care unit: why we should wait for nice-sugar. *Mayo Clin Proc*, 80(12):1546–8.

Bergman, R. N., Finegood, D. T., and Ader, M. (1985). Assessment of insulin sensitivity in vivo. *Endocr Rev*, 6(1):45–86.

Bergman, R. N., Ider, Y. Z., Bowden, C. R., and Cobelli, C. (1979). Quantitative estimation of insulin sensitivity. *Am J Physiol*, 236(6):E667–77.

Bergman, R. N., Phillips, L. S., and Cobelli, C. (1981). Physiologic evaluation of factors controlling glucose tolerance in man: measurement of insulin sensitivity and beta-cell glucose sensitivity from the response to intravenous glucose. *J Clin Invest*, 68(6):1456–1467.

Bergman, R. N., Prager, R., Volund, A., and Olefsky, J. M. (1987). Equivalence of the insulin sensitivity index in man derived by the minimal model method and the euglycemic glucose clamp. *J Clin Invest*, 79(3):790–800.

Bidiwala, K. S., Lorenz, J. M., and Kleinman, L. I. (1988). Renal function correlates of postnatal diuresis in preterm infants. *Pediatrics*, 82(1):50–8.

Binder, N. D., Raschko, P. K., Benda, G. I., and Reynolds, J. W. (1989). Insulin infusion with parenteral nutrition in extremely low birth weight infants with hyperglycemia. *The Journal of pediatrics*, 114(2):273–80.

Bistrian, B. R. (2001). Hyperglycemia and infection: which is the chicken and which is the egg? *JPEN J Parenter Enteral Nutr*, 25(4):180–181.

Blakemore, A., Wang, S., Le Compte, A., Shaw, G., Wong, X., Lin, J., Lotz, T., Hann, C., and Chase, J. (2008). Model-based insulin sensitivity as a sepsis diagnostic in critical care. *Journal of Diabetes Science and Technology*, 2(3):468–477.

Bloomfield, P. (2000). *Fourier analysis of time series: An introduction*. Wiley Series in Probability and Statistics. John Wiley & Sons, New York, 2nd edition.

Bloomgarden, Z. T. (2003). Inflammation and insulin resistance. *Diabetes Care*, 26(6):1922–1926.

Bolli, G., Defeo, P., Perriello, G., Ventura, M., and Brunetti, P. (1986). A Decrease in hepatic insulin sensitivity, not an increase in plasma-insulin clearance, causes the dawn phenomenon in IDDM. *Diabetes*, 35:A92–A92.

Box, G. and Jenkins, G. (1976). *Time Series Analysis: Forecasting and Control*. Holden-Day, San Francisco.

Branco, R. G., Garcia, P. C., Piva, J. P., Casartelli, C. H., Seibel, V., and Tasker, R. C. (2005). Glucose level and risk of mortality in pediatric septic shock. *Pediatr Crit Care Med*, 6(4):470–2.

Butler, S. O., Btaiche, I. F., and Alaniz, C. (2005). Relationship between hyperglycemia and infection in critically ill patients. *Pharmacotherapy*, 25(7):963–76.

Capes, S. E., Hunt, D., Malmberg, K., and Gerstein, H. C. (2000). Stress hyperglycaemia and increased risk of death after myocardial infarction in patients with and without diabetes: a systematic overview. *Lancet*, 355(9206):773–778.

Cardinal Health (2008). *Alaris CC Syringe Pump - Directions For Use*. Cardinal Health.

Carson, E. R. and Cobelli, C. (2001). *Modelling methodology for physiology and medicine*. Academic Press Series in Biomedical Engineering. Academic Press, San Diego.

Cassady, G. (1966). Plasma volume studies in low birth weight infants. *Pediatrics*, 38(6):1020–7.

Castillo, C., Bogardus, C., Bergman, R., Thuillez, P., and Lillioja, S. (1994). Interstitial insulin concentrations determine glucose uptake rates but not insulin resistance in lean and obese men. *J Clin Invest*, 93(1):10–6.

Chase, J., Shaw, G. M., Wong, X. W., Lotz, T., Lin, J., and Hann, C. E. (2006a). Model-based glycaemic control in critical care - a review of the state of the possible. *Biomedical Signal Processing and Control*, 1(1):3–21.

Chase, J. G., Andreassen, S., Jensen, K., and Shaw, G. M. (2008a). Impact of human factors on clinical protocol performance: A proposed assessment framework and case examples. *Journal of Diabetes Science and Technology*, 2(3):409–416.

Chase, J. G., Lin, J., Lee, D. S., Wong, X. W., Hann, C. E., and Shaw, G. M. (2006b). Stochastic insulin sensitivity models for tight glycaemic control. In *6th IFAC Symposium on Modeling and Control in Biomedical Systems (MCBMS)*, pages 345–50, Reims, France.

Chase, J. G., Lonergan, T., Le Compte, A., Willacy, M., Shaw, G. M., Wong, X. W., Lin, J., Lotz, T., and Hann, C. E. (2005a). Tight glucose control in critically ill patients using a specialized insulin-nutrition table. In *Proc. of the 12th International Conf on Biomedical Engineering (ICBME 2005)*, Singapore.

Chase, J. G., Shaw, G., Le Compte, A., Lonergan, T., Willacy, M., Wong, X. W., Lin, J., Lotz, T., Lee, D., and Hann, C. (2008b). Implementation and evaluation of the SPRINT protocol for tight glycaemic control in critically ill patients: a clinical practice change. *Critical Care*, 12(2):R49.

Chase, J. G., Shaw, G. M., Lin, J., Doran, C. V., Bloomfield, M., Wake, G. C., Broughton, B., Hann, C., and Lotz, T. (2004). Impact of insulin-stimulated glucose removal saturation on dynamic modelling and control of hyperglycaemia. *International Journal of Intelligent Systems Technologies and Applications (IJISTA)*, 1(1/2):79–94.

Chase, J. G., Shaw, G. M., Lin, J., Doran, C. V., Hann, C., Lotz, T., Wake, G. C., and Broughton, B. (2005b). Targeted glycemic reduction in critical care using closed-loop control. *Diabetes Technol Ther*, 7(2):274–82.

Chase, J. G., Shaw, G. M., Lin, J., Doran, C. V., Hann, C., Robertson, M. B., Browne, P. M., Lotz, T., Wake, G. C., and Broughton, B. (2005c). Adaptive

bolus-based targeted glucose regulation of hyperglycaemia in critical care. *Med Eng Phys*, 27(1):1–11.

Chase, J. G., Shaw, G. M., Lotz, T., Le Compte, A., Wong, J., Lin, J., Lonergan, T., Willacy, M., and Hann, C. E. (2007). Model-based insulin and nutrition administration for tight glycaemic control in critical care. *Curr Drug Deliv*, 4(4):283–96.

Chase, J. G., Wong, X. W., Singh-Levett, I., Hollingsworth, L. J., Hann, C. E., Shaw, G. M., Lotz, T., and Lin, J. (2008c). Simulation and initial proof-of-concept validation of a glycaemic regulation algorithm in critical care. *Control Engineering Practice*, 16(3):271–285.

Chatfield, C. (2000). *Time-series forecasting*. Chapman & Hall/CRC, Boca Raton, 1st edition.

Chatfield, C. (2004). *The analysis of time series - An introduction*. Statistical Science. Chapman & Hall/CRC, Boca Raton, 6th edition.

Chee, F., Fernando, T., and van Heerden, P. V. (2003a). Closed-loop glucose control in critically ill patients using continuous glucose monitoring system (cgms) in real time. *IEEE Trans Inf Technol Biomed*, 7(1):43–53.

Chee, F., Fernando, T. L., Savkin, A. V., and van Heeden, V. (2003b). Expert pid control system for blood glucose control in critically ill patients. *IEEE Trans Inf Technol Biomed*, 7(4):419–25.

Chen, E. T., Nichols, J. H., Duh, S. H., and Hortin, G. (2003). Performance evaluation of blood glucose monitoring devices. *Diabetes Technol Ther*, 5(5):749–68.

Chiu, K. C., Cohan, P., Lee, N. P., and Chuang, L. M. (2000). Insulin sensitivity differs among ethnic groups with a compensatory response in beta-cell function. *Diabetes care*, 23(9):1353–8.

Christensen, D. (2001). Critical care: Sugar limit saves lives. *Science News*, 159(26):159.

Clarke, W. L. (2005). The original Clarke Error Grid Analysis (EGA). *Diabetes Technol Ther*, 7(5):776–9.

Cobelli, C., Toffolo, G., and Ferrannini, E. (1984). A model of glucose kinetics and their control by insulin, compartmental and noncompartmental approaches. *Mathematical Biosciences*, 72(2):291–315.

Collins, J. W., Hoppe, M., Brown, K., Edidin, D. V., Padbury, J., and Ogata, E. S. (1991). A controlled trial of insulin infusion and parenteral nutrition in extremely low birth weight infants with glucose intolerance. *The Journal of pediatrics*, 118(6):921–7.

Cornblath, M., Hawdon, J. M., Williams, A. F., Aynsley-Green, A., Ward-Platt, M. P., Schwartz, R., and Kalhan, S. C. (2000). Controversies regarding definition of neonatal hypoglycemia: suggested operational thresholds. *Pediatrics*, 105(5):1141–5.

Coulthard, M. G. and Hey, E. N. (1999). Renal processing of glucose in well and sick neonates. *Arch Dis Child Fetal Neonatal Ed*, 81(2):F92–8.

Coursin, D. B. and Murray, M. J. (2003). How sweet is euglycemia in critically ill patients? *Mayo Clin Proc*, 78(12):1460–2.

Cowett, R. M. and Farrag, H. M. (2004). Selected principles of perinatal-neonatal glucose metabolism. *Semin Neonatol*, 9(1):37–47.

Cowett, R. M., Oh, W., and Schwartz, R. (1983). Persistent glucose production during glucose infusion in the neonate. *J Clin Invest*, 71(3):467–75.

Dandona, P., Chaudhuri, A., Ghanim, H., and Mohanty, P. (2006). Anti-inflammatory effects of insulin and pro-inflammatory effects of glucose: relevance to the management of acute myocardial infarction and other acute coronary syndromes. *Rev Cardiovasc Med*, 7 Suppl 2:S25–34.

Darlow, B. A., Cust, A. E., and Donoghue, D. A. (2003). Improved outcomes for very low birthweight infants: evidence from New Zealand national population based data. *Arch Dis Child Fetal Neonatal Ed*, 88(1):F23–8.

Das, U. N. (2003). Insulin in sepsis and septic shock. *J Assoc Physicians India*, 51:695–700.

Demissie, K., Rhoads, G. G., Ananth, C. V., Alexander, G. R., Kramer, M. S., Kogan, M. D., and Joseph, K. S. (2001). Trends in preterm birth and neonatal mortality among blacks and whites in the United States from 1989 to 1997. *Am J Epidemiol*, 154(4):307–15.

Deutsch, T., Gergelya, T., and Trunovc, V. (2004). A computer system for interpreting blood glucose data. *Computer Methods and Programs in Biomedicine*, 76(1):41–51.

Diderholm, B., Ewald, U., Ahlsson, F., and Gustafsson, J. (2007). Energy substrate production in infants born small for gestational age. *Acta Paediatr*, 96(1):29–34.

Diringer, M. N. (2005). Improved outcome with aggressive treatment of hyperglycemia - hype or hope? *Neurology*, 64(8):1330–1331.

Ditzenberger, G. R., Collins, S. D., and Binder, N. (1999). Continuous insulin intravenous infusion therapy for vlbw infants. *J Perinat Neonatal Nurs*, 13(3):70–82.

Doran, C. V. (2004). *Modelling and control of hyperglycemia in critical care patients*. Master's thesis, University of Canterbury.

Dweck, H. S. and Cassady, G. (1974). Glucose intolerance in infants of very low birth weight. *Pediatrics*, 53(2):189.

Egi, M., Bellomo, R., Stachowski, E., French, C. J., and Hart, G. (2006). Variability of blood glucose concentration and short-term mortality in critically ill patients. *Anesthesiology*, 105(2):244–52.

Erichsen, L., Agbaje, O. F., Luzio, S. D., Owens, D. R., and Hovorka, R. (2004). Population and individual minimal modeling of the frequently sampled insulin-modified intravenous glucose tolerance test. *Metabolism*, 53(10):1349–54.

Ertl, T., Gyarmati, J., Gaal, V., and Szabo, I. (2006). Relationship between hyperglycemia and retinopathy of prematurity in very low birth weight infants. *Biology of the neonate*, 89(1):56–9.

Esposito, K., Marfella, R., and Giugliano, D. (2003). Stress hyperglycemia, inflammation, and cardiovascular events. *Diabetes Care*, 26(5):1650–1651.

Farrag, H. M. and Cowett, R. M. (2000). Glucose homeostasis in the micropremie. *Clinics in Perinatology*, 27(1):1–22.

Farrag, H. M., Dorcus, E. J., and Cowett, R. M. (1996). Maturation of the glucose utilization response to insulin occurs before that of glucose production in the preterm neonate. *Pediatric Research*, 39(4):308.

Farrag, H. M., Nawrath, L. M., Healey, J. E., Dorcus, E. J., Rapoza, R. E., Oh, W., and Cowett, R. M. (1997). Persistent glucose production and greater peripheral sensitivity to insulin in the neonate vs. the adult. *Am J Physiol*, 272(1 Pt 1):E86–93.

Fendler, W. M. and Mlynarski, W. M. (2009). Insulin therapy in very-low-birth-weight infants. *N Engl J Med*, 360(5):535–6; author reply 536–7.

Finney, S. J., Zekveld, C., Elia, A., and Evans, T. W. (2003). Glucose control and mortality in critically ill patients. *JAMA*, 290(15):2041–2047.

Fuloria, M., Friedberg, M. A., DuRant, R. H., and Aschner, J. L. (1998). Effect of flow rate and insulin priming on the recovery of insulin from microbore infusion tubing. *Pediatrics*, 102(6):1401–6.

Garg, R., Agthe, A. G., Donohue, P. K., and Lehmann, C. U. (2003). Hyperglycemia and retinopathy of prematurity in very low birth weight infants. *Journal of perinatology*, 23(3):186–94.

Goldberg, P. A., Bozzo, J. E., Thomas, P. G., Mesmer, M. M., Sakharova, O. V., Radford, M. J., and Inzucchi, S. E. (2006). "Glucometrics"-assessing the quality of inpatient glucose management. *Diabetes Technol Ther*, 8(5):560–9.

Goldman, S. L. and Hirata, T. (1980). Attenuated response to insulin in very low birthweight infants. *Pediatric research*, 14(1):50–3.

Graafmans, W. C., Richardus, J. H., Macfarlane, A., Rebagliato, M., Blondel, B., Verloove-Vanhorick, S. P., and Mackenbach, J. P. (2001). Comparability of published perinatal mortality rates in Western Europe: the quantitative impact of differences in gestational age and birthweight criteria. *BJOG*, 108(12):1237–45.

Gruetter, R., Ugurbil, K., and Seaquist, E. R. (1998). Steady-state cerebral glucose concentrations and transport in the human brain. *J Neurochem*, 70(1):397–408.

Gubern, C., Lopez-Bermejo, A., Biarnes, J., Vendrell, J., Ricart, W., and Fernandez-Real, J. M. (2006). Natural antibiotics and insulin sensitivity: the role of bactericidal/permeability-increasing protein. *Diabetes*, 55(1):216–24.

Guyton, A. C. and Hall, J. E. (2000). *Textbook of medical physiology*. Saunders, Philadelphia ; London, 10th edition.

Hall, N. J., Peters, M., Eaton, S., and Pierro, A. (2004). Hyperglycemia is associated with increased morbidity and mortality rates in neonates with necrotizing enterocolitis. *J Pediatr Surg*, 39(6):898–901.

Hann, C., Chase, J., and Shaw, G. (2006). Integral-based identification of patient specific parameters for a minimal cardiac model. *Computer Methods and Programs in Biomedicine*, 81(2):181–192.

Hann, C. E., Chase, J. G., Lin, J., Lotz, T., Doran, C. V., and Shaw, G. M. (2005). Integral-based parameter identification for long-term dynamic verification of a glucose-insulin system model. *Comput Methods Programs Biomed*, 77(3):259–270.

Hansen, T. K., Thiel, S., Wouters, P. J., Christiansen, J. S., and Van den Berghe, G. (2003). Intensive insulin therapy exerts antiinflammatory effects in critically ill patients and counteracts the adverse effect of low mannose-binding lectin levels. *The Journal of clinical endocrinology and metabolism*, 88(3):1082–8.

Hartnoll, G. (2003). Basic principles and practical steps in the management of fluid balance in the newborn. *Seminars in neonatology*, 8(4):307–13.

Hartnoll, G., Betremieux, P., and Modi, N. (2000). Body water content of extremely preterm infants at birth. *Archives of disease in childhood*, 83(1):F56–9.

Hay, W. W. (2006). Early postnatal nutritional requirements of the very preterm infant based on a presentation at the NICHD-AAP workshop on research in neonatology. *J Perinatol*, 26(S2):S13–S18.

Hay, W. W. J., Lucas, A., Heird, W. C., Ziegler, E., Levin, E., Grave, G. D., Catz, C. S., and Yaffe, S. J. (1999). Workshop summary: nutrition of the extremely low birth weight infant. *Pediatrics*, 104(6):1360–8.

Hays, S. P., Smith, B., and Sunehag, A. L. (2006). Hyperglycemia is a risk factor for early death and morbidity in extremely low birth-weight infants. *Pediatrics*, 118(5):1811–1818.

Heimann, K., Peschgens, T., Kwiecien, R., Stanzel, S., Hoernchen, H., and Merz, U. (2007). Are recurrent hyperglycemic episodes and median blood glucose level a prognostic factor for increased morbidity and mortality in premature infants ¡=1500 g? *Journal of perinatal medicine*, 35(3):245–8.

Hemachandra, A. H. and Cowett, R. M. (1999). Neonatal hyperglycemia. *Pediatrics in Review*, 20(7):16–24.

Hertz, D. E., Karn, C. A., Liu, Y. M., Liechty, E. A., and Denne, S. C. (1993). Intravenous glucose suppresses glucose production but not proteolysis in extremely premature newborns. *The Journal of clinical investigation*, 92(4):1752–8.

Hewson, M., Nawadra, V., Oliver, J., Odgers, C., Plummer, J., and Simmer, K. (2000). Insulin infusions in the neonatal unit: Delivery variation due to adsorption. *J. Paed. Child Health*, 36(3):216–220.

Hey, E. (2005). Hyperglycaemia and the very preterm baby. *Seminars in fetal & neonatal medicine*, 10(4):377–87.

Hirsch, I. B. and Brownlee, M. (2005). Should minimal blood glucose variability become the gold standard of glycemic control? *J Diabetes Complications*, 19(3):178–81.

Ho, K. C., Roessmann, U., Hause, L., and Monroe, G. (1981). Newborn brain weight in relation to maturity, sex, and race. *Annals of neurology*, 10(3):243–6.

Holm, C., Horbrand, F., Mayr, M., von Donnersmarck, G. H., and Muhlbauer, W. (2004). Acute hyperglycaemia following thermal injury: friend or foe? *Resuscitation*, 60(1):71–7.

Hovorka, R., Canonico, V., Chassin, L. J., Haueter, U., Massi-Benedetti, M., Federici, M. O., Pieber, T. R., Schaller, H. C., Schaupp, L., Vering, T., and Wilinska, M. E. (2004). Nonlinear model predictive control of glucose concentration in subjects with type 1 diabetes. *Physiological Measurement*, 25(4):905–920.

Hovorka, R., Kremen, J., Blaha, J., Matias, M., Anderlova, K., Bosanska, L., Roubicek, T., Wilinska, M. E., Chassin, L. J., Svacina, S., and Haluzik, M. (2007). Blood glucose control by a model predictive control algorithm with variable sampling rate versus a routine glucose management protocol in cardiac surgery patients: A randomized controlled trial. *J Clin Endocrinol Metab*, 92(8):2960–2964.

Hovorka, R., Shojaee-Moradie, F., Carroll, P. V., Chassin, L. J., Gowrie, I. J., Jackson, N. C., Tudor, R. S., Umpleby, A. M., and Jones, R. H. (2002). Partitioning glucose distribution/transport, disposal, and endogenous production during ivgtt. *Am J Physiol Endocrinol Metab*, 282(5):E992–1007.

Hume, R., Burchell, A., Williams, F. L., and Koh, D. K. (2005). Glucose homeostasis in the newborn. *Early Hum Dev*, 81(1):95–101.

Insel, P. A., Kramer, K. J., Sherwin, R. S., Liljenquist, J. E., Tobin, J. D., Andres, R., and Berman, M. (1974). Modeling the insulin-glucose system in man. *Fed Proc*, 33(7):1865–8.

Jackson, L., Burchell, A., McGeechan, A., and Hume, R. (2003). An inadequate glycaemic response to glucagon is linked to insulin resistance in preterm infants? *Arch. Dis. Child. Fetal Neonatal Ed.*, 88(1):F62–66.

Jeremitsky, E., Omert, L. A., Dunham, C. M., Wilberger, J., and Rodriguez, A. (2005). The impact of hyperglycemia on patients with severe brain injury. *J Trauma*, 58(1):47–50.

Jeschke, M. G., Klein, D., and Herndon, D. N. (2004). Insulin treatment improves the systemic inflammatory reaction to severe trauma. *Annals of surgery*, 239(4):553–60.

Joslin, E. (1985). *Joslin's Diabetes Mellitus*. Lea & Febiger, 12th edition.

Kalhan, S. (2003). Metabolism of glucose and methods of investigation in the fetus and newborn. In *Fetal and Neonatal Physiology*, pages 449–464.

Kalhan, S. C., Oliven, A., King, K. C., and Lucero, C. (1986). Role of glucose in the regulation of endogenous glucose production in the human newborn. *Pediatric research*, 20(1):49–52.

Kanarek, K. S., Santeiro, M. L., and Malone, J. I. (1991). Continuous infusion of insulin in hyperglycemic low-birth weight infants receiving parenteral nutrition with and without lipid emulsion. *J Parenter Enteral Nutr*, 15(4):417–20.

Kao, L. S., Morris, B. H., Lally, K. P., Stewart, C. D., Huseby, V., and Kennedy, K. A. (2006). Hyperglycemia and morbidity and mortality in extremely low birth weight infants. *Journal of perinatology*, 26(12):730–6.

Kern, J. W., McDonald, T. L., Amstrup, S. C., Durner, G. M., and Erickson, W. P. (2003). Using the bootstrap and fast fourier transform to estimate confidence intervals of 2d kernel densities. *Environmental and Ecological Statistics*, 10:405–418.

Kiely, J. L. (1998). What is the population-based risk of preterm birth among twins and other multiples? *Clin Obstet Gynecol*, 41(1):3–11.

Kovatchev, B. P., Clarke, W. L., Breton, M., Brayman, K., and McCall, A. (2005). Quantifying temporal glucose variability in diabetes via continuous glucose monitoring: Mathematical methods and clinical application. *Diabetes Technol Ther*, 7(6):849–62.

Kovatchev, B. P., Gonder-Frederick, L. A., Cox, D. J., and Clarke, W. L. (2004). Evaluating the accuracy of continuous glucose-monitoring sensors: continuous glucose-error grid analysis illustrated by therasense freestyle navigator data. *Diabetes Care*, 27(8):1922–8.

Krinsley, J. S. (2003a). Association between hyperglycemia and increased hospital mortality in a heterogeneous population of critically ill patients. *Mayo Clin Proc*, 78(12):1471–1478.

Krinsley, J. S. (2003b). Decreased mortality of critically ill patients with the use of an intensive glycemic management protocol. *Crit Care Med*, 31:A19.

Krinsley, J. S. (2004). Effect of an intensive glucose management protocol on the mortality of critically ill adult patients. *Mayo Clin Proc*, 79(8):992–1000.

Krinsley, J. S. (2008). Glycemic variability: a strong independent predictor of mortality in critically ill patients. *Crit Care Med*, 36(11):3008–13.

Laird, A. M., Miller, P. R., Kilgo, P. D., Meredith, J. W., and Chang, M. C. (2004). Relationship of early hyperglycemia to mortality in trauma patients. *J Trauma*, 56(5):1058–62.

Langouche, L., Vanhorebeek, I., Vlasselaers, D., Vander Perre, S., Wouters, P. J., Skogstrand, K., Hansen, T. K., and Van den Berghe, G. (2005). Intensive insulin therapy protects the endothelium of critically ill patients. *J Clin Invest*, 115(8):2277–86.

Leipala, J. A., Talme, M., Viitala, J., Turpeinen, U., and Fellman, V. (2003). Blood volume assessment with hemoglobin subtype analysis in preterm infants. *Biol Neonate*, 84(1):41–4.

Lin, J. (2007). *Robust modelling and control of the glucose-insulin regulatory system for tight glycemic control of critical care patients*. PhD thesis, University of Canterbury.

Lin, J., Lee, D., Chase, J., Hann, C., Lotz, T., and Wong, X. (2006). Stochastic modelling of insulin sensitivity variability in critical care. *Biomedical Signal Processing & Control*, 1:229–242.

Lin, J., Lee, D., Chase, J. G., Shaw, G. M., Le Compte, A., Lotz, T., Wong, J., Lonergan, T., and Hann, C. E. (2008). Stochastic modelling of insulin sensitivity and adaptive glycemic control for critical care. *Computer Methods and Programs in Biomedicine*, 89(2):141–152.

Lonergan, T., Le Compte, A., Willacy, M., Chase, J. G., Shaw, G. M., Hann, C. E., Lotz, T., Lin, J., and Wong, X. W. (2006a). A pilot study of the SPRINT protocol for tight glycemic control in critically Ill patients. *Diabetes Technol Ther*, 8(4):449–62.

Lonergan, T., Le Compte, A., Willacy, M., Chase, J. G., Shaw, G. M., Wong, X. W., Lotz, T., Lin, J., and Hann, C. E. (2006b). A simple insulin-nutrition protocol for tight glycemic control in critical illness: development and protocol comparison. *Diabetes Technol Ther*, 8(2):191–206.

Lorenz, J. M., Kleinman, L. I., Ahmed, G., and Markarian, K. (1995). Phases of fluid and electrolyte homeostasis in the extremely low birth weight infant. *Pediatrics*, 96(3 Pt 1):484–9.

Lotz, T. F., Chase, J. G., McAuley, K. A., Lee, D. S., Lin, J., Hann, C. E., and Mann, J. I. (2006). Transient and steady-state euglycemic clamp validation of a model for glycemic control and insulin sensitivity testing. *Diabetes Technol Ther*, 8(3):338–46.

Lotz, T. F., Chase, J. G., McAuley, K. A., Shaw, G. M., Wong, X. W., Lin, J., Le Compte, A., Hann, C. E., and Mann, J. I. (2008). Monte Carlo analysis of a new model-based method for insulin sensitivity testing. *Comput Methods Programs Biomed*, 89(3):215–25.

Lucas, A., Morley, R., and Cole, T. (1988). Adverse neurodevelopmental outcome of moderate neonatal hypoglycaemia. *Br Med J*, 297(6659):1304–1308.

Lumley, J. (2003). Defining the problem: the epidemiology of preterm birth. *BJOG: An International Journal of Obstetrics & Gynaecology*, 110(s20):3–7.

Mackenzie, I., Ingle, S., Zaidi, S., and Buczaski, S. (2005). Tight glycaemic control: a survey of intensive care practice in large English hospitals. *Intensive Care Med*, 31(8):1136.

Mantell, C. D., Craig, E. D., Stewart, A. W., Ekeroma, A. J., and Mitchell, E. A. (2004). Ethnicity and birth outcome: New Zealand trends 1980-2001: Part 2. Pregnancy outcomes for Maori women. *Australian and New Zealand Journal of Obstetrics and Gynaecology*, 44(6):537–540.

Mari, A. (1998). Assessment of insulin sensitivity and secretion with the labelled intravenous glucose tolerance test: improved modelling analysis. *Diabetologia*, 41(9):1029–39.

Mari, A., Pacini, G., Murphy, E., Ludvik, B., and Nolan, J. J. (2001). A model-based method for assessing insulin sensitivity from the oral glucose tolerance test. *Diabetes Care*, 24(3):539–548.

Mari, A., Stojanovska, L., Proietto, J., and Thorburn, A. W. (2003). A circulatory model for calculating non-steady-state glucose fluxes. Validation and comparison with compartmental models. *Computer Methods and Programs in Biomedicine*, 71(3):269–281.

Marik, P. E. and Raghavan, M. (2004). Stress-hyperglycemia, insulin and immunomodulation in sepsis. *Intensive Care Medicine*, 30(5):748–756.

Marquardt, D. W. (1979). Citation classic - algorithm for least-squares estimation of non-linear parameters. *Current Contents/Engineering Technology & Applied Sciences*, (27).

McCowen, K. C., Malhotra, A., and Bistrian, B. R. (2001). Stress-induced hyperglycemia. *Crit Care Clin*, 17(1):107–124.

McDonnell, C. M., Donath, S. M., Vidmar, S. I., Werther, G. A., and Cameron, F. J. (2005). A novel approach to continuous glucose analysis utilizing glycemic variation. *Diabetes Technol Ther*, 7(2):253–63.

Meetze, W., Bowsher, R., Compton, J., and Moorehead, H. (1998). Hyperglycemia in extremely- low-birth-weight infants. *Biol Neonate*, 74(3):214–21.

Mena, P., Llanos, A., and Uauy, R. (2001). Insulin homeostasis in the extremely low birth weight infant. *Semin Perinatol*, 25(6):436–46.

Mesotten, D., Swinnen, J. V., Vanderhoydonc, F., Wouters, P. J., and Van den Berghe, G. (2004). Contribution of circulating lipids to the improved outcome of critical illness by glycemic control with intensive insulin therapy. *J Clin Endocrinol Metab*, 89(1):219–26.

Mitanchez-Mokhtari, D., Lahlou, N., Kieffer, F., Magny, J.-F., Roger, M., and Voyer, M. (2004). Both relative insulin resistance and defective islet beta-cell processing of proinsulin are responsible for transient hyperglycemia in extremely preterm infants. *Pediatrics*, 113(3):537–541.

Mizock, B. A. (2001). Alterations in fuel metabolism in critical illness: hyperglycaemia. *Best Pract Res Clin Endocrinol Metab*, 15(4):533–51.

Natali, A., Gastaldelli, A., Camastra, S., Sironi, A. M., Toschi, E., Masoni, A., Ferrannini, E., and Mari, A. (2000). Dose-response characteristics of insulin action on glucose metabolism: a non-steady-state approach. *Am J Physiol Endocrinol Metab*, 278(5):E794–801.

Ng, S. M., May, J. E., and Emmerson, A. J. (2005). Continuous insulin infusion in hyperglycaemic extremely-low- birth-weight neonates. *Biol Neonate*, 87(4):269–72.

Oddo, M., Schaller, M. D., Calandra, T., and Liaudet, L. (2004). New therapeutic strategies in severe sepsis and septic shock. *Rev Med Suisse Romande*, 124(6):329–32.

Ostertag, S., Jovanovic, L., Lewis, B., and Auld, P. (1986). Insulin pump therapy in the very low birth weight infant. *Pediatrics*, 78(4):625–630.

Pacini, G. and Bergman, R. N. (1986). Minmod: a computer program to calculate insulin sensitivity and pancreatic responsivity from the frequently sampled intravenous glucose tolerance test. *Comput Methods Programs Biomed*, 23(2):113–22.

Peet, A. C., Kennedy, D. M., Hocking, M. D., and Ewer, A. K. (2002). Near-patient testing of blood glucose using the Bayer Rapidlab 860 analyser in a regional neonatal unit. *Ann Clin Biochem*, 39(Pt 5):502–8.

Pildes, R. S., Hart, R. J., Warrner, R., and Cornblath, M. (1969). Plasma insulin response during oral glucose tolerance tests in newborns of normal and gestational diabetic mothers. *Pediatrics*, 44(1):76.

Pildes, R. S. and Pyati, S. P. (1986). Hypoglycemia and hyperglycemia in tiny infants. *Clin Perinatol*, 13(2):351–75.

Plank, J., Blaha, J., Cordingley, J., Wilinska, M. E., Chassin, L. J., Morgan, C., Squire, S., Haluzik, M., Kremen, J., Svacina, S., Toller, W., Plasnik, A.,

Ellmerer, M., Hovorka, R., and Pieber, T. R. (2006). Multicentric, randomized, controlled trial to evaluate blood glucose control by the model predictive control algorithm versus routine glucose management protocols in intensive care unit patients. *Diabetes Care*, 29(2):271–6.

Poindexter, B. B., Karn, C. A., and Denne, S. C. (1998). Exogenous insulin reduces proteolysis and protein synthesis in extremely low birth weight infants. *J Pediatrics*, 132(6):948–53.

Powers, W. J., Rosenbaum, J. L., Dence, C. S., Markham, J., and Videen, T. O. (1998). Cerebral glucose transport and metabolism in preterm human infants. *J Cereb Blood Flow Metab*, 18(6):632–8.

Prigeon, R. L., Roder, M. E., Porte, D., J., and Kahn, S. E. (1996). The effect of insulin dose on the measurement of insulin sensitivity by the minimal model technique. evidence for saturable insulin transport in humans. *J Clin Invest*, 97(2):501–7.

Raney, M., Donze, A., and Smith, J. R. (2008). Insulin infusion for the treatment of hyperglycemia in low birth weight infants: examining the evidence. *Neonatal Netw*, 27(2):127–40.

Rasio, E. A., Hampers, C. L., Soeldner, J. S., and Cahill, G. F., J. (1967). Diffusion of glucose, insulin, inulin, and evans blue protein into thoracic duct lymph of man. *J Clin Invest*, 46(6):903–10.

Richardson, D. K., Gray, J. E., Gortmaker, S. L., Goldmann, D. A., Pursley, D. M., and McCormick, M. C. (1998). Declining severity adjusted mortality: evidence of improving neonatal intensive care. *Pediatrics*, 102(4):893–9.

Rizza, R. A., Mandarino, L. J., and Gerich, J. E. (1981). Dose-response characteristics for effects of insulin on production and utilization of glucose in man. *Am J Physiol*, 240(6):E630–639.

Saltiel, A. R. and Kahn, C. R. (2001). Insulin signalling and the regulation of glucose and lipid metabolism. *Nature*, 414(6865):799–806.

Shaw, G. M., Chase, J. G., Lee, D. S., Bloomfield, M., Doran, C. V., Lin, J., and Lotz, T. (2005). Peak and range of blood glucose are also associated with ICU mortality. *Critical Care Medicine*, 32(12):A125.

Sherwin, R. S., Kramer, K. J., Tobin, J. D., Insel, P. A., Liljenquist, J. E., Berman, M., and Andres, R. (1974). A model of the kinetics of insulin in man. *J Clin Invest*, 53(5):1481–92.

Simpson, J. and Stephenson, T. (1993). Regulation of extracellular fluid volume in neonates. *Early Hum Dev*, 34(3):179–90.

Sjostrand, M., Holmang, A., and Lonnroth, P. (1999). Measurement of interstitial insulin in human muscle. *Am J Physiol*, 276(1 Pt 1):E151–4.

Soop, M., Duxbury, H., Agwunobi, A. O., Gibson, J. M., Hopkins, S. J., Childs, C., Cooper, R. G., Maycock, P., Little, R. A., and Carlson, G. L. (2002). Euglycemic hyperinsulinemia augments the cytokine and endocrine responses to endotoxin in humans. *Am J Physiol Endocrinol Metab*, 282(6):E1276–85.

Steil, G. M., Ader, M., Moore, D. M., Rebrin, K., and Bergman, R. N. (1996). Transendothelial insulin transport is not saturable in vivo. no evidence for a receptor-mediated process. *J Clin Invest*, 97(6):1497–503.

Sunehag, A., Haymond, M., Schanler, R., Reeds, P., and Bier, D. (1999). Gluconeogenesis in very low birth weight infants receiving total parenteral nutrition. *Diabetes*, 48(4):791–800.

Thabet, F., Bourgeois, J., Guy, B., and Putet, G. (2003). Continuous insulin infusion in hyperglycaemic very-low-birth-weight infants receiving parenteral nutrition. *Clin Nutr*, 22(6):545–7.

Thombs, L. A. and Schucany, W. R. (1990). Bootstrap prediction intervals for autoregression. *Journal of the American Statistical Association*, 85(410):486–492.

Thorell, A., Rooyackers, O., Myrenfors, P., Soop, M., Nygren, J., and Ljungqvist, O. H. (2004). Intensive insulin treatment in critically ill trauma patients normalizes glucose by reducing endogenous glucose production. *J Clin Endocrinol Metab*, 89(11):5382–6.

Toffolo, G., Campioni, M., Basu, R., Rizza, R. A., and Cobelli, C. (2006). A minimal model of insulin secretion and kinetics to assess hepatic insulin extraction. *Am J Physiol Endocrinol Metab*, 290(1):E169–76.

Toffolo, G., Cefalu, W. T., and Cobelli, C. (1999). Beta-cell function during insulin-modified intravenous glucose tolerance test successfully assessed by the c-peptide minimal model. *Metabolism*, 48(9):1162–6.

Tucker, J. and McGuire, W. (2004). Epidemiology of preterm birth. *BMJ*, 329(7467):675–8.

Tyrala, E. E., Chen, X., and Boden, G. (1994). Glucose metabolism in the infant weighing less than 1100 grams. *The Journal of pediatrics*, 125(2):283–7.

Umpierrez, G. E., Isaacs, S. D., Bazargan, N., You, X., Thaler, L. M., and Kitabchi, A. E. (2002). Hyperglycemia: an independent marker of in-hospital mortality in patients with undiagnosed diabetes. *J Clin Endocrinol Metab*, 87(3):978–982.

Van Cauter, E., Polonsky, K. S., and Scheen, A. J. (1997). Roles of circadian rhythmicity and sleep in human glucose regulation. *Endocr Rev*, 18(5):716–38.

Van den Berghe, G. (2004a). How does blood glucose control with insulin save lives in intensive care? *J Clin Invest*, 114(9):1187–95.

Van den Berghe, G. (2004b). How to compare adequacy of algorithms to control blood glucose in the intensive care unit? *Crit Care*, 8(3):151–2.

Van den Berghe, G., Schoonheydt, K., Becx, P., Bruyninckx, F., and Wouters, P. J. (2005). Insulin therapy protects the central and peripheral nervous system of intensive care patients. *Neurology*, pages 1348–1353.

Van den Berghe, G., Vlasselaers, D., and Vanhorebeek, I. (2009). Insulin therapy in very-low-birth-weight infants. *N Engl J Med*, 360(5):535; author reply 536–7.

Van den Berghe, G., Wilmer, A., Hermans, G., Meersseman, W., Wouters, P. J., Milants, I., Van Wijngaerden, E., Bobbaers, H., and Bouillon, R. (2006). Intensive insulin therapy in the medical ICU. *N Engl J Med*, 354(5):449–61.

Van den Berghe, G., Wouters, P., Weekers, F., Verwaest, C., Bruyninckx, F., Schetz, M., Vlasselaers, D., Ferdinande, P., Lauwers, P., and Bouillon, R. (2001). Intensive insulin therapy in the critically ill patients. *N Engl J Med*, 345(19):1359–1367.

Van den Berghe, G., Wouters, P. J., Bouillon, R., Weekers, F., Verwaest, C., Schetz, M., Vlasselaers, D., Ferdinande, P., and Lauwers, P. (2003). Outcome

benefit of intensive insulin therapy in the critically ill: Insulin dose versus glycemic control. *Crit Care Med*, 31(2):359–366.

Van Kempen, A. A., Romijn, J. A., Ruiter, A. F., Ackermans, M. T., Endert, E., Hoekstra, J. H., Kok, J. H., and Sauerwein, H. P. (2003). Adaptation of glucose production and gluconeogenesis to diminishing glucose infusion in preterm infants at varying gestational ages. *Pediatric research*, 53(4):628–34.

Vander, A., Sherman, J., and Luciano, D. (2001). *Human Physiology: The Mechanisms of Body Function*. McGraw-Hill, New York, 8th edition.

Vaucher, Y. E., Walson, P. D., and Morrow, G. (1982). Continuous insulin infusion in hyperglycemic, very low birth weight infants. *Journal of pediatric gastroenterology and nutrition*, 1(2):211–7.

Vicini, P. and Cobelli, C. (2001). The iterative two-stage population approach to IVGTT minimal modeling: improved precision with reduced sampling. Intravenous glucose tolerance test. *Am J Physiol Endocrinol Metab*, 280(1):E179–86.

Vlasselaers, D., Milants, I., Desmet, L., Wouters, P. J., Vanhorebeek, I., van den Heuvel, I., Mesotten, D., Casaer, M. P., Meyfroidt, G., Ingels, C., Muller, J., Van Cromphaut, S., Schetz, M., and Van den Berghe, G. (2009). Intensive insulin therapy for patients in paediatric intensive care: a prospective, randomised controlled study. *Lancet*, 373(9663):547–56.

Vogelzang, M., van der Horst, I., and Nijsten, M. (2004). Hyperglycaemic index as a tool to assess glucose control: A retrospective study. *Crit Care*, 8(3):R122–R127.

Weekers, F., Giulietti, A. P., Michalaki, M., Coopmans, W., Van Herck, E., Mathieu, C., and Van den Berghe, G. (2003). Metabolic, endocrine, and immune effects of stress hyperglycemia in a rabbit model of prolonged critical illness. *Endocrinology*, 144(12):5329–38.

Wilinska, M. E., Ludovic, J. C., and Hovorka, R. (2008). In-silico testing - impact on the progress of the closed loop insulin infusion for critically ill patients project. *Journal of Diabetes Science and Technology*, 2(3):417–423.

Wong, X., Chase, J., Hann, C., Lotz, T., Lin, J., Le Compte, A., and Shaw, G. (2008). Development of a clinical type 1 diabetes metabolic system model and in silico simulation tool. *Journal of Diabetes Science and Technology (JoDST)*, 2(3):424–435.

Wong, X. W., Chase, J. G., Shaw, G. M., Hann, C. E., Lotz, T., Lin, J., Singh-Levett, I., Hollingsworth, L. J., Wong, O. S., and Andreassen, S. (2006a). Model predictive glycaemic regulation in critical illness using insulin and nutrition input: a pilot study. *Med Eng Phys*, 28(7):665–81.

Wong, X. W., Shaw, G. M., Chase, J. G., Hann, C. E., Lotz, T., and Lin, J. (2005). Active insulin control with variable nutrition for targeted glucose control in critically ill patients. *New Zealand Medical Journal*, 118(1218):3.

Wong, X. W., Singh-Levett, I., Hollingsworth, L. J., Shaw, G. M., Hann, C. E., Lotz, T., Lin, J., Wong, O. S., and Chase, J. G. (2006b). A novel, model-based insulin and nutrition delivery controller for glycemic regulation in critically ill patients. *Diabetes Technol Ther*, 8(2):174–90.

Yang, Y. J., Hope, I. D., Ader, M., and Bergman, R. N. (1989). Insulin transport across capillaries is rate limiting for insulin action in dogs. *J Clin Invest*, 84(5):1620–8.

Yang, Y. J., Youn, J. H., and Bergman, R. N. (1987). Modified protocols improve insulin sensitivity estimation using the minimal model. *Am J Physiol*, 253(6 Pt 1):E595–602.

Zahid, N., Taylor, K. M., Gill, H., Maguire, F., and Shulman, R. (2008). Adsorption of insulin onto infusion sets used in adult intensive care unit and neonatal care settings. *Diabetes Res Clin Pract*, 80(3):e11–3.

Zheng, Y. and Zhao, M. (2005). Modified minimal model using a single-step fitting process for the intravenous glucose tolerance test in type 2 diabetes and healthy humans. *Comput Methods Programs Biomed*, 79(1):73–79.

Zhou, D., Qian, J., Liu, C. X., Chang, H., and Sun, R. P. (2008). Repetitive and profound insulin-induced hypoglycemia results in brain damage in newborn rats: an approach to establish an animal model of brain injury induced by neonatal hypoglycemia. *European Journal of Pediatrics*, 167(10):1169–74.

Zylberberg, R. and Pepper, M. (2001). Continuous insulin infusion: promoting growth in low birth-weight infants. *Neonatal Network*, 20(1):21–28.